

**The Palladium(II) Directed Synthesis
of Mechanically Interlocked
Molecular Architectures**

By

D. Barney Walker

Degree of Doctor of Philosophy

School of Chemistry

University of Edinburgh

October 2005



Dedicated to My Family

Table of Contents

Abstract	iv
Declaration	v
Lectures and Meetings Attended.....	vi
Acknowledgements	vii
List of Abbreviations.....	ix
General Comments on Experimental Data.....	xi
Chapter 1: The Use of Transition Metal Ions in the Assembly of Mechanically Interlocked Molecules	1
Preface	2
1.1 Background	3
1.1.1 Definitions and Nomenclature.....	3
1.1.2 Historical Origins and Early Synthetic Methodologies.....	3
1.1.3 The Assembly of Mechanically Interlocked Molecules Using Non-TM Template-Based Methodologies.....	5
1.2 TM-Based Mechanically Interlocked Architectures	12
1.2.1 Molecular Architectures Containing Metal Ions Within Their Interlocked Framework.....	12
1.2.2 TM-Directed Synthesis of Catenanes, Knots, Rotaxanes, and Borromean Rings.....	22
1.3 Conclusions and Perspectives	45
1.4 Thesis Layout	46
1.5 References	46
Chapter 2: Structural Requirements for the Assembly of a Square Planar Metal-Coordinated [2]Rotaxane	59
2.1 Introduction	60
2.1 Results and Discussion.....	61
2.3 Experimental Section	66
2.4 References and Notes	77
Chapter 3: A Square Planar Palladium [2]Catenate and Two Non-Interlocked Isomers	83
3.1 Introduction	84

3.2 Results and Discussion.....	86
3.3 Conclusions	97
3.4 Experimental Section	98
3.5 References and Notes	113
Chapter 4: Rare and diverse binding modes introduced through mechanical bonding.....	121
4.1 Introduction	122
4.2 Results and Discussion.....	124
4.3 Experimental Section	134
4.3.1 Solution Host-Guest Binding Experiments	134
4.3.2. Preparation of Sulfonic Acid Complexes.....	136
4.3.3 Preparation of TM Complexes	137
4.4 References and Notes	140
Chapter 5: Half-Rotation in a [2]catenane <i>via</i> Interconvertible Pd(II) Coordination modes	146
5.1 Introduction	147
5.2 Results and Discussion.....	147
5.3 Experimental Section	151
5.3.1 Compound Analysis	151
5.3.2 Interconversion of [2]Catenane Species.....	152
5.4 References and Notes	152
Chapter 6: Kinetically fixed half-rotation in a [2]catenane <i>via</i> transition metal chelation	156
6.1 Introduction	157
6.2 Results and Discussion.....	157
6.3 Experimental	161
6.4 References and Notes	166
Appendix 1: Glossary of Compounds.....	170
Appendix 2: Published Papers	172

Abstract

The template synthesis of mechanically interlocked molecules has allowed their comprehensive study. In particular the transition metal-mediated synthesis of catenanes and rotaxanes has proven to be a useful methodology. The well defined primary coordination sphere of transition metal ions can be relied upon to orient multiple ligands in a predictable manner thus directing subsequent cyclisation reactions. This thesis describes the use of Pd(II) as a template in the synthesis of mechanically interlocked molecular architectures and is in three parts.

Firstly, the steric and electronic parameters governing the synthesis of a [2]rotaxane utilising the preferred square planar coordination geometry of Pd(II) were investigated. Using a tridentate pyridine 2,6-dicarboxamido macrocyclic precursor and a 2,6-dimethoxypyridine unit capped with bulky terminating groups the [2]rotaxane was accessed using ring closing olefin metathesis in the crucial cyclisation step. Based on these findings the assembly of a similar [2]catenane was achieved. In this case the desired product and two of its molecular isomers were prepared selectively depending on the order in which the precursor units were cyclised.

Secondly, both catenanes and rotaxanes assembled in this way were shown to contain an unusual intercomponent pyridine-amide-pyridine hydrogen bond motif following abstraction of the Pd(II) template. As a result, a range of diverse noncovalent binding interactions were observed with the [2]rotaxane and [2]catenane that are not found with similar, but not mechanically interlocked, fragments including non-native transition metal coordination and encapsulation of a sulfonic acid guest. All the neutral, anionic and cationic complexes were characterised in solution using ^1H NMR spectroscopy and in the solid state using X-ray crystallography.

Thirdly, the control of large amplitude sub-molecular motion in two novel [2]catenanes was achieved. In the first example, a 180° turn was produced *via* interconvertible Pd(II) coordination modes. In the second example, a [2]catenane containing one ring with two different TM binding moieties allowed for the kinetic control of a formal half-turn *via* chelation to either Co(III) or Pd(II). In both cases the co-conformation of the rings was confirmed in solution using ^1H NMR spectroscopy and in the solid state using X-ray crystallography.

Declaration

The scientific work described in this thesis was carried out in the School of Chemistry at the University of Edinburgh between October 2002 and September 2005. Unless otherwise stated, it is the work of the author and has not been submitted in whole or in support of an application for another degree or qualification of this or any other University or institute of learning.

Signed.

Date.....15.2.06.....

Lectures and Meetings Attended

1. **Organic Research Seminars**, School of Chemistry, University of Edinburgh, Scotland, 2001-2004.
2. **Perkin Organic Chemistry Conference**, University of Dundee, Scotland, 12/02.
3. **Perkin Organic Chemistry Conference**, School of Chemistry, University of Edinburgh, Scotland, 12/03. Presented poster entitled '*The Pd(II) directed synthesis of interlocked molecular architectures.*'
4. **UK Symposium of Macrocyclic Chemistry**, Sheffield, England, 1/04. Presented poster entitled '*The Pd(II) directed synthesis of interlocked molecular architectures.*'
5. **Dalton Inorganic Chemistry Conference**, Edinburgh, Scotland, 3/04. Presented poster entitled '*The Pd(II) directed synthesis of interlocked molecular architectures*' (joint 1st prize).
6. **XXIX International Symposium of Macrocyclic Chemistry**, Cairns, Australia, 7/04. 15 minute oral presentation entitled '*The Pd(II) directed synthesis of interlocked molecular architectures.*'
7. **USIC 2004**, Heriot Watt University, Edinburgh, Scotland, 9/04. 30-minute oral presentation entitled '*Rare and diverse binding modes introduced through mechanical bonding.*'
8. **ESF EuroConference on Smart Materials**, Tomar, Portugal, 9/04. Presented poster entitled '*Rare and diverse binding modes introduced through mechanical bonding.*'
9. **Perkin Organic Chemistry Conference**, School of Chemistry, University of Edinburgh, Scotland, 12/03.
10. **229th ACS National Meeting**, San Diego, California, USA, 3/05. 15-minute oral presentation '*Rare and diverse binding modes introduced through mechanical bonding.*'
11. **XXX International Symposium of Macrocyclic Chemistry**, Dresden, Germany, 7/05. Presented poster entitled '*Rare and diverse binding modes introduced through mechanical bonding.*'

Acknowledgements

I would like to thank my supervisor Prof. David A. Leigh for giving me the opportunity to work in his group, for providing all the resources an aspiring chemist could possibly need and for all he has taught me. I also thank him for staying late one particular cold February night to help me strip the tar from my fume-hood after I accidentally incinerated it. Special thanks to Dr. Paul Lusby, my long suffering laboratory mentor who has shown no small measure of patience over the last three years and taught me in the ways of synthetic chemistry.

I would also like to thank the following people: Prof. Alex Slawin for all her amazing work solving the X-ray crystal structures that are central to the research presented in this thesis. Dr. Dana Marlin for imparting some of his knowledge concerning the black art of crystal growing and the noble pursuit of surfing. Anne-Marie Fuller for her work on the various Pd(II) projects and for some eagle-eyed proof reading. Louise Hogg for the preparation of copious amounts of ‘stopper’ and ‘U-shape’ and for keeping Lab. 29 shipshape. Euan Kay and Andrew Thomson, my chemistry peers, for countless useful discussions over the last *eight* years and for proof reading various documents. Dr. Jeff Hannam, the human organic chemistry compendium, for sharing a fraction of his knowledge. Dr. Emilio Pérez and Dr. Gianni Bottari for passing on (some of) their NMR expertise to me (*algún día sere un galactico como ustedes!*). Diego Gonzales for taking over the role of NMR chief so proficiently. Juraj Bella and John Millar for helping to revive the NMR spectrometer when all seemed lost. All my laboratory mates over the last three years: Manashi, Isabel, Stuart, Elena, José, Diego, Ale, Laure, Roy, Andrea A, Andrea B, James, Phill, Popi, Weiquan, Chin Fa, Yun, Jong, Julia, Claire, Alem, Pepe, Bill, Smilja, Trent, Steve M., Steve G., Nick, Vince, Vivi, Raman, Steph and the others whom I must have missed (truly a Leigh group army!). The Turner group boys: Hyena, Tiger, Yak, Pigeon and Bear for lending me chemicals and for being most amusing neighbours. I thank all the staff at the University of Edinburgh School of chemistry for their help.

I would like to thank my good friends from 3F2 Mk. I and Mk. II: Mark, John, Little Kris-San, Big Dave, Sim, Rich, Paul, Ian and Ingy (where did the love go!); the 1F2 boys: Nod, Liam, Teva, Mike, Holly and Rupert (don't be a hero Johnny!); my karate comrades Steven Webster, Dave Orr and all the different team members I have competed with over the years (sweep the leg!). All of you have made living and working in Edinburgh a magnificent experience.

Finally, I would like to express most grateful thanks to my mum and dad, Pauline and Alex, and my brother Craig for their support throughout my 1st and 2nd degrees (both financial and otherwise!) and for their help proof reading the final draft of this thesis.

List of Abbreviations

Å	Angstrom
δ	Chemical shift
bipy	Bipyridine
Calcd.	Calculated
CPK	Corey-Pauling-Koltun
DB24C8	Dibenzo-24-crown-8
DIAD	Diisopropylazodicarboxylate
DMAP	4-dimethylaminopyridine
DMF	<i>N,N'</i> -dimethylformamide
DMSO	Dimethylsulfoxide
DNA	Deoxyribonucleic acid
<i>E</i>	<i>trans</i> isomer
EDCI	1-(3-dimethylaminopropyl)-3-ethyl-carbodiimide hydrochloride
EDTA	Ethylenediamine tetraacetic acid
en	Ethylenediamine
equiv	Equivalent
ESI	Electrospray Ionisation
Et	Ethyl
FAB	Fast Atom Bombardment
g	Grams
h	Hours
H-bonding	Hydrogen bonding
HRMS	High Resolution Mass Spectrometry
<i>J</i>	Coupling constant
LRMS	Low Resolution Mass Spectrometry
MeOH	Methanol
Me	Methyl
mg	Milligram
MHz	Mega hertz
min	Minutes

mL	Millilitres
mmol	Millimoles
m.p.	Melting point
MS	Mass Spectrometry
<i>m/z</i>	Mass-to-charge ratio
NMR	Nuclear Magnetic Resonance
phen	Phenanthroline
ppm	Part per million
RCM	Ring Closing Metathesis
terpy	Terpyridine
THF	Tetrahydrofuran
TFA	Trifluoroacetic acid
TfOH	trifluoromethanesulfonic acid
TLC	Thin Layer Chromatography
TM	Transition Metal
VT	Variable Temperature
<i>E</i>	cis isomer

General Comments on Experimental Data

Unless stated otherwise, all reagents and anhydrous solvents were purchased from Aldrich Chemicals and used without further purification. Column chromatography was carried out using Kiesegel C60 (Merck, Germany) as the stationary phase, and TLC was performed on precoated silica gel plates (0.25 mm thick, 60F₂₅₄, Merck, Germany) and observed under UV light. All ¹H and ¹³C NMR spectra were recorded on a Bruker AV400 instrument at a constant temperature of 25 °C. Chemical shifts are reported in parts per million from low to high field and referenced to TMS. Coupling constants (*J*) are reported in hertz (Hz). Standard abbreviations indicating multiplicity were used as follows: m = multiplet, br = broad, d = doublet, q = quadruplet, t = triplet, s = singlet. All melting points were determined using Sanyo Gallenkamp apparatus and are reported uncorrected. ESI mass spectrometry was performed with a Micromass Platform II mass spectrometer controlled using Masslynx v2.3 software while FAB mass spectrometry was carried out by the laboratory services at the University of Edinburgh.

Chapter 1: The Use of Transition Metal Ions in the Assembly of Mechanically Interlocked Molecules

"Chemists are a strange class of mortals, impelled by an almost maniacal impulse to seek their pleasures amongst smoke and vapour, soot and flames, poisons and poverty, yet amongst all these evils I seem to live so sweetly, that I would rather die than change places with the King of Persia."

Johann Joachim Becher, *Physica subterranea*, 1667

Source: Paul Strathern, "Mendeleev's dream"

Preface

During the latter half of the 20th century a more comprehensive and rigorous understanding of the forces that govern intermolecular interactions evolved into the interdisciplinary field now known as supramolecular chemistry.^[1] The joint award of the Nobel prize in 1987 to Cram,^[2] Lehn^[3] and Pedersen,^[4] as well as the breadth of research currently being undertaken in this area across the globe, is testimony to the importance of “*chemistry beyond the molecule*” in contemporary science. One particularly impressive application of supramolecular chemistry has been the exploitation of noncovalent forces in the synthesis of mechanically interlocked molecules. The study of such compounds – where two or more fragments are held together in a single molecular species by a mechanical bond – was once the domain of a handful of pioneering chemists, but has rapidly developed over the last twenty years into an important field in its own right. Currently there are potential applications in materials chemistry^[5] and molecular electronics^[6, 7] amongst others that have to be considered as more than just whimsical dreams. Furthermore, through the study of these unique molecular entities, scientists are starting to formulate criteria for the mimicry of nature’s biological motors, paving the way for the realisation of synthetic molecular machines that can perform physical tasks in the macroscopic world.^[8]

Such is the current wealth of knowledge in this field that a fully comprehensive review of the area, including the synthesis, properties and applications of interlocked molecular systems, would fill several volumes.^[9, 10] With regard to the content of this thesis, specific emphasis has been placed on the role of TM ions in the development of mechanically interlocked molecules, although a brief overview of the area will be presented initially, to illustrate the diversity of this lively field of research.

1.1 Background

1.1.1 Definitions and Nomenclature

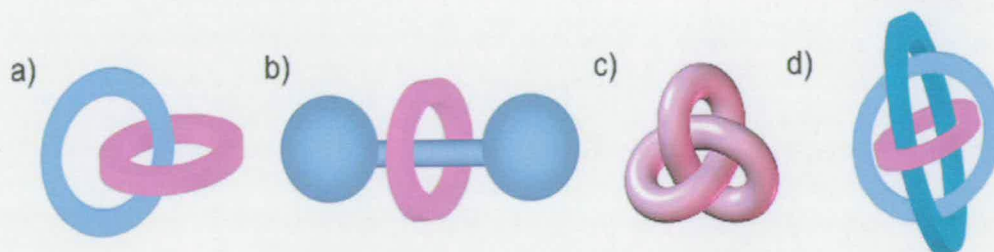


Figure 1.1. Cartoon representations of a) a [2]catenane, b) a [2]rotaxane, c) a trefoil knot, d) a Borromean ring.

Unambiguous scientific definitions have been assigned to the different classes of mechanically interlocked molecular architectures. A catenane (Figure 1.1 a) consists of two or more interlocked macrocycles connected like links in a chain. In a rotaxane (Figure 1.1 b) one or more macrocycles circumscribe a 'thread' comprised of a linear component terminated by two bulky end groups. Normally, a numerical prefix is added to the descriptor to denote the number of species that are kinetically associated, e.g. a [3]catenane is made up of three linked macrocycles. A trefoil knot (Figure 1.1 c) is the simplest non-trivial entangled molecule and, as its name suggests, contains three crossing points within its structure. Finally, a Borromean ring (Figure 1.1 d) is comprised of three rings linked together in such a way that cleavage of any ring results in complete dissociation of the 'locked' species (*see section 1.2.2.3*). Critically, all four species depicted in Figure 1.1 are molecules *not supramolecular complexes*, as covalent bonds must be broken in order to separate the mechanically bound fragments.^[11]

1.1.2 Historical Origins and Early Synthetic Methodologies

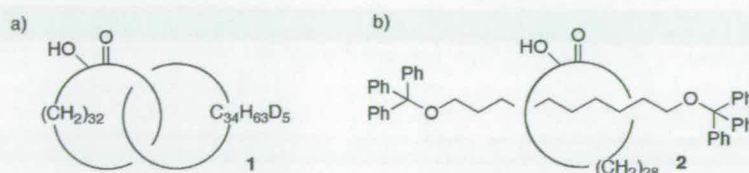
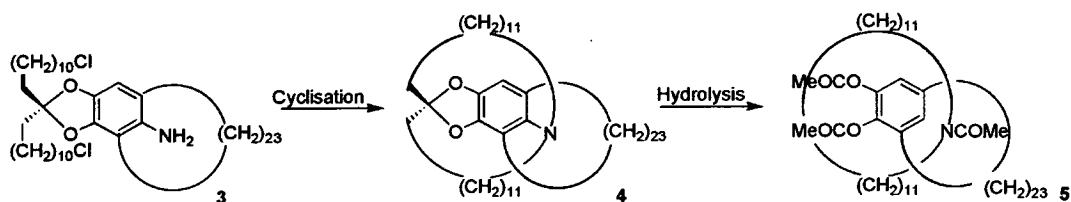


Figure 1.2. Early examples of interlocked molecules reported by a) Wasserman, b) Harrison.

The first mechanically interlocked architectures to be realised synthetically were assembled in the absence of any favourable intercomponent interactions using a technique commonly referred to as the ‘statistical’ method. An aleatory approach to the synthesis of mechanically interlocked rings was originally proposed in the early 1900s, and was finally realised synthetically in 1960 as **1** by Wasserman (Figure 1.2 a).^[12] The first [2]rotaxane **2** was assembled seven years later using a solid phase protocol by Harrison (Figure 1.2 b).^[13]



Scheme 1.1. Schill's covalent bond-directed synthesis of a [2]catenane.

Four years after Wasserman reported the first [2]catenane synthesis, Schill described the use of covalent bonds as templates in the first ‘directed’ synthesis of a mechanically interlocked molecule (Scheme 1.1).^[9, 14] The cyclisation of **3** is directed to either side of the preformed macrocyclic unit by the tetrahedral geometry of the acetal group – which essentially functions as a negative template – to form **4**. The relatively labile aryl-nitrogen and acetal linkages were then hydrolysed to form the [2]catenane **5**. The feasibility of constructing mechanically interlocked architectures using a covalent bond template is well illustrated by Schill's ingenious synthetic routes. However, such routes require many synthetic steps and a high level of technical expertise, thereby limiting the study of these novel compounds.

1.1.3 The Assembly of Mechanically Interlocked Molecules Using Non-TM Template-Based Methodologies

1.1.3.1 Hydrophobic Interactions

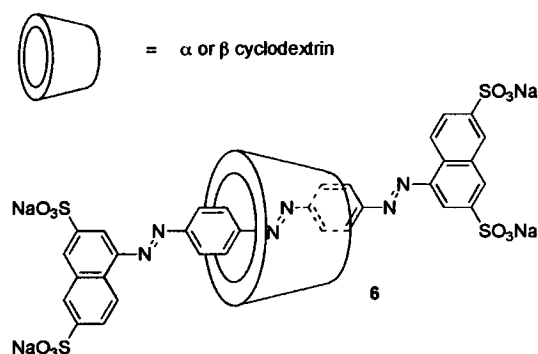
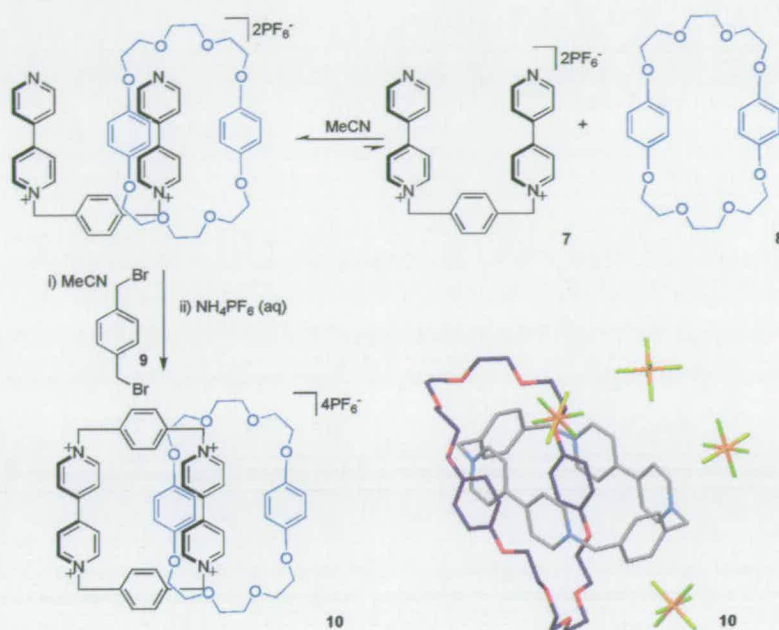


Figure 1.3. Anderson's cyclodextrin-based [2]rotaxane.

In 1981 Ogino reported the first synthesis of a rotaxane using a cyclodextrin ring (*see section 1.2.1.2.1*).^[15] Since then several groups have successfully employed the hydrophobic effect to synthesise interlocked molecules based on these ubiquitous cyclic oligosaccharides. In particular, Harada^[16] and Anderson^[17] have intensively investigated cyclodextrin-based rotaxane and polyrotaxane formation. In one fascinating example, Anderson and co-workers report on cyclodextrin-dye [2]rotaxane **6** wherein the cyclic oligosaccharide bestows exceptional stability on a normally reactive diazo species (Figure 1.3).^[18] It proved more difficult to assemble catenanes using cyclodextrins,^[19] but such molecules were realised for the first time by Stoddart in 1993.^[20]

1.1.3.2 Aromatic Interactions



Scheme 1.2. Synthesis and X-ray crystal structure of Stoddart's original paraquat-crown ether [2]catenane.

The discussion of synthetic molecular architectures assembled using aromatic interactions must be centred on the extensive research of Stoddart and co-workers. Stoddart's constructs were developed from research into host-guest complexes of the π -electron deficient herbicide paraquat derivative **7** and π -electron donating macrocycles such as **8** (bis-*p*-phenylene-34-crown-10).^[21] The first catenane based on this system was synthesised in 1989 (Scheme 1.2).^[22] Treatment of an acetonitrile solution of paraquat-derived macrocyclic precursor **7** and crown ether **8** with 1,4-dibenzyl bromide (**9**) resulted in the formation of catenane **10** in an impressive 70% yield. This robust methodology was subsequently used by Stoddart to generate an array of progressively more complex interlocked architectures including [5]catenanes,^[23] [7]catenanes^[24] and a trefoil knot.^[25]

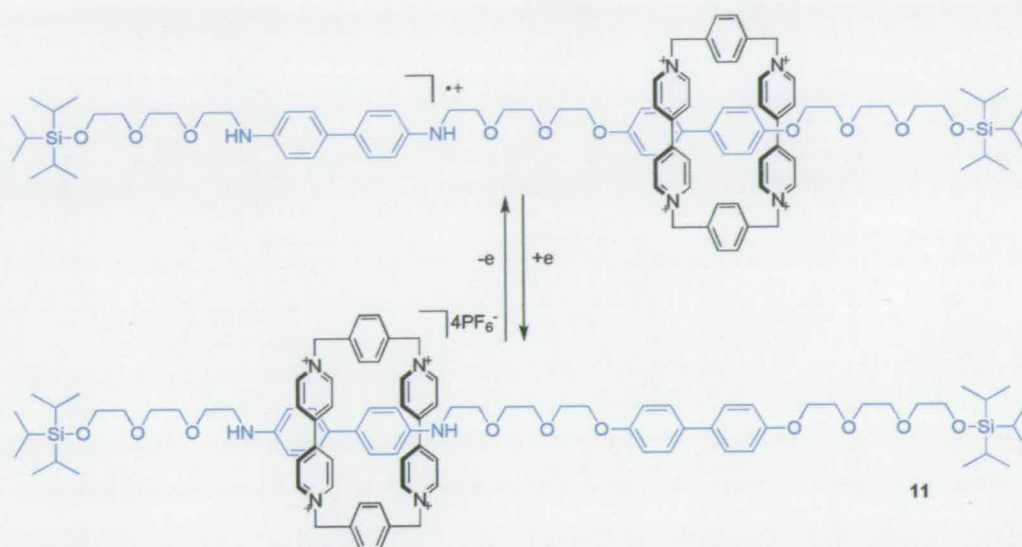


Figure 1.4. Electrochemically induced switching in the first stimuli-responsive molecular shuttle. The co-conformation of the rotaxane can also be mediated by pH (not shown).

Rotaxanes have also been assembled using the same paraquat-crown ether recognition motif.^[26] In 1991 Stoddart reported the first example of a molecular shuttle.^[27] This was followed by the seminal stimuli-responsive molecular shuttle **11** in 1994,^[28] wherein the co-conformation^[29] of the rotaxane is controlled using an electrochemical stimulus (Figure 1.4). The work of the UCLA-based group remains at the forefront of research into molecular devices and machines and they are making particularly impressive progress assembling molecular-level electronic devices.^[7, 30]

1.1.3.3 Hydrogen Bonding Interactions

Typically, hydrogen bonds are much weaker than covalent bonds or those in many metal complexes. As a consequence, effective H-bonding templates are generally made up of multi-point recognition sites. Whilst their geometric requirements are less rigid than those of TM-based templates, the most effective H-bonding templates are those with a high level of preorganisation.

1.1.3.3.1 Ammonium-Crown Ether-Based Rotaxanes

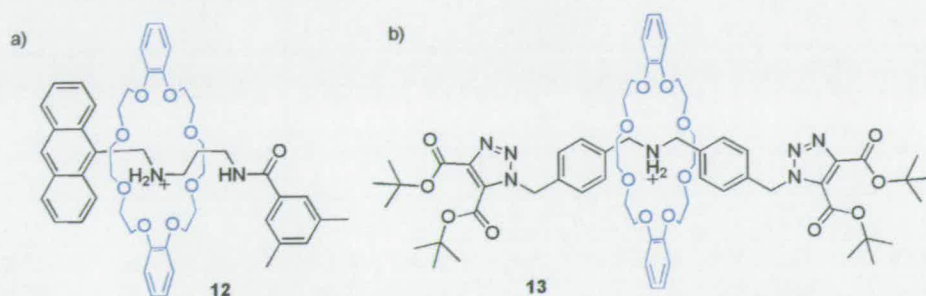
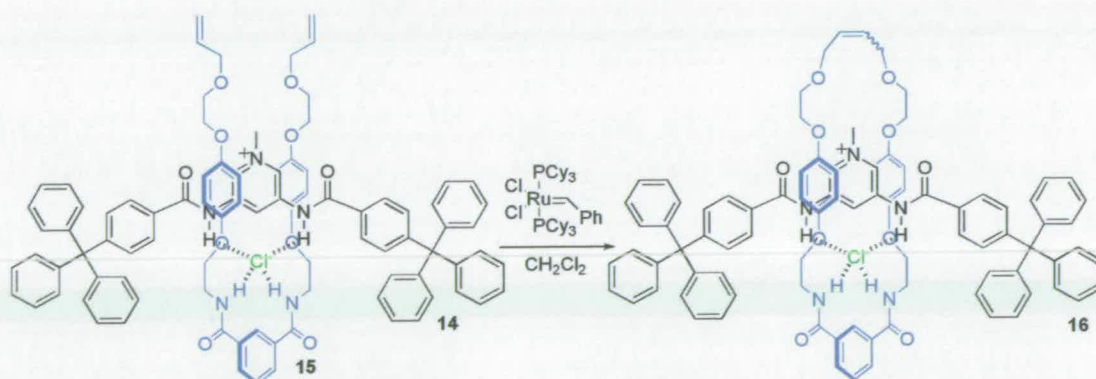


Figure 1.5. Original ammonium-crown ether rotaxanes reported by a) Busch, b) Stoddart.

Concurrently, Stoddart and Busch demonstrated that DB24C8 could form strong complexes with secondary dialkylammonium cations in a way that resulted in the penetration of the macrocycle by the positively charged species. The first [2]rotaxane (**12**) assembled using this system was published by Busch and co-workers in 1995 (Figure 1.5 a).^[31] Stoddart and co-workers showed that the same crown ether and a dibenzyl ammonium ion formed a 1:1 complex, and went on to describe the synthesis of rotaxanes (e.g. **13**) by ‘capping’ the thread component with bulky terminating groups (Figure 1.5 b).^[32] Stoddart has utilised this templating array to synthesise mechanically interlocked molecules under thermodynamic control, exploiting the reversible nature of imine^[33] and olefin^[34] bonds to form the energetically favoured mechanically bound species.

1.1.3.3.2 Anion-Based Catenanes and Rotaxanes



Scheme 1.3. Synthesis of Beer's [2]rotaxane assembled using a chloride/pyridinium ion pair as a template.

Vögtle reported the first example of a rotaxane assembled around an anionic phenolate template in 1999.^[35] More recently, Beer and co-workers have elegantly shown how chloride ion recognition can be utilised to assemble rotaxanes^[36] and catenanes.^[37] This approach relies on the affinity of strongly ion paired methyl pyridinium chloride thread **14** with isophthaloyl macrocycle precursor **15**. The close association of the two fragments in a non-competitive solvent directs the Grubbs' catalyst mediated RCM of two terminal olefin groups around the thread forming rotaxane **16** in 47% yield (Scheme 1.3).

1.1.3.3 Amide-Based Catenanes and Rotaxanes

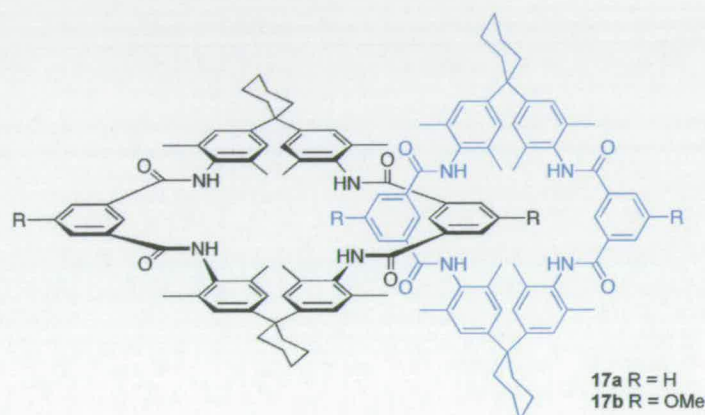
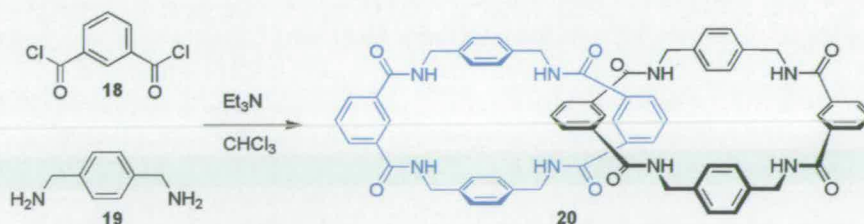


Figure 1.6. The first amide-based [2]catenane reported by Hunter (R = H) and Vögtle (R = OMe).

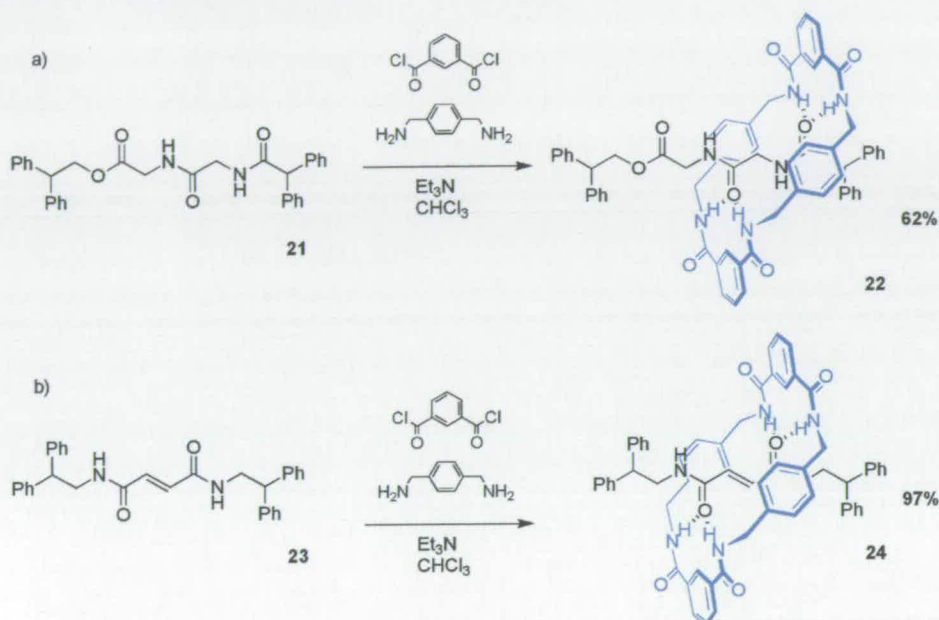
Hunter reported the first amide-based catenane **17a** – wherein multiple H-bonds direct the synthesis of two interlocking rings – in 1992.^[38] This was closely followed by the publication of very similar molecules by Vögtle **17b** (Figure 1.6).^[39] Subsequent accumulation of a large body of work by the latter has led to some elaborate molecular topologies being realised synthetically.^[40]



Scheme 1.4. Synthesis of Leigh's serendipitously discovered [2]catenane.

A much simpler amide-based [2]catenane was first described in 1995 by Leigh and co-workers.^[41] The combination of isophthaloyl chloride (**18**) and p-xylylene

diamine (**19**) at high dilution was expected to form the 2 + 2 macrocyclic adduct, but instead the [2]catenane **20** formed in 20% yield (Scheme 1.4). In a simultaneously published article, the tolerance of this system was demonstrated through the synthesis of a series of [2]catenanes using inexpensive, commercially available starting materials.^[42] Subsequently, it was observed that, if the acid chloride/diamine condensation was carried out in the presence of a suitably stoppered benzylic 1,3 diamide thread, [2]rotaxanes could be formed.^[43]



Scheme 1.5. Synthesis of a) glycylglycine [2]rotaxane, b) fumaric [2]rotaxane.

In both cases the mechanism for the formation of these interlocked molecules appeared to involve the directed assembly of a preformed macrocycle precursor around two *E*-amide bonds. Divergent H-bonding sites in a similar spatial arrangement occur in adjacent amino acid residues in peptide chains, and in 1997 Leigh showed that, when glycylglycine was incorporated into thread **21**, formation of [2]rotaxane **22** occurred in yields of up to 62% (Scheme 1.5 a).^[44] By further preorganising the orientation of the carbonyl groups using a fumaramide moiety (**23**), [2]rotaxane **24** was assembled in a near quantitative 97% yield (Scheme 1.5 b).^[45]

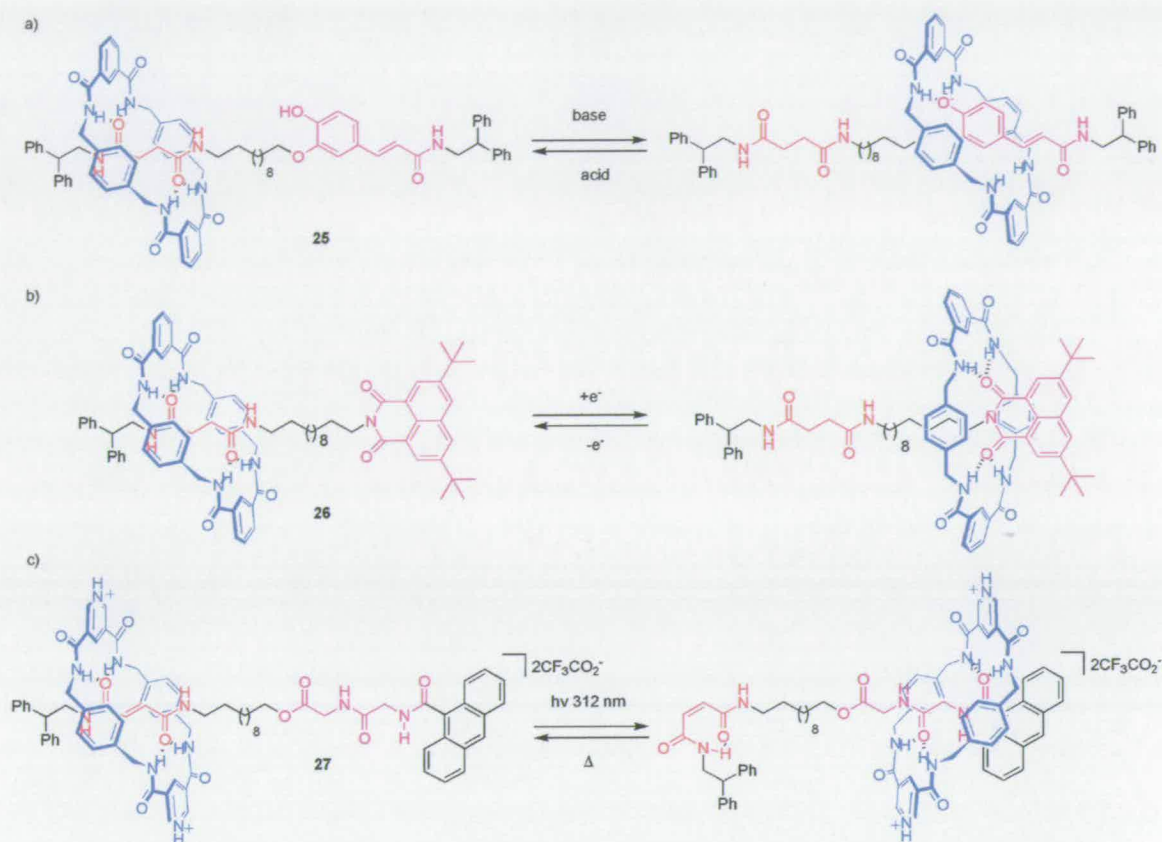


Figure 1.7. Selected examples of amide-based stimuli-responsive molecular shuttles controlled by a) pH, b) addition or removal of electrons, c) light/thermal energy.

The structural simplicity of these amide-based catenanes and rotaxanes has facilitated the comprehensive study of their inherent dynamics.^[46] Furthermore, reliable control over the formation of the mechanical bond has allowed for the expeditious development of a series of stimuli responsive molecular shuttles (e.g. [2]rotaxanes **25-27**). Molecular shuttles in which the macrocycle undergoes a well defined positional change in response to pH (Figure 1.7 a),^[47] redox processes (Figure 1.7 b),^[48] photochemical and thermal stimuli (Figure 1.7 c),^[49] and covalent bond formation^[50] have all been recently described. Recently, the first examples of unidirectional molecular rotors based on mechanically interlocked molecules have been prepared using this versatile synthetic methodology.^[51]

1.2 TM-Based Mechanically Interlocked Architectures

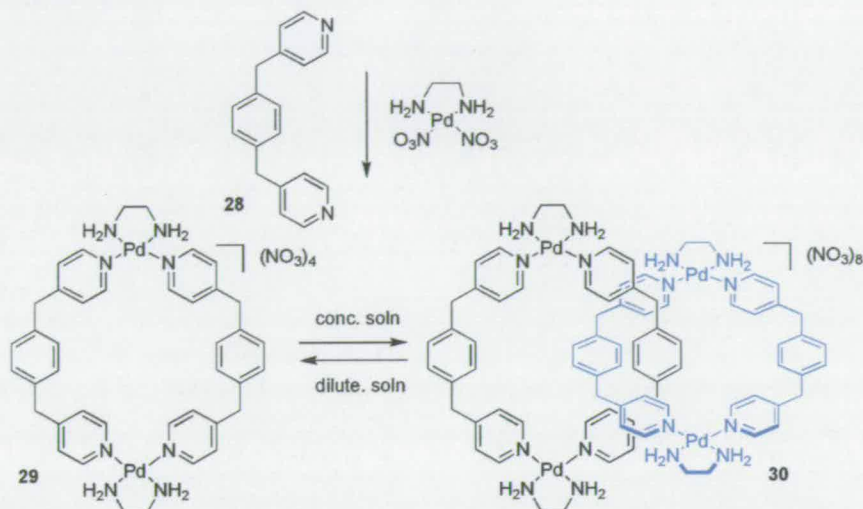
Broadly speaking, TM-based mechanically interlocked molecular architectures can be divided into two classes: complexes in which the TM ion comprises an integral structural feature (i.e. the complex dissociates in the absence of the metal); and discrete organic molecules that are assembled around a TM template (i.e. template abstraction yields a kinetically bound wholly organic molecule).

1.2.1 Molecular Architectures Containing Metal Ions Within Their Interlocked Framework

1.2.1.1 [2]Catenanes Containing TM Ions in Their Framework

The rich variation in properties (preferred coordination number, donor type and primary coordination geometry) of TMs and alkali metals has led to an exotic selection of [2]catenanes containing metal ions in their structure being reported in the literature, which at first sight seem to have little in common. The relationship between the complexes, other than their obvious topological congruity, is their thermodynamically controlled assembly. Evidently, a cyclic structure containing reversible coordination bonds can reorganise to form a stable interpenetrated TM complex provided the energetic gain in stability achieved through intercomponent recognition outweighs the entropic cost of unifying the two species.

1.2.1.1.1 Palladium and Platinum Systems



Scheme 1.6. Fujita's original Pd(II) catenane synthesis.

This field of research is dominated by the work of Fujita^[52] who, in 1994, reported a Pd(II) containing [2]catenane accessed *via* the quantitative self-assembly of simple component molecules.^[53] By mixing $\text{Pd}(\text{NO}_3)_2(\text{en})$ with 1,4-bis[(4-pyridyl)methyl]benzene **28** in aqueous solution, macrocycle **29** and corresponding [2]catenane **30** were shown to be in rapid equilibrium with one another (Scheme 1.6). Consequently, by Le Chatelier's Principle, at concentrations of greater than 50 mM, the reaction conditions favour the single component [2]catenane species **30**. These remarkable compounds were characterised initially by ^1H NMR and ESI-MS. An X-ray crystal structure was obtained of the Pt(II) analogue **31** (Figure 1.8).^[54]

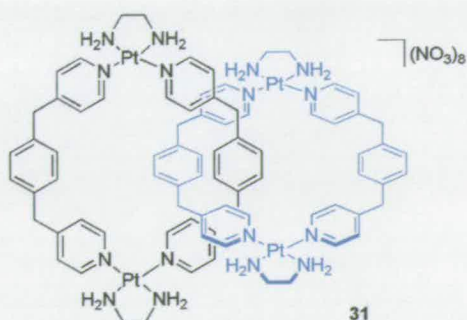
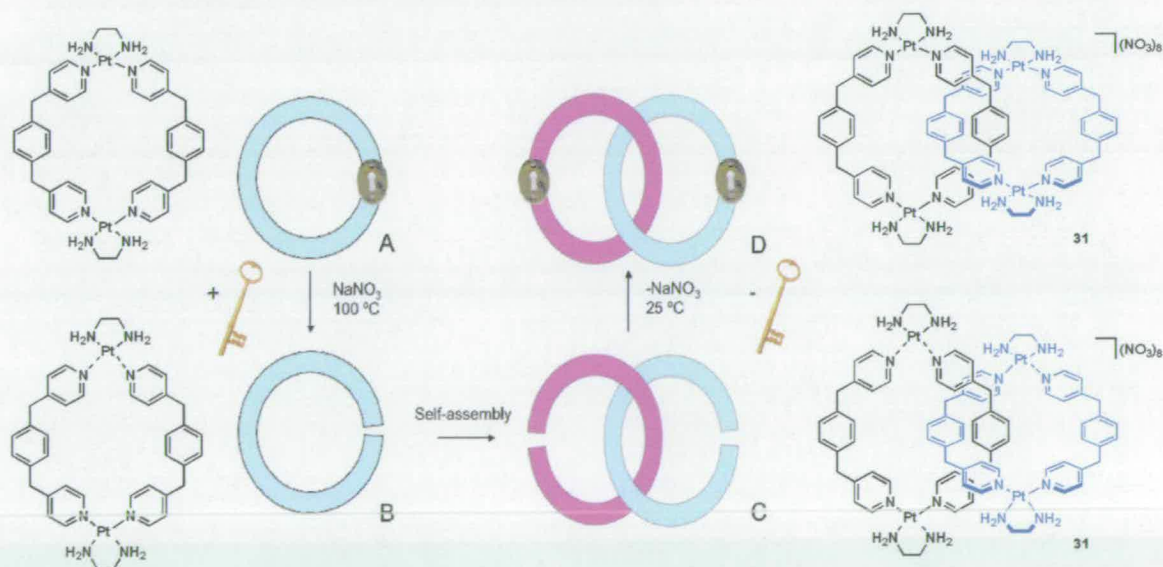


Figure 1.8. Fujita's Pt(II) [2]catenane.

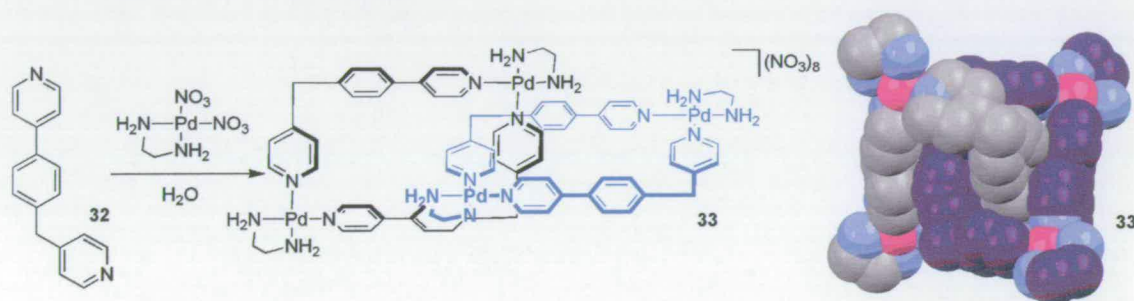
It has been suggested that the [2]catenane spontaneously forms as a result of double molecular recognition, i.e. the molecules bind each other in their respective hydrophobic cavities. By increasing the polarity of the reaction medium through addition of NaNO_3 , the yield of [2]catenane **30** was increased to greater than 99% even at high dilution, which supports this hypothesis. This observation facilitated the irreversible formation of [2]catenane **31**, using a 'molecular lock' strategy (Scheme 1.7). The Pt(II)-pyridine bond can be described as a thermally controlled lock as it is irreversible under ambient conditions, but becomes reversible in highly polar media at elevated temperatures. Initially the ring is locked (A) but it is released by adding salt and heating (B) to enable self-assembly of the [2]catenane (C). The framework is then locked again by cooling and salt removal (D).



Scheme 1.7. Fujita's molecular lock strategy.

In order to further improve the synthesis of catenanes, ligand **28** was replaced by ligand **32** as theoretical calculations predicted that the monomeric molecular box

formed by complexation of **32** with Pd(II) would contain a hydrophobic cavity more ideally suited for aromatic π -stacking with an exact copy of itself. This was shown to be the case experimentally when catenane **33** was assembled quantitatively and characterised by X-ray crystallography (Scheme 1.8).^[55] The crucial parameter for interlocking is the 3.5 Å interplane separation which favours catenane formation through π -stacking interactions and destabilises the non-interlocked Pd(II) box compound. In the same study, the Japanese research group showed that [2]catenanes could be assembled selectively from a three component mixture and that larger more flexible interlocked structures were thermodynamically privileged, provided the aromatic cleft was of sufficient dimensions. Recently the thermodynamically controlled self assembly of Fujita's catenanes has been employed in the synthesis of an extremely large macrocycle.^[56]



Scheme 1.8. Synthesis and X-ray-crystal structure (space filling representation) of a ‘made to order’ [2]catenane.

An alternative use of Pt(II) ions in the synthesis of interlocked architectures was described by Kim in 2002.^[57] In this case, the relatively inert Pt(II)-pyridine bond aligns multiple cucurbituril/dialkylammonium pseudorotaxanes resulting in the formation of [5]catenanes (**34**) as ‘molecular necklaces’ (Figure 1.9).^[58] Puddephatt and co-workers have used Pd(II) as a reversible linker in the H-bond directed assembly of chiral [2]catenanes.^[59]

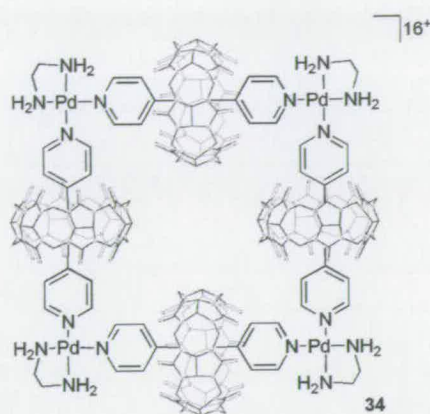


Figure 1.9. A [5]catenane molecular necklace.

1.2.1.1.2 Gold Systems

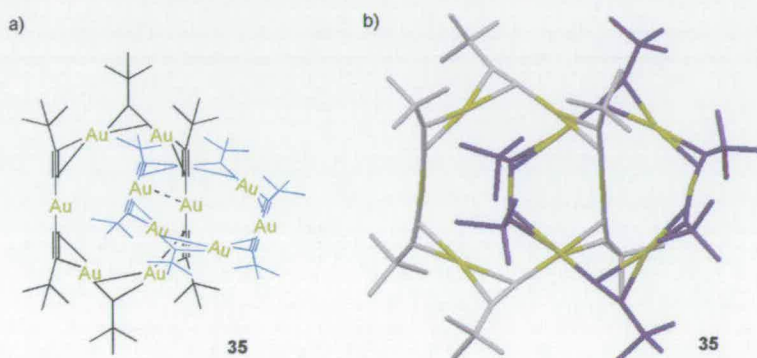
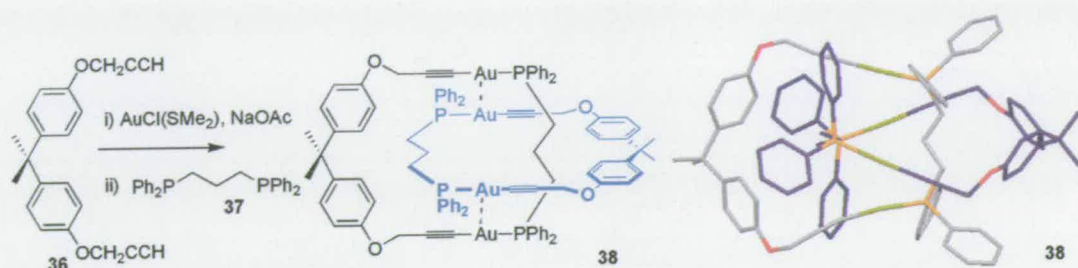


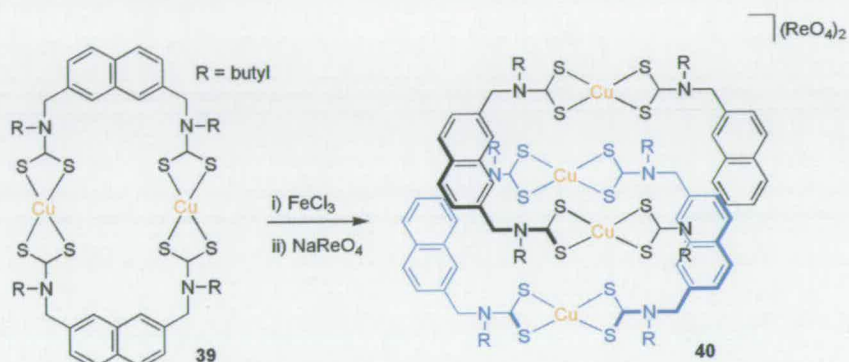
Figure 1.10. a) Chemical and b) X-ray crystal structure of the first gold-containing [2]catenane.

The original gold containing [2]catenane **35**, reported in 1995 by Mingos and co-workers is made up of alternate Au(I) and acetylenic units with the driving force for interlocking being intercomponent gold-gold or aurophilic interactions (Figure 1.10).^[60] This aesthetically pleasing organometallic structure was followed, from 1999 onwards, by a series of systematic studies by Puddephatt on the assembly of catenanes using the same Au(I)-acetylene linkage. In the original synthesis, deprotonation of diacetyl compound **36** followed by addition of AuCl(SMe₂) generated a polymeric gold species, which, on addition of diphosphine ligand **37**, reorganises to form [2]catenane **38** (Scheme 1.9). It was later shown that, only slightly varying the length of either the diacetyl or the diphosphine ‘hinge’ linkage directs the selective formation of either macrocycles,^[61] [2]catenanes^[62] or doubly braided [2]catenanes.^[63] Further to this research, self assembled chiral [2]catenanes have also been described.^[64]



Scheme 1.9. Synthesis and X-ray crystal structure of Puddephatt's original Au(I) [2]catenane.

1.2.1.1.3 Copper Systems



Scheme 1.10. Synthesis of Beer's Cu(II)/Cu(III) [2]catenane.

Beer and co-workers serendipitously discovered a fascinating example of a copper-based [2]catenane in 2001.^[65] The facile oxidation of a dithiocarbamate/Cu(II) macrocycle **39** with FeCl_3 leads to the exclusive formation of a mixed valence Cu(II)/Cu(III) catenane **40** (Scheme 1.10) as evidenced by X-ray crystallography (Figure 1.11 a). The solid-state structure reveals the stacked arrangement of the TM centres (Figure 1.11 b). It was concluded that intercomponent charge transfer between the interdigitated Cu(II) and Cu(III) ions drives the formation of the interlocked compound. Further studies have shown that it is possible to utilise the same interaction with Cu(II)/Au(III) systems to generate a library of mixed metal [2]catenanes.^[66]

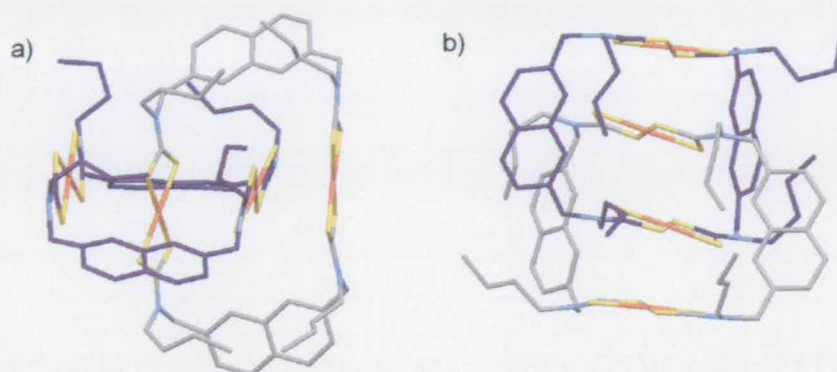


Figure 1.11. a) Top view and b) side view of the X-ray crystal structure of [2]catenane **40**.

1.2.1.1.4 Iron/silver and zinc systems

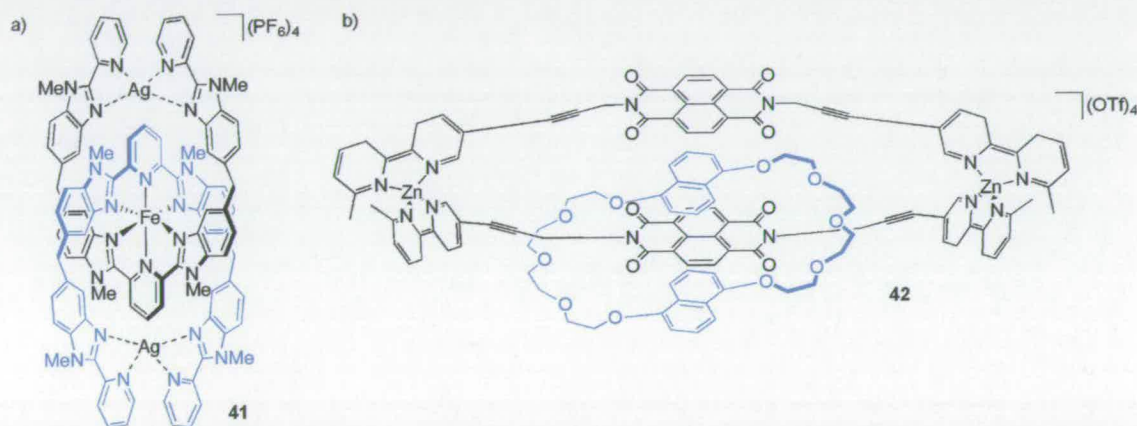


Figure 1.12. a) An iron/silver containing [2]catenane, b) Zn(II) linked [2]catenane associated *via* aromatic interactions

A remarkable self-assembling [2]catenane incorporating one Fe(II) ion and two Ag(I) ions was reported in 1995 (Figure 1.12 a). The complex **41** exists as two helical diastereomers that have been individually characterised in the solid state using X-ray crystallography.^[67] Self assembly was also employed in the five component synthesis of [2]catenane **42** (Figure 1.12 b). As with Fujita's catenanes, favourable aromatic interactions were used to select the interlocked product, although in this case a dinaphtho-crown ether (π -electron rich) and an aromatic diimido compound (π -electron deficient) were employed as recognition elements.^[68]

1.2.1.2 Rotaxanes Containing a Metal Ion in Their Framework

1.2.1.2.1 Discrete Metal Containing [2]Rotaxanes

The first metal containing rotaxane was reported by Ogino in 1981.^[15] The Co(III)/cyclodextrin rotaxane **43** – wherein the TM ions comprise the bulky stoppering groups – was prepared by spontaneous threading of β -cyclodextrin over a hydrophobic 1,12-diaminododecane thread in DMSO. The complex was ‘capped’ with a Co(III) complex to give rotaxane in 19% yield (Figure 1.13 a). A similar rotaxane **44**, incorporating Fe(II) instead of Co(III), was subsequently prepared by Macartney (Figure 1.13 b).^[69] Sauvage has also described [2]rotaxanes (e.g. **45**) with TM complexes as stoppers (Figure 1.13 c). In this example, two Ru(II) ions complexed with two terpy ligands (one on the thread, one as a free ligand) kinetically trap the interlocked species.^[70]

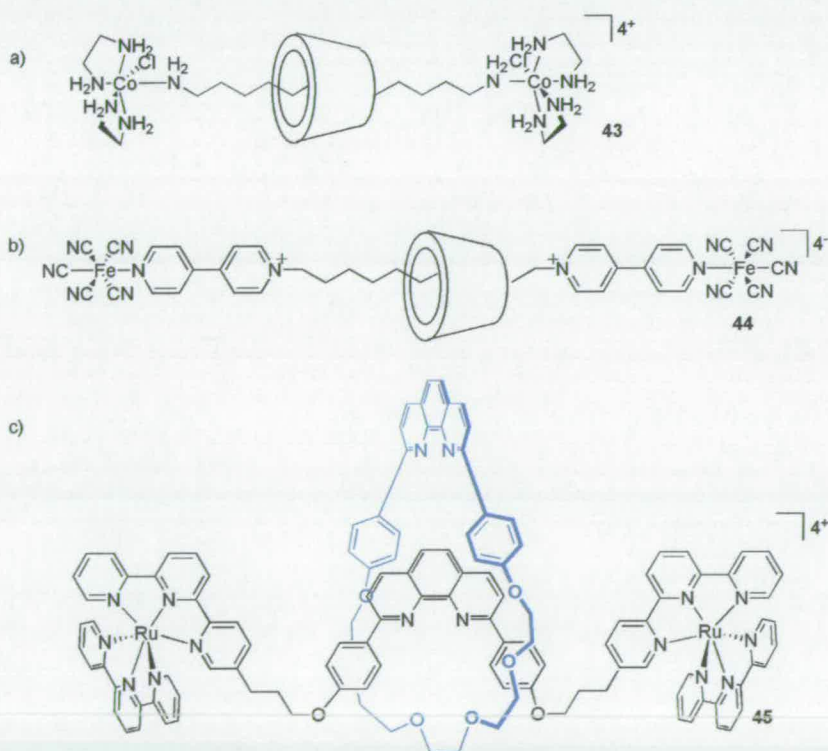


Figure 1.13. a) Ogino's Co(III) rotaxane, b) Macartney's Fe(II) rotaxane, c) Sauvage's Ru(II) rotaxane.

Rather than utilising TM ions as stoppers, Jeong and co-workers have developed a novel interlocked assembly where an Os(VI) ion comprises part of the

macrocycle.^[71] Rotaxane **46** is thermodynamically favoured over its constituent parts as a result of two intercomponent NH-CO H-bonds that can only be satisfied through intermolecular penetration (Figure 1.14 a). The reversible nature of the osmium-pyridine bond allows the thread to access the internal cavity of the macrocycle *via* a ‘clipping’ mechanism and thus the energetically favoured mechanically interlocked species is formed.

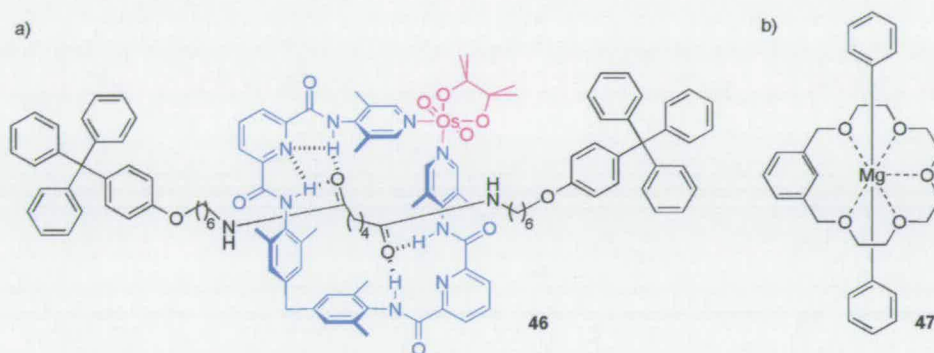
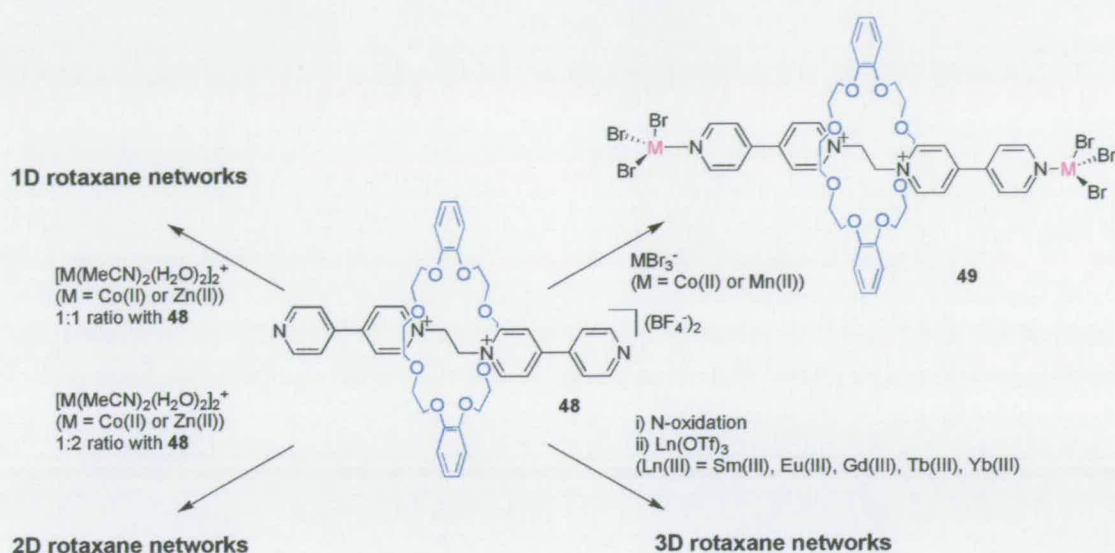


Figure 1.14. a) Os(VI) containing rotaxane, b) Mg(II) containing rotaxane.

Group 1 and 2 metal containing mechanically interlocked molecules are rare. An example of a polyether based rotaxane **47**, and an analogous catenane, assembled around a Mg(II) ion has been reported (Figure 1.14 b).^[72] It was not possible to isolate the compound as it was in rapid equilibrium with its individual components.

1.2.1.2.2 Metal-Organic Rotaxane Frameworks (MORFs)



Scheme 1.11. Illustration of the various rotaxane-based coordination networks accessible using Loeb's pseudorotaxane **48**.

It is straightforward to envisage how a bidentate pseudo-[2]rotaxane such as **48** could be incorporated into a polyrotaxane framework if the host-guest complex is regarded simply as a bridging ligand (Scheme 1.11). Loeb and co-workers have realised 1D, 2D and 3D networks using a pseudo-[2]rotaxane **48**^[73] in this way.^[74] It has been shown that complexation of **48** with two equivalents of MBr_3^- ($M = \text{Mn(II)}, \text{Co(II)}$) generates the neutral [2]rotaxane **49** (Figure 1.15 a),^[75] but, by using a more labile metal complex $[M(\text{MeCN})_2(\text{H}_2\text{O})_2]^{2+}$ ($M = \text{Zn(II)}, \text{Co(II)}$), a 1D array was realised where each bridging ligand is encapsulated by a macrocycle (Figure 1.15 b). This was extended to two dimensions using a 2:1 pseudo-[2]rotaxane to TM ion ratio (Figure 1.15 c),^[76] and to three dimensions using the doubly N-oxidised analogue of **48** and Ln(III) ions ($\text{Sm(III)}, \text{Eu(III)}, \text{Gd(III)}, \text{Tb(III)}, \text{Yb(III)}$).^[77] This type of long range order in materials containing mechanically bonded substrates lends itself to the concept of molecular-level solid-state devices, although the stability of these networks is not yet optimal and addressable systems have yet to be realised.

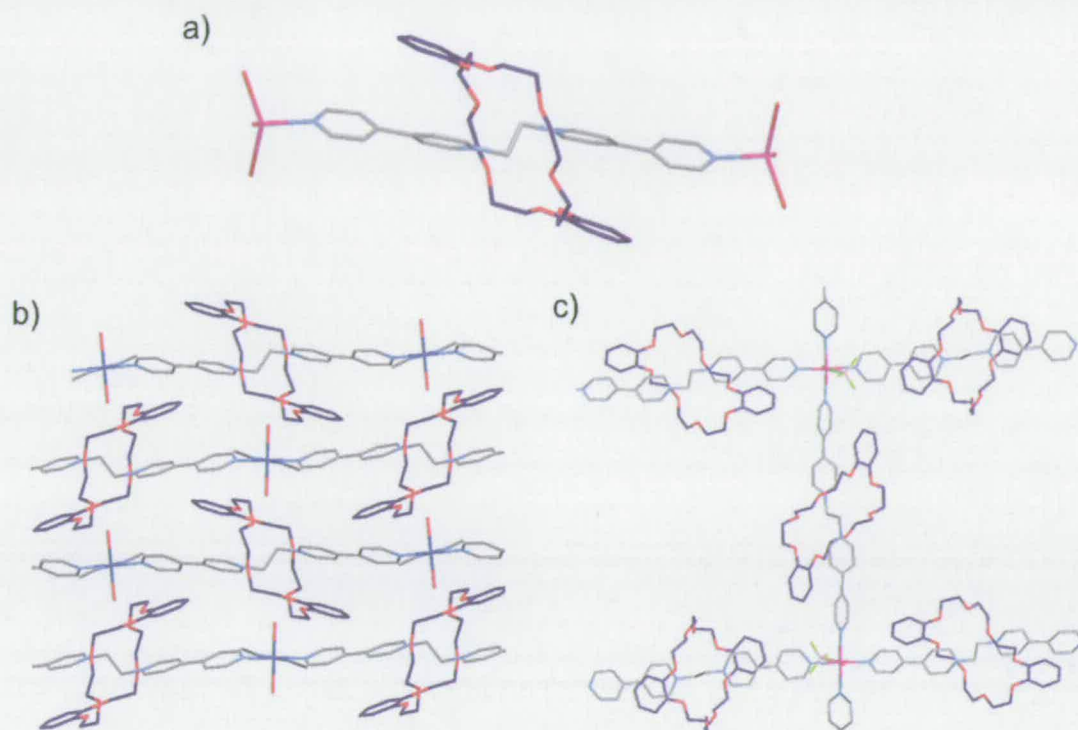


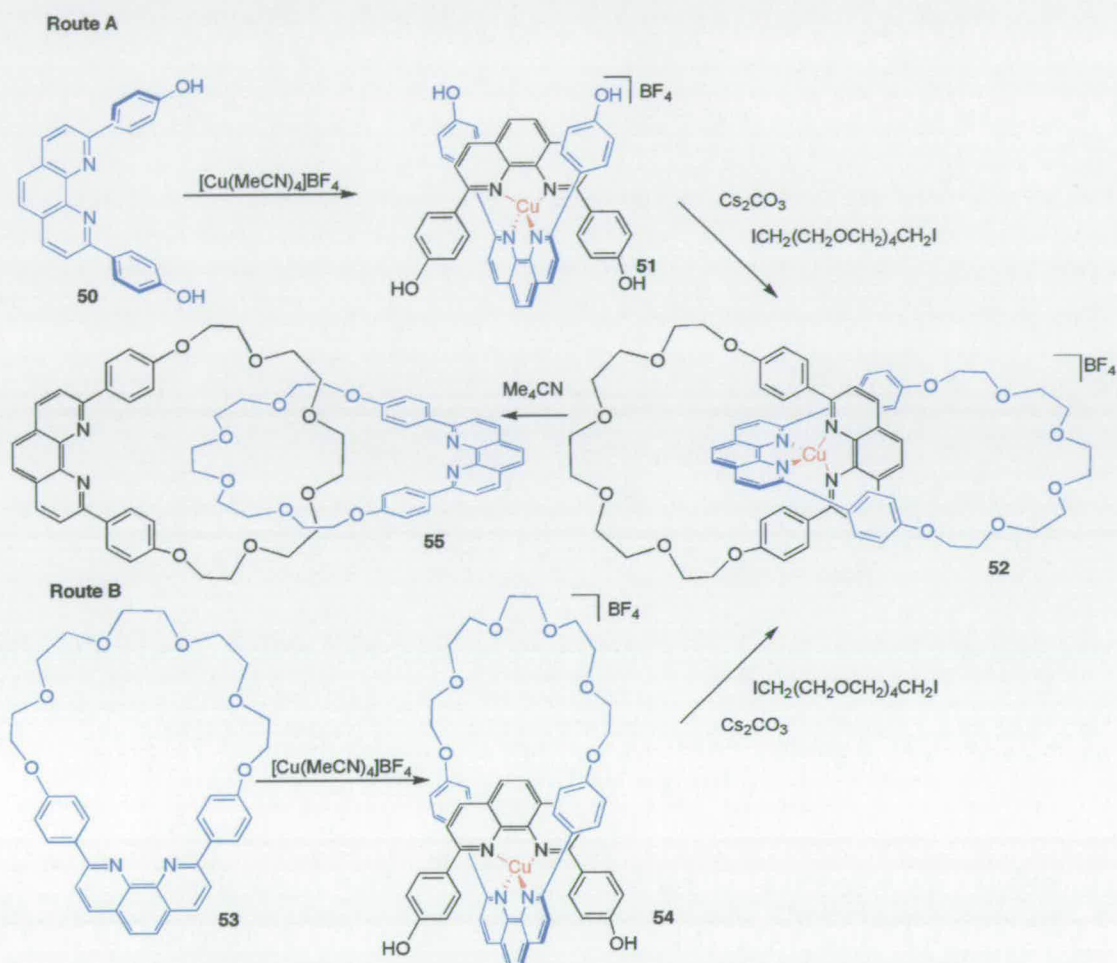
Figure 1.15. X-ray crystal structures of a) Discrete [2]rotaxane 49, b) 1D rotaxane network, c) 2D rotaxane network.

1.2.2 TM-Directed Synthesis of Catenanes, Knots, Rotaxanes, and Borromean Rings

1.2.2.1 Mechanically Interlocked Molecular Architectures Accessed Using a Cu(I)-Phenanthroline Methodology

The use of TM ions as templates in the synthesis of catenates, as implemented by Sauvage in 1983, represents an important landmark in the history of mechanically interlocked architectures. It could be argued that his insightful accomplishments bridge the gap between the work of the early pioneers and the extensive research of the modern day specialists.^[78]

1.2.2.1.1 [2]catenanes



Scheme 1.12. Sauvage's original Cu(I) directed [2]catenane synthesis.

Central to the original strategy developed by the Strasbourg group is the tetrahedral geometric preference of the primary coordination sphere of Cu(I), which promotes the orthogonal arrangement of two functionalised phen ligands (**50**) around the TM centre (Scheme 1.12 Route A).^[79] Subsequent reaction of tetra phenol complex **51** with 1,14-diiodo-3,6,9,12-tetraoxatetradecane in DMF at high dilution results in the formation of the catenate **52** in 27% yield with the remainder of the products being non-interlocked macrocycle **53** (20%) and various oligomeric species ($M_r > 1500$). The yield of catenane was increased to 42% by preforming one of the ligands as macrocycle **53** and cyclising complex **54** (Scheme 1.12 Route B).

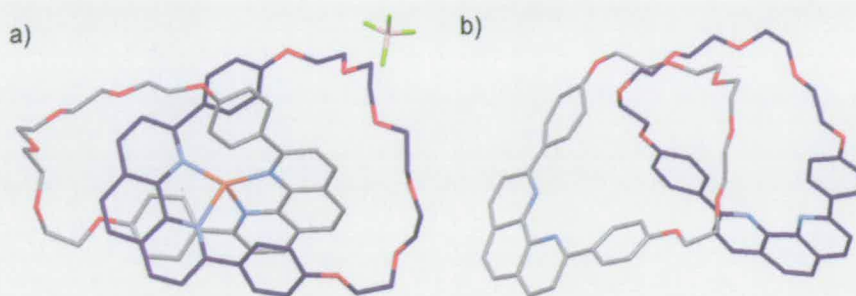


Figure 1.16. X-ray crystal structures of: a) [2]catenane **52** and [2]catenand **55**.

Abstraction of the Cu(I) ion using tetramethylammonium cyanide furnishes the free catenand **55**. In the Cu(I) catenane the four coordinating nitrogen groups ‘lock’ the two ligands in a well defined co-conformation around the TM ion. In contrast, removal of the Cu(I) template allows the rings to rotate freely (the ^1H NMR spectrum of the catenand is remarkably similar to that of the non-interlocked macrocycle suggesting that the two rings pirouette rapidly on the NMR timescale in CD_2Cl_2) although it was expected that the uncomplexed phen moieties would repel one another. This rearrangement was observed in the solid state following X-ray analysis of the catenane **52** (Figure 1.16 a) and the catenand **55** (Figure 1.16 b).^[80]

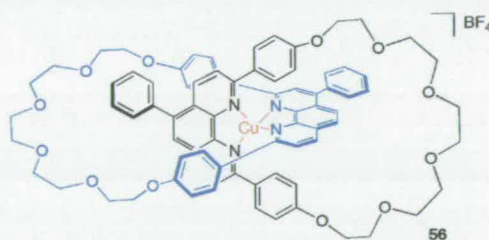
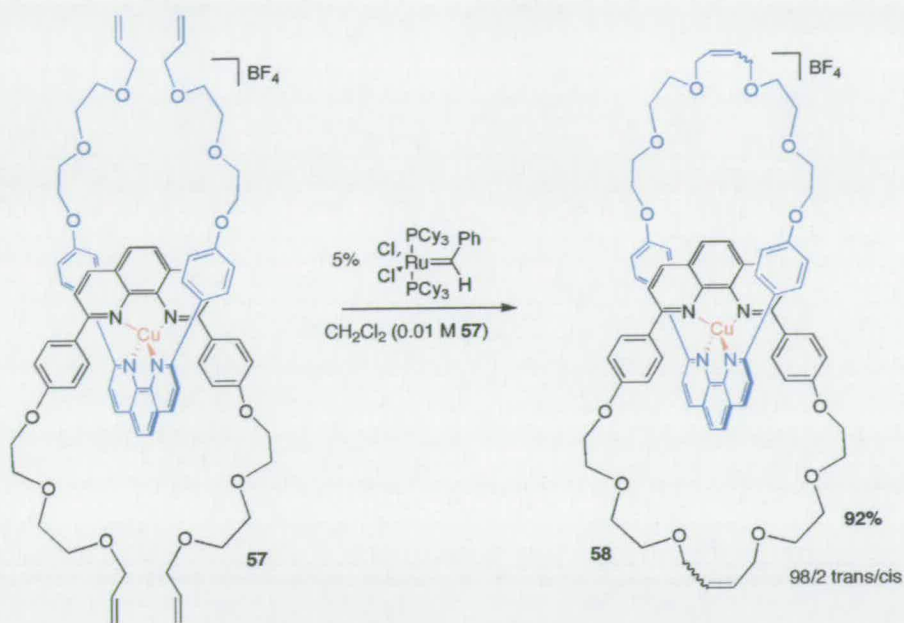


Figure 1.17 A topologically chiral [2]catenane.

Subsequently, the chiral [2]catenane **56** was reported wherein the substitution of a phenyl ring on the phen backbone (Figure 1.17) introduces topological chirality to the molecule (i.e. the chirality is introduced through the mechanical bond rather than a stereocentre present in one of the sub-molecular fragments).^[81]

An important advance from a synthetic perspective was introduced in 1997, when the yield of the key cyclisation step was greatly improved using intramolecular RCM (Scheme 1.13).^[82] It was found that 5 mol % of Grubbs’ 1st generation catalyst cleanly converted tetra-olefin complex **57** into unsaturated [2]catenane **58** in a 92% yield.



Scheme 1.13. Synthesis of a [2]catenane using RCM.

1.2.2.1.2 The Catenand Effect

It was quickly realised that catenands represented a fascinating new class of chelating ligands. They are unique in that the topology of the interlocked ligand is necessarily maintained during any complexation-decomplexation processes as no covalent bonds are cleaved. However, such a process instigates a profound change in the topography of the molecule due to the drastic change in shape it affects. The influence of the mechanical bond on the properties of the ligating species was accordingly termed '*the catenand effect*' and was investigated intensively by Sauvage following his initial discovery. The first of these phenomena to be quantified was its effect on the rate of reaction with potassium cyanide.^[83] It was found that catenane **52** was about ten times more stable than its monocyclic analogue **54** and dissociates several orders of magnitude slower than its bis-acyclic analogue **51**, perhaps as might be expected of such a highly preorganised molecule. Congruent with these results it was found that both reducing ring size and sterically hindering the molecule, further reduced the rate of demetallation.^[84]

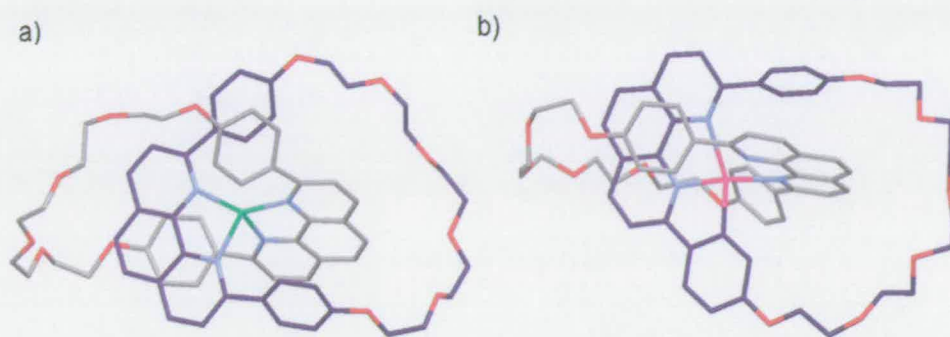
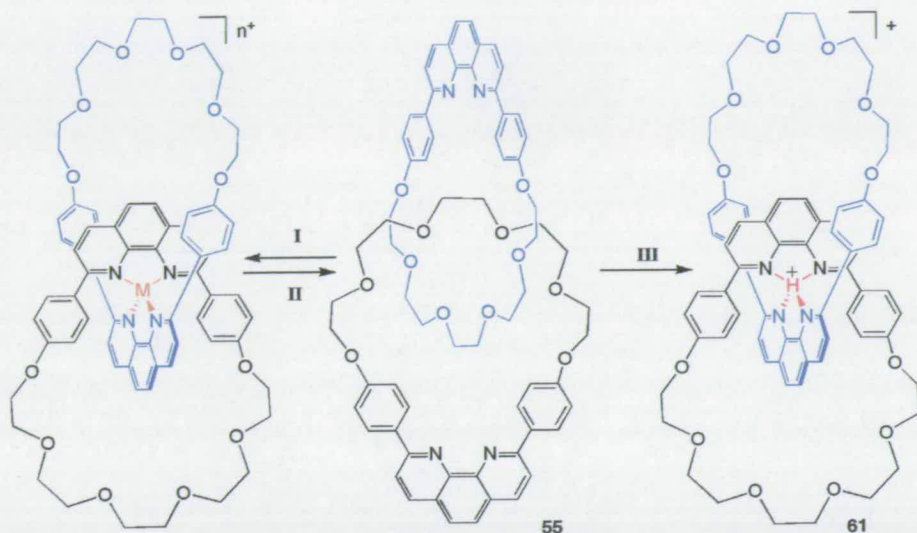
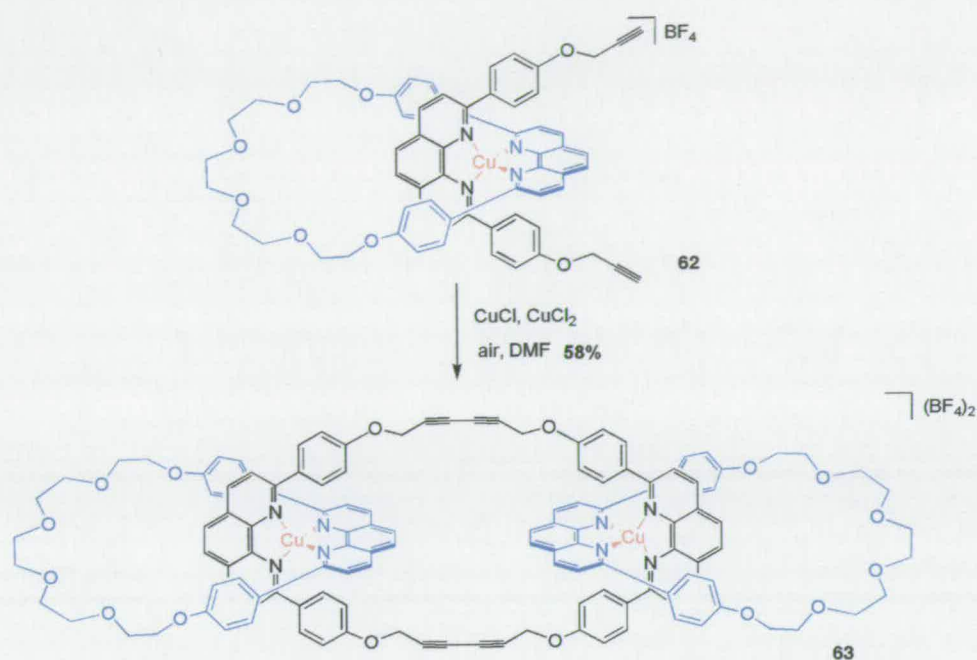


Figure 1.18. X-ray crystal structures of a) Ni(I) [2]catenate **59**, b) Pd(II) [2]catenate **60**.

The influence of the catenand effect on the properties of various encapsulated metals has also been rigorously investigated. A series of metals, (Li(I), Cu(I), Ag(I), Co(II), Ni(II), Zn(II), Pd(II) and Cd(II)) have been coordinated to ligand **55** and the electrochemical,^[85] luminescent^[86] and kinetic^[87] properties of the resulting complexes have been examined. Introduction of a Cu(I) ion was shown to be much slower than with its acyclic analogues, with the catenand complexing as a unimolecular species. The interlocked geometry of the Cu(I) catenate strongly favours a tetrahedral donor arrangement around the TM centre. As such, the complex was shown to highly favour the Cu(I) oxidation state with an existence range of around 2.2 V, although both the Cu(II) and Cu metal species were shown to be stable in solution. The ability of the catenand to stabilise low oxidation states is also observed for other metal complexes. In particular, Co(II) and Fe(II) are so strongly favoured that oxidation of the ligand occurs prior to the TM centre. Ni(I) was introduced to the interlocked ligand system *via* single electron reduction of the divalent species and the air stable Ni(I) complex **59** was characterised in the solid state (Figure 1.18 a).^[88] In an atypical example, addition of Pd(OAc)₂ to **55** resulted in the orthometalation of the catenane, with an N₃C donor set making up a distorted square planar primary coordination sphere in **60** (Figure 1.18 b).^[89] A third interesting feature of the interlocked phen ligands is the enhancement of basicity brought about as a result of the mechanical bond. Protonation of the catenand to form **61** with one equivalent of HClO₄ brought about a topographical, or large amplitude, rearrangement of the molecule which is stabilised not only by binding to the proton but also by the increased π -accepting ability of the phen core, allowing it to stack more effectively with the π -donor benzyl groups of the opposing molecular fragment. Selected key features of the catenand effect are summarised in Scheme 1.14.



Scheme 1.14. Summary of the catenand effect. **I** The rate of complexation of either native Cu(I) ion or other metal ions (Li(I), Cu(I), Ag(I), Co(II), Ni(II), Zn(II), Pd(II) and Cd(II)) by the mechanically linked ligand **55** is significantly reduced. **II** Demetallation is several orders of magnitude slower than for the non-interlocked ligands. **III** Addition of H^+ results in a topographical arrangement similar to the metal bound species with topographical factors increasing the basicity of the catenand by several orders of magnitude.

1.2.2.1.3 Multi-Ring ($n > 2$) Catenates

Scheme 1.15. Synthesis of a [3]catenate using a Glazer coupling reaction.

Following the same basic procedure as for [2]catenates, dicopper [3]catenates were first synthesised in 1985 in very low yields.^[90] A more selective route was described a year later utilising the acetylenic homo-coupling of **62** in the key cyclisation step to form the [3]catenate **63** in a 58% yield (Scheme 1.15).^[91] Solution ¹H NMR and solid state X-ray analysis (Figure 1.19) proved to be in excellent agreement, with the two metallic centres pulled together (Cu-Cu distance *ca.* 8.1 Å) by the rigidity of the four alkyne linkages,^[92] a consequence being a slight perturbation in redox potentials for selected dimetallic complexes relative to the analogous [2]catenate.^[93] In the same reaction, higher order multiring catenates were observed using ESI-MS.^[94]

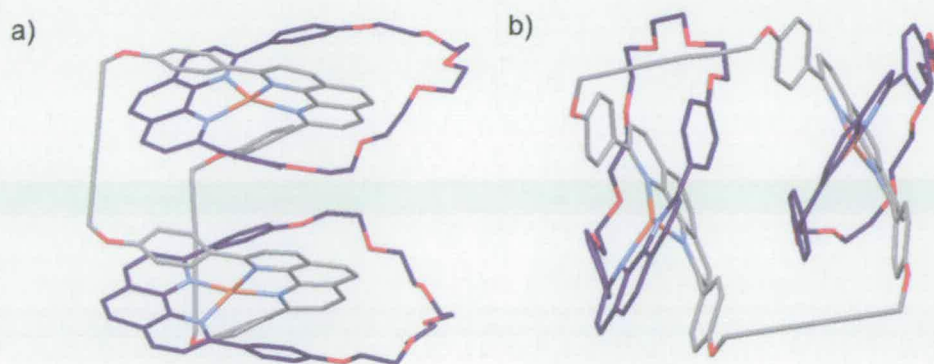
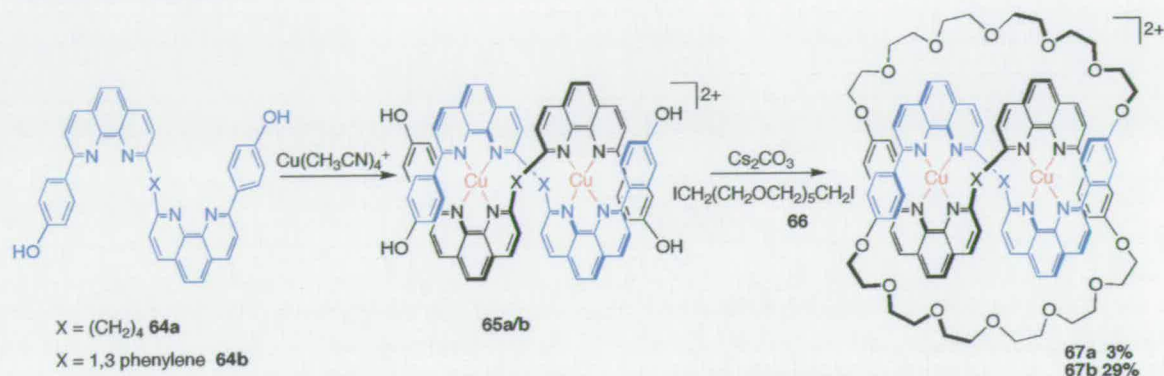


Figure 1.19. a) Side view and b) top view of the X-ray crystal structure of [3]catenate **63**.

1.2.2.1.4 Knots



Scheme 1.16. Synthesis of a trefoil knot.

Following early attempts at their preparation by Schill,^[9] Sauvage reported the first molecular trefoil knot in 1989^[95] with its intertwined topology confirmed irrefutably by X-ray crystallography a year later (Figure 1.20 a).^[96] The initial ligand **64a** used to fashion the knot is shown in Scheme 1.16. The short (CH₂)₄ linker between the two phen units prevents the complexation of the ligand around a single Cu(I) ion, but it was observed that the desired helical complex **65a** was relatively labile and thus able to interconvert with its co-planar analogue. This facile exchange led to a modest 3% yield of **67a** following cyclisation, but this was increased to 29% by replacing the (CH₂)₄ linker with a 1,3-phenylene group (**64b**→**67b**).^[97] Access to knotted compounds was further optimised following the introduction of olefin RCM in the cyclisation step.^[98]

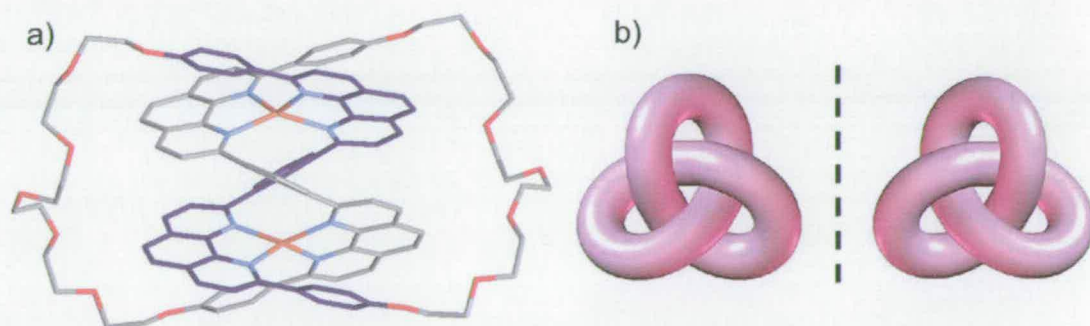
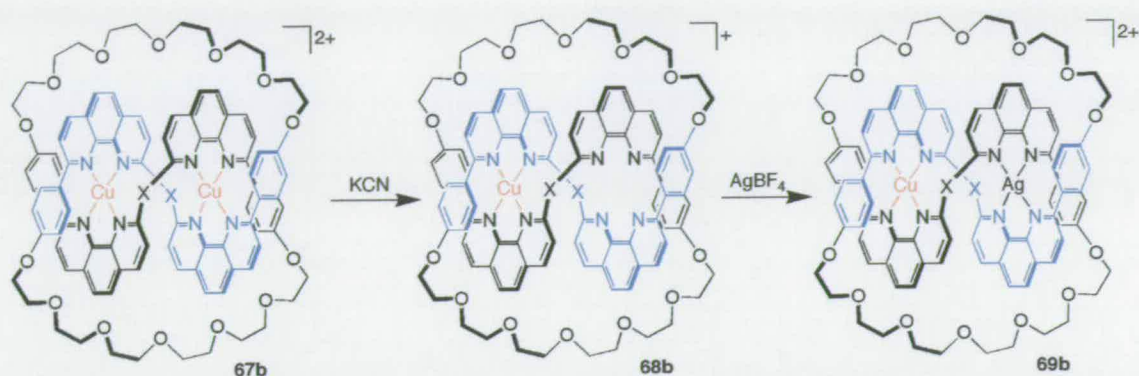


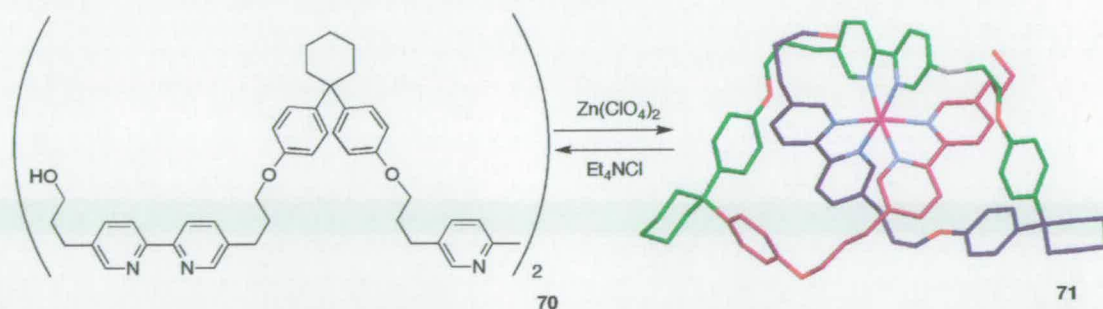
Figure 1.20. a) X-ray crystal structure of knot **67a** assembled around two tetrahedral metal centres. b) Cartoon illustration of the two topological enantiomers of the trefoil knot.



Scheme 1.17. Monodemetalation of a knot followed by generation of a heterodimetallic complex.

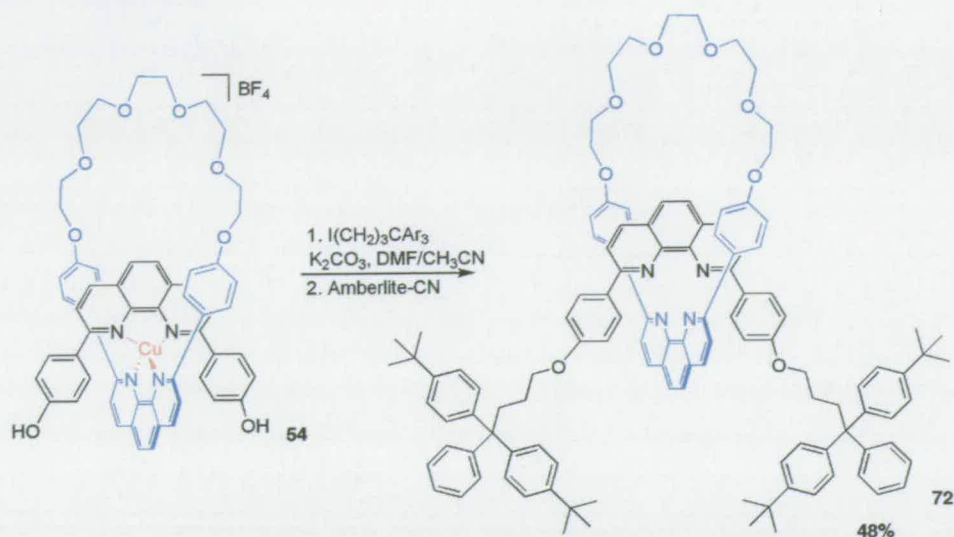
Unlike catenanes, knots are intrinsically chiral molecules. Two enantiomers of a trefoil knot are depicted as cartoons in Figure 1.20 b. In the original synthesis knot **67a/b** was isolated as a mixture of enantiomers, but ingenious methods for separation of the two chiral species were subsequently developed.^[99] Further to this important advance in the synthesis of topologically entangled molecules, more complex composite knots have been described,^[100] and recently the enantioselective synthesis of a knot from a chiral starting material was reported.^[101] As with the [2]catenanes, the effect of the topological links in **67a/b** has been meticulously examined.^[97, 102] In addition, the properties of selected heteronuclear complexes (e.g. mixed copper/silver complex **69b**) accessible due to the relative stability of the monometalated complex **68b** have been described (Scheme 1.17).^[103]

An intriguing example of an open knot complex has been reported by Hunter.^[104] The oligomeric ligand **70** contains three bipy units which all coordinate to a Zn(II) ion in a fashion that entwines the biphenyl units to form open knot complex **71**. Addition of excess Cl^- regenerates the free ligand.



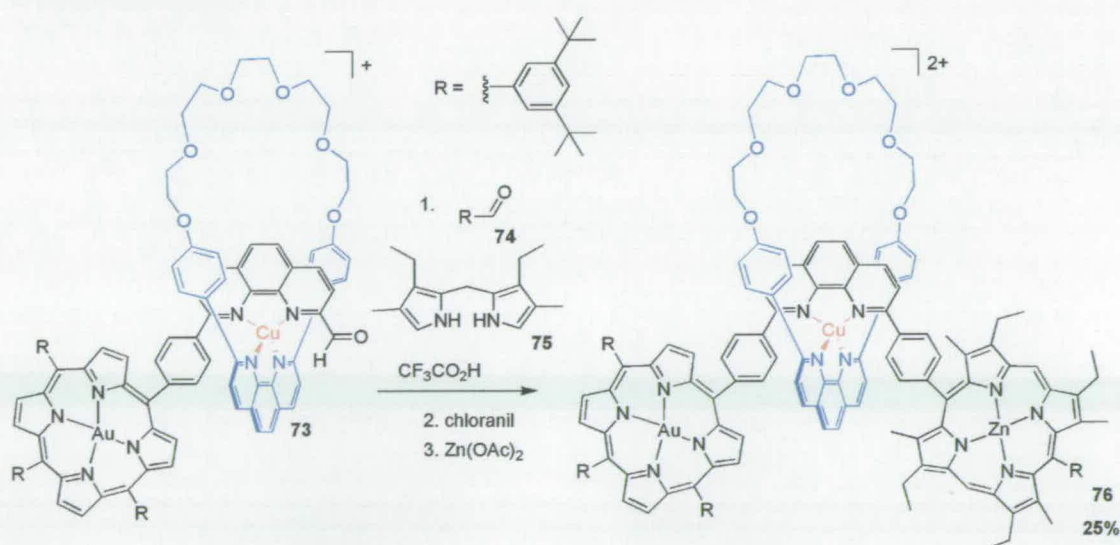
Scheme 1.18. Reversible formation of an open knot complex mediated by counterion exchange.

1.2.2.1.5 Rotaxanes



Scheme 1.19. Gibson's Cu(I)-phen based rotaxane synthesis.

The first rotaxane synthesised using TM-directed methods was reported in 1991 by Gibson.^[105] Rotaxane **72** was prepared *via* bis-alkylation of complex **54** with two bulky end groups that were sufficiently large so as to prevent the dethreading of the species following demetallation (Scheme 1.19). Sauvage followed this in 1992 with his own rotaxane synthesis, the crucial reaction step being the *in situ* formation of a porphyrin ring *via* the condensation reaction of complex **73** with **74** and **75**, furnishing rotaxane **76** in 25% yield (Scheme 1.20).^[106] These mixed Au(III)/Zn(II) porphyrin stoppered rotaxanes were subsequently investigated as vehicles for electron transfer.^[107]



Scheme 1.20. Sauvage's porphyrin rotaxane synthesis.

Multiporphyrinic rotaxanes such as **77** were introduced in 1997 (Figure 1.21) where the macrocycle has an appended electron accepting porphyrin ring (A) and the two stoppering groups of the thread are electron donating (D) units.^[108] In these intricate molecules, it was proven possible to mediate electron transfer through using metal cation coordination.^[109] More recently it was demonstrated that linear porphyrin containing rotaxanes could also be formed *via* amide bond formation.^[110]

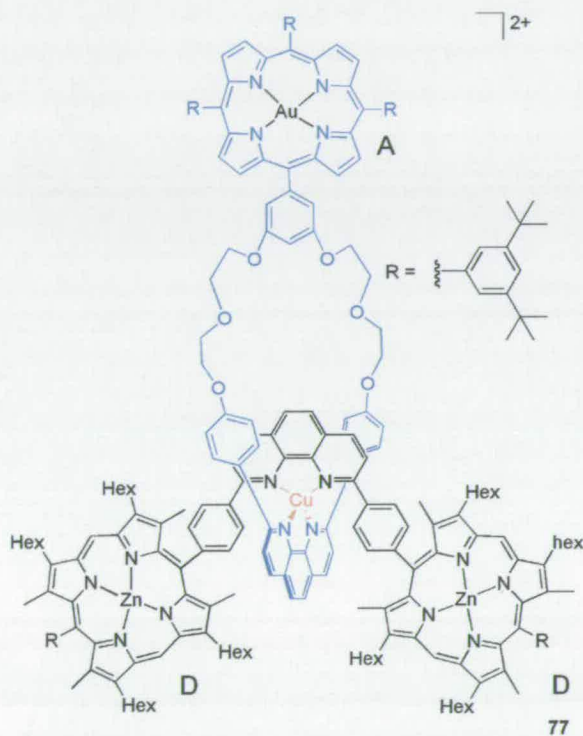


Figure 1.21. A multiporphyrin [2]rotaxane.

Fullerene terminated rotaxane **78** was also realised (Figure 1.22),^[111] and its electrochemistry probed with a view to exploiting the strongly electron accepting nature of the C_{60} group.^[112] The subtle mechanism of photoinduced electron transfer in rotaxane architectures is the subject of a number of reviews.^[113]

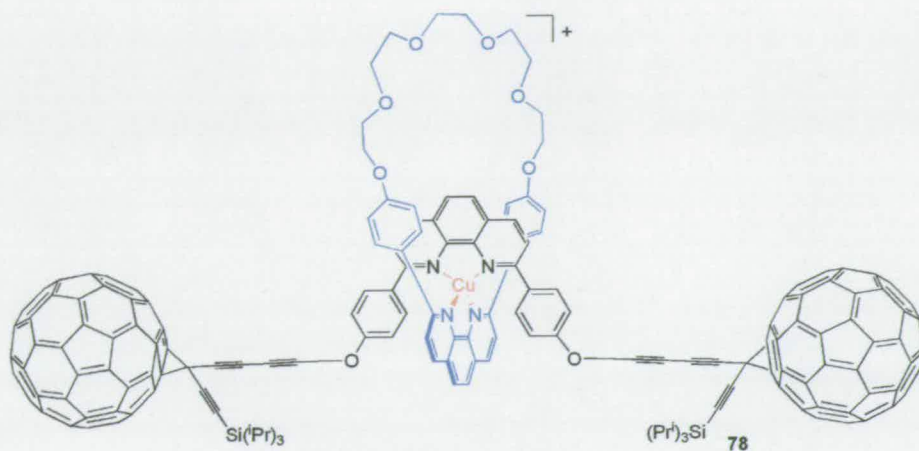


Figure 1.22. A fullerene [2]rotaxane.

Also noteworthy is the compelling work of Swager and co-workers who have utilised the ubiquitous Cu(I)-bis-phen motif to assemble conducting polymetalorotaxanes.^[114] In addition, the synthesis of a rotaxane exciplex – an electronically excited complex of definite stoichiometry, non-bonding in the ground state – has been reported by the same group.^[115]

1.2.2.1.6 Hybrid Systems

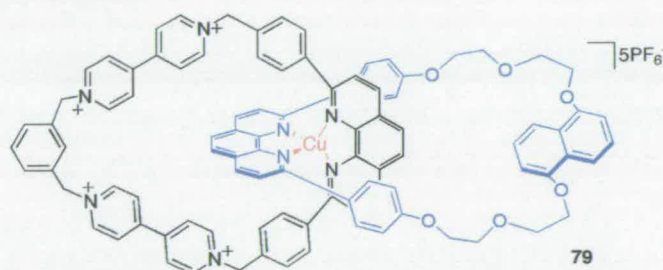


Figure 1.23. Sauvage/Stoddart hybrid [2]catenate.

Several successful collaborations have occurred over the last 10 years between the group of Sauvage and other chemists in the field of interlocked molecules: the products of which can be described as ‘hybrid systems’ or species that contain multiple types of non-covalent intercomponent interactions. Sauvage and Stoddart published the first of these bimodal compounds jointly in 1996. The [2]catenate **79** contains both the supramolecular motifs (Cu(I)-phen and π - π interactions) exploited so successfully by the separate research groups (Figure 1.23).^[116] The co-conformation of the de-metallated molecule can be controlled *via* pH where an

excess of acid orients the molecule so that the phen- H^+ moiety is encapsulated within the centre of the molecule and the addition of base restores it to the π -stacked arrangement. The topography of the molecule can also be controlled using lithium ion coordination, but decomplexation proved unsuccessful.

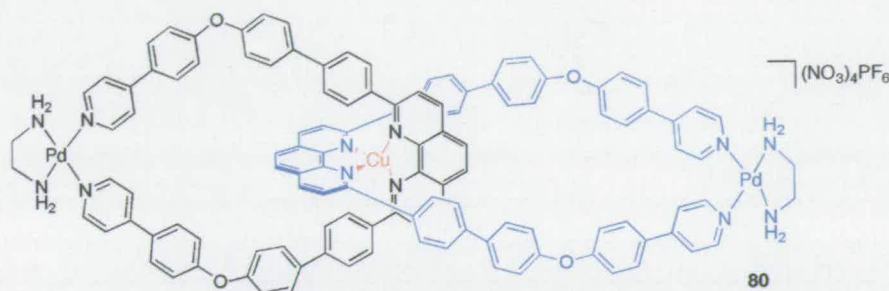
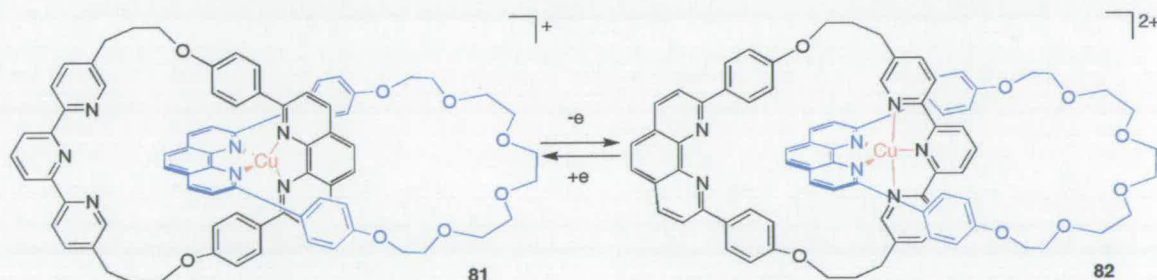


Figure 1.24. Sauvage/Fujita hybrid [2]catenate.

Another union of methodologies is the combination of Fujita's Pd(II)-based self-assembled catenanes with Sauvage's Cu(I)-phen motif. This collaboration led to both doubly interlocked catenanes^[117] and an enlarged [2]catenate **80**, where formation of the Pd(II)-pyridine bond closes the two rings (Figure 1.25).^[118]

1.2.2.1.7 Redox Active Molecular Machine Prototypes



Scheme 1.21. Sauvage's original redox switchable [2]catenate.

An important goal in the field of interlocked molecules is the reversible control of large amplitude molecular motion. In 1994 Sauvage introduced a novel system wherein the topography of the molecule was controlled by a reversible redox process.^[119] In **81** the tetrahedral arrangement of the two phen units is favoured by the Cu(I) ion (Scheme 1.21). On removal of one electron the Cu(II) ion is formed, which has a preference for a higher coordination number. Consequently the terpy

containing ligand undergoes a 'gliding' motion and revolves 180° , allowing the metal to access to the tridentate moiety, forming **82**. The main drawback associated with this elegant, bistable complex is the time that the 4-coordinate divalent complex takes to relax into its thermodynamically stable form (several hours). Accordingly, various improvements were made to the system,^[120] and the current lead rotaxane **83** is shown in Figure 1.25^[121] In this system, the steric restrictions previously imposed on the pirouetting ring are relieved by replacing the 1,10 phen unit in the thread with a 2,2'-bipy unit, allowing the redox mediated rearrangements to take place on the millisecond timescale.

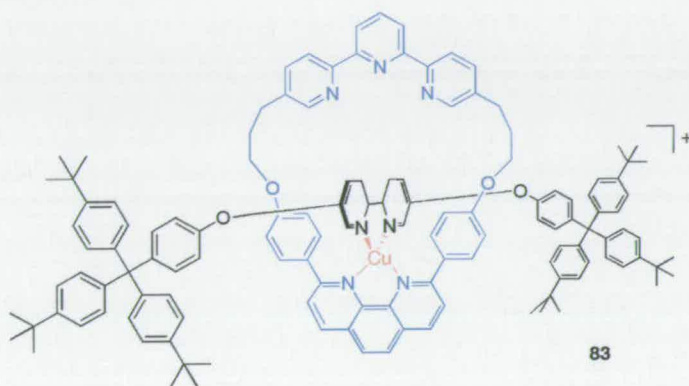
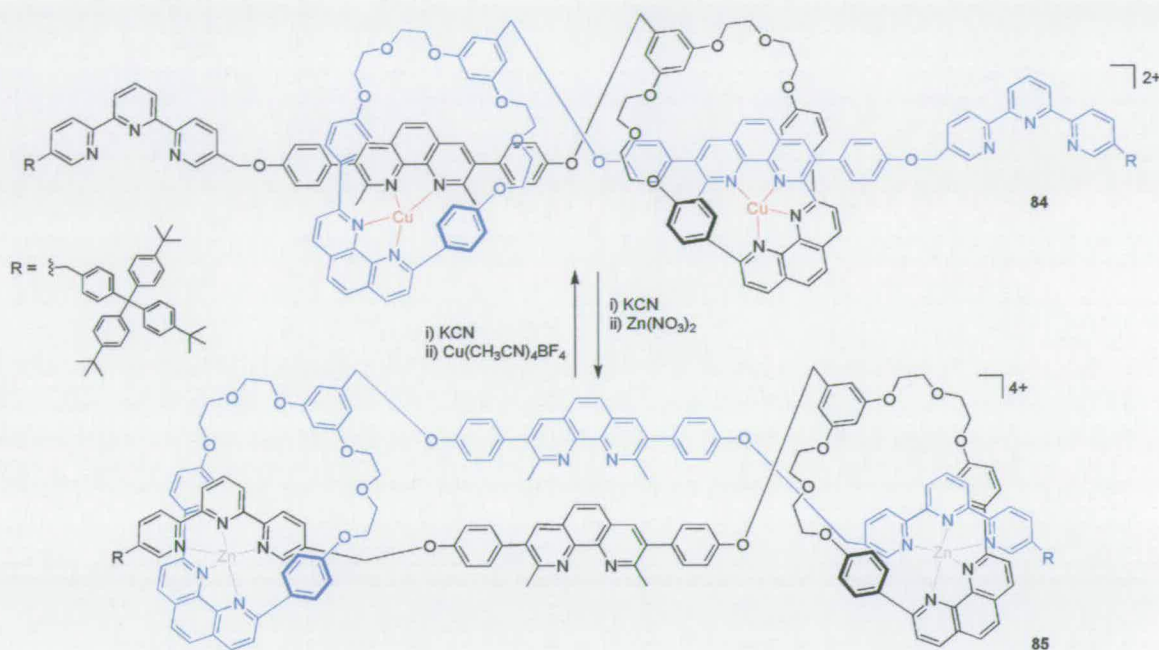


Figure 1.25. A redox controlled [2]rotaxane where addition/removal of $1 e^-$ induces a pirouetting motion in the macrocycle.

The fabrication of the first artificial molecular muscle represents one of the more impressive TM-directed synthetic feats achieved to date.^[122] Although controlled by metal ion coordination rather than redox processes, this symmetrical system functions by the same mechanism as described above. When bound to two Cu(I) ions the dimer is in its extended state **84**. Treatment with KCN followed by excess $Zn(NO_3)_2$ contracts the molecule by about 27%, as a result of the higher coordinative demands of the Zn(II) ion, forming **85**.



Scheme 1.22. Interconversion between extended and contracted forms of a molecular muscle.

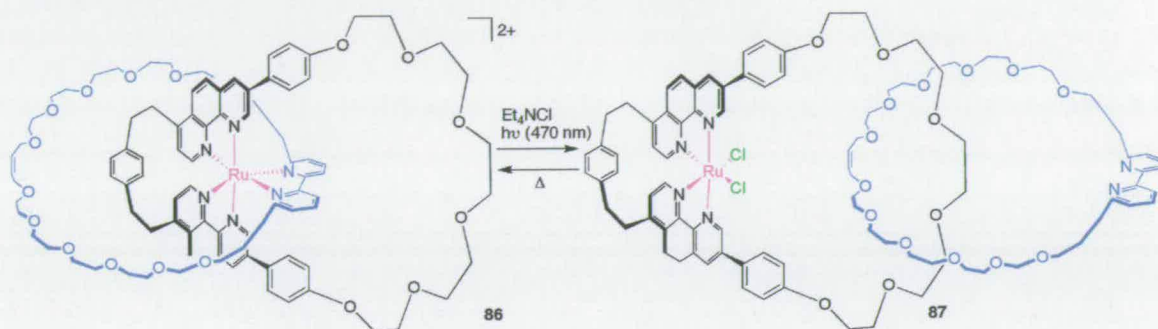
1.2.2.2 6-coordinate TM-Templates

For almost twenty years, the development of mechanically interlocked molecular systems constructed around TM ions has proceeded with Sauvage's original catenate assembly system largely unchanged. Nevertheless, the application of a TM template methodology utilising higher valence transition metals with an alternative geometric preference has obvious appeal and was originally proposed as early as 1973.^[123]

1.2.2.2.1 Rhodium and Ruthenium Directed Synthesis of Interlocked Molecules

The first example of a catenate assembled around an 6-coordinate TM was reported in 1991 when two appropriately substituted terpy ligands were coordinated to a Ru(II) ion and cyclised.^[124] The modest 11% yield of final macrocyclisation and the inert nature of the final ruthenium complex were addressed in a subsequent article in which Fe(II) was used as a more labile template and RCM was employed in the key cyclisation step.^[125] However, in this case, preferential formation of the isomeric 58 membered large macrocycle was observed, leading the authors to recognise the utility of the original Cu-phen approach. Nevertheless, Sauvage and co-workers have recently demonstrated how 6-coordinate ruthenium^[126] and rhodium^[127] ions can be used as templates in the synthesis of catenanes *via* a '4 + 2' strategy.^[128] In the case

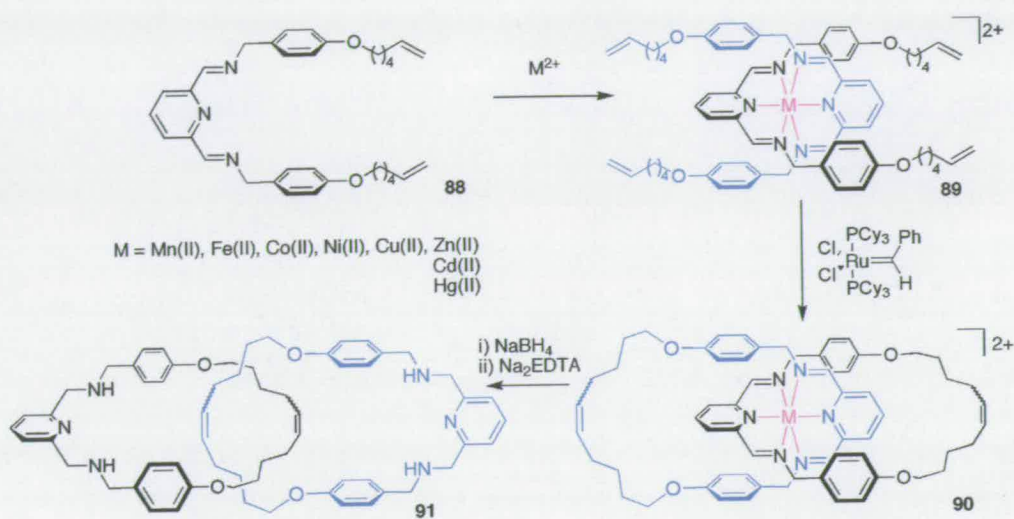
of the former, the well established photochemistry of Ru(II) centres facilitated the development of the first TM-based light driven molecular machine prototype **86** (Scheme 1.23).^[129] Exposure of [2]catenate **86** to light (*ca.* 470 nm) in the presence of Et₄NCl results in the topographical rearrangement to complex **87** with two chloride ions occupying the coordination site vacated by the bidentate macrocycle. Thermal energy is required to initiate the reverse process.



Scheme 1.23. Operation of a light switchable Ru(II) [2]catenate.

1.2.2.2.2 A Simple General Ligand System for the Assembly of Catenates and Rotaxanes

In 2001 Leigh and co-workers reported a general system for the synthesis of catenanes around a range of divalent TM ions.^[130] The ligands used were developed from benzylic amide macrocycles, which are well suited for incorporation into analogous metal chelating systems. The isophthaloyl group ensures a 180° turn that, as well as prearranging potential donor groups in a convergent fashion, also holds the appended aromatic rings parallel at a distance suitable for π -stacking with an orthogonally bound guest. Such an arrangement also favours intracomponent cyclisation of suitably chosen end groups. In order to orthogonally chelate divalent TM ions with an octahedral geometric preference, the isophthaloyl group was replaced by a 2,6-pyridine moiety. Finally, the phenolic esters were replaced with ether bonds for stability reasons and terminal olefins selected as end groups based on previously reported successful RCM reactions.^[131]



Scheme 1.24. Synthesis of [2]catenates around a range of divalent TM ions.

With the critical design features formulated, the Schiff-base ligand **88** was then readily prepared in three steps using standard organic transformations and combined with of $\text{Zn}(\text{ClO}_4)_2(\text{H}_2\text{O})_6$ to furnish the zinc perchlorate complex **89** ($M = \text{Zn(II)}$). Free imines are not normally compatible with ring closing metathesis conditions but, in this case, coordination to the TM ion effectively ‘protects’ the sensitive functionality allowing Grubbs’ 1st generation catalyst to mediate the clean conversion of the tetra-olefin complex to the zinc catenate as a mixture of olefin diastereomers (Scheme 1.24). An extended reaction time of four days allowed the mixture to equilibrate forming the thermodynamically favoured isomer *E,E*- Zn(II) **90** almost exclusively.

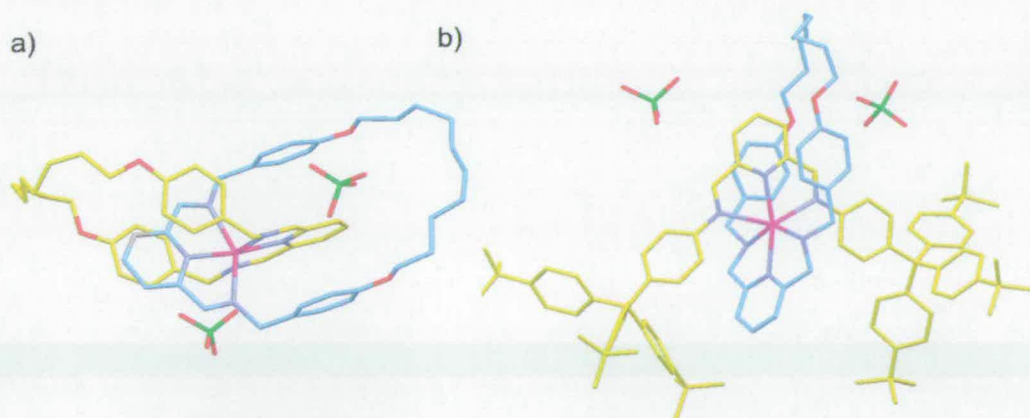
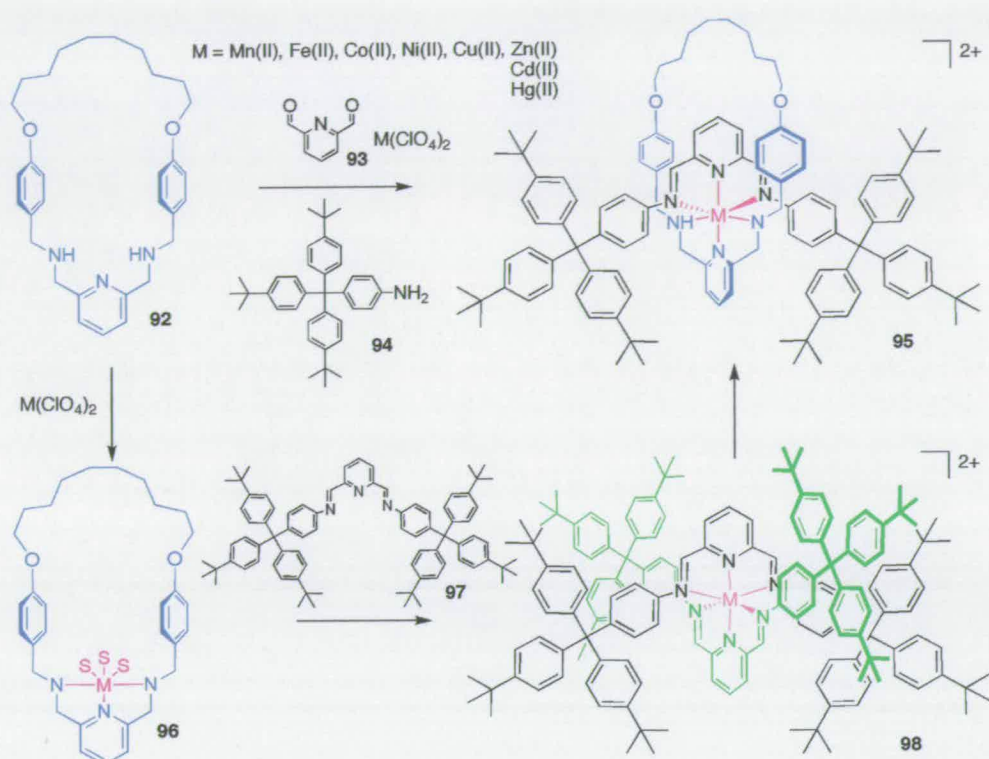


Figure 1.26. X-ray crystal structures of a) the Zn(II) catenate **90**, b) the Zn(II) Rotaxane **95**.

X-ray crystallography confirmed the interlocked structure of the zinc catenate **90** and is in excellent agreement with solution phase analysis (^1H NMR spectroscopy),

showing both the π -stacking of the benzyl aromatic rings with the orthogonally bound pyridine and the stereochemistry of the internal olefins (Figure 1.26 a). The tolerance of this approach was investigated using a range of divalent TM ions with a preferred octahedral geometric preference (Mn(II)-Zn(II)) across the 1st row TMs and Zn(II)-Hg(II) down group 12) and it was discovered that catenane assembly was favoured in each case. The highly preorganised hexadentate ligand system introduces high kinetic stability to the interlocked complex and it was necessary to first reduce the imines using sodium borohydride to allow demetallation with a standard Na₂EDTA chelant to liberate the catenand **91**.

The success of benzylic imine ligand catenate formation prompted investigation into the synthesis of more challenging interlocked molecular architectures. The next logical step was to attempt the synthesis of a [2]rotaxane around a divalent octahedral TM template using a similar ligand system. The challenge of constructing a rotaxane, or indeed any heterocircuit system, around a TM template arises because of the need to simultaneously coordinate two different ligands to the metal centre. In this case the previously employed tetra-imine ligand system is not well suited to forming rotaxanes because thread-thread and macrocycle-macrocycle (catenate) ligand systems can form in competition with the desired thread-metal-macrocycle assembly. Replacement of the bisimine macrocycle with preformed bisamine analogue **92** eliminated the possibility of catenate formation and allowed the researchers to tailor the reaction conditions to favour rotaxane formation under thermodynamic control (Scheme 1.25).^[132]



Scheme 1.25. Synthesis of rotaxanes under thermodynamic control.

Sequential treatment of **92** with $M(\text{ClO}_4)_2(\text{H}_2\text{O})_6$, **93** and **94** resulted in exclusive formation of the desired [2]metallorotaxane **95** (analogous to the [2]catenate assembly, rotaxane formation can be achieved using a range of divalent TM templates). The X-ray crystal structure of the Cd(II)-rotaxane confirmed the spatial arrangement of the two ligands around the metal centre and that the expected π - π interactions between the macrocycle with the pyridyl unit of the thread persist in the solid state (Figure 1.26 b). In order to confirm the rotaxane was the thermodynamic product, the macrocycle complex **96** was treated with two equivalents of the preformed thread **97**. Initially, the *bis*-thread complex **98** was formed due the enhanced ligating ability of imines relative to amines, but after 24 h only the thermodynamically favoured metallo-rotaxane species **95** was observed.

1.2.2.2.3 Getting Harder: The Assembly of Catenates and Rotaxanes Around Cobalt Ions

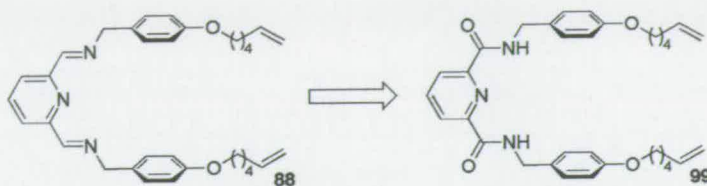
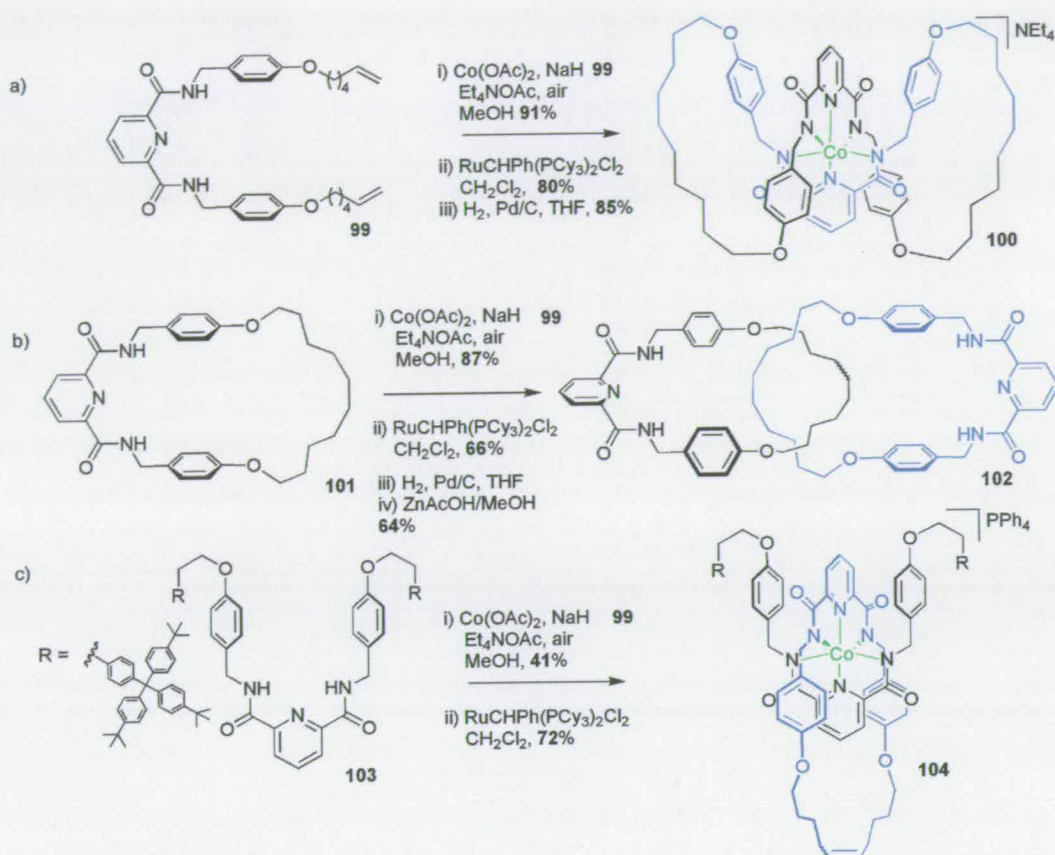


Figure 1.27. Conversion of ligands.

In coordination chemistry, deprotonated carboxamide (carboxamido) ligands are known to be well suited to binding ‘hard’ TM ions such as Fe(III) and Co(III) and have been rigorously examined primarily with a view to mimicking natural processes.^[133] It was thought that replacement of the imines with amides in the ligand described above (**88**→**90**) would – following deprotonation – facilitate binding to trivalent TM ions whilst conserving features previously shown to be essential to promote interlocking, such as intercomponent π -stacking and the preorganised 180° turn that forces the ligands to converge (Figure 1.27).^[134] The initial strategy for catenate synthesis relied on the simultaneous RCM of two alkene terminated macrocycle precursors that were held in a mutually orthogonal alignment by the metal template (Scheme 1.26 a). However, cyclisation of the Co(III) complex using Grubbs’ 1st generation catalyst resulted in the exclusive formation of the covalently linked isomer **100**, as indicated by X-ray crystallography (Figure 1.28 a).



Scheme 1.26. Synthesis of a) tetra-amide macrocycle **100**, b) tetra-amide [2]catenane **102**, c) tetra-amide [2]rotaxane **104**.

Thus the [2]catenane was accessed by an alternative strategy, that is the fabrication of one of the macrocycles (**101**) prior to complexation. Following this protocol (Scheme 1.26 b) it was possible to synthesize the desired [2]catenane (**102**) in reasonable yield as confirmed by X-ray crystallography (Figure 1.28 b). A more quantitative understanding of how a relatively subtle change in chemical structure (from imines to amides) completely changes the product selectivity of the cyclisation reaction from imine catenane *E,E*-**90** to amide macrocycle **100** is currently being pursued. It was also shown to be possible to access [2]rotaxane **104** by replacing macrocycle **101** with thread **103** (Scheme 1.26 c) albeit in modest overall yield due to the low yielding statistical complexation step.

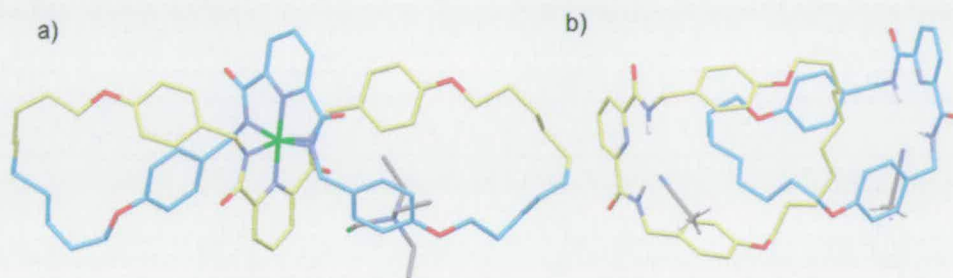
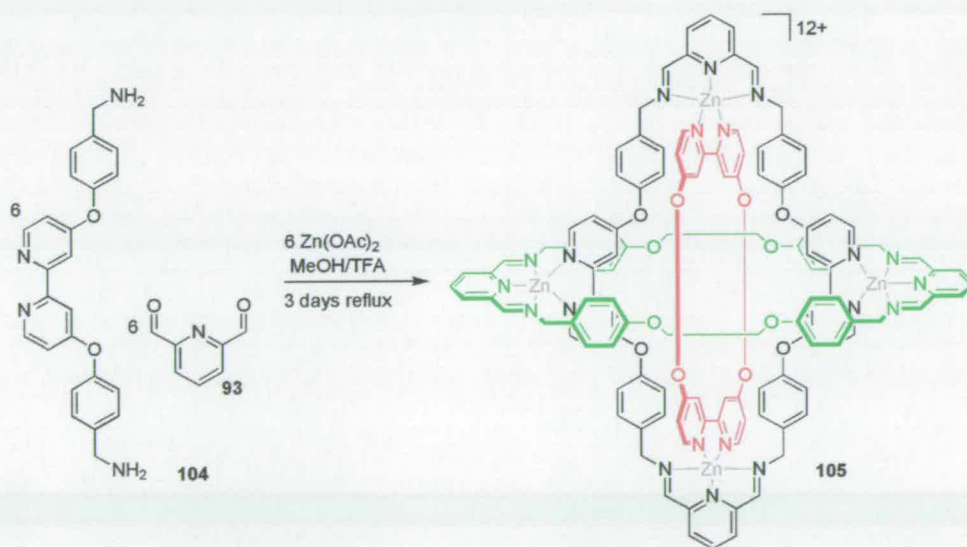


Figure 1.28. X-ray crystal structure of macrocycle **100** and [2]catenane **102**.

1.2.2.3 5-coordinate TM-templates and the Self Assembly of Borromean Rings

To date penta-coordinated TM centres have rarely been used as templates for the assembly of mechanically interlocked architectures.^[135] However, in 2004 Stoddart and co-workers reported the self assembly of Borromean rings from 18 discrete building blocks; arguably one of the most impressive thermodynamically controlled multi-component reactions described to date.^[136] The Borromean symbol has its roots buried in mysticism and was adopted as an insignia by an 18th century Italian family from which it now derives its name.^[137] From a topological viewpoint the connectivity of the three rings is fascinating, as the molecule is locked rather than interlocked and consequently cleavage of any one of the three rings results in complete dissociation of all three fragments.



Scheme 1.27. The 18 component self-assembly of the first [3]Borromean ring.

In this spectacular synthesis, the readily prepared bis-amine ligand **104** was stirred with 2,6-diformylpyridine (**93**) and $\text{Zn}(\text{OAc})_2$ in MeOH/TFA solution at reflux for

three days. By following the reaction with ^1H NMR in CD_3OD it was observed that after two days the major (>90%) product was a single highly symmetrical species that ESI-MS indicated to be the desired Borromean ring complex **105**. This was confirmed on elucidation of the X-ray crystal structure (Figure 1.29), which also illustrated that the various non-covalent forces act convergently in a way that thermodynamically favours the locked multi-ring structure. More specifically, each bipy unit is flanked by a pair of phenolic rings at a distance ideally suited for π -stacking. This complements the six penta-coordinate $\text{Zn}(\text{II})$ ions bound following formation of the imine groups. The reversible nature of the imine bond is crucial in the synthesis as it allows any 'errors' in the synthesis to be corrected allowing the exclusive formation of the thermodynamically privileged Borromean ring. Further studies have shown that the Borromean ring organic ligand is stable in the absence of the $\text{Zn}(\text{II})$ ions following reduction of the imines and that cleavage of any one of the links results in complete dissociation of the two remaining rings.^[138]

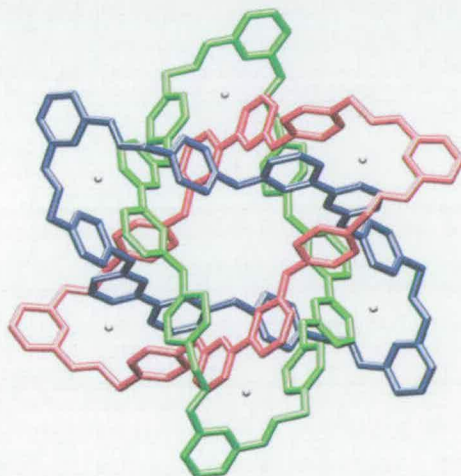


Figure 1.29. X-ray crystal structure of Borromean ring complex **105**.

Prior to Stoddart's discovery Seeman and co-workers achieved the synthesis of Borromean rings using DNA strands.^[139] The step-wise assembly of molecular ring-in-ring compounds has been realised by various groups,^[140] but attempts to complete the Borromean ring structure in this manner have proved unsuccessful to date and it remains a synthetic challenge for contemporary chemists.

1.3 Conclusions and Perspectives

It is without question that TM ions have played a central role in the development of mechanically interlocked molecular architectures. The fact that many of the ‘firsts’ in this area – such as the original template directed [2]catenane, trefoil knot and Borromean ring synthesis – were achieved using a TM-based template is testimony to the utility of this approach. It seems likely that the complexity of these molecules, in terms of function as well as structure, will continue to rapidly advance.

There is now a range of robust methodologies for the synthesis of mechanically interlocked molecules. Most routes rely on a kinetically controlled reaction in the final step, but there are a few that utilise thermodynamically controlled bond formation in the crucial interlocking reaction. The latter is clearly the more facile approach, provided the interlocked species is energetically favoured, and perhaps will become more prominent over the next few years. In all protocols described up until now, the template-directed synthesis of mechanically interlocked molecules has relied on intercomponent interactions to hold the fragments together that ‘live on’ in the interlocked molecule. A system where the template was also the catalyst for the reaction would allow access to a whole new class of interlocked molecules.

Both within the field and in wider circles of the scientific community, researchers are becoming increasingly interested in the potential applications of these uniquely linked molecules. So far, molecular shuttles have been utilised in solid-state electronic devices (perhaps forerunners to efficient molecular level electronic systems) and to initiate macroscopic property changes (such as fluorescence and variation in surface wettability). One particular goal is the assembly of true ‘molecular machines’ that actually perform useful tasks or ‘do work’ at the nanoscopic level. Important steps have been made towards realising such species, but the field of molecular machinery is still in its infancy. The outcome of an increased understanding of the mechanism by which nature’s own motors operate, coupled with the rapid advances in the synthesis and control of mechanically interlocked molecules will be fascinating.

1.4 Thesis Layout

This thesis describes the use of Pd(II) as a template in the synthesis of mechanically interlocked molecular architectures. Chapter two describes the synthesis of a [2]rotaxane using this approach and describes some of the steric and electronic factors that govern its preparation. Chapter three describes the synthesis of a [2]catenane and two of its noninterlocked isomers. Chapter four addresses the unusual binding properties observed for the [2]rotaxane and [2]catenane described in the previous chapters. Chapters five and six describe two novel methods for inducing a half turn in a [2]catenane. The first is achieved through interconvertible coordination modes, the second *via* TM ion exchange in a kinetically controlled system.

Chapters two to five are presented in the form of articles that have already been published in peer-reviewed journals. No attempt has been made to rewrite the work out of context, although the compounds have been renumbered so they are consistent throughout the thesis (*see Appendix 1*). Instead, a brief synopsis has been attached to each chapter to put the research in perspective and to acknowledge gratefully the contributions of my fellow researchers. A consequence of presenting the work in this way is that many of the sad stories involving failed synthetic routes and insoluble macrocycles have been left out. I hope the reader will forgive such omissions as well as the slight repetition that occurs in the introduction and bibliography of each chapter.

1.5 References

- [1] J.-M. Lehn, J. L. Atwood, J. E. D. Davies, D. D. MacNicol, F. Vögtle (Eds), *Comprehensive Supramolecular Chemistry*, Pergamon, Oxford, 1996.
- [2] D. J. Cram, J. M. Cram, *Science* 1974, 183, 803-809; E. P. Kyba, R. C. Helgeson, K. Madan, G. W. Gokel, T. L. Tarnowski, S. S. Moore, D. J. Cram, *J. Am. Chem. Soc.* 1977, 99, 2564-2571; D. J. Cram, J. M. Cram, *Acc. Chem. Res.* 1978, 11, 8-14; D. J. Cram, K. N. Trueblood, *Top. Curr. Chem.* 1981, 98, 43-106; D. J. Cram, *Science* 1983, 219, 1177-1183; D. J. Cram,

- Angew. Chem. Int. Ed. Engl.* **1986**, *25*, 1039-1057; D. J. Cram, *Angew. Chem. Int. Ed. Engl.* **1988**, *27*, 1009-1020.
- [3] J.-M. Lehn, *Science* **1985**, *227*, 849-856; J.-M. Lehn, *Angew. Chem. Int. Ed. Engl.* **1988**, *27*, 89-112; *Supramolecular Chemistry. Concepts and Perspectives* (Ed.: J.-M. Lehn), Wiley-VCH, Weinheim, **1995**.
- [4] C. J. Pedersen, *J. Am. Chem. Soc.* **1967**, *89*, 7017-7036; C. J. Pedersen, *Angew. Chem. Int. Ed. Engl.* **1988**, *27*, 1021-1027.
- [5] D. A. Leigh, M. A. F. Morales, E. M. Pérez, J. K. Y. Wong, C. G. Saiz, A. M. Z. Slawin, A. J. Carmichael, D. M. Haddleton, A. M. Brouwer, W. J. Buma, G. W. H. Wurpel, S. León, F. Zerbetto, *Angew. Chem. Int. Ed.* **2005**, *44*, 3062-3067.
- [6] A. R. Pease, J. O. Jeppesen, J. F. Stoddart, Y. Luo, C. P. Collier, J. R. Heath, *Acc. Chem. Res.* **2001**, *34*, 433-444; A. H. Flood, R. J. A. Ramirez, W. Q. Deng, R. P. Muller, W. A. Goddard, J. F. Stoddart, *Aust. J. Chem.* **2004**, *57*, 301-322; P. M. Mendes, A. H. Flood, J. F. Stoddart, *Appl. Phys. A.* **2005**, *80*, 1197-1209.
- [7] A. H. Flood, J. F. Stoddart, D. W. Steurman, J. R. Heath, *Science* **2004**, *306*, 2055-2056.
- [8] "Synthetic Molecular Machines": E. R. Kay, D. A. Leigh, in *Functional Artificial Receptors* (Eds.: T. Schrader, A. D. Hamilton), Wiley-VCH, Weinheim, **2005**, 333-406.
- [9] G. Schill, *Catenanes, Rotaxanes and Knots*, Academic Press, New York, **1971**.
- [10] D. B. Amabilino, J. F. Stoddart, *Chem. Rev.* **1995**, *95*, 2725-2828; J.-P. Sauvage, C. O. Dietrich-Buchecker (Eds.) *Catenanes, Rotaxanes and Knots*, Wiley-VCH, Weinheim, **1999**; V. Balzani, A. Credi, F. M. Raymo, J. F. Stoddart, *Angew. Chem. Int. Ed.* **2000**, *39*, 3349-3391.
- [11] J. S. Hannam, S. M. Lacy, D. A. Leigh, C. G. Saiz, A. M. Z. Slawin, S. Stitchell, *Angew. Chem. Int. Ed.* **2004**, *43*, 3260-3264.
- [12] E. Wasserman, *J. Am. Chem. Soc.* **1960**, *82*, 4433-4434; H. L. Frisch, E. Wasserman, *J. Am. Chem. Soc.* **1961**, *83*, 3789-3795.
- [13] I. T. Harrison, S. Harrison, *J. Am. Chem. Soc.* **1967**, *89*, 5723-5724; I. T. Harrison, *J. Chem. Soc. Perkin Trans. 1* **1974**, 301-304.
- [14] G. Schill, A. Lüttringhaus, *Angew. Chem. Int. Ed. Engl.* **1964**, *3*, 546-547.

- [15] H. Ogino, *J. Am. Chem. Soc.* **1981**, *103*, 1303-1304.
- [16] A. Harada, J. Li, M. Kamachi, *Nature* **1992**, *356*, 325-327; A. Harada, J. Li, T. Nakamitsu, M. Kamachi, *J. Org. Chem.* **1993**, *58*, 7524-7528; A. Harada, *Coord. Chem. Rev.* **1996**, *148*, 115-133; A. Harada, *Acta Polym.* **1998**, *49*, 3-17; T. Hoshino, M. Miyauchi, Y. Kawaguchi, H. Yamaguchi, A. Harada, *J. Am. Chem. Soc.* **2000**, *122*, 9876-9877; H. Shigekawa, K. Miyake, J. Sumaoka, A. Harada, M. Komiyama, *J. Am. Chem. Soc.* **2000**, *122*, 5411-5412; A. Harada, *Acc. Chem. Res.* **2001**, *34*, 456-464.
- [17] S. Anderson, T. D. W. Claridge, H. L. Anderson, *Angew. Chem. Int. Ed. Engl.* **1997**, *36*, 1310-1313; M. R. Craig, T. D. W. Claridge, M. G. Hutchings, H. L. Anderson, *Chem. Commun.* **1999**, 1537-1538; J. E. H. Buston, J. R. Young, H. L. Anderson, *Chem. Commun.* **2000**, 905-906; C. A. Stanier, M. J. O'Connell, W. Clegg, H. L. Anderson, *Chem. Commun.* **2001**, 493-494; F. Cacialli, J. S. Wilson, J. J. Michels, C. Daniel, C. Silva, R. H. Friend, N. Severin, P. Samori, J. P. Rabe, M. J. O'Connell, P. N. Taylor, H. L. Anderson, *Nature Mater.* **2002**, *1*, 160-164; J. J. Michels, M. J. O'Connell, P. N. Taylor, J. S. Wilson, F. Cacialli, H. L. Anderson, *Chem. Eur. J.* **2003**, *9*, 6167-6176.
- [18] M. R. Craig, M. G. Hutchings, T. D. W. Claridge, H. L. Anderson, *Angew. Chem. Int. Ed.* **2001**, *40*, 1071-1074.
- [19] A. Lüttringhaus, F. Cramer, H. Prinzbach, F. M. Henglein, *Annal. Chem.* **1958**, *613*, 185-198.
- [20] D. Armspach, P. Ashton, C. P. Moore, N. Spencer, J. F. Stoddart, T. J. Wear, D. J. Williams, *Angew. Chem. Int. Ed. Engl.* **1993**, *32*, 854-858.
- [21] B. L. Allwood, N. Spencer, H. Shahriarizavareh, J. F. Stoddart, D. J. Williams, *J. Chem. Soc. Chem. Commun.* **1987**, 1064-1066; B. Odell, M. V. Reddington, A. M. Z. Slawin, N. Spencer, J. F. Stoddart, D. J. Williams, *Angew. Chem. Int. Ed. Engl.* **1988**, *27*, 1547-1550; J. Y. Ortholand, A. M. Z. Slawin, N. Spencer, J. F. Stoddart, D. J. Williams, *Angew. Chem. Int. Ed. Engl.* **1989**, *28*, 1394-1395.
- [22] P. R. Ashton, T. T. Goodnow, A. E. Kaifer, M. V. Reddington, A. M. Z. Slawin, N. Spencer, J. F. Stoddart, C. Vicent, D. J. Williams, *Angew. Chem. Int. Ed. Engl.* **1989**, *28*, 1396-1399.

- [23] D. B. Amabilino, P. R. Ashton, A. S. Reder, N. Spencer, J. F. Stoddart, *Angew. Chem. Int. Ed. Engl.* **1994**, *33*, 433-437.
- [24] D. B. Amabilino, P. R. Ashton, S. E. Boyd, J. Y. Lee, S. Menzer, J. F. Stoddart, D. J. Williams, *Angew. Chem. Int. Ed. Engl.* **1997**, *36*, 2070-2072.
- [25] P. R. Ashton, O. A. Matthews, S. Menzer, F. M. Raymo, N. Spencer, J. F. Stoddart, D. J. Williams, *Liebigs Ann. Recl.* **1997**, 2485-2494.
- [26] P. R. Ashton, M. Grognoz, A. M. Z. Slawin, J. F. Stoddart, D. J. Williams, *Tetrahedron Lett.* **1991**, *32*, 6235-6238; P. L. Anelli, P. R. Ashton, R. Ballardini, V. Balzani, M. Delgado, M. T. Gandolfi, T. T. Goodnow, A. E. Kaifer, D. Philp, M. Pietraszkiewicz, L. Prodi, M. V. Reddington, A. M. Z. Slawin, N. Spencer, J. F. Stoddart, C. Vicent, D. J. Williams, *J. Am. Chem. Soc.* **1992**, *114*, 193-218.
- [27] P. L. Anelli, N. Spencer, J. F. Stoddart, *J. Am. Chem. Soc.* **1991**, *113*, 5131-5133.
- [28] R. A. Bissell, E. Cordova, A. E. Kaifer, J. F. Stoddart, *Nature* **1994**, *369*, 133-137.
- [29] M. C. T. Fyfe, P. T. Glink, S. Menzer, J. F. Stoddart, A. J. P. White, D. J. Williams, *Angew. Chem. Int. Ed. Engl.* **1997**, *36*, 2068-2070.
- [30] Y. Luo, C. P. Collier, J. O. Jeppesen, K. A. Nielsen, E. Delonno, G. Ho, J. Perkins, H.-R. Tseng, T. Yamamoto, J. F. Stoddart, J. R. Heath, *Chemphyschem* **2002**, *3*, 519-525; T. J. Huang, H.-R. Tseng, L. Sha, W. X. Lu, B. Brough, A. H. Flood, B. D. Yu, P. C. Celestre, J. P. Chang, J. F. Stoddart, C. M. Ho, *Nano Letters* **2004**, *4*, 2065-2071; S. S. Kang, S. A. Vignon, H.-R. Tseng, J. F. Stoddart, *Chem. Eur. J.* **2004**, *10*, 2555-2564; D. W. Steuerman, H.-R. Tseng, A. J. Peters, A. H. Flood, J. O. Jeppesen, K. A. Nielsen, J. F. Stoddart, J. R. Heath, *Angew. Chem. Int. Ed.* **2004**, *43*, 6486-6491.
- [31] A. G. Kolchinski, D. H. Busch, N. W. Alcock, *J. Chem. Soc. Chem. Commun.* **1995**, 1289-1291.
- [32] P. R. Ashton, P. T. Glink, J. F. Stoddart, P. A. Tasker, A. J. P. White, D. J. Williams, *Chem. Eur. J.* **1996**, *2*, 729-736.
- [33] S. J. Cantrill, S. J. Rowan, J. F. Stoddart, *Org. Lett.* **1999**, *1*, 1363-1366.

- [34] J. D. Badjic, V. Balzani, A. Credi, S. Silvi, J. F. Stoddart, *Science* **2004**, *303*, 1845-1849; J. D. Badjic, S. J. Cantrill, R. H. Grubbs, E. N. Guidry, R. Orenes, J. F. Stoddart, *Angew. Chem. Int. Ed.* **2004**, *43*, 3273-3278.
- [35] G. M. Hubner, J. Glaser, C. Seel, F. Vögtle, *Angew. Chem. Int. Ed.* **1999**, *38*, 383-386.
- [36] J. A. Wisner, P. D. Beer, M. G. B. Drew, M. R. Sambrook, *J. Am. Chem. Soc.* **2002**, *124*, 12469-12476.
- [37] M. R. Sambrook, P. D. Beer, J. A. Wisner, R. L. Paul, A. R. Cowley, *J. Am. Chem. Soc.* **2004**, *126*, 15364-15365.
- [38] C. A. Hunter, *J. Am. Chem. Soc.* **1992**, *114*, 5303-5311.
- [39] F. Vögtle, S. Meier, R. Hoss, *Angew. Chem. Int. Ed. Engl.* **1992**, *31*, 1619-1622.
- [40] C. A. Schalley, T. Weilandt, J. Bruggemann, F. Vögtle, in *Templates In Chemistry I, Vol. 248*, **2004**, pp. 141-200; O. Lukin, F. Vögtle, *Angew. Chem. Int. Ed.* **2005**, *44*, 1456-1477.
- [41] A. G. Johnston, D. A. Leigh, R. J. Pritchard, M. D. Deegan, *Angew. Chem. Int. Ed. Engl.* **1995**, *34*, 1209-1212.
- [42] A. G. Johnston, D. A. Leigh, L. Nezhat, J. P. Smart, M. D. Deegan, *Angew. Chem. Int. Ed. Engl.* **1995**, *34*, 1212-1216.
- [43] A. G. Johnston, D. A. Leigh, A. Murphy, J. P. Smart, M. D. Deegan, *J. Am. Chem. Soc.* **1996**, *118*, 10662-10663.
- [44] D. A. Leigh, A. Murphy, J. P. Smart, A. M. Z. Slawin, *Angew. Chem. Int. Ed. Engl.* **1997**, *36*, 728-732.
- [45] F. G. Gatti, D. A. Leigh, S. A. Nepogodiev, A. M. Z. Slawin, S. J. Teat, J. K. Y. Wong, *J. Am. Chem. Soc.* **2001**, *123*, 5983-5989.
- [46] M. S. Deleuze, D. A. Leigh, F. Zerbetto, *J. Am. Chem. Soc.* **1999**, *121*, 2364-2379; V. Bermudez, N. Capron, T. Gase, F. G. Gatti, F. Kajzar, D. A. Leigh, F. Zerbetto, S. W. Zhang, *Nature* **2000**, *406*, 608-611; D. A. Leigh, A. Troisi, F. Zerbetto, *Angew. Chem. Int. Ed.* **2000**, *39*, 350-353; F. G. Gatti, S. Leon, J. K. Y. Wong, G. Bottari, A. Altieri, M. A. F. Morales, S. J. Teat, C. Frochot, D. A. Leigh, A. M. Brouwer, F. Zerbetto, *Proc. Natl. Acad. Sci. U.S.A* **2003**, *100*, 10-14.
- [47] C. M. Keaveney, D. A. Leigh, *Angew. Chem. Int. Ed.* **2004**, *43*, 1222-1224.

- [48] A. M. Brouwer, C. Frochot, F. G. Gatti, D. A. Leigh, L. Mottier, F. Paolucci, S. Roffia, G. W. H. Wurpel, *Science* **2001**, *291*, 2124-2128; A. Altieri, F. G. Gatti, E. R. Kay, D. A. Leigh, D. Martel, F. Paolucci, A. M. Z. Slawin, J. K. Y. Wong, *J. Am. Chem. Soc.* **2003**, *125*, 8644-8654.
- [49] E. M. Pérez, D. T. F. Dryden, D. A. Leigh, G. Teobaldi, F. Zerbetto, *J. Am. Chem. Soc.* **2004**, *126*, 12210-12211.
- [50] D. A. Leigh, E. M. Pérez, *Chem. Commun.* **2004**, 2262-2263.
- [51] D. A. Leigh, J. K. Y. Wong, F. Dehez, F. Zerbetto, *Nature* **2003**, *424*, 174-179; J. V. Hernández, E. R. Kay, D. A. Leigh, *Science* **2004**, *306*, 1532-1537.
- [52] M. Fujita, K. Ogura, *Coord. Chem. Rev.* **1996**, *148*, 249-264; M. Fujita, *Acc. Chem. Res.* **1999**, *32*, 53-61; M. Fujita, *Chem. Soc. Rev.* **1998**, *27*, 417-425.
- [53] M. Fujita, F. Ibukuro, H. Hagihara, K. Ogura, *Nature* **1994**, *367*, 720-723.
- [54] M. Fujita, F. Ibukuro, K. Yamaguchi, K. Ogura, *J. Am. Chem. Soc.* **1995**, *117*, 4175-4176.
- [55] M. Fujita, M. Aoyagi, F. Ibukuro, K. Ogura, K. Yamaguchi, *J. Am. Chem. Soc.* **1998**, *120*, 611-612.
- [56] A. Hori, T. Sawada, K. Yamashita, M. Fujita, *Angew. Chem. Int. Ed.* **2005**, *44*, 4896-4899.
- [57] K. Kim, *Chem. Soc. Rev.* **2002**, *31*, 96-107.
- [58] K. M. Park, S. Y. Kim, J. Heo, D. Whang, S. Sakamoto, K. Yamaguchi, K. Kim, *J. Am. Chem. Soc.* **2002**, *124*, 2140-2147.
- [59] T. J. Burchell, D. J. Eisler, R. J. Puddephatt, *Dalton Trans.* **2005**, 268-272.
- [60] D. Michael, P. Mingos, J. Yau, S. Menzer, D. J. Williams, *Angew. Chem. Int. Ed. Engl.* **1995**, *34*, 1894-1895.
- [61] C. P. McArdle, M. C. Jennings, J. J. Vittal, R. J. Puddephatt, *Chem. Eur. J.* **2001**, *7*, 3572-3583.
- [62] C. P. McArdle, M. J. Irwin, M. C. Jennings, R. J. Puddephatt, *Angew. Chem. Int. Ed.* **1999**, *38*, 3376-3378.
- [63] C. P. McArdle, J. J. Vittal, R. J. Puddephatt, *Angew. Chem. Int. Ed.* **2000**, *39*, 3819-3822.
- [64] C. P. McArdle, S. Van, M. C. Jennings, R. J. Puddephatt, *J. Am. Chem. Soc.* **2002**, *124*, 3959-3965.
- [65] M. E. Padilla-Tosta, O. D. Fox, M. G. B. Drew, P. D. Beer, *Angew. Chem. Int. Ed.* **2001**, *40*, 4235-4239.

- [66] W. W. H. Wong, J. Cookson, E. A. L. Evans, E. J. L. McInnes, J. Wolowska, J. P. Maher, P. Bishop, P. D. Beer, *Chem. Commun.* **2005**, 2214-2216.
- [67] C. Piguet, G. Bernardinelli, A. F. Williams, B. Bocquet, *Angew. Chem. Int. Ed. Engl.* **1995**, *34*, 582-584.
- [68] A. C. Try, M. M. Harding, D. G. Hamilton, J. K. M. Sanders, *Chem. Commun.* **1998**, 723-724.
- [69] R. S. Wylie, D. H. Macartney, *J. Am. Chem. Soc.* **1992**, *114*, 3136-3138.
- [70] D. J. Cardenas, J.-P. Sauvage, *Inorg. Chem.* **1997**, *36*, 2777-2783; D. J. Cardenas, P. Gavina, J.-P. Sauvage, *J. Am. Chem. Soc.* **1997**, *119*, 2656-2664.
- [71] K. S. Jeong, J. S. Choi, S. Y. Chang, H. Y. Chang, *Angew. Chem. Int. Ed.* **2000**, *39*, 1692-1695; S. Y. Chang, J. S. Choi, K. S. Jeong, *Chem. Eur. J.* **2001**, *7*, 2687-2697; S. Y. Chang, H. Y. Jang, K. S. Jeong, *Chem. Eur. J.* **2003**, *9*, 1535-1541; S. Y. Chang, K. S. Jeong, *J. Org. Chem.* **2003**, *68*, 4014-4019; K. S. Jeong, K. J. Chang, Y. J. An, *Chem. Commun.* **2003**, 1450-1451.
- [72] G. J. M. Gruter, F. J. J. Dekanter, P. R. Markies, T. Nomoto, O. S. Akkerman, F. Bickelhaupt, *J. Am. Chem. Soc.* **1993**, *115*, 12179-12180.
- [73] S. J. Loeb, J. A. Wisner, *Angew. Chem. Int. Ed.* **1998**, *37*, 2838-2840.
- [74] S. J. Loeb, *Chem. Commun.* **2005**, 1511-1518.
- [75] G. J. E. Davidson, S. J. Loeb, N. A. Parekh, J. A. Wisner, *J. Chem. Soc., Dalton Trans.* **2001**, 3135-3136.
- [76] G. J. E. Davidson, S. J. Loeb, *Angew. Chem. Int. Ed.* **2003**, *42*, 74-77.
- [77] D. J. Hoffart, S. J. Loeb, *Angew. Chem. Int. Ed.* **2005**, *44*, 901-904.
- [78] J.-P. Sauvage, *Acc. Chem. Res.* **1990**, *23*, 319-327; J.-P. Sauvage, *Acc. Chem. Res.* **1998**, *31*, 611-619; J.-P. Collin, C. Dietrich-Buchecker, P. Gavina, M. C. Jiménez-Moleró, J.-P. Sauvage, *Acc. Chem. Res.* **2001**, *34*, 477-487.
- [79] C. O. Dietrich-Buchecker, J.-P. Sauvage, J. P. Kintzinger, *Tetrahedron Lett.* **1983**, *24*, 5095-5098; C. O. Dietrich-Buchecker, J.-P. Sauvage, J.-M. Kern, *J. Am. Chem. Soc.* **1984**, *106*, 3043-3045. In these seminal papers the term 'catenate' and 'catenand' were defined. Derived from the original descriptors for 'cryptate' and 'cryptand', a catenate describes a catenane assembled around a TM ion that still contains its native template. A catenand describes a catenane assembled around a TM ion that no longer contains the template. The same nomenclature has been applied recently to 'Borromates' and 'Borromands'.

- [80] M. Cesario, C. O. Dietrich-Buchecker, J. Guilhem, C. Pascard, J.-P. Sauvage, *J. Chem. Soc., Chem. Commun.* **1985**, 244-247.
- [81] D. K. Mitchell, J.-P. Sauvage, *Angew. Chem. Int. Ed. Engl.* **1988**, *27*, 930-931.
- [82] B. Mohr, M. Weck, J.-P. Sauvage, R. H. Grubbs, *Angew. Chem. Int. Ed. Engl.* **1997**, *36*, 1308-1310; M. Weck, B. Mohr, J.-P. Sauvage, R. H. Grubbs, *J. Org. Chem.* **1999**, *64*, 5463-5471.
- [83] A. M. Albrechtgary, Z. Saad, C. O. Dietrich-Buchecker, J.-P. Sauvage, *J. Am. Chem. Soc.* **1985**, *107*, 3205-3209.
- [84] A. M. Albrechtgary, C. Dietrich-Buchecker, Z. Saad, J.-P. Sauvage, J. Weiss, *J. Chem. Soc., Chem. Commun.* **1986**, 1325-1327.
- [85] C. Dietrich-Buchecker, J.-P. Sauvage, J.-M. Kern, *J. Am. Chem. Soc.* **1989**, *111*, 7791-7800.
- [86] N. Armaroli, L. Decola, V. Balzani, J.-P. Sauvage, C. O. Dietrich-Buchecker, J.-M. Kern, A. Bailal, *J. Chem. Soc., Dalton Trans.* **1993**, 3241-3247.
- [87] A. M. Albrechtgary, C. O. Dietrich-Buchecker, Z. Saad, J.-P. Sauvage, *J. Am. Chem. Soc.* **1988**, *110*, 1467-1472.
- [88] C. O. Dietrich-Buchecker, J.-M. Kern, J.-P. Sauvage, *J. Chem. Soc., Chem. Commun.* **1985**, 760-762.
- [89] A. J. Blake, C. O. Dietrich-Buchecker, T. I. Hyde, J.-P. Sauvage, M. Schroder, *J. Chem. Soc., Chem. Commun.* **1989**, 1663-1665.
- [90] J.-P. Sauvage, J. Weiss, *J. Am. Chem. Soc.* **1985**, *107*, 6108-6110.
- [91] C. O. Dietrich-Buchecker, A. Khemiss, J.-P. Sauvage, *J. Chem. Soc., Chem. Commun.* **1986**, 1376-1378.
- [92] C. O. Dietrich-Buchecker, J. Guilhem, A. K. Khemiss, J. P. Kintzinger, C. Pascard, J.-P. Sauvage, *Angew. Chem. Int. Ed. Engl.* **1987**, *26*, 661-664.
- [93] C. O. Dietrich-Buchecker, C. Hemmert, A. K. Khemiss, J.-P. Sauvage, *J. Am. Chem. Soc.* **1990**, *112*, 8002-8008.
- [94] F. Bitsch, C. O. Dietrich-Buchecker, A. K. Khemiss, J.-P. Sauvage, A. Vandorsselaer, *J. Am. Chem. Soc.* **1991**, *113*, 4023-4025.
- [95] C. O. Dietrich-Buchecker, J.-P. Sauvage, *Angew. Chem. Int. Ed. Engl.* **1989**, *28*, 189-192.
- [96] C. O. Dietrich-Buchecker, J. Guilhem, C. Pascard, J.-P. Sauvage, *Angew. Chem. Int. Ed. Engl.* **1990**, *29*, 1154-1156.

- [97] C. O. Dietrich-Buchecker, J. F. Nierengarten, J.-P. Sauvage, N. Armaroli, V. Balzani, L. Decola, *J. Am. Chem. Soc.* **1993**, *115*, 11237-11244.
- [98] C. Dietrich-Buchecker, G. N. Rapenne, J.-P. Sauvage, *Chem. Commun.* **1997**, 2053-2054.
- [99] G. Rapenne, C. Dietrich-Buchecker, J.-P. Sauvage, *J. Am. Chem. Soc.* **1996**, *118*, 10932-10933.
- [100] R. F. Carina, C. Dietrich-Buchecker, J.-P. Sauvage, *J. Am. Chem. Soc.* **1996**, *118*, 9110-9116.
- [101] L. E. Perret-Aebi, A. von Zelewsky, C. D. Dietrich-Buchecker, J.-P. Sauvage, *Angew. Chem. Int. Ed.* **2004**, *43*, 4482-4485.
- [102] M. Meyer, A. M. Albrecht-Gary, C. O. Dietrich-Buchecker, J.-P. Sauvage, *J. Am. Chem. Soc.* **1997**, *119*, 4599-4607; C. Dietrich-Buchecker, N. G. Hwang, J.-P. Sauvage, *New J. Chem.* **1999**, *23*, 911-914.
- [103] C. O. Dietrich-Buchecker, J.-P. Sauvage, N. Armaroli, P. Ceroni, V. Balzani, *Angew. Chem. Int. Ed. Engl.* **1996**, *35*, 1119-1121.
- [104] H. Adams, E. Ashworth, G. A. Breault, J. Guo, C. A. Hunter, P. C. Mayers, *Nature* **2001**, *411*, 763-763.
- [105] C. Wu, P. R. Lecavalier, Y. X. Shen, H. W. Gibson, *Chem. Mater.* **1991**, *3*, 569-572.
- [106] J. C. Chambron, V. Heitz, J.-P. Sauvage, *J. Chem. Soc., Chem. Commun.* **1992**, 1131-1133.
- [107] J. C. Chambron, A. Harriman, V. Heitz, J.-P. Sauvage, *J. Am. Chem. Soc.* **1993**, *115*, 6109-6114; J. C. Chambron, V. Heitz, J.-P. Sauvage, *J. Am. Chem. Soc.* **1993**, *115*, 12378-12384; J. C. Chambron, S. Chardonnoibat, A. Harriman, V. Heitz, J.-P. Sauvage, *Pure Appl. Chem.* **1993**, *65*, 2343-2349; J. C. Chambron, A. Harriman, V. Heitz, J.-P. Sauvage, *J. Am. Chem. Soc.* **1993**, *115*, 7419-7425.
- [108] M. Linke, J.-C. Chambron, V. Heitz, J.-P. Sauvage, *J. Am. Chem. Soc.* **1997**, *119*, 11329-11330.
- [109] M. Andersson, M. Linke, J. C. Chambron, J. Davidsson, V. Heitz, L. Hammarstrom, J.-P. Sauvage, *J. Am. Chem. Soc.* **2002**, *124*, 4347-4362.
- [110] M. J. Blanco, J. C. Chambron, V. Heitz, J.-P. Sauvage, *Org. Lett.* **2000**, *2*, 3051-3054.

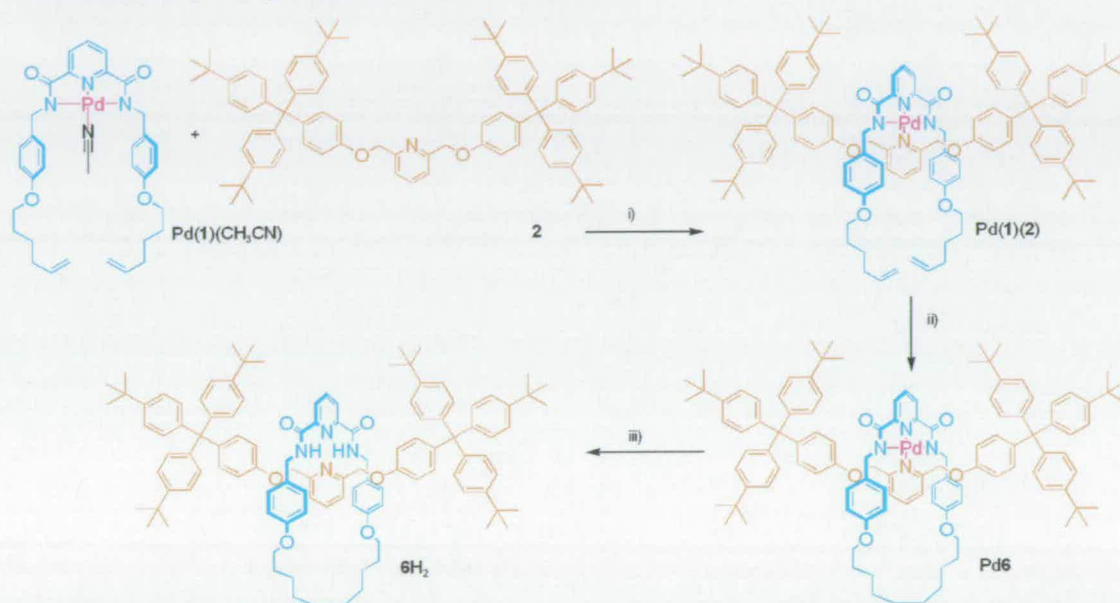
- [111] F. Diederich, C. Dietrich-Buchecker, J. F. Nierengarten, J.-P. Sauvage, *J. Chem. Soc., Chem. Commun.* **1995**, 781-782.
- [112] N. Armaroli, F. Diederich, C. O. Dietrich-Buchecker, L. Flamigni, G. Marconi, J. F. Nierengarten, J.-P. Sauvage, *Chem. Eur. J.* **1998**, *4*, 406-416.
- [113] J. C. Chambron, J.-P. Sauvage, *Chem. Eur. J.* **1998**, *4*, 1362-1366; J. C. Chambron, J.-P. Collin, J. O. Dalbavie, C. O. Dietrich-Buchecker, V. Heitz, F. Odobel, N. Solladie, J.-P. Sauvage, *Coord. Chem. Rev.* **1998**, *180*, 1299-1312; M.-J. Blanco, M. C. Jimenez, J.-C. Chambron, V. Heitz, M. Linke, J.-P. Sauvage, *Chem. Soc. Rev.* **1999**, *28*, 293-305.
- [114] S. S. Zhu, P. J. Carroll, T. M. Swager, *J. Am. Chem. Soc.* **1996**, *118*, 8713-8714; P. H. Kwan, M. J. MacLachlan, T. M. Swager, *J. Am. Chem. Soc.* **2004**, *126*, 8638-8639; B. J. Holliday, T. M. Swager, *Chem. Commun.* **2005**, 23-36; P. H. Kwan, T. M. Swager, *J. Am. Chem. Soc.* **2005**, *127*, 5902-5909.
- [115] M. J. MacLachlan, A. Rose, T. M. Swager, *J. Am. Chem. Soc.* **2001**, *123*, 9180-9181.
- [116] D. B. Amabilino, C. O. Dietrich-Buchecker, A. Livoreil, L. Perez-Garcia, J.-P. Sauvage, J. F. Stoddart, *J. Am. Chem. Soc.* **1996**, *118*, 3905-3913.
- [117] F. Ibukuro, M. Fujita, K. Yamaguchi, J.-P. Sauvage, *J. Am. Chem. Soc.* **1999**, *121*, 11014-11015.
- [118] C. Dietrich-Buchecker, B. Colasson, M. Fujita, A. Hori, N. Geum, S. Sakamoto, K. Yamaguchi, J.-P. Sauvage, *J. Am. Chem. Soc.* **2003**, *125*, 5717-5725.
- [119] A. Livoreil, C. O. Dietrich-Buchecker, J.-P. Sauvage, *J. Am. Chem. Soc.* **1994**, *116*, 9399-9400.
- [120] D. J. Cardenas, A. Livoreil, J.-P. Sauvage, *J. Am. Chem. Soc.* **1996**, *118*, 11980-11981; A. Livoreil, J.-P. Sauvage, N. Armaroli, V. Balzani, L. Flamigni, B. Ventura, *J. Am. Chem. Soc.* **1997**, *119*, 12114-12124; P. Gavina, J.-P. Sauvage, *Tetrahedron Lett.* **1997**, *38*, 3521-3524; N. Armaroli, V. Balzani, J.-P. Collin, P. Gaviña, J.-P. Sauvage, B. Ventura, *J. Am. Chem. Soc.* **1999**, *121*, 4397-4408.
- [121] I. Poleschak, J.-M. Kern, J.-P. Sauvage, *Chem. Commun.* **2004**, 474-476.
- [122] M. C. Jimenez, C. Dietrich-Buchecker, J.-P. Sauvage, *Angew. Chem. Int. Ed.* **2000**, *39*, 3284-3287.

- [123] V. I. Sokolov, *Uspekhi Khimii* **1973**, *42*, 1037-1059; *Russ. Chem. Rev. (Eng. Transl.)* **1973**, *42*, 452-463.
- [124] J.-P. Sauvage, M. Ward, *Inorg. Chem.* **1991**, *30*, 3869-3874.
- [125] N. Belfrekh, C. Dietrich-Buchecker, J.-P. Sauvage, *Inorg. Chem.* **2000**, *39*, 5169-5172.
- [126] F. Arico, P. Mobian, J.-M. Kern, J.-P. Sauvage, *Org. Lett.* **2003**, *5*, 1887-1890; P. Mobian, J.-M. Kern, J.-P. Sauvage, *J. Am. Chem. Soc.* **2003**, *125*, 2016-2017.
- [127] P. Mobian, J.-M. Kern, J.-P. Sauvage, *Inorg. Chem.* **2003**, *42*, 8633-8637.
- [128] J. C. Chambron, J.-P. Collin, V. Heitz, D. Jouvenot, J.-M. Kern, P. Mobian, D. Pomeranc, J.-P. Sauvage, *Eur. J. Org. Chem.* **2004**, 1627-1638.
- [129] P. Mobian, J.-M. Kern, J.-P. Sauvage, *Angew. Chem. Int. Ed.* **2004**, *43*, 2392-2395.
- [130] D. A. Leigh, P. J. Lusby, S. J. Teat, A. J. Wilson, J. K. Y. Wong, *Angew. Chem. Int. Ed.* **2001**, *40*, 1538-1543.
- [131] T. J. Kidd, D. A. Leigh, A. J. Wilson, *J. Am. Chem. Soc.* **1999**, *121*, 1599-1600.
- [132] L. Hogg, D. A. Leigh, P. J. Lusby, A. Morelli, S. Parsons, J. K. Y. Wong, *Angew. Chem. Int. Ed.* **2004**, *43*, 1218-1221.
- [133] F. A. Chavez, J. M. Rowland, M. M. Olmstead, P. K. Mascharak, *J. Am. Chem. Soc.* **1998**, *120*, 9015-9027; J. C. Noveron, M. M. Olmstead, P. K. Mascharak, *Inorg. Chem.* **1998**, *37*, 1138-1139; D. S. Marlin, M. M. Olmstead, P. K. Mascharak, *Inorg. Chem.* **1999**, *38*, 3258-3260; J. C. Noveron, M. M. Olmstead, P. K. Mascharak, *J. Am. Chem. Soc.* **1999**, *121*, 3553-3554; F. A. Chavez, P. K. Mascharak, *Acc. Chem. Res.* **2000**, *33*, 539-545; D. S. Marlin, P. K. Mascharak, *Chem. Soc. Rev.* **2000**, *29*, 69-74; L. A. Tyler, J. C. Noveron, M. M. Olmstead, P. K. Mascharak, *Inorg. Chem.* **2000**, *39*, 357-362; J. C. Noveron, M. M. Olmstead, P. K. Mascharak, *J. Am. Chem. Soc.* **2001**, *123*, 3247-3259.
- [134] D. A. Leigh, A. Morelli, P. J. Lusby, A. M. Z. Slawin, A. R. Thomson, D. B. Walker, (*unpublished results*).
- [135] C. Hamann, J.-M. Kern, J.-P. Sauvage, *Inorg. Chem.* **2003**, *42*, 1877-1883.
- [136] K. S. Chichak, S. J. Cantrill, A. R. Pease, S. H. Chiu, G. W. V. Cave, J. L. Atwood, J. F. Stoddart, *Science* **2004**, *304*, 1308-1312.

- [137] S. J. Cantrill, K. S. Chichak, A. J. Peters, J. F. Stoddart, *Acc. Chem. Res.* **2005**, *38*, 1-9.
- [138] K. S. Chichak, S. J. Cantrill, J. F. Stoddart, *Chem. Commun.* **2005**, 3391-3393; A. J. Peters, K. S. Chichak, S. J. Cantrill, J. F. Stoddart, *Chem. Commun.* **2005**, 3394-3396.
- [139] C. D. Mao, W. Q. Sun, N. C. Seeman, *Nature* **1997**, *386*, 137-138.
- [140] J. C. Loren, M. Yoshizawa, R. F. Haldimann, A. Linden, J. S. Siegel, *Angew. Chem. Int. Ed.* **2003**, *42*, 5702-5705; M. Schmittel, A. Ganz, D. Fenske, *Org. Lett.* **2002**, *4*, 2289-2292.

Chapter Two Synopsis

Our group has previously reported on an efficient [2]catenate and [2]rotaxane synthesis based on divalent TM ions with a six coordinate (octahedral) primary coordination sphere that compliments Sauvage's original four coordinate (tetrahedral) Cu(I) system. Following this success we became interested in using four coordinate (square planar) geometries, specifically that of Pd(II), in the synthesis of mechanically interlocked molecular architectures. In the first instance, the construction of a [2]rotaxane was investigated.



Scheme 1. Synthesis of a [2]rotaxane using a Pd(II) template. Reagents and conditions: (i) CHCl₃, 50 °C 63% (ii) 1. Grubbs' catalyst (0.1 equiv), CH₂Cl₂; 2. H₂, Pd-C, THF, 6H₂ 98%, (over 2 steps); (iii) KCN, MeOH, CH₂Cl₂, 20 °C, 1 h and then 40 °C, 0.5 h, 97%.

With the idea of probing the electronic and structural requirements of such a strategy, a series of monodentate pyridine-based 'threads' were synthesised and combined with PdI(CH₃CN), a stable tridentate macrocycle precursor complex with a labile solvent molecule in its fourth coordination site (Scheme 1). We observed that only a 2,6-dimethoxyphenylene thread, 2, is suitable for rotaxane (Pd6) formation. In addition, following Pd(II) abstraction and protonation of the macrocycle, an unanticipated H-bond interaction between the two kinetically bound fragments was observed.

Chapter 2: Structural Requirements for the Assembly of a Square Planar Metal-Coordinated [2]Rotaxane

Published as “A 3D structure from a 2D template: Structural requirements for the assembly of a square planar metal-coordinated [2]rotaxane” A.-M. Fuller, D. A. Leigh, P. J. Lusby, I. D. H. Oswald, S. Parsons, D. B. Walker, *Angew. Chem. Int. Ed.* **2004**, *43*, 3914-3918.

Acknowledgements

The following people are gratefully acknowledged for their contribution to this chapter: Dr. P. Lusby synthesized rotaxane **6H₂** for the first time; Dr I. D. H. Oswald and Dr. S. Parsons solved the X-ray crystal structure of **Pd6**; A.-M. Fuller is thanked for her work attempting the synthesis of **6H₂** via alternative routes (not described here).

2.1 Introduction

The starting point for the revolution in catenane and rotaxane synthesis that occurred during the last part of the 20th century was Sauvage's realization that metal-ligand coordination geometries could fix molecular fragments in three-dimensional space such that they were predisposed to form mechanically interlocked architectures through macrocyclization or 'stopping' reactions.^[1] Efficient synthetic methods to rotaxanes were subsequently developed based on four^[2] (tetrahedral), five^[3] (trigonal bipyramidal and square pyramidal) and, most recently, six^[4] (octahedral) coordinate metal templates (Figure 1).^[5]

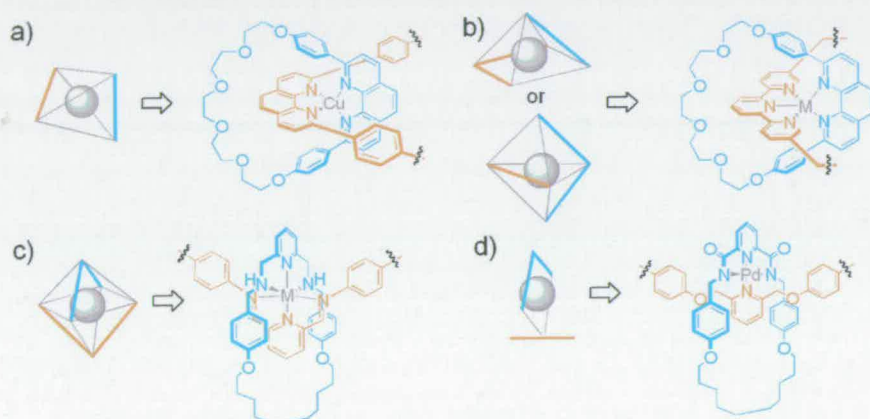


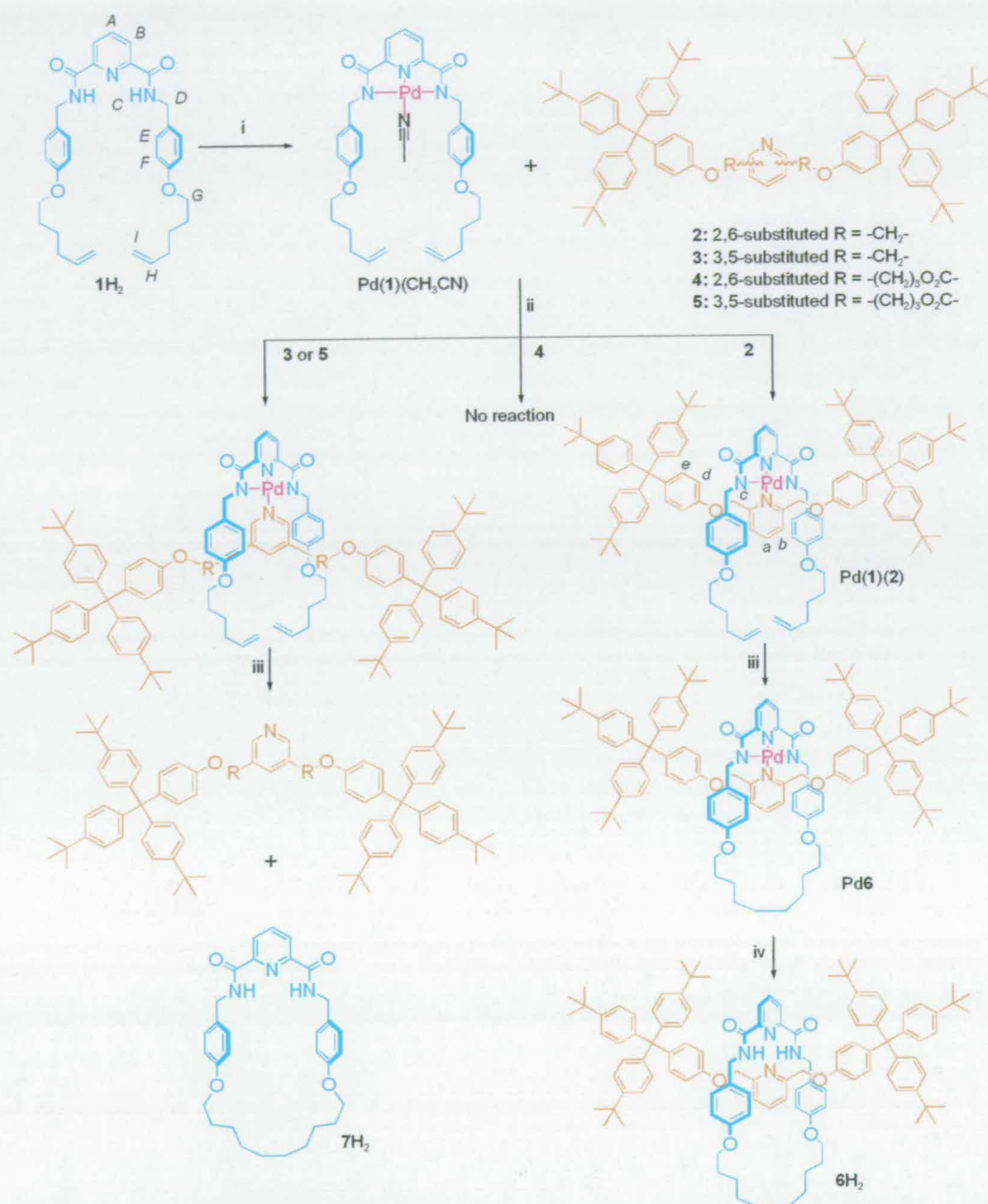
Figure 2.1. Exploiting transition metal-ligand geometries in the synthesis of mechanically interlocked architectures: a) tetrahedral, b) square pyramidal and trigonal bipyramidal, c) octahedral and d) square planar coordination motifs.

One of the benefits of using specific coordination motifs for such assemblies is that the resulting interlocked ligands often do not permit other metal geometries in their binding site, which can consequently be exploited either to lock a metal in an unusual geometry for its oxidation state^[6] or to bring about large amplitude 'shuttling' of the ligand components.^[3,7] Here we show that three dimensional interlocked architectures can also be assembled from two dimensional coordination templates, using steric and electronic restrictions to direct the synthesis in the third dimension. The resulting [2]rotaxane is the first example of a mechanically interlocked ligand that forms a four-coordinate square planar metal complex.^[8]

2.1 Results and Discussion

The square planar [2]rotaxane ligand design consists of a tridentate benzylic amide macrocycle and a monodentate thread (Figure 2.1 d). The macrocycle incorporates a 2,6-dicarboxyamidopyridine unit in order to exploit palladium chemistry recently developed^[9] by Hirao. The thread contains a pyridine donor substituted either 2,6- or 3,5- with appropriately bulky stoppers. It was envisioned that in the key intermediate, Pd(1)(2-5) (Scheme 2.1), the geometry of the precursor to the macrocycle (previously used to direct hydrogen bond assembly processes^[10]) would promote intercomponent π - π stacking, causing the pyridine donor of the thread to bind the metal orthogonally to the N₃-ligand (complimenting the normally preferred orientation^[11]) thus directing the assembly in the third dimension. A series of readily available threads 2-5 was investigated during the study.

The rotaxane synthesis was carried out according to Scheme 2.1. Treatment of 1H₂ with Pd(OAc)₂ in acetonitrile smoothly generated a complex Pd(1)(CH₃CN) in which the metal's fourth coordination site is occupied by a normally labile acetonitrile molecule. Nevertheless, displacement of the acetonitrile by *bis*-ester pyridine ligand 4 was unsuccessful (*vide infra*). However, simple combination of 5 or either of the *bis*-ether pyridine threads, 2 and 3, with Pd(1)(CH₃CN) in either dichloromethane or chloroform gave the desired complexes Pd(1)(5/2/3) in 97, 63 and 96% yields, respectively.



Scheme 2.1. Reagents and conditions: (i) Pd(OAc)₂, CH₃CN, 76%; (ii) CHCl₃, 50 °C; 2 63%, 3 96%, 4 0%, 5 97%; (iii) 1. Grubbs' catalyst (0.1 equiv), CH₂Cl₂; 2. H₂, Pd-C, THF, 6H₂ 98%, 3 + 7H₂ 63%, 5 + 7H₂ 69% (over 2 steps); (iv) KCN, MeOH, CH₂Cl₂, 20 °C, 1 h and then 40 °C, 0.5 h, 97%.

The ^1H NMR spectrum of Pd(1)(2) is shown in Figure 2.2 c. Comparison with the spectra of Pd(1)(CH₃CN) and 1H₂ (Figure 2.2 b and 2.2 a, respectively) shows features clearly indicative of metal coordination (the absence of H_C and shifts in H_A and H_B) and the anticipated aromatic stacking between the tridentate and monodentate ligands (particularly H_E and H_F). Similar chemical shift differences were observed for Pd(1)(3) and Pd(1)(5), however, ring closing olefin metathesis (RCM) followed by hydrogenation (Scheme 2.1, step iii) of the three complexes produced very different results. Whilst cyclisation of Pd(1)(2) gave the corresponding [2]rotaxane Pd6 in 77% yield following hydrogenation of the olefin, no [2]rotaxane was produced from RCM of Pd(1)(3) or Pd(1)(5), the only products in each case being uninterlocked macrocycle and thread. Why does only one of the four threads direct rotaxane synthesis in the desired manner?

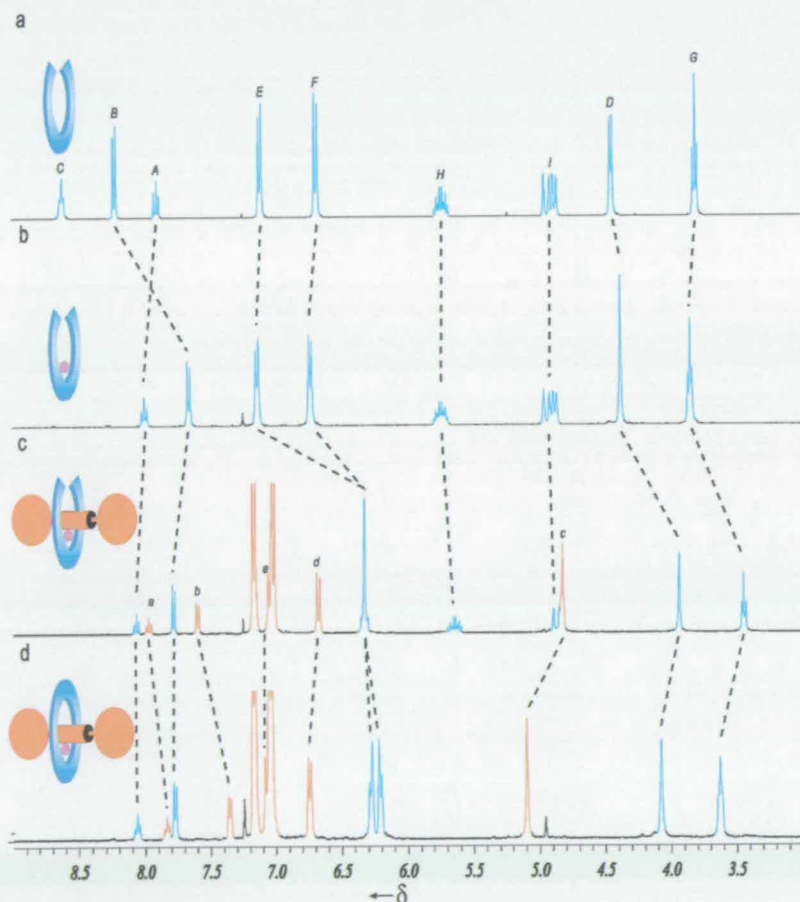


Figure 2.2. ^1H NMR spectra (400 MHz, 9:1 CDCl_3 : CD_3CN , 298 K) of: (a) 1H₂ (b) Pd(1)(CH₃CN) (c) Pd(1)(2) (d) [2]rotaxane Pd6. The lettering refers to the assignments in Scheme 2.1.

The ^1H NMR spectra of the [2]rotaxane (Pd6, Figure 2.2 d), mass spectrometry and the preserved association of the organic fragments upon demetallation, unambiguously confirmed the interlocked structure. In addition to the loss of the terminal olefin protons, some subtle differences in the ^1H NMR spectrum of Pd6 compared to Pd(1)(2) (Figure 2.2 c) indicates that some rearrangement of the ligands does occur on rotaxane formation. Single crystals of Pd6 suitable for X-ray crystallography^[12] were grown by slow cooling of a warm, saturated solution of the [2]rotaxane in acetonitrile.

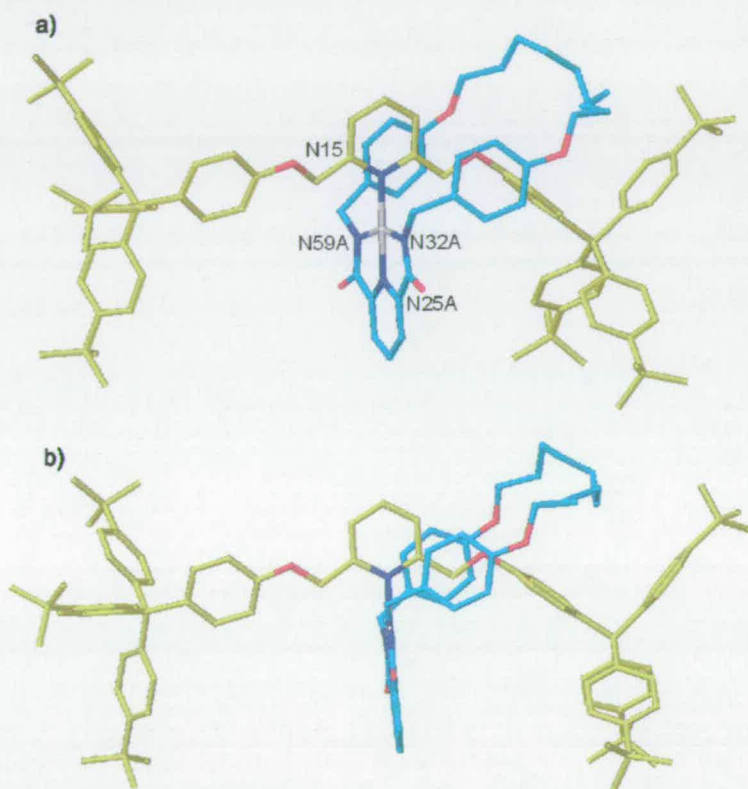


Figure 2.3. X-ray crystal structure of rotaxane Pd6 showing: a) staggered and b) side-on views.^[12] Carbon atoms of the macrocycle are shown in light blue and those of the thread in yellow; oxygen atoms are red, nitrogen dark blue, palladium grey. Selected bond lengths [Å]: Pd-N15 1.95, Pd-N25 1.86, Pd-N32 2.04, Pd-N59 2.02; other selected distance [Å]: N15-N25 3.81; macrocycle bite angle [°]: N59-Pd-N32 160.0. The macrocycle is disordered over two similar sites (50:50), but one is omitted for clarity together with the hydrogen atoms.

The solid state structure (Figure 2.3) shows the interlocked architecture and the pseudo- (the N_3 -bite angle is 160.0°) square planar geometry of the palladium. The π -stacking between the macrocycle and the pyridine of the thread so apparent in solution from the ^1H NMR shifts is significantly offset in the solid state (side-on view, figure 2.3 b). The co-conformation adopted by the macrocycle and thread in

the rotaxane crystal structure clearly illustrates why RCM of the complexes formed with the 3,5-disubstituted threads (Pd(1)(3) and Pd(1)(5)) can lead to uninterlocked products; even with both fragments attached to the metal, cyclization of **1** can readily occur without encircling a 3,5-substituted pyridine thread. Similarly, the conformation of the thread suggests a possible reason for the lack of reactivity of the 2,6-bis-ester thread, **4**, towards Pd(1)(CH₃CN). In the crystal structure the electron density of the ether oxygen atoms of the thread is directed away from the occupied d_{z²} orbital lobes which lie above and below the plane of the square planar geometry d⁸ palladium. Chelation by **4** to Pd1 has to occur orthogonally for steric reasons. Such an arrangement would force electron density from the ester carbonyl groups into this high energy space.

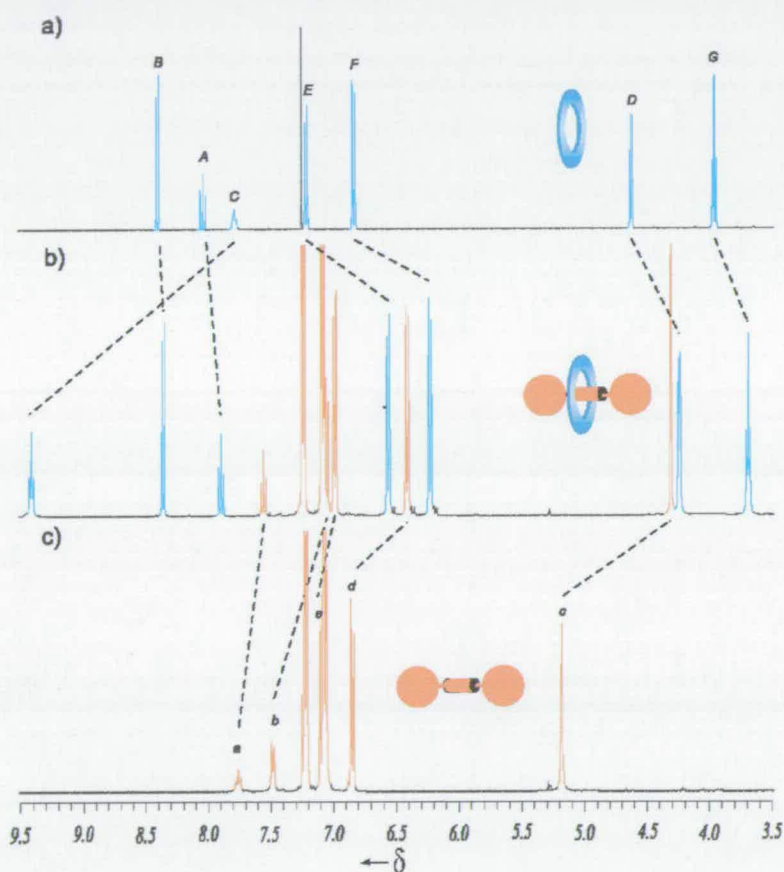


Figure 2.4. ¹H NMR spectra (400 MHz, CDCl₃, 298 K) of: (a) macrocycle 7H₂ (b) demetallated [2]rotaxane 6H₂ (c) thread 2. The lettering refers to the assignments in Scheme 1.1.

Demetallation of Pd6 with potassium cyanide (Scheme 2.1, step iv) generates the free [2]rotaxane 6H₂ in 97% yield confirming that once formed the coordination bonds are not required to stabilize the interlocked architecture. The ¹H NMR

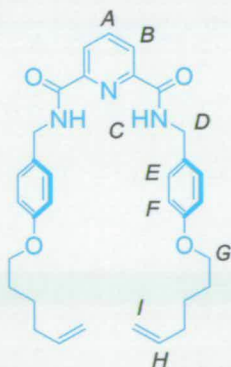
spectrum of **6H₂** and its uninterlocked components in CDCl₃ are shown in Figure 2.4. The shielding of the benzyl groups in the rotaxane compared to the free macrocycle, together with the large (1.7 ppm) downfield shift in the amide protons (H_C), indicate that specific hydrogen bonding interactions between the thread and the macrocycle are ‘switched on’ by the demetallation-protonation procedure. It appears that the amide groups of **6H₂** simultaneously hydrogen bond to the pyridine groups in both macrocycle and thread.

In conclusion, we have described methodology for assembling a three-dimensional interlocked molecular architecture from a two-dimensional metal template. A combination of steric and electronic factors direct the synthesis in the third dimension, either promoting or preventing interlocking. The resulting [2]rotaxane is the first derived from a square planar coordinated metal and completes the series of mechanically interlocked ligands for common transition metal geometries started by Sauvage in 1983.

2.3 Experimental Section

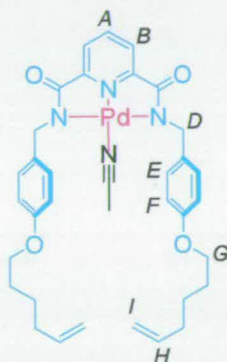
General

Unless stated otherwise, all reagents and anhydrous solvents were purchased from Aldrich Chemicals and used without further purification. (*p*-hydroxyphenyl)tris(*p*-*tert*-butylphenyl)methane^[16] and 4-(hex-5-enyloxy)benzylamine^[17] were prepared according to literature procedures.



N, N'-Bis[4-(hex-5-enyloxy)benzyl]-2,6-pyridinedicarboxamide 1H₂: To a solution of 4-(hex-5-enyloxy)benzylamine (2.18 g, 10.6 mmol) and triethylamine (1.07 g, 10.6 mmol) in dichloromethane (50 mL) at 0 °C under an atmosphere of

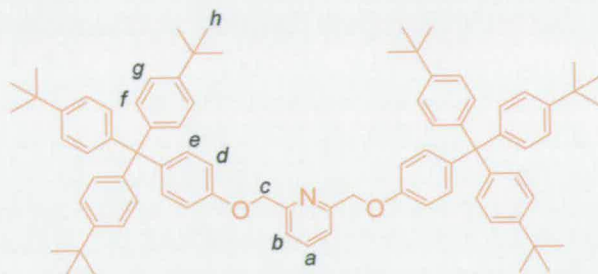
nitrogen was added slowly 2,6-pyridinedicarbonyl dichloride (1.08 g, 5.30 mmol). The reaction was then stirred at room temperature for 18 h. The solvent was removed under reduced pressure and the crude residue purified by column chromatography (1:9 EtOAc/CH₂Cl₂) and then recrystallised from acetonitrile to yield the title compound as a colourless crystalline solid (2.61 g, yield = 91%). m.p. 141.2-143.0 °C; ¹H NMR (400 MHz, CDCl₃, 298 K): δ = 1.46 (m, 4H, H_{alkyl}), 1.68 (m, 4H, H_{alkyl}), 2.02 (m, 4H, H_{alkyl}), 3.81 (t, 4H, *J* = 6.6 Hz, H_G), 4.44 (d, 4H, *J* = 6.3 Hz, H_D), 4.90 (m, 4H, H_I), 5.73 (m, 2H, H_H), 6.68 (d, 4H, *J* = 8.8 Hz, H_F), 7.11 (d, 4H, *J* = 8.8 Hz, H_E), 7.90 (t, 1H, *J* = 7.8 Hz, H_A), 8.22 (d, 2H, *J* = 7.8 Hz, H_B), 8.62 (t, 2H, *J* = 6.3 Hz, H_C); ¹³C NMR (100 MHz, CDCl₃, 298 K): δ = 25.3, 28.7, 33.4, 42.9, 67.8, 114.6, 114.8, 125.2, 129.0, 129.9, 138.5, 138.9, 148.8, 158.5, 163.5; LRFAB-MS (3-NOBA matrix): *m/z* = 541 [M]⁺, 564 [MNa]⁺; HRFAB-MS (3-NOBA matrix): *m/z* = 541.29425 (calcd. for C₃₃H₃₉N₃O₄, 541.29406).



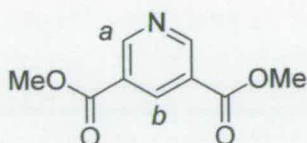
[(*N,N'*-Bis[4-(hex-5-enyloxy)benzyl]-2,6-pyridinedicarboxamido)palladium(II)

(acetonitrile)] Pd(1)(CH₃CN): To 1H₂ (0.480 g, 8.86x10⁻¹ mmol) and palladium(II) acetate (0.199 g, 8.86x10⁻¹ mmol) was added anhydrous acetonitrile (50 mL). The reaction was stirred at room temperature under an atmosphere of nitrogen for 4 h. The resulting suspension was filtered off, washed with excess acetonitrile (25 mL), and dried in air to yield the title compound as a yellow/green solid (0.465 g, yield = 76%). m.p. 120 °C (dec); ¹H NMR (400 MHz, 9:1 CDCl₃:CD₃CN, 298 K): δ = 1.47 (m, 4H, H_{alkyl}), 1.69 (m, 4H, H_{alkyl}), 1.93 (s, 3H, Pd-NCCH₃), 2.03 (m, 4H, H_{alkyl}), 3.85 (t, 4H, *J* = 6.3 Hz, H_G), 4.38 (s, 4H H_D), 4.89 (m, 4H, H_I), 5.74 (m, 2H, H_H), 6.73 (d, 4H, *J* = 8.6 Hz, H_F), 7.13 (d, 4H, *J* = 8.6 Hz, H_E), 7.65 (d, 2H, *J* = 7.6 Hz, H_B), 8.00 (t, 1H, *J* = 7.6 Hz, H_A); ¹³C NMR (100 MHz, 9:1 CDCl₃:CD₃CN, 298 K): δ = 0.5, 27.4, 32.1, 48.1, 66.5, 112.9, 113.3, 115.3, 123.4, 127.1, 132.1, 137.2, 139.8, 151.8, 156.4, 156.5, 169.1; LRFAB-MS (3-NOBA matrix): *m/z* = 646 [Pd1H]⁺,

HRFAB-MS (3-NOBA matrix): $m/z = 646.18925$ (calcd. for $C_{33}H_{38}N_3O_4Pd$, 646.18943).



2: To a THF solution (50 mL) of (*p*-hydroxyphenyl)tris(*p*-*tert*-butylphenyl)methane, (1.50 g, 2.97 mmol), 2,6-pyridinedimethanol (0.21 g, 1.49 mmol) and triphenylphosphine (0.778 g, 2.97 mmol), under an atmosphere of N_2 at 0 °C, was added dropwise DIAD (0.70 mL, 2.97 mmol). The solution was allowed to warm to room temperature and stirred for 18 h. The solvent was then removed under vacuum, and methanol (50 mL) added to the crude residue. The resulting white solid was filtered off, and purified by column chromatography ($CDCl_3$) to yield the title compound as a colourless solid (0.952 g, yield = 64%). m.p. 277 °C (dec); 1H NMR (400 MHz, $CDCl_3$, 298 K): $\delta = 1.29$ (s, 54H, H_h), 5.18 (s, 4H, H_c), 6.84 (d, 4H, $J = 8.8$ Hz, H_e), 7.08 (m, 16H, $H_d + H_g$), 7.22 (d, 12H, $J = 8.8$ Hz, H_f), 7.48 (d, 2H, $J = 7.6$ Hz, H_b), 7.76 (t, 1H, $J = 7.6$ Hz, H_a); LRFAB-MS (3-NOBA matrix): $m/z = 1112$ $[MH]^+$; HRFAB-MS (3-NOBA matrix): $m/z = 1112.72910$ (calcd. for $C_{81}H_{94}NO_2$, 1112.72846).

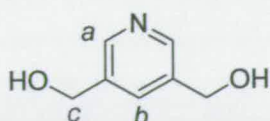


3

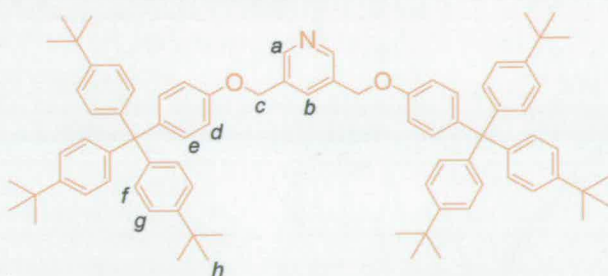
a) Pyridine-3,5-dicarboxylic acid methyl ester^[18]

EDCI (5.04 g, 26 mmol) was added to a solution of pyridine-3,5-dicarboxylic acid (2.00 g, 12 mmol) in methanol (50 mL) and the mixture was cooled to 0 °C. A solution of dimethylaminopyridine (0.587 g, 5 mmol) in methanol (10 mL) was added dropwise and the mixture was stirred for 3 h. The solvent was then removed under reduced pressure and the crude residue dissolved in dichloromethane (50 mL). The solution was washed with, 1 M hydrochloric acid (20 mL), saturated aqueous sodium bicarbonate (20 mL) and saturated aqueous sodium chloride (20 mL). The

dichloromethane washings were combined and dried with sodium sulfate and the solvent was removed under reduced pressure to yield the title compound as a white solid (2.13 g, yield = 91%). m.p. 85.5-86.3 °C; ^1H NMR (400 MHz, CDCl_3 , 298 K): $\delta = 3.97$ (s, 6H, CO_2CH_3), 8.85 (m, 1H, H_b), 9.34 (m, 2H, H_a); ^{13}C NMR (100 MHz, CDCl_3 , 298 K): 52.7, 125.9, 138.0, 154.2, 164.9; LRFAB-MS (3-NOBA matrix): $m/z = 196$ $[\text{MH}]^+$; HRFAB-MS (3-NOBA matrix): $m/z = 196.06095$ (calcd. for $\text{C}_9\text{H}_{10}\text{NO}_4$, 196.0698).

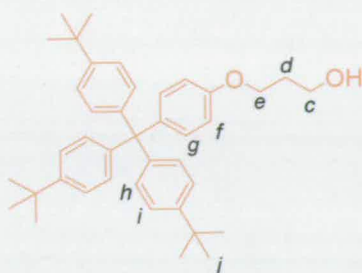


b) 3,5-pyridinedimethanol^[19]: Pyridine-3,5-dicarboxylic acid methyl ester (1.00 g, 5.13 mmol) dissolved in dry Et_2O (20 mL) was added dropwise to a suspension of LiAlH_4 (0.65 g, 17.1 mmol) in dry Et_2O (35 mL) at 0 °C. The resulting yellow mixture was refluxed for 2 h, cooled to room temperature and quenched with H_2O (10 mL). The suspension was filtered and the crude residue was extracted several times with hot methanol (4 x 30 mL). The solvent was removed under reduced pressure to yield the title compound as a pale yellow oil, (0.468 g, yield = 66%); ^1H NMR (400 MHz, MeOD, 298 K): $\delta = 4.67$ (s, 4H, H_c), 7.83 (m, 1H, H_b), 8.43 (m, 2H, H_a); ^{13}C NMR (100 MHz, MeOD, 298 K): 62.5, 135.5, 138.9, 147.6, 158.7; LRFAB-MS (3-NOBA matrix): $m/z = 140$ $[\text{MH}]^+$; HRFAB-MS (3-NOBA matrix): $m/z = 140.07132$ (calcd. for $\text{C}_9\text{H}_{10}\text{NO}_2$, 140.07115).



c) **3**: To a THF solution (50 mL) of (*p*-hydroxyphenyl)tris(*p*-*tert*-butylphenyl)methane, (0.725 g, 1.44 mmol), 3,5-pyridinedimethanol (0.100 g, 7.2×10^{-1} mmol) and triphenylphosphine (0.415 g, 1.60 mmol), under an atmosphere of N_2 at 0 °C, was added dropwise DIAD (0.3 mL, 1.6 mmol). The solution was allowed to warm to room temperature and stirred for 18 h. The solvent was then removed under vacuum, and methanol (50 mL) added to the crude residue. The resulting white solid was filtered off, and purified by column chromatography

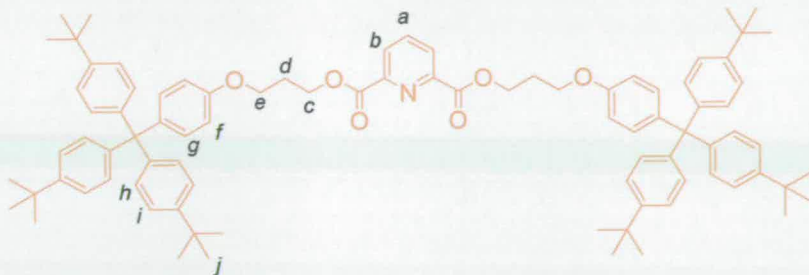
(CDCl₃) to yield the title compound as a white solid (0.480 g, yield = 60%). m.p. 265 °C (dec); ¹H NMR (400 MHz, CDCl₃, 298 K): δ = 1.28 (s, 54H, H_h), 5.08 (s, 4H, H_c), 6.83 (d, 4H, *J* = 9.2 Hz, H_e), 7.06 (d, 12H, *J* = 8.6 Hz, H_g), 7.11 (d, 4H, *J* = 9.2 Hz, H_d), 7.22 (d, 12H, *J* = 8.6 Hz, H_f), 7.92 (m, 1H, H_b), 8.65 (m, 2H, H_a); ¹³C NMR (100 MHz, CDCl₃, 298 K): 29.4, 32.4, 111.3, 122.1, 128.8 (x2), 130.5, 133.5, 138.6, 142.0, 146.4, 151.3, 154.1, 155.9, 205.1; LRFAB-MS (3-NOBA matrix): *m/z* = 1112 [MH]⁺; HRFAB-MS (3-NOBA matrix): *m/z* = 1112.72797 (calcd. for C₈₁H₉₄NO₂, 1112.72846).



3-{4-[Tris-(4-*tert*-butyl-phenyl)-methyl]-phenoxy}-propan-1-ol:

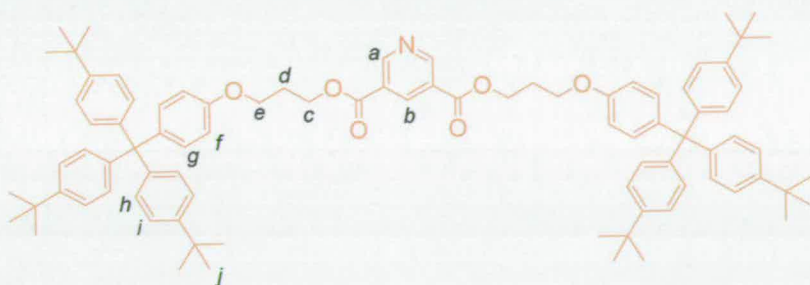
(*p*-

hydroxyphenyl)tris(*p*-*tert*-butylphenyl)methane (1.00 g, 2 mmol), 3-bromopropan-1-ol (0.268 g, 2.00 mmol), potassium carbonate (2.7 g, 20 mmol) and sodium iodide (0.01 g 0.07 mmol) were dissolved in butanone (100 mL) and the mixture was heated at reflux for 18 h. The solution was then filtered and the solvent was removed under vacuum. The crude residue was purified by column chromatography (1:9, EtOAc:CH₂Cl₂) to give the title compound as a white solid (0.991 g, yield = 88%). m.p. 290 °C (dec); ¹H NMR (400 MHz, CDCl₃, 298 K): δ = 1.29 (s, 27H, H_j), 2.02 (m, 2H, H_d), 3.85 (t, 2H, *J* = 6.0 Hz, H_e), 4.10 (t, 2H, *J* = 6.2 Hz, H_c), 6.76 (d, 2H, *J* = 9.0 Hz, H_g), 7.07 (m, 8H, H_f + H_i), 7.22 (d, 6H, *J* = 8.5 Hz, H_h); ¹³C NMR (100 MHz, CDCl₃, 298 K): δ = 25.4, 28.1, 28.4, 28.7, 42.9, 67.4, 114.7, 125.3, 129.2, 129.8, 148.8, 158.6, 163.3, 169.7; LRFAB-MS (3-NOBA matrix): *m/z* = 562 [M]⁺; HRFAB-MS (3-NOBA matrix): *m/z* = 562.38039 (calcd. for C₄₀H₅₀O₂, 562.38108).



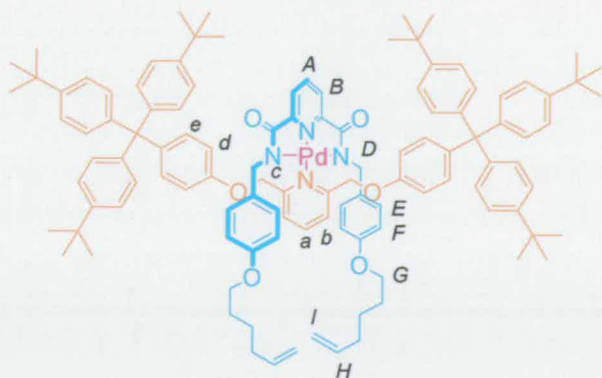
4: EDCI (0.182 g, 0.95 mmol) was added to a solution of pyridine-2,6-dicarboxylic acid (0.072 g, 4.3x10⁻¹ mmol) and 3-{4-[Tris-(4-*tert*-butyl-phenyl)-methyl]-

phenoxy}-propan-1-ol (0.484 g, 8.6×10^{-1} mmol) in dichloromethane (50 mL) and the mixture was cooled to 0 °C. A solution of DMAP (0.021 g, 1.7×10^{-1} mmol) in dichloromethane (10 mL) was added dropwise and the mixture was stirred for 3 h. The solution was then washed with, 1 M hydrochloric acid (20 mL), saturated aqueous sodium bicarbonate (20 mL) and saturated aqueous sodium chloride (20 mL). The dichloromethane washings were combined and dried with sodium sulfate and the solvent was removed under reduced pressure to yield the title compound as a white solid, (0.430 g, yield = 84%). m.p. 281-282 °C; ^1H NMR (400 MHz, CDCl_3 , 298 K): δ = 1.28 (s, 54H, H_j), 2.25 (m, 4H, H_d), 4.03 (t, 4H, J = 6.0 Hz, H_e), 4.52 (t, 4H, J = 6.4 Hz, H_c), 6.79 (d, 4H, J = 8.6 Hz, H_g), 7.28 (m, 16H, $\text{H}_f + \text{H}_i$), 7.21 (d, 12H, J = 8.4 Hz, H_h), 7.90 (t, 1H, J = 8.0 Hz, H_a), 8.18 (d, 2H, J = 8.0 Hz, H_b); ^{13}C NMR (100 MHz, CDCl_3 , 298 K): δ = 31.4, 34.3, 60.8, 65.8, 112.9, 124.1, 127.9, 130.7, 132.3, 138.2, 139.8, 144.1, 148.3, 148.5, 156.5, 157.9, 164.6, 183.8; LRFAB-MS (3-NOBA matrix): m/z = 1257 $[\text{MH}]^+$; HRFAB-MS (3-NOBA matrix): m/z = 1256.76819 (calcd. for $\text{C}_{87}\text{H}_{102}\text{NO}_6$, 1256.77072).

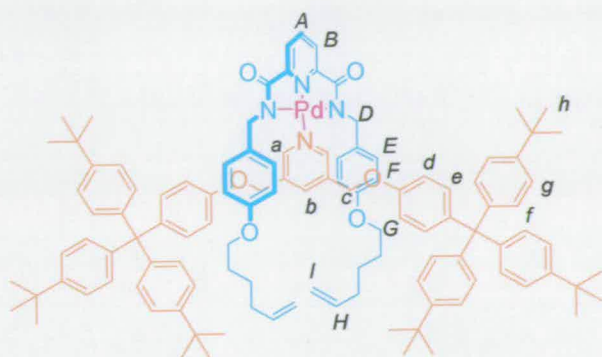


5: EDCI (0.182 g, 9.5×10^{-1} mmol) was added to a solution of pyridine-3,5-dicarboxylic acid (0.072 g, 4.3×10^{-1} mmol) and 3-{4-[tris-(4-*tert*-butyl-phenyl)-methyl]-phenoxy}-propan-1-ol (0.484 g, 8.6×10^{-1} mmol) in dichloromethane (50 mL) and the mixture was cooled to 0 °C. A solution of DMAP (0.021 g, 1.7×10^{-1} mmol) in dichloromethane (10 mL) was added dropwise and the mixture was stirred for 3 h. The solution was then washed with, 1 M hydrochloric acid (20 mL), saturated aqueous sodium bicarbonate (20 mL) and saturated aqueous sodium chloride (20 mL). The dichloromethane washings were combined and dried with sodium sulfate and the solvent was removed under reduced pressure to yield the title compound as a white solid, (0.40 g, yield = 83%). m.p. 276-277 °C; ^1H NMR (400 MHz, CDCl_3 , 298 K): δ = 1.28 (s, 54H, H_j), 2.25 (m, 4H, H_d), 4.08 (t, 4H, J = 6.0 Hz, H_e), 4.57 (t, 4H, J = 6.4 Hz, H_c), 6.74 (d, 4H, J = 8.6 Hz, H_g), 7.06 (m, 16H, $\text{H}_f + \text{H}_i$), 7.21 (d, 12H, J = 8.4 Hz, H_h), 8.81 (s, 1H, H_b), 9.35 (s, 2H, H_a); ^{13}C NMR

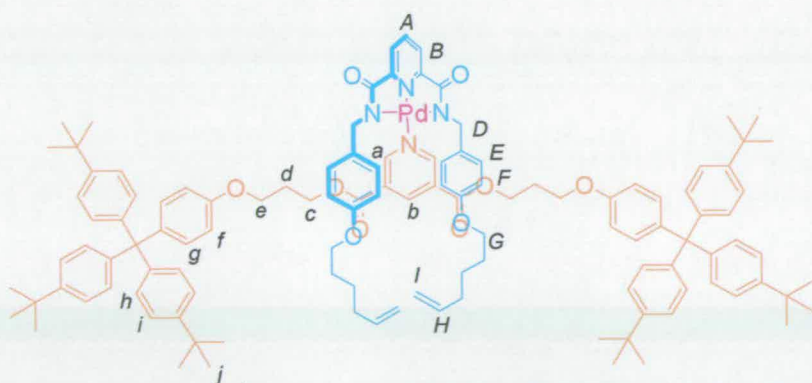
(100 MHz, CDCl₃, 298 K): δ = 26.8, 29.6, 32.1, 61.0, 62.0, 111.0, 122.4, 124.2, 128.5, 130.4, 136.1, 138.0, 142.2, 146.4, 152.3, 154.5, 155.9, 162.5; LRFAB-MS (3-NOBA matrix): m/z = 1257 [MH]⁺; HRFAB-MS (3-NOBA matrix): m/z = 1256.77142 (calcd. for C₈₇H₁₀₂NO₆, 1256.77072).



Pd(1)(2): **2** (0.344 g, 3.09x10⁻¹ mmol) and [Pd(1)(CH₃CN)] (0.255 g, 3.71x10⁻¹ mmol) were gently heated (50 °C) in CHCl₃ (25 mL) for 10 minutes, and then stirred for a further 1 h at room temperature. The solvent was removed under reduced pressure, and the crude residue purified by column chromatography (1:24 EtOAc:CH₂Cl₂) to give the title compound as a yellow solid (0.344 g, yield = 63%). m.p. 172 °C (dec); ¹H NMR (400 MHz, CD₂Cl₂, 298 K): δ = 1.28 (s, 54H, H_h), 1.38 (m, 4H, H_{alkyl}), 1.54 (m, 4H, H_{alkyl}), 2.00 (m, 4H, H_{alkyl}), 3.53 (t, 4H, J = 6.3 Hz H_G), 3.94 (s, 4H, H_D), 4.90 (m, 4H, H_I), 4.93 (s, 4H, H_c), 5.74 (m, 2H, H_H), 6.39 (s, 8H, H_E + H_F), 6.76 (d, 4H, J = 8.8 Hz, H_e), 7.12 (m, 16H, H_d + H_g), 7.25 (d, 12H, J = 8.8 Hz, H_j), 7.63 (d, 2H, J = 7.8 Hz, H_b), 7.77 (d, 2H, J = 7.8 Hz, H_B), 8.01 (t, 1H, J = 7.8 Hz, H_a), 8.09 (t, 1H, J = 7.8 Hz, H_A); ¹³C NMR (100 MHz, CD₂Cl₂, 298 K): δ = 25.7, 29.1, 31.5, 33.8, 34.6, 48.9, 63.5, 67.8, 69.5, 114.0, 114.5, 114.7, 122.6, 124.6, 125.0, 128.4, 130.8, 132.4, 133.3, 139.0, 140.1, 141.2, 141.2, 144.7, 148.9, 153.2, 155.7, 158.2, 159.3, 171.3; LRFAB-MS (3-NOBA matrix): m/z = 1757 [M]⁺; HRFAB-MS (3-NOBA matrix): m/z = 1757.90693 (calcd. for ¹²C₁₁₃¹³CH₁₃₀N₄O₆¹⁰⁶Pd, 1757.90559).

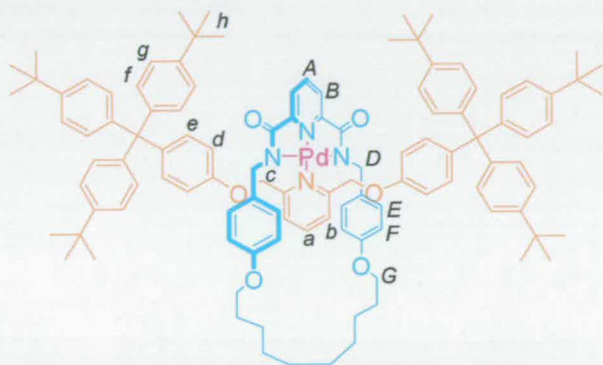


Pd(1)(3): 3 (0.100 g, 9×10^{-2} mmol) and $[\text{Pd(1)}(\text{CH}_3\text{CN})]$ (0.062 g, 9×10^{-2} mmol) were gently heated (50 °C) in dichloromethane (10 mL) for 10 minutes, and then stirred for a further 1 h at room temperature. The solvent was removed under reduced pressure to give the title compound as a yellow solid (0.152 g, yield = 96%). m.p. 187 °C (dec); ^1H NMR (400 MHz, CDCl_3 , 298 K): δ = 1.28 (s, 54H, H_h), 1.41 (m, 8H, H_{alkyl}), 1.97 (m, 4H, H_{alkyl}), 3.71 (t, 4H, J = 6.5 Hz, H_G), 4.15 (s, 4H, H_C), 4.69 (s, 4H, H_D), 4.90 (m, 4H, H_I), 5.70 (m, 2H, H_H), 6.49 (d, 4H, J = 8.5 Hz, H_F), 6.58 (d, 4H, J = 8.5 Hz, H_E), 6.80 (d, 4H, J = 8.5 Hz, H_e), 7.05 (d, 12H, J = 8.5 Hz, H_g), 7.15 (d, 4H, J = 8.5 Hz, H_d), 7.21 (d, 12H, J = 8.5 Hz, H_f), 7.73 (s, 1H, H_a), 7.76 (s, 2H, H_b), 7.85 (d, 2H, J = 8.0 Hz, H_B), 8.09 (t, 1H, J = 8.0 Hz, H_A); ^{13}C NMR (100 MHz, CDCl_3 , 298 K): δ = 25.3, 28.7, 31.4, 33.4, 34.3, 48.0, 65.6, 67.7, 113.1, 113.9, 114.8, 124.1, 124.8, 127.8, 130.7, 132.6, 133.0, 134.9, 135.1, 138.4, 140.6, 141.1, 143.9, 148.5, 153.1, 155.4, 157.3, 157.8, 157.9, 170.8; LRFAB-MS (3-NOBA matrix): m/z = 1758 $[\text{M}]^+$; HRFAB-MS (3-NOBA matrix): m/z = 1757.90303 (calcd. for $^{12}\text{C}_{113}^{13}\text{CH}_{130}\text{N}_4\text{O}_6^{106}\text{Pd}$, 1757.90559).



Pd(1)(5): 5 (0.268 g, 2.1×10^{-1} mmol) and $[\text{Pd(1)}(\text{CH}_3\text{CN})]$ (0.147 g, 2.1×10^{-1} mmol) were gently heated (50 °C) in dichloromethane (20 mL) for 10 minutes, and then stirred for a further 1 h at room temperature. The solvent was removed under reduced pressure to give the title compound as a yellow solid (0.386 g, yield = 97%). m.p.

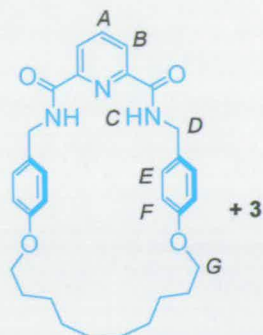
193 °C (dec); ^1H NMR (400 MHz, CD_2Cl_2 , 298 K): δ = 1.22 (s, 54H, H_j), 1.42 (m, 4H, H_{alkyl}), 1.64 (m, 4H, H_{alkyl}), 2.00 (m, 4H, H_{alkyl}), 2.21 (m, 4H, H_d), 3.69 (t, 4H, J = 6.5 Hz, H_G), 4.03 (t, 4H, J = 6.0 Hz, H_c), 4.15 (s, 4H, H_D), 4.45 (t, 4H, J = 6.5 Hz, H_e), 4.88 (m, 4H, H_l), 5.68 (m, 2H, H_H), 6.37 (d, 4H, J = 8.5 Hz, H_F), 6.50 (d, 4H, J = 8.5 Hz, H_E), 6.77 (d, 4H, J = 8.6 Hz, H_g), 7.02 (m, 16H, $\text{H}_f + \text{H}_i$), 7.14 (d, 12H, J = 8.5 Hz, H_h), 7.79 (d, 2H, J = 8.0 Hz, H_B), 8.04 (t, 1H, J = 8.0 Hz, H_A), 8.42 (s, 2H, H_a), 8.55 (s, 1H, H_b); ^{13}C NMR (100 MHz, CD_2Cl_2 , 298 K): δ = 23.3, 26.6, 27.8, 29.4, 31.5, 32.3, 46.2, 62.0, 65.7, 110.9, 112.2, 112.9, 122.1, 123.0, 125.3, 125.5, 126.4, 128.7, 130.4, 130.6, 131.2, 136.4, 138.1, 138.9, 142.1, 146.4, 151.1, 152.2, 154.4, 155.6, 156.0, 160.0, 168.8 ; LRFAB-MS (3-NOBA matrix): m/z = 1902 [M] $^+$; HRFAB-MS (3-NOBA matrix): m/z = 1901.94173 (calcd. for $^{12}\text{C}_{119}^{13}\text{CH}_{138}\text{N}_4\text{O}_{10}^{106}\text{Pd}$, 1901.94785).



Pd6: (a) To an anhydrous dichloromethane solution (400 mL) of Grubbs' catalyst (0.031 g, 3.74×10^{-2} mmol) under an atmosphere of N_2 , was added *via* a double ended needle, Pd(1)(2) (0.657 g, 3.74×10^{-1} mmol) in anhydrous dichloromethane (100 mL). The solution was stirred at room temperature for 18 h. The solvent was removed under vacuum and the crude residue purified by column chromatography (1:24 EtOAc: CH_2Cl_2) to give a yellow solid (0.50 g).

(b) A mixture of the yellow solid obtained in part (a) (0.50 g) in THF (50 mL), and 10% w/w Pd-C (0.100 g) was stirred under an atmosphere of H_2 for 18 h. The Pd-C was then removed by filtration through a plug of Celite, and the solvent was removed under reduced pressure to give the title compound as a yellow solid (0.499 g, yield = 77% over 2 steps). m.p. 292 °C (dec); ^1H NMR (400 MHz, CD_2Cl_2 , 298 K): δ = 1.21 (m, 8H, H_{alkyl}), 1.29 (s, 54H, H_h), 1.41 (m, 4H, H_{alkyl}), 1.55 (m, 4H, H_{alkyl}), 3.71 (t, 4H, J = 6.3 Hz, H_G), 4.11 (s, 4H, H_D), 5.19 (s, 4H, H_c), 6.30 (d, 4H, J = 8.3 Hz H_F), 6.35 (d, 4H, J = 8.3 Hz, H_E), 6.85 (d, 4H, J = 8.8 Hz, H_e), 7.18 (m, 16H, $\text{H}_d + \text{H}_g$), 7.26 (d, 12H, J = 8.3 Hz, H_f), 7.43 (d, 2H, J = 7.8 Hz, H_b), 7.77 (d, 2H, J = 7.8 Hz,

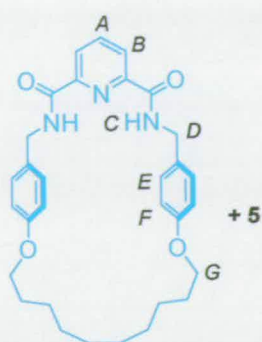
H_B), 7.90 (t, 1H, $J = 7.8$ Hz, H_A), 8.09 (t, 1H, $J = 7.8$ Hz, H_A); ^{13}C NMR (100 MHz, CD_2Cl_2 , 298 K): $\delta = 24.7, 27.7, 27.8, 28.6, 30.3, 33.3, 48.8, 62.4, 66.4, 69.2, 113.8, 114.0, 121.1, 123.6, 123.9, 127.2, 129.6, 131.2, 132.1, 138.6, 140.0, 140.5, 143.6, 147.6, 152.0, 154.5, 156.9, 158.0, 170.5$; LRFAB-MS (3-NOBA matrix): $m/z = 1730$ $[M]^+$; HRFAB-MS (3-NOBA matrix): $m/z = 1731.89199$ (calcd. for $^{12}\text{C}_{111}^{13}\text{CH}_{128}\text{N}_4\text{O}_6\text{Pd}$, 1731.88994).



Ring closing metathesis and hydrogenation of Pd(1)(3)

(a) To an anhydrous dichloromethane solution (60 mL) of Grubbs' catalyst (0.031 g, 3.74×10^{-2} mmol) under an atmosphere of N_2 , was added *via* a double ended needle, Pd(1)(3) (0.140 g, 8.0×10^{-2} mmol) in anhydrous dichloromethane (30 mL). The solution was stirred at room temperature for 18 h. The solvent was removed under vacuum to give a dark green solid (0.20 g).

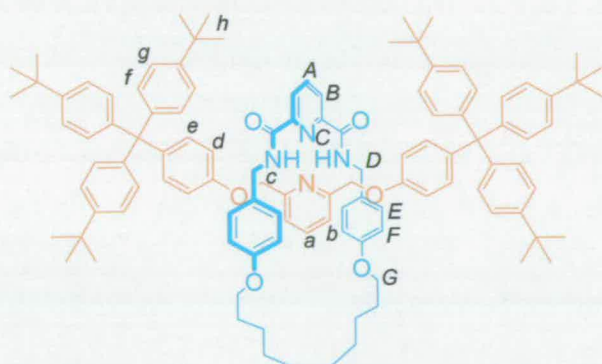
(b) A mixture of the green solid obtained in part (a) (0.20 g) in THF (20 mL), and 10% w/w Pd-C (0.020 g) was stirred under an atmosphere of H_2 for 18 h. The Pd-C was then removed by filtration through a plug of Celite, and the solvent was removed under reduced pressure. The crude mixture was purified using column chromatography to give two colorless compounds that were identified as **3** (0.056 g, yield = 63% over 2 steps) and macrocycle 7H_2 (0.027 g, yield = 65% over 2 steps). Macrocycle (7H_2); m.p. 258-260 °C; ^1H NMR (400 MHz, CDCl_3 , 298 K): $\delta = 1.30$ (m, 12H, H_{alkyl}), 1.70 (m, 4H, H_{alkyl}), 3.86 (t, 4H, $J = 6.0$ Hz, H_G), 4.52 (d, 4H, $J = 6.0$ Hz, H_D), 6.71 (d, 4H, $J = 8.5$ Hz, H_F), 7.10 (d, 4H, $J = 8.5$ Hz, H_E), 7.94 (m, 3H, $H_A + H_C$), 8.29 (d, 2H, $J = 8.0$ Hz, H_B); ^{13}C NMR (100 MHz, CDCl_3 , 298 K): $\delta = 25.4, 28.1, 28.4, 28.7, 42.9, 67.4, 114.7, 125.3, 129.2, 129.8, 138.9, 148.8, 158.6, 163.1$; LRFAB-MS (3-NOBA matrix): $m/z = 516$ $[MH]^+$; HRFAB-MS (3-NOBA matrix): $m/z = 516.28550$ (calcd. for $\text{C}_{12}\text{H}_{38}\text{N}_3\text{O}_4$, 516.28623).



Ring closing metathesis and hydrogenation of Pd(1)(5)

(a) To an anhydrous dichloromethane solution (200 mL) of Grubbs' catalyst (0.016 g, 1.9×10^{-2} mmol) under an atmosphere of N_2 , was added *via* a double ended needle, Pd(1)(5) (0.367 g, 1.93×10^{-1} mmol) in anhydrous dichloromethane (50 mL). The solution was stirred at room temperature for 18 h. The solvent was removed under vacuum to give a dark green solid (0.352 g).

(b) A mixture of the yellow solid obtained in part (a) (0.33 g) in THF (30 mL), and 10% w/w Pd-C (0.033 g) was stirred under an atmosphere of H_2 for 18 h. The Pd-C was then removed by filtration through a plug of Celite, and the solvent was removed under reduced pressure. The crude mixture was purified using column chromatography to give two colorless compounds that were identified as **5** (0.17 g yield = 69% over 2 steps) and **7H₂** (0.071 g, yield = 71% over 2 steps).



6H₂: To Pd6 (0.131 g, 7.56×10^{-2} mmol) in dichloromethane (10 mL) and methanol (10 mL) was added potassium cyanide (0.075 g, 1.15 mmol) in methanol (2 mL). The solution was stirred for 1 hour at room temperature and then heated gently to reduce the overall volume to less than 5 mL. The resulting mixture was portioned between dichloromethane (25 mL) and water (25 mL). The organic layer was collected and the water extracted with further dichloromethane (10 mL). The combined organic extracts were washed with further water (25 mL) and then dried over anhydrous sodium sulfate. After filtration, the solvent was removed under reduced pressure and the crude residue purified by column chromatography (1:99

EtOAc:CH₂Cl₂) to give the title compound as a colourless solid (0.119 g, yield = 97%). m.p. 157 °C (dec); ¹H NMR (400 MHz, CDCl₃, 298 K): δ= 1.32 (m, 8H, H_{alkyl}), 1.37 (s, 54H, H_h), 1.46 (m, 4H, H_{alkyl}), 1.71 (m, 4H, H_{alkyl}), 3.76 (t, 4H, *J* = 6.3 Hz, H_G), 4.31 (d, 4H, *J* = 6.1 Hz, H_D), 4.38 (s, 4H, H_c), 6.30 (d, 4H, *J* = 8.6 Hz, H_F), 6.48 (d, 4H, *J* = 8.8 Hz, H_e), 6.63 (d, 4H, *J* = 8.6 Hz, H_E), 7.06 (d, 4H, *J* = 8.8 Hz, H_d), 7.14 (m, 14H, H_b + H_g), 7.31 (d, 12H, *J* = 7.3 Hz, H_f), 7.63 (t, 1H, *J* = 7.8 Hz, H_a), 7.97 (t, 1H, *J* = 7.8 Hz, H_A) 8.43 (d, 2H, *J* = 7.8 Hz, H_B), 9.49 (t, 2H, *J* = 6.1 Hz, H_C); ¹³C NMR (100 MHz, CDCl₃, 298 K): δ= 24.4, 27.3, 27.4, 28.2, 30.4, 33.3, 41.6, 62.0, 65.8, 67.6, 111.9, 112.0, 119.1, 123.1, 124.3, 127.6, 128.4, 129.6, 131.1, 136.1, 137.6, 139.2, 143.0, 147.3, 148.1, 154.6, 155.2, 156.8, 162.8; LRFAB-MS (3-NOBA matrix): *m/z* = 1627 [*M*]⁺; HRFAB-MS (3-NOBA matrix): *m/z* = 1628.00326 (calcd. for ¹²C₁₁₁¹³CH₁₃₀N₄O₆, 1628.00239).

2.4 References and Notes

- [1] C. O. Dietrich-Buchecker, J.-P. Sauvage, J.-P. Kintzinger, *Tetrahedron Lett.* **1983**, *24*, 5095-5098.
- [2] a) J.-P. Sauvage, C. Dietrich-Buchecker, G. Rapenne in *Molecular Catenanes, Rotaxanes and Knots* (Eds.: J.-P. Sauvage, C. Dietrich-Buchecker), Wiley-VCH, **1999**; b) J.-P. Collin, C. Dietrich-Buchecker, P. Gaviña, M. C. Jimenez-Molero, J.-P. Sauvage, *Acc. Chem. Res.* **2001**, *34*, 477-487.
- [3] a) N. Armaroli, V. Balzani, J.-P. Collin, P. Gaviña, J.-P. Sauvage, B. Ventura, *J. Am. Chem. Soc.* **1999**, *121*, 4397-4408; b) L. Raehm, J.-M. Kern, J.-P. Sauvage, *Chem. Eur. J.* **1999**, *5*, 3310-3317.
- [4] a) D. Pomeranc, D. Jouvenot, J.-C. Chambron, J.-P. Collin, V. Heitz, J.-P. Sauvage, *Chem. Eur. J.*, **2003**, *9*, 4247-4254; b) L. Hogg, D. A. Leigh, P. J. Lusby, A. Morelli, S. Parsons, J. K. Y. Wong, *Angew. Chem.* **2004**, *116*, 1238-1241; *Angew. Chem. Int. Ed.* **2004**, *43*, 1218-1221.
- [5] For complexes in which metal coordination forms part of the macrocycle in a rotaxane see: a) K.-S. Jeong, J. S. Choi, S.-Y. Chang, H.-Y. Chang, *Angew. Chem.* **2000**, *112*, 1758-1761; *Angew. Chem. Int. Ed.* **2000**, *39*, 1692-1695; b) S.-Y. Chang, J. S. Choi, K.-S. Jeong, *Chem. Eur. J.* **2001**, *7*, 2687-2697; c) S.-Y. Chang, K.-S. Jeong, *J. Org. Chem.* **2003**, *68*, 4014-4019; d) S.-Y. Chang, H.-Y. Jang, K.-S. Jeong, *Chem. Eur. J.* **2003**, *9*, 1535-1541. For complexes in which metal coordination forms

part of the thread in a rotaxane see: e) K.-M. Park, D. Whang, E. Lee, J. Heo, K. Kim, *Chem. Eur. J.* **2002**, *8*, 498-508. For complexes in which metal coordination forms the stoppers in a rotaxane see: f) R. B. Hannak, G. Färber, R. Konrat, B. Kräutler, *J. Am. Chem. Soc.* **1997**, *119*, 2313-2314; g) J.-C. Chambron, J.-P. Collin, J.-O. Dalbavie, C. O. Dietrich-Buchecker, V. Heitz, F. Odobel, N. Solladié, J.-P. Sauvage, *Coord. Chem. Rev.* **1998**, *178-180*, 1299-1312; h) A. J. Baer, D. H. Macartney, *Inorg. Chem.* **2000**, *39*, 1410-1417; i) G. J. E. Davidson, S. J. Loeb, N. A. Parekh, J. A. Wisner, *J. Chem. Soc., Dalton Trans.* **2001**, 3135-3136. For polyrotaxanes based on metal coordination polymers see: j) S. R. Batten, R. Robson, *Angew. Chem.* **1998**, *110*, 1558-1595; *Angew. Chem. Int. Ed.* **1998**, *37*, 1460-1494; k) A. J. Blake, N. R. Champness, P. Hubberstey, W.-S. Li, M. A. Withersby, M. Schröder, *Coord. Chem. Rev.* **1999**, *183*, 117-138; l) K. Kim, *Chem. Soc. Rev.* **2002**, *31*, 96-107.

[6] N. Armaroli, L. De Cola, V. Balzani, J.-P. Sauvage, C. O. Dietrich-Buchecker, J.-M. Kern, A. Bailal, *J. Chem. Soc. Dalton Trans.* **1993**, 3241-3247.

[7] M. Consuelo Jiménez, C. Dietrich-Buchecker, J.-P. Sauvage, *Angew. Chem.* **2000**, *112*, 3422-3425; *Angew. Chem. Int. Ed.* **2000**, *39*, 3284-3287.

[8] For a rotaxane which utilizes square planar metal complexes as the stoppers see S. J. Loeb, J. A. Wisner, *Chem. Commun.* **1998**, 2757-2758. For a pseudo-rotaxane based on a square planar metal geometry see C. Hamann, J.-M. Kern, J.-P. Sauvage, *Dalton Trans.* **2003**, 3770-3775.

[9] T. Moriuchi, S. Bandoh, M. Miyaishi, T. Hirao, *Eur. J. Inorg. Chem.* **2001**, 651-657.

[10] a) T. J. Kidd, D. A. Leigh, A. J. Wilson, *J. Am. Chem. Soc.* **1999**, *121*, 1599-1600; b) J. S. Hannam, T. J. Kidd, D. A. Leigh, A. J. Wilson, *Org. Lett.* **2003**, *5*, 1907-1910.

[11] a) J. E. Kickham, S. J. Loeb, *Inorg. Chem.* **1994**, *33*, 4351-4359; b) G. R. Newkome, T. Kawato, D. K. Kohli, W. E. Puckett, B. D. Olivier, G. Chiari, F. R. Fronczek, W. A. Deutsch, *J. Am. Chem. Soc.* **1981**, *103*, 3423-3429.

[12] **L6Pd**: C₁₂₁H_{141.5}N_{8.5}O₆Pd, *M* = 1917.33, yellow block, crystal size 0.47 × 0.31 × 0.27 mm³, triclinic, *P* $\bar{1}$, *a* = 15.7840(10), *b* = 15.9967(10), *c* = 22.8029(14) Å, α = 84.9850(10), β = 71.8430(10), γ = 80.5460(10)°, *V* = 5392.5(6) Å³, *Z* = 2, ρ_{calcd} = 1.193 Mg m⁻³; Mo *K* α radiation (graphite monochromator, λ = 0.71073 Å), μ = 0.231

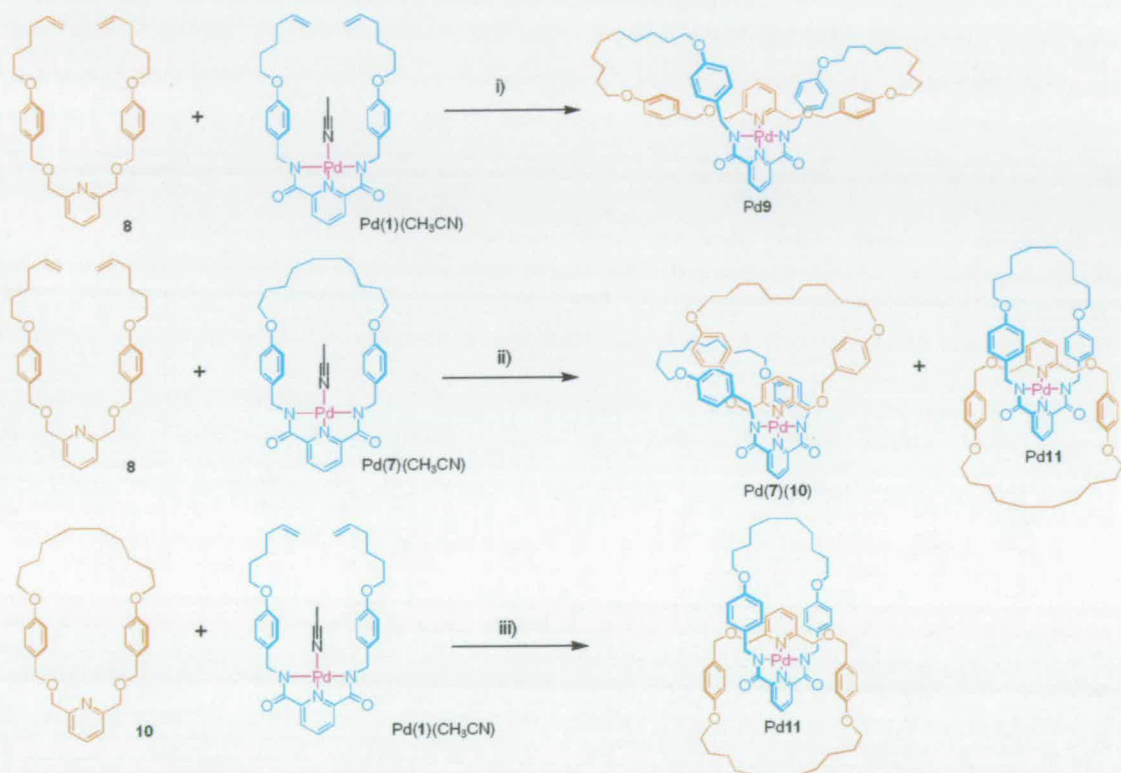
mm⁻¹, $T = 150(2)$ K. 34043 data (15412 unique, $R_{\text{int}} = 0.0331$, $2.06 < \theta < 23.26^\circ$), were collected on a Bruker SMART CCD diffractometer using narrow frames (0.5° in ω), and were corrected semiempirically for absorption and incident beam decay. Data beyond 0.9 \AA were weak and were not used for refinement. The structure was solved by direct methods (SIR92)^[13] and refined by full-matrix least-squares against F^2 .^[14] Phenyl groups were constrained to be rigid hexagons and hydrogen atoms were placed in calculated positions. The whole macrocyclic component, inclusive of the Pd atom, is disordered (50:50) over two positions. The alkyl chain is further disordered and the refinement of this portion of the structure was controlled by application of restraints to both 1, 2 and 1, 3 distances and use of a common isotropic displacement parameter for all C-atoms forming the chain. The only disorder present in the thread is in two of the *t*-butyl groups. That based on C244 is rotationally disordered (70:30) with the central carbon atom (C244) fully occupied and the two alternative sets of methyl positions related by a 60° rotation about the C244-C243 bond. All atoms in the groups were refined with anisotropic displacement parameters (adps), those of 'opposite' C-atoms being constrained to be equal. The *t*-butyl group attached to C263 is disordered (70:30) over two positions and was refined isotropically. Similarity restraints were applied to chemically equivalent 1,2 and 1,3 distances in both disordered *t*-butyl groups. In the latter stages of refinement there was still significant unassigned electron density associated with diffuse solvent. This density was modelled using the procedure of van der Sluis and Spek,^[15] comprising 199 electrons per unit cell, which corresponds to approximately 4.5 MeCN solvent molecules per asymmetric unit; values of M , $F(000)$, μ etc. have been calculated on this assumption. $wR = \{\Sigma[w(F_o^2 - F_c^2)^2] / \Sigma[w(F_o^2)^2]\}^{1/2} = 0.2527$, conventional $R = 0.0806$ for F values of 15412 reflections with $F_o^2 > 2\sigma(F_o^2)$, $S = 1.115$ for 885 parameters. Residual electron density extremes were 1.03 and -0.94 e\AA^{-3} . Crystallographic data have been deposited with the Cambridge Crystallographic Data Centre as supplementary publication no. CCDC-229418. These data can be obtained free of charge via <http://www.ccdc.cam.ac.uk/conts/retrieving.html> or from the Cambridge Crystallographic Data Centre, 12 Union Road, Cambridge CB2 1EZ, UK; fax: +44 1223 336033; or deposit@ccdc.cam.ac.uk.

[13] A. Altomare, G. Cascarano, C. Giacovazzo and A. Guagliardi. *J. Appl. Cryst.* **1993**, *26*, 343-350.

- [14] G. M. Sheldrick, University of Göttingen, Germany, 1997.
- [15] P. Van der Sluis and A. L. Spek, *Acta. Cryst.* **1990**, *A46*, 194-201.
- [16] H. W. Gibson, S. H. Lee, P. T. Engen, P. LeCavalier, J. Sze, Y. X. Shen, M. Bheda, *J. Org. Chem.*, **1993**, *58*, 3748 – 3756.
- [17] D. A. Leigh, P. J. Lusby, S. J. Teat, A. J. Wilson, J. K.Y. Wong, *Angew. Chem.* **2001**, *113*, 1586-1591; *Angew. Chem. Int. Ed.* **2001**, *40*, 1538-1543.
- [18] M. Kristiansen, J. Eriksen, K. A. Joergensen, *J.Chem.Soc. Perkin Trans. 1*, **1990**, 101-103.
- [19] K. Tsuda, N. Ikeawa, R. Takasaki, Y. Yamakawa, *Pharm. Bull.*, **1953**, 142-145.

Chapter Three Synopsis

In chapter two the structural requirements for the synthesis of a [2]rotaxane around a Pd(II) ion were described. Using this knowledge we then attempted to assemble an analogous [2]catenane in the same manner. We explored several routes to a Pd(II)-[2]catenane, varying the sequence that the rings were cyclised, and it proved possible to selectively form each of the isomers shown in Scheme 1.



Scheme 1. The selective synthesis of three isomeric complexes, Pd9, Pd(7)(10) and Pd11. Reagents and conditions: (i) 1. CH₂Cl₂, 1 h, 93%; 2a. 1st generation Grubbs' catalyst (Cy₃P)₂Cl₂RuCHPh, 0.2 equiv, CH₂Cl₂, 20 h; 2b. H₂, Pd-C, THF, 4 h, 75% (over 2 steps). (ii) 1. CH₂Cl₂, 1 h, a 3:2 ratio of Pd(7)(exo-8): Pd(7)(endo-8), isolated in 89% yield; 2a. 1st generation Grubbs' catalyst (0.1 equiv), CH₂Cl₂, 22 h; 2b. H₂, Pd-C, Na₂CO₃, THF, 18 h. (iii) 1. CH₂Cl₂, 1 h, 78%; 2a. Grubbs' 1st generation catalyst (0.1 equiv), CH₂Cl₂, 22 h; 2b. H₂, Pd-C, THF, 4 h, 78% (over 2 steps).

Double macrocyclisation of Pd(1)(CH₃CN) and 8 with both ligands coordinated to the TM centre resulted in exclusive formation of the covalently linked macrocycle complex Pd9. Cyclisation of the monodentate ligand 8 following complexation with macrocycle complex Pd(7)(CH₃CN) resulted in a mixture of two products (catenane Pd11 and non-interlocked ring isomer Pd(7)(10)). However, cyclisation of the tridentate ligand Pd(1)(CH₃CN), following complexation with macrocycle 10,

resulted in exclusive formation of the desired [2]catenate Pd(11). In summary it proved possible to select topology and connectivity through metal-directed macrocyclisation reactions.

Chapter 3: A Square Planar Palladium [2]Catenate and Two Non-Interlocked Isomers

Published as “*Selecting topology and connectivity through metal-directed macrocyclization reactions: a square planar palladium [2]catenate and two non-interlocked isomers*” A.-M. L. Fuller, D. A. Leigh, P. J. Lusby, A. M. Z. Slawin, D. B. Walker, *J. Am. Chem. Soc.* **2005**, *127*, 12612-12619.

Acknowledgements

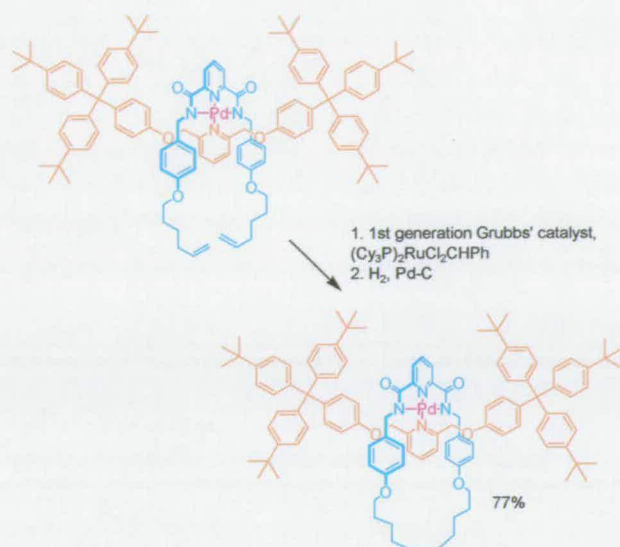
The following people are gratefully acknowledged for their contribution to this chapter: Dr. P. Lusby synthesized catenand **11H₂** for the first time and investigated the interconversion of the two atropisomers Pd(7)(*exo*-**8**):Pd(7)(*endo*-**8**); A.-M. L. Fuller synthesized macrocycle **9H₂** for the first time and synthesized catenand **11H₂** from the mixture of atropisomers; Prof. A. M. Z. Slawin solved the X-ray crystal structures of Pd**9**, Pd**11** and Pd(7)(**10**).

3.1 Introduction

The use of transition metal ions to direct the synthesis of interlocked architectures remains amongst the most efficient strategies available.¹⁻⁸ In addition to exploiting reversible coordination chemistry to deliver high yields of thermodynamically privileged catenanes incorporating metals in their ring frameworks,² catenanes – metal complexes of organic interlocked macrocyclic ligands – can be formed through metal template macrocyclization reactions. However, whilst the use of tetrahedral copper(I) geometry to hold bidentate ligands in a geometry suitable for subsequent interlocking macrocyclization reactions has been extensively developed over a twenty year period,³⁻⁸ the transposition of this basic concept to other coordination modes has been slow to develop. Although Sokolov alluded to the possibility of using octahedral ions to template catenane synthesis as early as 1973,⁹ attempts to prepare interlocked architectures in this way initially met with limited success^{2c,10} and it is only recently¹¹ that efficient synthetic routes based on octahedral coordination have been developed. There is also a single example¹² of 5-coordinate zinc(II) being used to direct the formation of a [2]catenane and a remarkable crown ether-threaded organometallic catenane templated about a magnesium atom that also forms part of one ring.¹³

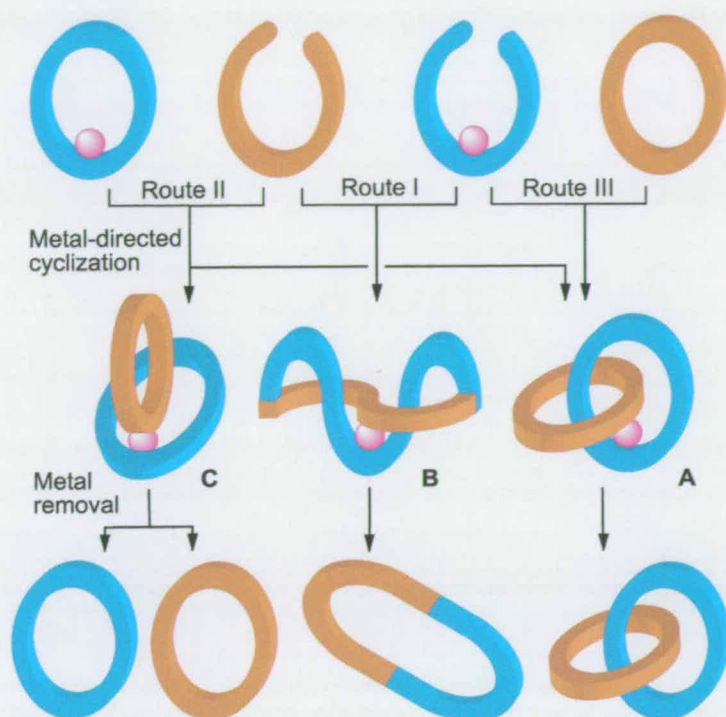
At first sight the use of a template strategy to produce interlocked macrocyclic ligands for metals with a square planar coordination geometry might appear somewhat counter-intuitive. Square planar coordination obviously involves a 2D donor set, whilst interlocking of the two rings requires two crossing points (one positive, one negative¹⁴) necessitating control over the nature of covalent bond formation in the third dimension. However, by using a tridentate-monodentate ligand combination, the relative orientation of the ligands coordinated to the metal can be varied (formally by rotation about the monodentate ligand-metal bond) and therefore, in principle, systems can be designed to extend above and below the plane of the square planar coordination mode and direct a subsequent ring closure reaction. Indeed, there are several examples^{15,16} of the orthogonal alignment of organic fragments using such a '3+1' donor set of ligands and we recently found it was possible to exploit this effect to form a mechanically interlocked structure (Scheme 3.1).¹⁷ Through a combination of electronic and steric factors, the square planar

palladium holds the monodentate 2,6-dimethylenoxy-pyridine thread orthogonal to a *bis*-olefin terminated tridentate benzylic amide macrocycle-precursor such that cyclization by ring closing olefin metathesis (RCM) results in a [2]rotaxane in 77% yield.



Scheme 3.1. The palladium(II)-directed synthesis of a [2]rotaxane.¹⁷

However, extending this strategy to catenane synthesis is not straightforward. Even though oligomer and polymer formation could be minimized by metal chelation of the acyclic building blocks, a double macrocyclization strategy could produce three different isomeric products (**A-C**, Scheme 3.2) and even pre-forming one of the rings prior to attaching the building blocks to the metal could still afford either the interlocked (**B**) or non-interlocked (**C**) complex. We therefore explored several potential routes to a square planar coordination [2]catenane, varying the sequence that the rings were cyclized and whether or not the building blocks were attached to the metal prior to macrocyclization. Remarkably, in this way it proved possible to find synthetic routes to each of the isomers **A-C** shown in Scheme 3.2.



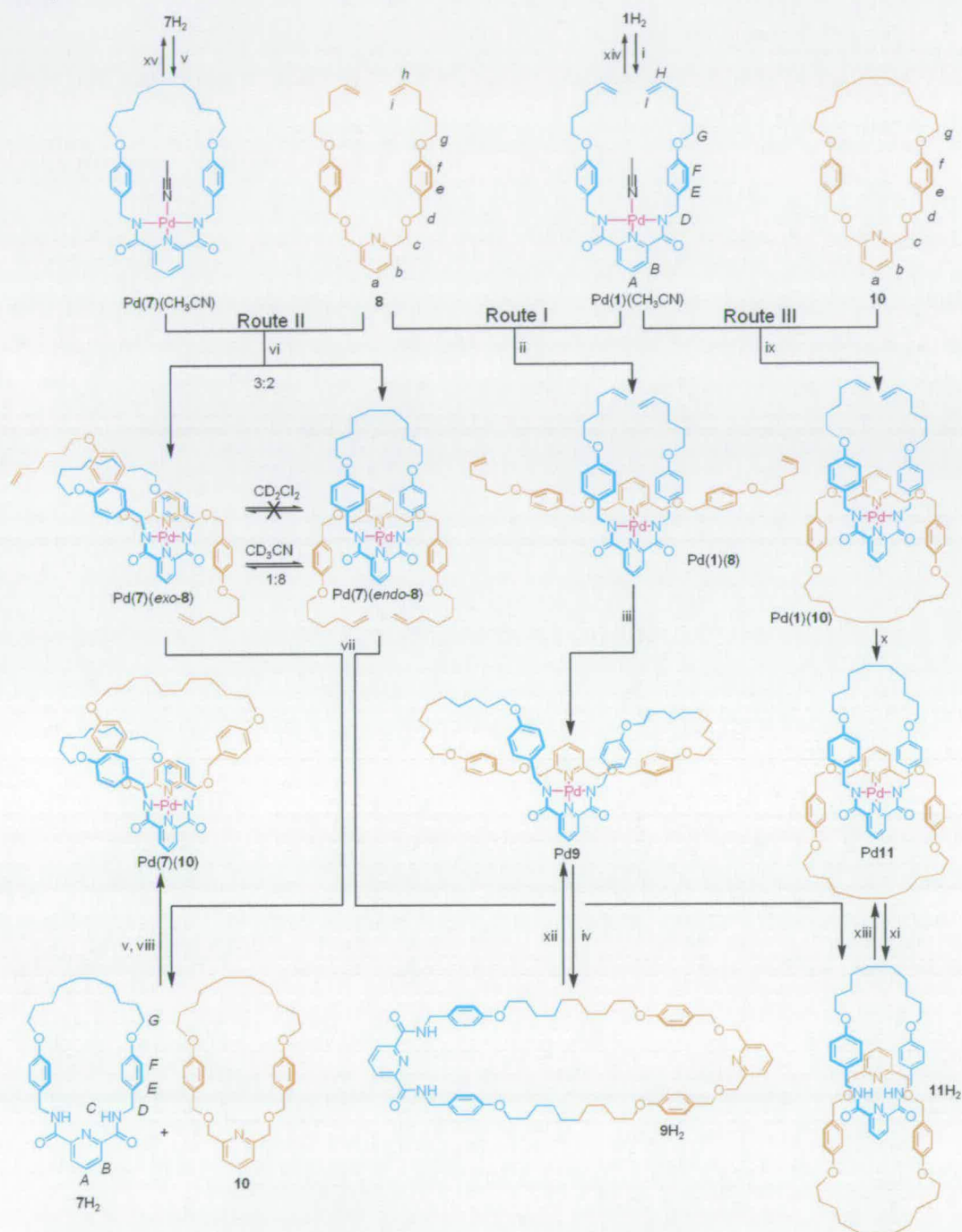
Scheme 3.2. Schematic representation of the three isomers that result from synchronous or simultaneous metal-directed cyclization of two acyclic building blocks. Homo-dimerization is avoided by using one tridentate ligand (blue) and one monodentate ligand (orange) and a metal with a preferred square planar coordination geometry. Other possible reaction products could potentially include knots – although knotted isomers of A-C are easily precluded by limiting the size of the building blocks – and higher cyclic, catenated and knotted oligomers and polymers resulting from the condensation of more than just one of each building block (minimized by carrying out the cyclization reactions at high dilution).

3.2 Results and Discussion

Route I – Simultaneous metal-directed olefin metathesis of 1 and 8

The first route we investigated was the possible double macrocyclization of the tridentate (**1H**₂) and monodentate **8** building blocks, with both ligands already coordinated to a square planar metal, Pd(**1**)(**8**) (Scheme 3.3, Route I). The monodentate ligand **8** was prepared in two steps from 4-hydroxybenzyl alcohol (see experimental section). When combined with the known Pd(**1**)(CH₃CN) complex in dichloromethane this provided the tetra-terminal olefin complex, Pd(**1**)(**8**), in 93% yield (Scheme 3.3, ii), ¹H NMR confirming the exchange of the acetonitrile ligand for **8** (Figure 3.1 a and 3.1 b, note the upfield shift of the aromatic resonances of **1**

(H_E and H_F) by 0.8 and 0.2 ppm respectively due to stacking with the pyridine group of **8**).



Scheme 3.3. Reagents and conditions: (i) $\text{Pd}(\text{OAc})_2$, CH_3CN , 1 h, 76%; (ii) CH_2Cl_2 , 1 h, 93%; (iii) a. 1st generation Grubbs' catalyst $(\text{Cy}_3\text{P})_2\text{Cl}_2\text{RuCHPh}$, 0.2 equiv, CH_2Cl_2 , 20 h; b. H_2 , Pd-C, THF, 4 h, 75% (over 2 steps); (iv) KCN, MeOH, CH_2Cl_2 , 20 °C, 1 h and then 40 °C, 0.5 h, 94%; (v) $\text{Pd}(\text{OAc})_2$, CH_3CN , 1 h, 93%; (vi) CH_2Cl_2 , 1 h, a 3:2 ratio of $\text{Pd}(7)(\text{exo-}8)$: $\text{Pd}(7)(\text{endo-}8)$, isolated in 89% yield; (vii) a. 1st generation Grubbs' catalyst (0.1 equiv), CH_2Cl_2 , 22 h; b. H_2 , Pd-C, Na_2CO_3 , THF, 18 h; c. KCN, MeOH, CH_2Cl_2 , 20 °C, 1 h and then 40 °C, 0.5 h, 7H_2 (44% over 3 steps), **10** (41%), **11H₂** (25%); (viii) part (v) and then CH_2Cl_2 , 1 h, 78%; (ix) CH_2Cl_2 , 1 h, 69%; (x) a. Grubbs' 1st generation catalyst (0.1 equiv), CH_2Cl_2 , 22 h; b. H_2 , Pd-C, THF, 4 h, 78% (over 2 steps); (xi) KCN, MeOH,

CH_2Cl_2 , 20 °C, 1 h and then 40 °C, 0.5 h, 97%; (xii) $\text{Pd}(\text{OAc})_2$, CH_3CN , 60 °C, 4 h, 85%; (xiii) $\text{Pd}(\text{OAc})_2$, CH_3CN , 60 °C, 4 h, 79%; (xiv) KCN , MeOH , CH_2Cl_2 , 20 °C, 1 h and then 40 °C, 0.5 h, 98%; (xv) KCN , MeOH , CH_2Cl_2 , 20 °C, 1 h and then 40 °C, 0.5 h, 95%.

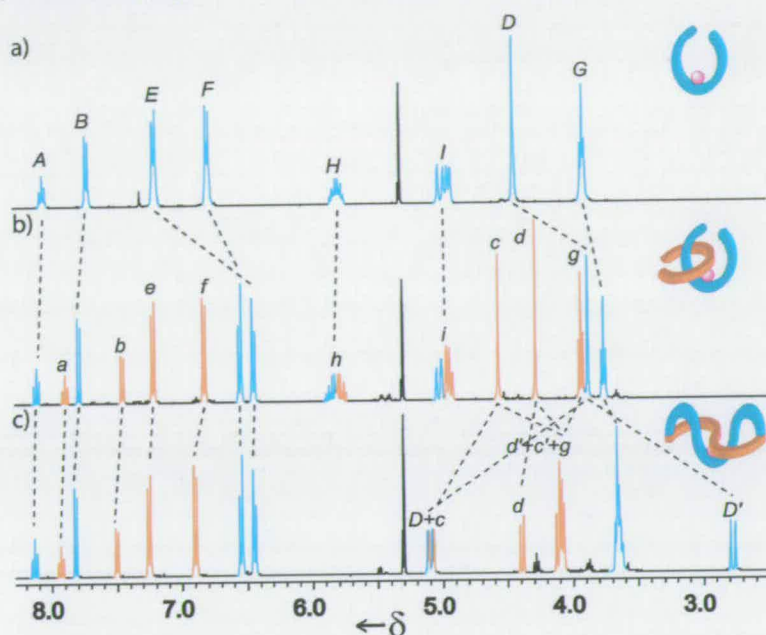


Figure 3.1. ^1H NMR spectra (400 MHz, 19:1 CD_2Cl_2 : CD_3CN , 298 K) of (a) $\text{Pd}(\mathbf{1})(\text{CH}_3\text{CN})$ (b) $\text{Pd}(\mathbf{1})(\mathbf{8})$ (c) $\text{Pd}\mathbf{9}$. The lettering refers to the assignments shown in Scheme 3.

Subjecting $\text{Pd}(\mathbf{1})(\mathbf{8})$ to RCM using the first generation Grubbs olefin metathesis catalyst,¹⁸ followed by hydrogenation of the resulting internal double bond (Scheme 3.3, iii), gave a single species in 75% isolated yield for the two steps. FAB mass spectrometry confirmed that the complex had the molecular weight ($m/z = 1110$, MH^+) necessary to be one of the isomers A-C and the ^1H NMR spectrum (Figure 3.1c) showed significant differences from $\text{Pd}(\mathbf{1})(\mathbf{8})$, most notably in the region 2.5–5.5 ppm, indicating that some change in orientation of the building blocks had occurred upon RCM. Treatment of the complex with potassium cyanide (Scheme 3.3, iv) gave a single organic compound (confirmed by mass spectrometry and ^1H NMR), ruling out the possibility that the product of the RCM was the two non-interlocked ring isomer, C, i.e. the product of Route I could not be $\text{Pd}(\mathbf{7})(\mathbf{10})$.

The ^1H NMR spectrum (Figure 3.2 c) of the de-metallated structure did not show the shielding effects characteristic of benzylic amide macrocycle interlocked systems, the chemical shifts being virtually identical to the independently prepared free ligands, $\mathbf{7H}_2$ and $\mathbf{10}$ (Figure 3.2 a and 3.2 d, respectively). This suggested that the ligand isomer formed from Route I was probably $\mathbf{9H}_2$, the single large macrocycle

(B) resulting from intercomponent metathesis between the **1** and **8** olefin groups. This assignment was confirmed when single crystals suitable for X-ray crystallography were grown from slow cooling of a hot, saturated acetonitrile solution of the complex formed by Route I. The solid state structure (Figure 3.3) shows the tetradentate 58-membered single macrocycle satisfying the square planar coordination geometry of the palladium, with the tridentate 2,6-dicarboxamidopyridine moiety held orthogonally to the monodentate 2,6-bis(oxymethylene)pyridine group. This results in twisting of the macrocycle, providing a single cross-over point in a distinctive figure-of-eight conformation (Figure 3.3 b). Although rare, this shape is not unique amongst coordination complexes of large flexible macrocycles, with other examples – based on octahedral metals – reported by the groups of Sauvage (a 58-membered hexadentate *bis*-terpy macrocycle bound to iron(II))¹⁰ and Busch (a 40-membered ring coordinating to nickel(II) *via* 2,6-diiminopyridine groups).¹⁹ In all cases the metal ion provides the cross-over point, imposing helical chirality on what would otherwise be intrinsically achiral macrocycles (for Pd**9** both enantiomers are observed in the unit cell). Re-examination of the ¹H NMR spectrum (Figure 3.1 c) reveals that the ring conformation of Pd**9** is conserved from the solid state to solution. The low (C₂) symmetry results in the individual protons of the H_D, H_C and H_d methylene groups (H_D, H_D', H_C, H_C', H_d and H_d') being held in diastereotopic environments, the magnitude of the splittings following their proximity to the cross-over point (H_D and H_D' are split by nearly 2.5 ppm, H_C and H_C' by 1.0 ppm, and H_d and H_d' by just 0.4 ppm). Interestingly, the aromatic region of Pd**9** is virtually identical to that of Pd(**1**)(**8**) (Figure 3.1b) suggesting that whilst the alkyl residues may be mobile, the rest of the acyclic precursor complex is well-organized for intercomponent olefin metathesis.

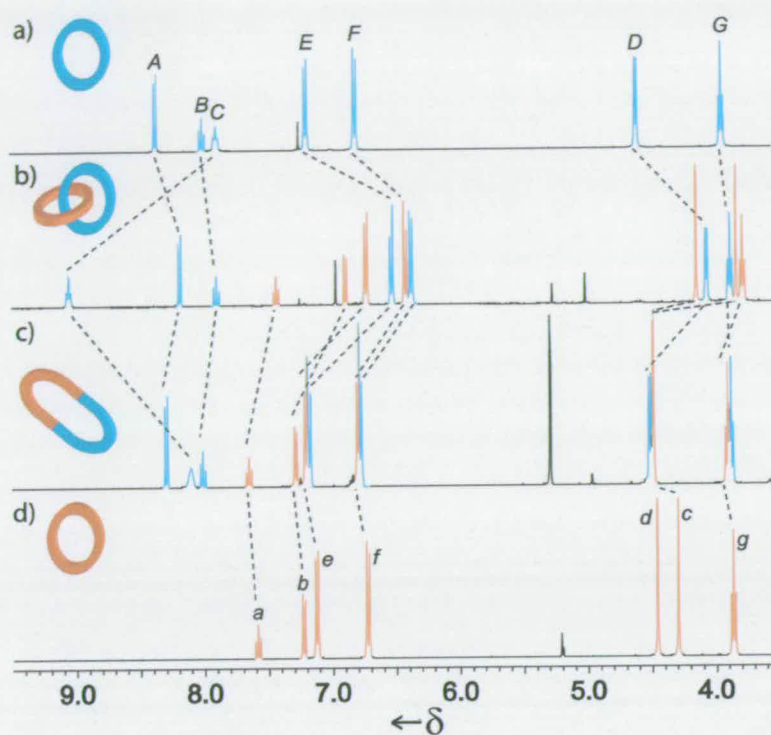


Figure 3.2. ^1H NMR spectra (400 MHz, CDCl_3 , 298 K) of (a) 7H_2 (b) 11H_2 (c) 9H_2 (d) **10**. The lettering refers to the assignments shown in Scheme 3.

Since the attempted simultaneous double macrocyclization strategy had given rise to intercomponent bond formation, we sought to exclude this possibility²⁰ by pre-forming one or other of the rings prior to the second, metal-directed, cyclization reaction (Scheme 3.3, Routes II and III).

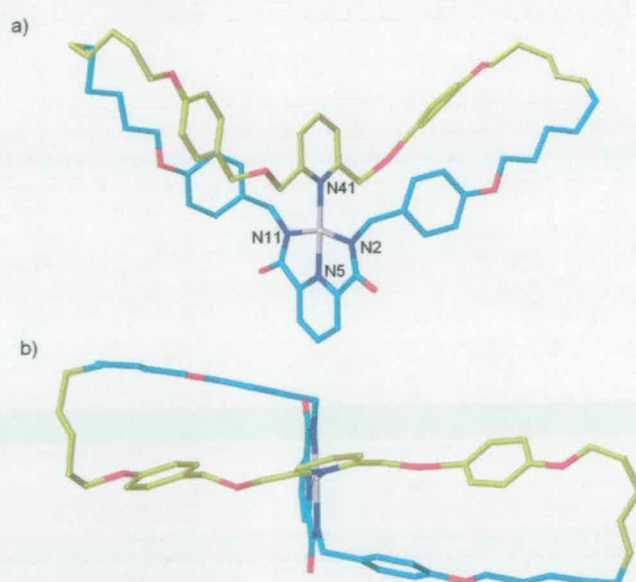


Figure 3.3. X-ray crystal structure of ‘figure-of-eight’ complex Pd**9** grown by slow cooling of a warm, saturated solution of the complex in acetonitrile. a) Side-on and b) top views. Carbon atoms

originating from **1** are shown in light blue, those from **8** in yellow. Oxygen atoms are red, nitrogen dark blue, palladium grey. Selected bond lengths [Å]: Pd-N2 2.015, Pd-N5 1.941, Pd-N11 2.027, Pd-N41 2.052; tridentate fragment bite angle [°]: N2-Pd-N11 161.0.

Route II – Metal-directed RCM of **8**

Tridentate macrocycle **7H₂** was prepared in 57% yield by treatment of pyridine-2,6-dicarbonyl dichloride with the appropriate diamine under high dilution conditions (see Supporting Information). Subsequent complexation with palladium(II) acetate afforded Pd(**7**)(CH₃CN) (93%, scheme 3.3, v). Threading of **8** through the cavity of Pd(**7**)(CH₃CN) *via* the substitution of the coordinated acetonitrile was attempted by simple mixing of the two in dichloromethane at room temperature (Scheme 3.3, vi). While mass spectrometry confirmed the ligand exchange, the ¹H NMR spectrum of the crude product was unexpectedly complex. Closer inspection of the thin layer chromatographic analysis of the reaction mixture revealed two products with very similar R_f values in a ratio of approximately 2:3. Despite their proximity, these proved amenable to separation by preparative thin layer chromatography on silica gel-coated plates (CH₂Cl₂:MeOH, 98.5:1.5 as eluent). The isolated complexes gave indistinguishable fragmentation patterns by electrospray ionization mass spectrometry, the molecular mass ion suggesting they were both isomers of Pd(**7**)(**8**). However, the ¹H NMR spectra exhibited important differences between the two products. When compared to the spectra of the starting materials, the minor isomer (lower R_f, Figure 3.4 d), showed significant shielding of the **7** benzyl rings (H_E and H_F) indicative of aromatic stacking with the pyridine group of **8**. In contrast, the major isomer (higher R_f, Figure 3.4 b), showed no evidence of stacking interactions but a greater degree of complexity in both the **8** signals (two sets of non-equivalent H_b, H_c, H_d, H_e and H_f resonances) and the H_D methylene groups (an AB system with a 2.5 ppm separation between the two proton environments) of **7**. From this we tentatively assigned the two products as ‘non-threaded’ (major isomer) and ‘threaded’ (minor isomer) atropisomers,²¹ Pd(**7**)(*exo*-**8**) and Pd(**7**)(*endo*-**8**) respectively (Scheme 3.3).

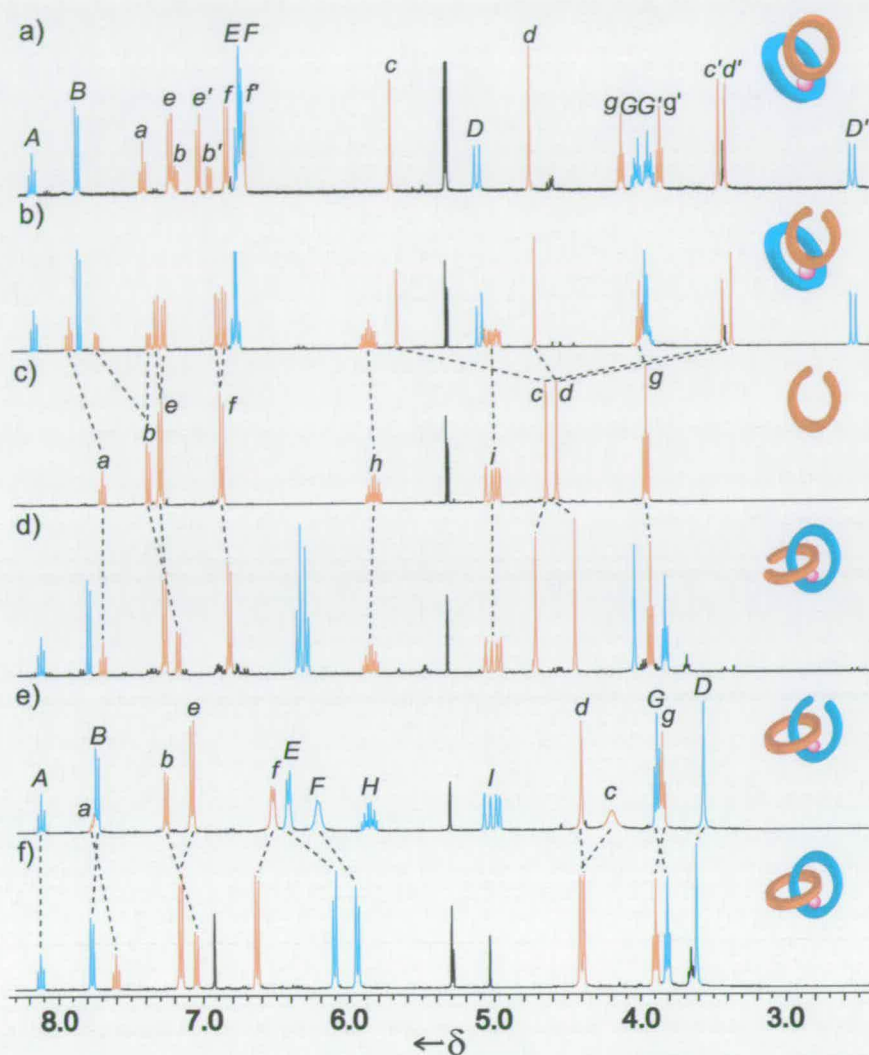


Figure 3.4. ^1H NMR spectra (400 MHz, CD_2Cl_2 , 298 K) of (a) Pd(7)(**10**) (b) Pd(7)(*exo*-**8**) (c) **8** (d) Pd(7)(*endo*-**8**) (e) Pd(1)(**10**) (f) Pd11. The lettering refers to the assignments shown in Scheme 3.

Intriguingly, CPK models suggested that cyclization of **8** could occur with *each* atropisomer of Pd(7)(**8**), suggesting that two compounds of identical connectivity but different conformations²² are predisposed to form topological isomeric products upon RCM – the [2]catenate, **B**, and the analogous non-interlocked double macrocycle structure, **C**. Sure enough, treatment of the 2:3 mixture of atropisomers with Grubbs' catalyst in CH_2Cl_2 , followed by hydrogenation and demetallation (Scheme 3.3, vii (three steps – the mixtures of topological and olefin isomers preventing the isolation of pure products until the end of the reaction sequence)) afforded three products: macrocycles 7H_2 (44%) and **10** (41%²³) arising from complex Pd(7)(**10**), and a further compound, which mass spectrometry confirmed to be a different isomer of 9H_2 , in 25% overall yield for the three steps.

^1H NMR spectroscopy of the new compound in CDCl_3 (Figure 3.2 b) revealed shielding of most resonances compared to the free macrocycles 7H_2 (Figure 3.2 a) and 10 (Figure 3.2 d) characteristic of interdigitation, suggesting that it was indeed the [2]catenand 11H_2 . The exception to the upfield trend in shifts were the amide protons (H_C), which were shifted significantly downfield (*ca.* 1.3 ppm) in the catenand compared to those of 7H_2 , indicative of a significant hydrogen-bonding interaction between the amide protons of one ring and the pyridine nitrogen of the other. In contrast, the analogous amide protons in the 58-membered free macrocycle 9H_2 occur at 8.11 ppm in CDCl_3 (Figure 3.2 c), only slightly downfield of their position in 7H_2 (7.88 ppm, Figure 3.2 a), meaning that little intramolecular hydrogen bonding is occurring in the large flexible macrocycle. Why is this internal hydrogen bonding absent when it is so clearly present in the mechanically bonded isomer 11H_2 ? Firstly, the size and nature of the solvent-exposed surfaces of the compact [2]catenand structure and the large, relatively open, macrocycle must be very different, making desolvation of the amide and pyridine residues in the catenane a significantly less energetically costly process. Secondly, with the 2,6-bis(oxymethylene)pyridine and 2,6-pyridinecarboxamide groups on different components, the macrocycles in 11H_2 can orientate themselves for inter-residue hydrogen bonding with little more than the loss of a single rotational degree of freedom. In contrast, alignment of the groups to enable a similar interaction within 9H_2 would significantly restrict the number of conformations accessible by the alkyl chains in the large flexible ring, the resulting losses in degrees of freedom raising the energy of the hydrogen bonded structure. This unusual orthogonal double bifurcated *bis*-pyridine hydrogen bonding interaction is also observed in the related [2]rotaxane system.¹⁷

Re-introduction of Pd(II) into the free ligand systems ($9\text{H}_2 \rightarrow \text{Pd}9$, Scheme 3.3, xii; $11\text{H}_2 \rightarrow \text{Pd}11$, Scheme 3.3, xiii; $7\text{H}_2 \rightarrow \text{Pd}(7)(\text{CH}_3\text{CN}) + 10 \rightarrow \text{Pd}(7)(10)$, Scheme 3.3, v, viii) proceeded smoothly in each case, the last two providing pure samples of complexes formed previously as intermediates during each pathway of the Route II syntheses. ESI mass spectrometry initially identified the formation of $\text{Pd}(7)(10)$, confirming that both macrocycles could simultaneously bind to palladium without being interlocked. ^1H NMR spectroscopy (Figure 3.4a) corroborated this result and

showed significant similarity (a diastereotopic environment for H_D , and two sets of signals for each H_b , H_c , H_d , H_e , H_f and H_g) to the presumed ‘non-threaded’ isomer of Pd(7)(8) (Figure 3.4b). These spectral features are consistent with orthogonal binding of the rings to the square planar geometry metal, with neither macrocycle being able to pass through the cavity of the other nor rotate (at least not rapidly on the NMR time scale in the case of the monodentate ligand) about the plane of the square planar coordination geometry. This means both macrocycles are perforce desymmetrized in the plane that they coordinate to the metal, i.e. top from bottom in **7** and left from right in **10** (as Pd(7)(10) is depicted in Figure 3.5a).

Pleasingly, the pure samples of Pd(7)(10) and Pd11 both provided single crystals suitable for structure elucidation by X-ray crystallography (Figure 3.5 and Figure 3.6, respectively). Between them, the X-ray crystal structures of Pd9, Pd(7)(10) and Pd11 not only confirm the identity of the metal complexes – a unique set of topological (Pd(7)(8) and Pd11) and constitutional (Pd9 and Pd(7)(10)/Pd11) isomers – but also the structural assignments of the free ligands inferred by the earlier ^1H NMR and mass spectrometry analysis.

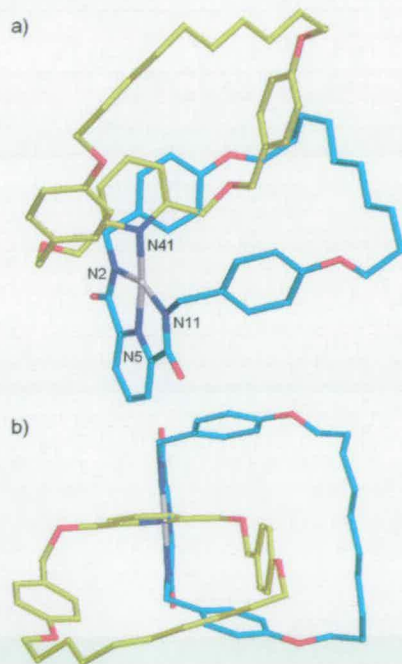


Figure 3.5. X-ray crystal structure of non-interlocked double macrocycle complex Pd(7)(10) grown from a saturated solution of the complex in acetone. a) Side-on and b) top views. Carbon atoms of the **7** macrocycle are shown in light blue and those of the **10** macrocycle in yellow; oxygen atoms are red, nitrogen dark blue, palladium grey. Selected bond lengths [\AA]: N2-Pd 2.032, N5-Pd 1.943, N11-Pd 2.032, N41-Pd 2.077; tridentate fragment bite angle [$^\circ$]: N2-Pd-N11 160.8.

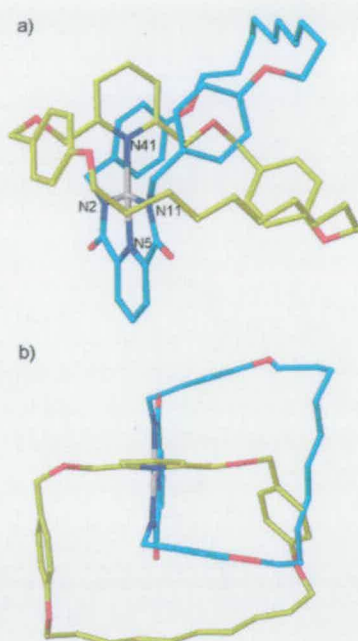


Figure 3.6. X-ray crystal structure of palladium [2]catenate Pd11 grown by slow cooling of a warm, saturated solution of the complex in acetonitrile. a) Side-on and b) top views. Carbon atoms of the 7 macrocycle are shown in light blue and those of the 10 macrocycle in yellow; oxygen atoms are red, nitrogen dark blue, palladium grey. Selected bond lengths [Å]: Pd-N2 1.934, Pd-N5 2.041, Pd-N11 2.036, Pd-N41 2.079; tridentate fragment bite angle [°]: N2-Pd-N11 160.2.

Atropisomer-specific synthesis of different topological isomers

Although RCM (and subsequent hydrogenation and de-metallation) of the mixture of the two Pd(7)(8) atropisomers gives a ratio of isolated interlocked to non-interlocked products similar to the starting atropisomer ratio, it does not necessarily follow that one atropisomer leads solely to one product. The interconversion of the two Pd(7)(8) atropisomers in solution was investigated by ^1H NMR spectroscopy. The initial ‘threaded’:‘non-threaded’ ratio of *ca.* 2:3 remained unchanged over 7 days in CD_2Cl_2 at RT. Similarly, spectra of pure samples of each of the compounds were invariant under these conditions, demonstrating that the atropisomers are kinetically stable at room temperature in a non-coordinating solvent. However, addition of $\sim 10\%$ CD_3CN to either of the pure atropisomer solutions or the 2:3 mixture led to a gradual change in the ‘threaded’:‘non-threaded’ ratio, rising to *ca.* 7:3 after 4 days. This suggests that the ‘threaded’ isomer is thermodynamically favored and that atropisomer interconversion can take place via the dissociation of **8** from either form of Pd(7)(8), the vacant coordination site being temporarily filled by a molecule of CD_3CN .

Accordingly, the reaction between **8** and Pd(7)(CH₃CN) was repeated in refluxing acetonitrile. After several hours, ¹H NMR spectroscopy showed a 7:3 ratio of the 'threaded':'non-threaded' forms of Pd(7)(**8**). Heating over two days increased the ratio to 8:1 after which no further change occurred.

RCM of single atropisomer samples of Pd(7)(**8**) in CH₂Cl₂ did, indeed, generate a single new species in each case. The product of RCM of the presumed Pd(7)(*endo*-**8**) complex was hydrogenated to give solely the [2]catenate, Pd**11**; the product of RCM of presumed Pd(7)(*exo*-**8**) proved unstable to hydrogenation,²³ so the metal was removed instead (KCN, MeOH, CH₂Cl₂, 20 °C, 1 h and then 40 °C, 0.5 h), liberating two different macrocycles, 7H₂ (96%) and the unsaturated olefin analogue of **10** (93%).

Route III - Metal-directed RCM of 1

Finally, we investigated the product distribution arising from pre-forming the monodentate macrocycle and applying metal-directed cyclization of the tridentate ligand (Scheme 3, Route III). Pd(**1**)(CH₃CN) and **10** were stirred together in dichloromethane at room temperature (Scheme 3.3, ix) and, in contrast to the analogous step in Route II, reacted to give a single product rather than a mixture of atropisomers. The ¹H NMR spectrum of Pd(**1**)(**10**) (Figure 3.4e) suggests the two ligands are threaded, the upfield shift of H_E and H_F compared to similar protons in the non-threaded Pd(**7**)(**10**) and Pd(**7**)(*exo*-**8**) complexes (Figure 3.4a and 3.4b, respectively) indicating π -stacking of the benzyl groups of **1** with the pyridine unit of **10**. It is difficult to distinguish between whether Pd(**1**)(**10**) can exist as threaded/non-threaded atropisomers but is formed solely as the Pd(*exo*-**1**)(**10**) isomer, or rather threaded and non-threaded forms of Pd(**1**)(**10**) are in equilibrium with the threaded conformation being thermodynamically preferred by several kcal mol⁻¹. In any event, RCM of Pd(**1**)(**10**) and subsequent hydrogenation (Scheme 3.3, x) afforded exclusively the [2]catenate, Pd**11**, in 78% yield, making this route both synthetically efficient and completely selective for the mechanically interlocked topological isomer.

3.3 Conclusions

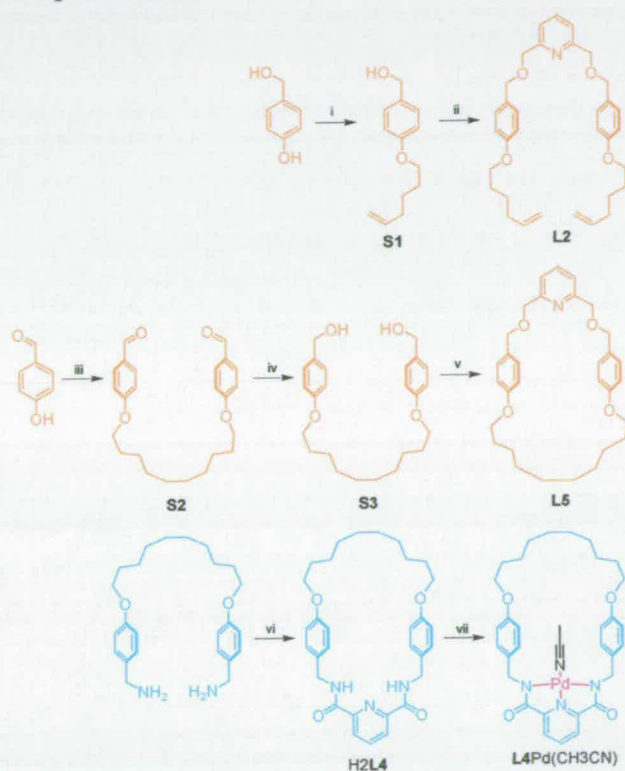
A [2]catenate and the isomeric single macrocycle and double macrocycle metal complexes can each be efficiently assembled about a palladium(II) template *via* RCM. The order in which the tridentate and monodentate ligand cyclization reactions and coordination steps are performed determines the outcome of the synthetic pathway, providing selective routes to each of the three topological and constitutional isomers. In one case, pre-forming the tridentate macrocycle followed by its coordination along with the acyclic monodentate ligand to the Pd, produces threaded and non-threaded atropisomers. These can be isolated and, whilst the individual forms are stable in dichloromethane, they can be interconverted in a coordinating solvent through ligand exchange. Each atropisomer was shown to be a true intermediate to a different topological product meaning that, in this reaction, the choice of solvent can determine whether the [2]catenate is formed or its non-

interlocked isomer. It is remarkable to see how topology and connectivity can be selected so exquisitely – in three different forms – using just one set of organic building blocks and a metal atom with a two dimensional coordination geometry.

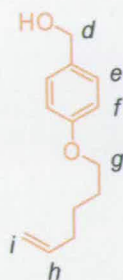
3.4 Experimental Section

General

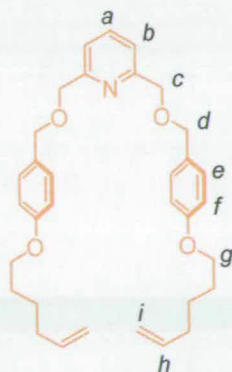
Unless stated otherwise, all reagents and anhydrous solvents were purchased from Aldrich Chemicals and used without further purification. 1,10-bis[*p*-(aminomethyl)phenoxy]decane²⁴, **1H₂**²⁵ and Pd(**1**)(CH₃CN)²⁵ were prepared according to literature procedures.



Scheme 3.4. Reagents and conditions: i) 6-bromohex-1-ene, K₂CO₃, NaI, butan-2-one, Δ, 18 h, 70%; ii) 2, 6-bis(bromomethyl)pyridine, NaH, THF, Δ, 18 h, 70%; iii) 1,10-dibromodecane, K₂CO₃, NaI, butan-2-one, Δ, 18 h, 75%; iv) NaBH₄, CHCl₃/MeOH, Δ, 4 h, 73%; v) 2, 6-bis(bromomethyl)pyridine, NaH, THF, Δ, 18h, 60%; vi) 1,10-bis[*p*-(aminomethyl)phenoxy]decane, 2,6-pyridinedicarbonyl dichloride, Et₃N, CH₂Cl₂, 0 °C then warm to r.t., 18 h, 57%; vii) Pd(OAc)₂, CH₃CN, r.t., 1 h, 93%.

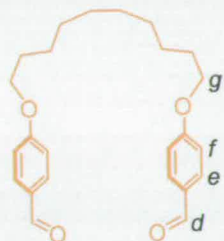


S1: To a solution of 4-hydroxybenzylalcohol (1.32 g, 10.6 mmol) and 6-bromohex-1-ene (1.73 g, 10.6 mmol) in butan-2-one (75 mL), were added potassium carbonate (7.32 g, 53.0 mmol) and a catalytic amount of sodium iodide. The suspension was refluxed for 18 h under an atmosphere of nitrogen. After cooling, the potassium carbonate was removed by filtration and the filtrate concentrated *in vacuo*. The resultant oil was re-dissolved in dichloromethane (50 mL) and washed with water (2 x 25 mL), followed by a saturated aqueous solution of sodium chloride (25 mL). The water layers were combined and re-extracted with dichloromethane (25 mL). The combined organic layers were dried over anhydrous magnesium sulfate, concentrated *in vacuo* and the crude product purified by column chromatography (CH_2Cl_2) to yield **S1** as a colourless oil (1.54 g, yield = 70%). ^1H NMR (400 MHz, CDCl_3 , 298 K): δ = 1.61 (m, 2H, H_{alkyl}), 1.84 (m, 2H, H_{alkyl}), 2.18 (m, 2H, H_{alkyl}), 2.77 (s, 1H, OH), 3.98 (t, 2H, J = 6.5 Hz, H_g), 4.56 (s, 2H, H_d), 5.06 (m, 2H, H_i), 5.88 (m, 1H, H_h), 6.90 (d, 2H, J = 8.3 Hz, H_j), 7.27 (d, 2H, J = 8.3 Hz, H_e); ^{13}C NMR (100 MHz, CDCl_3 , 298 K): δ = 25.1, 28.5, 33.3, 64.5, 67.6, 114.3, 114.6, 128.4, 132.8, 138.3, 158.4; LRFAB-MS (3-NOBA matrix): m/z = 206 [M] $^+$; HRFAB-MS (3-NOBA matrix): m/z = 206.13060 (calcd. for $\text{C}_{13}\text{H}_{18}\text{O}_2$, 206.13068).

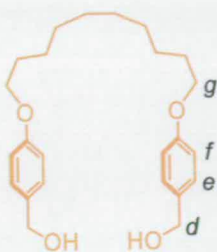


8: To a solution of **S1** (1.11 g, 5.38 mmol) in anhydrous THF (20 mL), under an atmosphere of nitrogen at 0 °C was added sodium hydride (0.174 g, 7.25 mmol) (60% dispersion in oil). After 30 minutes a solution of 2, 6-

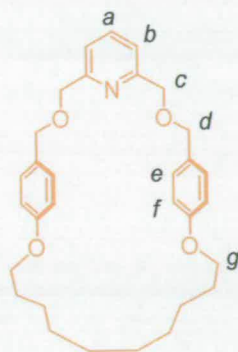
bis(bromomethyl)pyridine (0.713 g, 2.69 mmol) in anhydrous THF (15 mL) was added using a transfer needle and the suspension refluxed under an atmosphere of nitrogen for 18 h. Upon cooling the reaction mixture was filtered, concentrated *in vacuo* and the resultant crude oil re-dissolved in dichloromethane, washed with water (2 x 25 mL), and a saturated aqueous solution of sodium chloride (25 mL). The water layers were combined and re-extracted with dichloromethane (25 mL). The combined organic layers were dried over anhydrous magnesium sulfate, concentrated *in vacuo* and the crude product purified by column chromatography (95:5 CH₂Cl₂:EtOAc) to yield **8** as a colourless oil (0.970 g, yield = 70%). ¹H NMR (400 MHz, CDCl₃, 298 K): δ = 1.49 (m, 4H, H_{alkyl}), 1.72 (m, 4H, H_{alkyl}), 2.05 (m, 4H, H_{alkyl}), 3.88 (t, 4H, *J* = 6.4 Hz, H_g), 4.49 (s, 4H, H_d), 4.57 (s, 4H, H_c), 4.94 (m, 4H, H_i), 5.76 (m, 2H, H_h), 6.80 (d, 4H, *J* = 8.6 Hz, H_f), 7.22 (d, 4H, *J* = 8.6 Hz, H_e), 7.31 (d, 2H, *J* = 7.8 Hz, H_b), 7.62 (t, 1H, *J* = 7.8 Hz, H_a); ¹³C NMR (100 MHz, CDCl₃, 298 K): δ = 25.2, 28.6, 33.4, 67.7, 72.6, 72.7, 114.3, 114.7, 119.9, 129.4, 129.8, 137.2, 138.5, 157.9, 158.7; LRFAB-MS (3-NOBA matrix): *m/z* = 516 [MH]⁺; HRFAB-MS (3-NOBA matrix): *m/z* = 516.31141 (calcd. for C₃₃H₄₂NO₄, 516.31138).



S2 (4,4'-decanediyldioxy-dibenzaldehyde)^[26]: The synthesis of **S2** was carried out as for **S1** but using 4-hydroxybenzaldehyde (1.62 g, 13.3 mmol), 1,10-dibromodecane (2.00 g, 6.66 mmol), potassium carbonate (9.20 g, 66.6 mmol) and a catalytic amount of sodium iodide. The crude residue was recrystallized from methanol to yield the title compound as a colourless solid (1.91 g, yield = 75%). m.p. 78-79 °C (lit. 78-80 °C);^[26] ¹H NMR (400 MHz, CDCl₃, 298 K): δ = 1.21-1.47 (m, 12H, H_{alkyl}), 1.81 (m, 4H, H_{alkyl}), 4.02 (t, 4H, *J* = 6.6 Hz, H_g), 6.97 (d, 4H, *J* = 8.6 Hz, H_f), 7.81 (d, 4H, *J* = 8.6 Hz, H_e), 9.86 (s, 2H, H_d); ¹³C NMR (100 MHz, CDCl₃, 298 K): δ = 25.9, 29.0, 29.3, 29.4, 68.3, 114.7, 129.7, 132.0, 164.2, 190.8; LRFAB-MS (3-NOBA matrix): *m/z* = 383 [MH]⁺; HRFAB-MS (3-NOBA matrix): *m/z* = 383.22211 (calcd. for C₂₄H₃₁O₄, 383.22223).

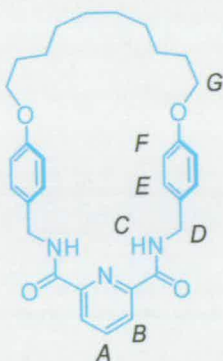


S3 (4,4'-[decane-1,10-diylbis(oxy)]bis[benzenemethanol])^[27]: To a solution of **S2** (1.80 g, 4.70 mmol) in chloroform (50 mL) and methanol (10 mL), was slowly added sodium borohydride (1.78 g, 47.0 mmol). The reaction mixture was then heated at reflux for 4 h, cooled to 0 °C and quenched with 1 M hydrochloric acid. The product was then extracted with dichloromethane (3 x 50 mL) and the combined organic extracts dried over anhydrous magnesium sulfate and concentrated in *vacuo* to yield **S3** as a colourless solid (1.33 g, yield = 73%). m.p. 131-132 °C; ¹H NMR (400 MHz, DMSO, 298 K): δ = 1.24-1.47 (m, 12H, H_{alkyl}), 1.71 (m, 4H, H_{alkyl}), 3.94 (t, 4H, J = 6.6 Hz, H_g), 4.42 (d, 4H, J = 4.8 Hz, H_d), 5.02 (t, 2H, J = 4.8 Hz, OH) 6.87 (d, 4H, J = 8.6 Hz, H_f), 7.22 (d, 4H, J = 8.6 Hz, H_e); ¹³C NMR (100 MHz, DMSO, 298 K): δ = 25.4, 28.6, 28.6, 28.8, 62.4, 67.2, 113.9, 127.8, 134.3, 157.2; LRFAB-MS (3-NOBA matrix): m/z = 386 [M]⁺; HRFAB-MS (3-NOBA matrix): m/z = 386.24509 (calcd. for C₂₄H₃₄O₄, 386.24571).



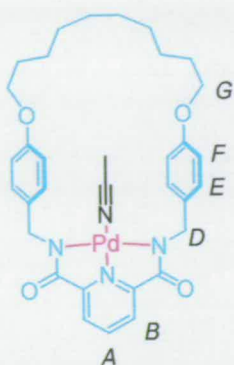
10: To a solution of **S3** (1.29 g, 3.34 mmol) and 2,6-bis(bromomethyl)pyridine (0.885 g, 3.34 mmol) in anhydrous THF (1 L) was added sodium hydride (0.176 g, 7.35 mmol, 60% in oil suspension) under an atmosphere of nitrogen. The reaction was refluxed under nitrogen for 18 h. Upon cooling, the suspension was filtered and the filtrate concentrated in *vacuo*. The crude residue was re-dissolved in dichloromethane, washed with water (25 mL), dried over anhydrous magnesium sulfate and concentrated in *vacuo*. The crude residue was purified by column chromatography (95:5 CH₂Cl₂:EtOAc) to yield **10** as a colorless crystalline solid

(0.981 g, yield = 60%). m.p. 61-62 °C; ^1H NMR (400 MHz, CDCl_3 , 298 K): δ = 1.22-1.48 (m, 12H, H_{alkyl}), 1.73 (m, 4H, H_{alkyl}), 3.97 (t, 4H, J = 6.3 Hz, H_g), 4.43 (s, 4H, H_d), 4.60 (s, 4H, H_c), 6.80 (d, 4H, J = 8.6 Hz, H_f), 7.23 (d, 4H, J = 8.6 Hz, H_e), 7.36 (d, 2H, J = 7.8 Hz, H_b), 7.69 (t, 1H, J = 7.8 Hz, H_a); ^{13}C NMR (100 MHz, CDCl_3 , 298 K): δ = 25.6, 28.5, 28.6, 29.3, 67.3, 71.2, 72.2, 114.5, 119.9, 129.2, 130.0, 137.1, 157.7, 158.7; LRFAB-MS (3-NOBA matrix): m/z = 490 $[\text{MH}]^+$; HRFAB-MS (3-NOBA matrix): m/z = 490.29495 (calcd. for $\text{C}_{31}\text{H}_{40}\text{NO}_4$, 490.29573).

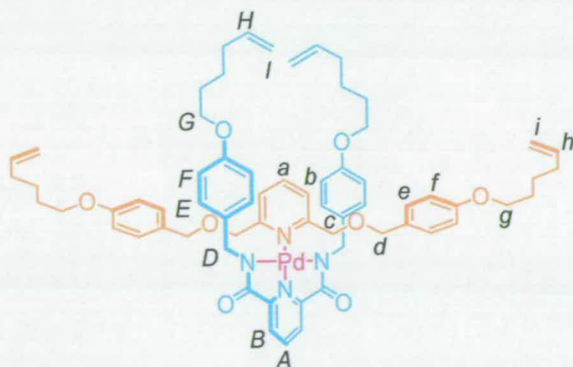


7H₂: Method 1: To a solution of 1,10-bis[*p*-aminomethyl]phenoxy]decane (5.00 g, 13.0 mmol) in anhydrous dichloromethane (2950 mL), at 0 °C under an atmosphere of nitrogen, was added triethylamine (2.93 g, 29.0 mmol). A solution of 2,6-pyridinedicarbonyl dichloride (2.65 g, 13.0 mmol) in anhydrous dichloromethane (50 mL) was slowly added dropwise over 3 h, while keeping the solution at 0 °C. The solution was then allowed to warm to room temperature and stirred for 18 h before being concentrated *in vacuo*. The crude residue was purified by column chromatography (50:50 CH_2Cl_2 :EtOAc) and recrystallized from acetonitrile to yield colorless crystals of the title compound (3.80 g, yield = 57%). m.p. 259-260 °C; ^1H NMR (400 MHz, CD_2Cl_2 , 298 K): δ = 1.23-1.46 (m, 12H, H_{alkyl}), 1.71 (m, 4H, H_{alkyl}), 3.91 (t, 4H, J = 6.3 Hz, H_G), 4.55 (d, 4H, J = 6.1 Hz, H_D), 6.77 (d, 4H, J = 8.6 Hz, H_F), 7.17 (d, 4H, J = 8.6 Hz, H_E), 8.00 (t, 1H, J = 7.8 Hz, H_A), 8.10 (br, 2H, H_C) 8.31 (d, 2H, J = 7.8 Hz, H_B); ^{13}C NMR (100 MHz, CD_2Cl_2 , 298 K): δ = 25.7, 28.4, 28.7, 29.1, 42.7, 67.6, 114.7, 125.2, 129.2, 130.6, 139.1, 149.2, 158.8, 163.5; LRFAB-MS (3-NOBA matrix): m/z = 516 $[\text{MH}]^+$; HRFAB-MS (3-NOBA matrix): m/z = 516.28550 (calcd. for $\text{C}_{31}\text{H}_{38}\text{N}_3\text{O}_4$, 516.28623).

Method 2 Synthesis as for **9H₂** using Pd(7)(CH_3CN) (0.050 g, 7.6×10^{-2} mmol) and potassium cyanide (0.05 g, 7.7×10^{-1} mmol). The crude residue was purified by column chromatography (50:50 CH_2Cl_2 :EtOAc) to yield **7H₂** (0.037 g, 95%).

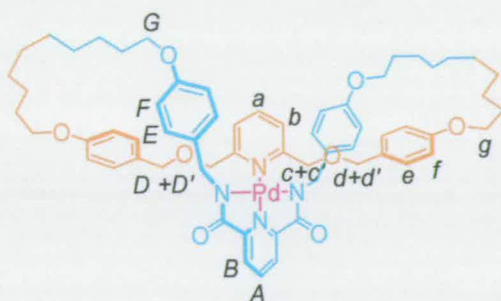


Pd(7)(CH₃CN): To a solution of **7**H₂ (1.55 g, 3.00 mmol) in anhydrous acetonitrile (50 mL), was added palladium(II) acetate (0.674 g, 3.00 mmol) and the reaction stirred at room temperature for 1 h under an atmosphere of nitrogen. The resulting precipitate was filtered, washed with acetonitrile (25 mL) and dried under suction to yield a yellow solid (1.84 g, yield = 93%). m.p. 240 °C (decomp.); ¹H NMR (400 MHz, 9:1 CD₂Cl₂:CD₃CN, 298 K): δ = 1.22-1.77 (m, 16H, H_{alkyl}), 1.95 (s, 3H, Pd-NCCCH₃), 3.92 (t, 4H, *J* = 6.3 Hz, H_G), 4.41 (s, 4H, H_D), 6.77 (d, 4H, *J* = 8.3 Hz, H_F), 7.13 (d, 4H, *J* = 8.3 Hz, H_E), 7.71 (d, 2H, *J* = 7.8 Hz, H_B), 8.07 (t, 1H, *J* = 7.8 Hz, H_A); ¹³C NMR (100 MHz, 9:1 CD₂Cl₂:CD₃CN, 298 K): δ = 0.5, 25.7, 28.4, 28.8, 29.3, 49.5, 67.4, 114.5, 115.5, 125.0, 128.5, 133.7, 141.4, 153.4, 158.2, 170.7; LRFAB-MS (3-NOBA matrix): *m/z* = 620 [MH-CH₃CN]⁺; HRFAB-MS (3-NOBA matrix): *m/z* = 660.19089 (calcd. for C₃₃H₃₈N₄O₄Pd, 660.19251).



Pd(1)(8): A solution of **8** (0.520 g, 1.01 mmol) and Pd(1)(CH₃CN) (0.687 g, 1.00 mmol) in anhydrous dichloromethane (25 mL) was stirred for 1 h at room temperature. The solution was concentrated *in vacuo* and the crude residue purified by column chromatography, (95:5 CH₂Cl₂:EtOAc) to yield Pd(1)(8) as a yellow, gummy solid (1.08 g, yield = 93%). m.p. 120 °C (decomp); ¹H NMR (400 MHz, CD₂Cl₂, 298 K): δ = 1.38-1.83 (m, 16H, H_{alkyl}), 1.99-2.15 (m, 8H, H_{alkyl}), 3.77 (t, 4H, *J* = 6.6 Hz, H_G), 3.85-3.95 (m, 8H, H_E + H_D), 4.29 (s, 4H, H_d), 4.57 (s, 4H, H_c), 4.99 (m, 8H, H_I + H_i), 5.82 (m, 4H, H_H + H_h), 6.46 (d, 4H, *J* = 8.6 Hz, H_E), 6.57 (d, 4H, *J*

= 8.6 Hz, H_F), 6.85 (d, 4H, $J = 8.6$ Hz, H_f), 7.24 (d, 4H, $J = 8.6$ Hz, H_e), 7.47 (d, 2H, $J = 7.8$ Hz, H_b), 7.81 (d, 2H, $J = 7.8$ Hz, H_B), 7.91 (t, 1H, $J = 7.8$ Hz, H_a), 8.13 (t, 1H, $J = 7.8$ Hz, H_A); ^{13}C NMR (100 MHz, CDCl_3 , 298 K): $\delta = 25.3, 25.3, 28.7, 28.7, 33.4, 33.4, 48.7, 67.7, 67.8, 71.8, 73.2, 114.1, 114.3, 114.7, 114.7, 121.8, 124.7, 128.5, 128.9, 129.3, 133.0, 138.4, 138.5, 139.1, 140.5, 152.8, 157.9, 158.9, 160.5, 171.0$. LRFAB-MS (3-NOBA matrix): $m/z = 1161$ $[\text{MH}]^+$; HRFAB-MS (3-NOBA matrix): $m/z = 1161.49253$ (calcd. for $\text{C}_{66}\text{H}_{79}\text{N}_4\text{O}_8\text{Pd}$, 1161.49299).



Pd9: Method 1 (a) A solution of Pd(1)(8) (0.452 g, 0.390 mmol) in anhydrous dichloromethane (150 mL) was added via a double ended needle to a solution of first generation Grubbs' catalyst (0.064 g, 7.8×10^{-2} mmol) in anhydrous dichloromethane (500 mL) under an atmosphere of nitrogen. The solution was stirred at room temperature for 18 h, concentrated *in vacuo* and the crude residue purified by column chromatography (96:4 CH_2Cl_2 :EtOAc) to yield a yellow solid (0.33 g).

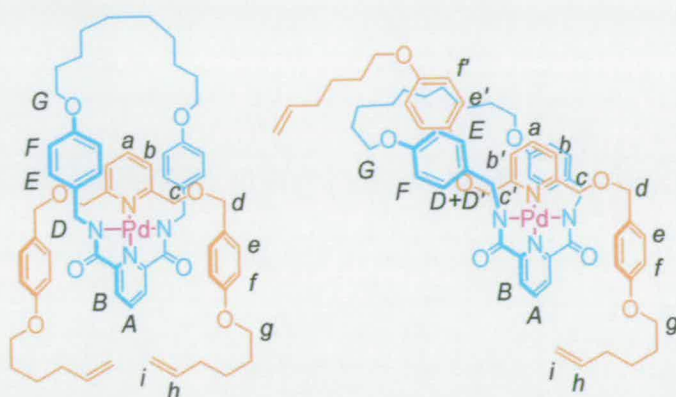
(b) To a stirred solution of the yellow solid obtained in part (a) (0.33 g) in THF (50 mL), was added 10% w/w Pd-C (0.050 g) and the resultant suspension stirred under an atmosphere of hydrogen for 18 h. The suspension was filtered through a plug of Celite, and the solution concentrated *in vacuo* to yield Pd9 as a yellow solid (0.32 g, yield = 75% over 2 steps). m.p. 196 °C (decomp); ^1H NMR (400 MHz, CD_2Cl_2 , 298 K): $\delta = 1.09$ -1.84 (m, 32H, H_{alkyl}), 2.70 (d, 2H, $J = 14.4$ Hz, $H_{D'}$), 3.64 (m, 4H, H_G), 4.0-4.13 (m, 8H, $H_g + H_c + H_{d'}$), 4.39 (d, 2H, $J = 10.6$ Hz, H_d), 5.04-5.14 (m, 4H, $H_c + H_D$), 6.38 (d, 4H, $J = 8.6$ Hz, H_E), 6.49 (d, 4H, $J = 8.6$ Hz, H_F), 6.84 (d, 4H, $J = 8.6$ Hz, H_f), 7.20 (d, 4H, $J = 8.6$ Hz, H_e), 7.45 (d, 2H, $J = 7.8$ Hz, H_b), 7.76 (d, 2H, $J = 7.8$ Hz, H_B), 7.88 (t, 1H, $J = 7.8$ Hz, H_a), 8.08 (t, 1H, $J = 7.8$ Hz, H_A); ^{13}C NMR (100 MHz, CDCl_3 , 298 K): $\delta = 23.7, 25.2, 25.5, 27.5, 27.5, 27.5, 28.6, 29.5, 48.5, 67.1, 68.1, 71.8, 73.2, 114.0, 114.8, 121.2, 124.8, 128.5, 128.7, 129.5, 132.8, 139.1, 140.7, 152.8, 158.1, 158.6, 160.6, 171.1$; LRFAB-MS (3-NOBA matrix): $m/z = 1109$ $[\text{MH}]^+$; HRFAB-MS (3-NOBA matrix): $m/z = 1109.46275$ (calcd. for $\text{C}_{62}\text{H}_{75}\text{N}_4\text{O}_8\text{Pd}$, 1109.46169).

Method 2

To a stirred solution of **9H₂** (0.050 g, 5.0×10^{-2} mmol) in anhydrous acetonitrile (10 mL) and dichloromethane (10 mL), palladium(II) acetate (0.011 g, 5.0×10^{-2} mmol) was added and the solution refluxed for 18 h under an atmosphere of nitrogen. The resulting precipitate was filtered, washed with acetonitrile (25 mL) and dried under suction to yield **Pd9** (0.047 g, 85%).



9H₂: To a solution of **9Pd** (0.100 g, 9.00×10^{-2} mmol) in dichloromethane (10 mL) and methanol (10 mL) was added potassium cyanide (0.091 g, 1.4 mmol) in methanol (2 mL). The solution was stirred at room temperature for 1 h, until it was colorless, and then heated gently to reduce the overall volume to less than 5 mL. The resultant mixture was dispersed in water (25 mL) and washed with dichloromethane (3 x 25 mL). The combined organic extracts were washed with further water (25 mL) and dried over anhydrous magnesium sulfate. After filtration, the solution was concentrated *in vacuo* and the crude residue purified by column chromatography (85:15 CH₂Cl₂:EtOAc) to give the title compound as a colorless solid (0.085 g, yield = 94%). m.p. 186 °C (decomp); ¹H NMR (400 MHz, CD₂Cl₂, 298 K): δ = 1.17-1.78 (m, 32H, H_{alkyl}), 3.84-3.96 (m, 8H, H_G + H_g), 4.48-4.54 (m, 12H, H_D + H_d + H_c), 6.76-6.84 (m, 8H, H_F + H_f), 7.15-7.24 (m, 8H, H_E + H_e), 7.30 (d, 2H, J = 7.8 Hz, H_b), 7.66 (t, 1H, J = 7.8 Hz, H_a), 8.02 (t, 1H, J = 7.8 Hz, H_A), 8.11 (br, 2H, H_C), 8.32 (d, 2H, J = 7.8 Hz, H_B). ¹³C NMR (100 MHz, CDCl₃, 298 K): δ = 25.9, 25.9, 29.0, 29.1, 29.2, 29.3, 29.3, 29.3, 43.0, 67.9, 68.0, 72.4, 72.4, 114.4, 114.7, 120.3, 125.2, 129.0, 129.6, 129.7, 129.8, 137.2, 139.0, 148.8, 157.9, 158.6, 158.8, 163.3; LRFAB-MS (3-NOBA matrix): m/z = 1006 [MH]⁺; HRFAB-MS (3-NOBA matrix): m/z = 1005.57406 (calcd. for C₆₂H₇₇N₄O₈, 1005.57414).

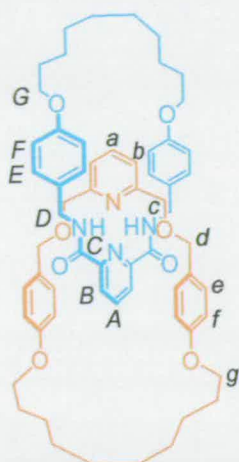


Pd(7)(endo-8)/Pd(7)(exo-8): The synthesis of Pd(7)(8) was carried out as for Pd(1)(8) but using 8 (0.300 g, 5.82×10^{-1} mmol) and Pd(7)(CH₃CN) (0.384 g, 5.82×10^{-1} mmol) as reactants. The crude residue was purified using column chromatography (85:15 CH₂Cl₂:EtOAc) to yield a 2:3 mixture of the two atropisomers as a yellow solid (0.587 g, 89%). The atropisomers were separated using preparative thin layer chromatography (98.5:1.5 CH₂Cl₂:MeOH).

Threaded atropisomer, Pd(7)(endo-8). ¹H NMR (400 MHz, CD₂Cl₂, 298 K): δ = 1.18-1.82 (m, 24H, H_{alkyl}), 2.10 (m, 4H, H_{alkyl}), 3.80 (t, 4H, J = 6.6 Hz, H_G), 3.90 (t, 4H, J = 6.6 Hz, H_E), 4.01 (s, 4H, H_D), 4.42 (s, 4H, H_d), 4.69 (s, 4H, H_c), 4.98 (m, 4H, H_i), 5.83 (m, 2H, H_h), 6.24-6.35 (m, 8H, H_E + H_F), 6.80 (d, 4H, J = 8.6 Hz, H_f), 7.15 (d, 2H, J = 7.8 Hz, H_b), 7.23 (d, 4H, J = 8.6 Hz, H_e), 7.66 (t, 1H, J = 7.8 Hz, H_a), 7.77 (d, 2H, J = 7.8 Hz, H_B), 8.10 (t, 1H, J = 7.8 Hz, H_A); ¹³C NMR (100 MHz, CD₂Cl₂, 298 K): δ = 25.7, 25.8 (x2), 28.8, 29.1 (x2), 29.8, 33.8, 49.9, 67.6, 72.3, 73.7, 114.6, 114.7, 114.8, 121.8, 124.8, 128.4, 129.6, 130.4, 132.0, 139.0, 139.1, 140.9, 153.2, 157.9, 159.4, 160.2, 171.5; LRESI-MS m/z = 1157 (M + Na⁺).

Non-threaded atropisomer, Pd(7)(exo-8) ¹H NMR (400 MHz, CD₂Cl₂, 298 K): δ = 0.73-1.81 (m, 24H, H_{alkyl}), 2.11 (m, 4H, H_{alkyl}), 2.49 (d, 2H, J = 14.4 Hz, H_{D'}), 3.33 (s, 2H, H_{d'}), 3.39 (s, 2H, H_{c'}), 3.93 (m, 8H, H_G + H_e), 4.68 (s, 2H, H_d), 5.00 (m, 6H, H_f + H_D), 5.63 (s, 2H, H_c), 5.83 (m, 2H, H_H), 6.74 (m, 8H, H_F + H_E), 6.85 (m, 4H, H_f + H_f), 7.28 (m, 5H, H_{e'} + H_e + H_{b'}), 7.72 (d, 1H, J = 7.8 Hz, H_b), 7.82 (d, 2H, J = 7.8 Hz, H_B), 7.88 (t, 1H, J = 7.8 Hz, H_a), 8.13 (t, 1H, J = 7.8 Hz, H_A); ¹³C NMR (100 MHz, CD₂Cl₂, 298 K): δ = 25.7, 25.9, 29.0, 29.1, 29.1, 29.2, 29.8, 33.9, 49.0, 67.9, 68.2, 68.3, 71.4, 72.2, 72.4, 73.8, 114.5, 114.7, 114.8, 114.8, 122.2, 122.5, 125.1, 128.6, 129.6, 130.1, 130.2, 130.5, 133.44, 139.1, 140.2, 141.25, 153.1, 158.3, 159.2, 159.5, 159.7, 162.3, 171.6; LRESI-MS m/z = 1157 (M + Na⁺).

Preparation of $7H_2$, 10 and $11H_2$ from the mixture of Pd(7)(*exo*-8) and Pd(7)(*endo*-8)

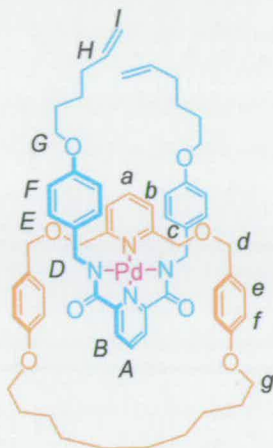


(a) A solution of Pd(7)(8) (0.362 g, 3.19×10^{-1} mmol) in anhydrous dichloromethane (150 mL) was added *via* a double ended needle to a solution of first generation Grubbs' catalyst (0.030 g, 3.6×10^{-2} mmol) in anhydrous dichloromethane (500 mL) under an atmosphere of nitrogen. The solution was stirred at room temperature for 18 h, after which it was concentrated *in vacuo* and the crude residue purified by column chromatography (9:1 $CH_2Cl_2:CH_3COCH_3$) to yield a yellow solid.

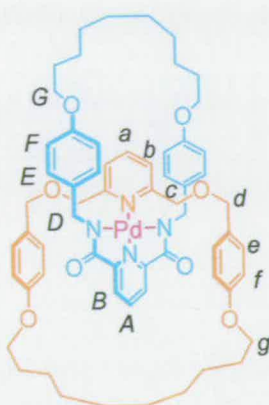
(b) To a solution of the yellow solid obtained from part (a) in THF (20 mL) was added PdEnCat™ (0.080 g, 3.2×10^{-2} mmol) and the resulting suspension stirred under an atmosphere of hydrogen (50 bar) for 18 h. The suspension was then filtered and the solution concentrated *in vacuo*.^[28]

(c) To a solution of the crude product obtained from part (b) in dichloromethane (10 mL) and methanol (10 mL) was added potassium cyanide (0.311 g, 4.79 mmol) in methanol (4 mL). The solution was stirred at room temperature for 1 h, until it was colorless, and then heated gently to reduce the overall volume to less than 5 mL. The resulting mixture was dispersed in water (25 mL) and washed with dichloromethane (3 x 25 mL). The combined organic extracts were washed with further water (25 mL) and dried over anhydrous magnesium sulfate. After filtration, the solution was concentrated *in vacuo* and the crude residue purified by column chromatography (99:1 $CH_2Cl_2:MeOH$) to give $7H_2$ (0.12 g), 10 (0.020 g) and $11H_2$ (0.081 g) in 73%, 13% and 25% yields respectively (over three steps). $11H_2$: m.p. 125-126 °C; 1H NMR (400 MHz, CD_2Cl_2 , 298 K): δ = 1.22-1.55 (m, 24H, H_{alkyl}), 1.63-1.76 (m, 8H, H_{alkyl}), 3.75-2.89 (m, 12H, $H_g + H_c + H_G$), 4.02 (d, 4H, $J = 6.3$, H_D), 4.16 (s, 4H, H_d), 6.32-6.42 (m, 8H, $H_f + H_F$), 6.48 (d, 4H, $J = 8.6$ Hz, H_E), 6.74 (d, 4H, $J = 8.6$ Hz, H_e), 6.85

(d, 2H, $J = 7.8$ Hz, H_b), 7.40 (t, 1H, $J = 7.8$ Hz, H_a), 7.91 (t, 1H, $J = 7.8$ Hz, H_A), 8.15 (d, 2H, $J = 7.8$ Hz, H_B), 9.01 (t, 2H, $J = 6.3$ Hz, H_C); ^{13}C NMR (100 MHz, CDCl_3 , 298 K): $\delta = 25.6, 25.8, 28.3, 28.5, 28.6, 28.7, 29.2, 29.4, 42.2, 67.0, 67.1, 70.0, 72.6, 113.6, 114.1, 118.9, 124.1, 128.3, 128.8, 129.8, 130.4, 136.5, 137.3, 148.6, 157.3, 157.5, 158.4, 163.2$; LRFAB-MS (3-NOBA matrix): $m/z = 1006$ $[\text{MH}]^+$; HRFAB-MS (3-NOBA matrix): $m/z = 1005.57494$ (calcd. for $\text{C}_{62}\text{H}_{77}\text{N}_4\text{O}_8$, 1005.57414).



1Pd10: The synthesis of Pd(1)(10) was carried out as for Pd(1)(8) but using 10 (0.279 g, 5.70×10^{-1} mmol) and Pd(1)(CH₃CN) (0.392 g, 5.70×10^{-1} mmol) as reactants. The resulting crude residue was purified by column chromatography (95:5 CH₂Cl₂:EtOAc) to yield Pd(1)(10) as a yellow solid (0.446 g, yield = 69%). m.p. 58–60 °C; ^1H NMR (400 MHz, CD_2Cl_2 , 298 K): $\delta = 1.19$ – 1.48 (m, 12H, H_{alkyl}), 1.50– 1.82 (m, 12H, H_{alkyl}), 2.13 (m, 4H, H_{alkyl}), 3.55 (s, 4H, H_D), 3.80– 3.91 (m, 8H, $H_G + H_H$), 4.18 (b, 4H, H_C), 4.39 (s, 4H, H_d), 5.00 (m, 4H, H_I), 5.86 (m, 2H, H_H), 6.21 (br, 4H, H_E), 6.41 (d, 4H, $J = 8.0$ Hz, H_F), 6.52 (d, 4H, $J = 8.3$ Hz, H_J), 7.07 (d, 4H, $J = 8.3$ Hz, H_e), 7.25 (d, 2H, $J = 7.8$ Hz, H_b), 7.71– 7.78 (m, 3H, $H_B + H_a$), 8.11 (t, 1H, $J = 7.8$ Hz, H_A). ^{13}C NMR (100 MHz, CD_2Cl_2 , 298 K): $\delta = 25.7, 26.0, 28.9, 29.0, 29.1, 29.9, 33.8, 48.5, 67.6, 68.1, 70.4, 73.1, 114.2, 114.4, 114.8, 123.5, 124.3, 128.6, 131.4, 133.6, 139.1, 139.3, 140.4, 153.0, 157.9, 158.2, 159.3, 159.8, 170.8$; LRFAB-MS (3-NOBA matrix): $m/z = 1135$ $[\text{MH}]^+$; HRFAB-MS (3-NOBA matrix): $m/z = 1135.47843$ (calcd. for $\text{C}_{64}\text{H}_{77}\text{N}_4\text{O}_8\text{Pd}$, 1135.47734).

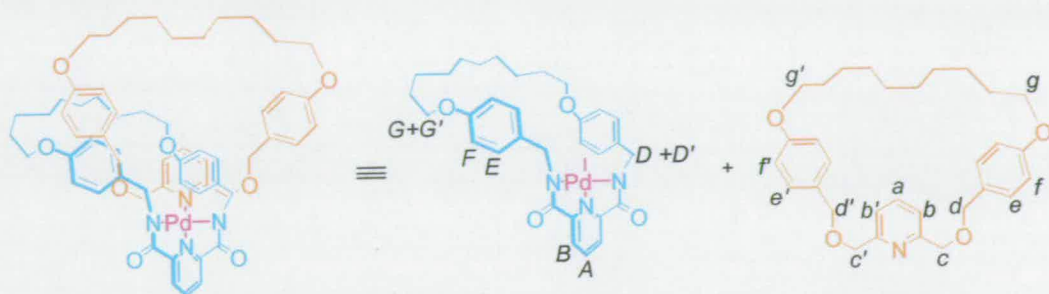
**Pd11:****Method 1**

(a) The synthesis of Pd11 was carried out as for Pd9 (method 1) but using Pd(1)(10) (0.352 g, 3.10×10^{-1} mmol) as the starting material and (0.030 g, 3.6×10^{-2} mmol) of Grubbs' catalyst. The crude residue was purified by column chromatography (96:4 CH₂Cl₂:EtOAc) to yield a yellow solid (0.34 g).

(b) The yellow solid obtained from part (a) (0.34 g) was treated with 10% w/w Pd-C (0.050 g) over H₂ in THF (20 mL) as for Pd9, yielding Pd11 (0.268 g, 78% over 2 steps). m.p. 134-135 °C; ¹H NMR (400 MHz, CD₂Cl₂, 298 K): δ = 1.04-1.50 (m, 24H, H_{alkyl}), 1.60 (m, 4H, H_{alkyl}), 1.70 (m, 4H, H_{alkyl}), 3.60 (s, 4H, H_D), 3.81 (t, 4H, J = 6.3 Hz, H_G), 3.89 (t, 4H, J = 6.3 Hz, H_E), 4.36-4.42 (m, 8H, H_d+ H_c), 5.94 (d, 4H, J = 8.6 Hz, H_F), 6.10 (d, 4H, J = 8.6 Hz, H_E), 6.63 (d, 4H, J = 8.6 Hz, H_f), 7.05 (d, 2H, J = 7.8 Hz, H_b), 7.15 (d, 4H, J = 8.6 Hz, H_e), 7.60 (t, 1H, J = 7.8 Hz, H_a), 7.76 (d, 2H, J = 7.6 Hz, H_B), 8.13 (t, 1H, J = 7.6 Hz, H_A); ¹³C NMR (100 MHz, CD₂Cl₂, 298 K): δ = 25.8, 26.0, 28.5, 28.7, 28.9, 29.2, 30.0, 30.1, 49.4, 67.1, 67.7, 69.6, 72.9, 114.5, 114.8, 121.2, 124.5, 128.2, 128.6, 131.7, 132.9, 138.8, 140.6, 153.1, 157.4, 159.5, 160.0, 171.1. LRFAB-MS (3-NOBA matrix): m/z = 1109 [MH]⁺; HRFAB-MS (3-NOBA matrix): m/z = 1109.46152 (calcd. for C₆₂H₇₅N₄O₈ Pd, 1109.46169).

Method 2

The synthesis of Pd11 was carried out as for Pd9 (method 2) but using 11H₂ (0.050 g, 5.0×10^{-2} mmol) as the starting complex and (0.011 g, 5.0×10^{-2} mmol) of palladium(II) acetate to yield Pd11 (0.044 g, 79%).



7Pd10: The synthesis of Pd(7)(10) was carried out as for Pd(1)(8) but using 10 (0.110 g, 2.25×10^{-1} mmol) and Pd(7)(CH₃CN) (0.149 g, 2.25×10^{-1} mmol) as reactants. The crude residue was purified by column chromatography (97.5:2.5 CH₂Cl₂:MeOH) to yield Pd(7)(10) as a yellow solid. (0.194 g, yield = 78%). m.p. 181 °C (decomp); ¹H NMR (400 MHz, CD₂Cl₂, 298 K): δ = 0.81-1.74 (m, 32H, H_{alkyl}), 2.50 (d, 2H, J = 14.8 Hz, H_{D'}), 3.34-3.44 (m, 4H, H_{d'} + H_{c'}), 3.78-4.02 (m, 6H, H_{g'} + H_{G'} + H_G), 4.09 (t, 2H, J = 6.3 Hz, H_g), 4.72 (s, 2H, H_d), 5.08 (d, 2H, J = 14.8 Hz, H_D), 5.67 (s, 2H, H_c), 6.64-6.84 (m, 12H, H_{f'} + H_{F'} + H_E + H_f), 6.92 (d, 1H, J = 7.8 Hz, H_{b'}), 6.99 (d, 2H, J = 8.6 Hz, H_{e'}), 7.12-7.22 (m, 3H, H_b + H_e), 7.38 (t, 1H, J = 7.8 Hz, H_a), 7.83 (d, 2H, J = 7.8 Hz, H_B), 8.13 (t, 1H, J = 7.8 Hz, H_A); ¹³C NMR (100 MHz, CD₂Cl₂, 298 K): δ = 25.6, 25.9 (x2), 28.5, 29.0, 29.1, 29.3, 29.4, 29.4, 29.6, 29.8, 29.9, 49.2, 67.8, 67.9, 68.3, 72.1, 72.8, 73.4, 76.3, 114.8, 114.9, 115.4, 122.0, 122.7, 125.1, 128.3, 129.9, 130.3, 130.5, 131.4, 133.0, 138.4, 141.3, 153.0, 158.2, 158.7, 159.6, 160.6, 161.9, 171.6; LRESI-MS m/z = 1131 (M + Na⁺).

11H₂: The synthesis of H₂11 was carried out as for 9H₂ but using Pd11 (0.210 g, 1.90×10^{-1} mmol) as the starting complex and potassium cyanide (0.190 g, 2.92 mmol). The crude residue was purified using column chromatography (85:15 CH₂Cl₂:EtOAc) to yield 11H₂ as a colorless solid (0.185 g, yield = 97%).

X-ray Crystallographic structure determinations. Pd9: C₆₂H₇₄N₄O₈Pd, M = 1109.65, yellow prism, crystal size 0.3 × 0.2 × 0.15 mm, monoclinic, $P2(1)/n$ (# 14), a = 11.839(17), b = 17.17(2), c = 27.07(8) Å, β = 92.689(19)°, V = 5497(19) Å³, Z = 4, ρ_{calcd} = 1.341 Mg m⁻³; MoK α radiation (confocal optic, λ = 0.71073 Å), μ = 0.397 mm⁻¹, T = 93(2) K. 25519 data (8839 unique, R_{int} = 0.0352, $2.37 < \theta < 25.35^\circ$), were collected on a Rigaku MM007/Mercury CCD diffractometer and were corrected for absorption. The structure was solved by direct methods and refined by full-matrix least-squares on F^2 values of all data (G. M. Sheldrick, SHELXTL, Bruker AXS

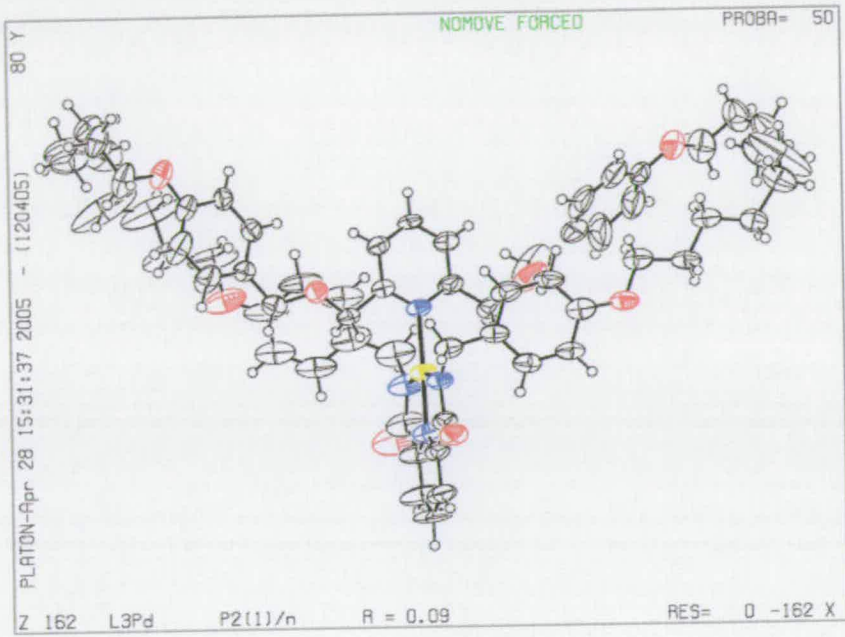
Madison WI, USA, 2001, version 6.1) to give $wR = \{\Sigma[w(F_o^2 - F_c^2)^2] / \Sigma[w(F_o^2)^2]\}^{1/2} = 0.2821$, conventional $R = 0.0919$ for F values of reflections with $F_o^2 > 2\sigma(F_o^2)$, [6956 observed reflections] $S = 0.919$ for 677 parameters. Residual electron density extremes were 2.085 and $-1.443 \text{ e}\text{\AA}^{-3}$.

Pd(7)(10). $0.5\text{CH}_3\text{COCH}_3$: $\text{C}_{63.5}\text{H}_{77}\text{N}_4\text{O}_{8.5}\text{Pd}$, $M = 1138.69$, yellow plate, crystal size $0.2 \times 0.1 \times 0.02 \text{ mm}$, triclinic, $P-1$, $a = 16.191(15)$, $b = 24.30(2)$, $c = 30.6665(5) \text{ \AA}$, $\alpha = 105.54(5)$, $\beta = 101.08(5)$, $\gamma = 90.607(11)^\circ$, $V = 11381(24) \text{ \AA}^3$, $Z = 848$ (four independent molecules), $\rho_{\text{calcd}} = 1.329 \text{ Mg m}^{-3}$; $\text{CuMoK}\alpha$ radiation (confocal optic, $\lambda = 0.71073 \text{ \AA}$, 1.54178 \AA), $\mu = 3.109 \text{ mm}^{-1}$, $T = 173(2) \text{ K}$. 143757 data (38597 unique, $R_{\text{int}} = 0.0354$, $2.08 < \theta < 68.13^\circ$), were collected on a Rigaku MM007/Saturn9270 CCD diffractometer and were corrected for absorption. The structure was solved by direct methods and refined by full-matrix least-squares on F^2 values of all data (G. M. Sheldrick, SHELXTL, Bruker AXS Madison WI, USA, 2001, version 6.1) to give $wR = \{\Sigma[w(F_o^2 - F_c^2)^2] / \Sigma[w(F_o^2)^2]\}^{1/2} = 0.1198$, conventional $R = 0.0452$ for F values of reflections with $F_o^2 > 2\sigma(F_o^2)$ [38597 observed reflections], $S = 1.068$ for 2803 parameters. Residual electron density extremes were 1.879 and $-1.247 \text{ e}\text{\AA}^{-3}$.

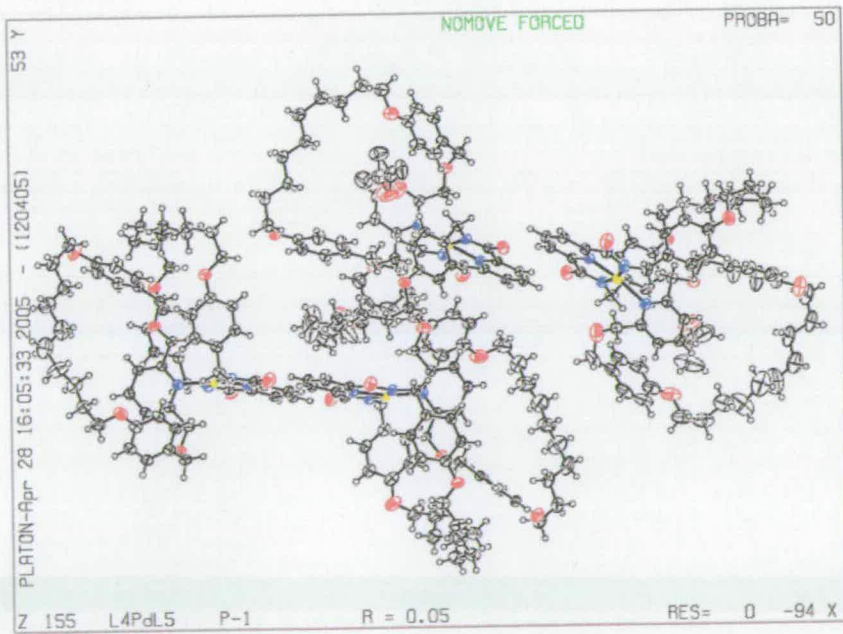
Pd11: $\text{C}_{62}\text{H}_{74}\text{N}_4\text{O}_8\text{Pd}$, $M = 1109.65$, yellow prism, crystal size $0.3 \times 0.2 \times 0.15 \text{ mm}$, monoclinic, $P2(1)$ (# 4), $a = 11.3837(6)$, $b = 36.2251(19)$, $c = 13.6178(8) \text{ \AA}$, $\beta = 97.838(3)^\circ$, $V = 5563.2(5) \text{ \AA}^3$, $Z = 4$, $\rho_{\text{calcd}} = 1.325 \text{ Mg m}^{-3}$; $\text{MoK}\alpha$ radiation (confocal optic, $\lambda = 0.71073 \text{ \AA}$), $\mu = 0.392 \text{ mm}^{-1}$, $T = 93(2) \text{ K}$. 37193 data (16752 unique, $R_{\text{int}} = 0.0600$, $2.57 < \theta < 25.34^\circ$), were collected on a Rigaku MM007/Saturn70 CCD diffractometer and were corrected for absorption. The structure was solved by direct methods and refined by full-matrix least-squares on F^2 values of all data (G. M. Sheldrick, SHELXTL, Bruker AXS Madison WI, USA, 2001, version 6.1) to give $wR = \{\Sigma[w(F_o^2 - F_c^2)^2] / \Sigma[w(F_o^2)^2]\}^{1/2} = 0.1571$, conventional $R = 0.0624$ for F values of reflections with $F_o^2 > 2\sigma(F_o^2)$ [16035 observed reflections], $S = 1.066$ for 1353 parameters. Residual electron density extremes were 0.811 and $-1.526 \text{ e}\text{\AA}^{-3}$.

X-ray crystal structure thermal ellipsoids

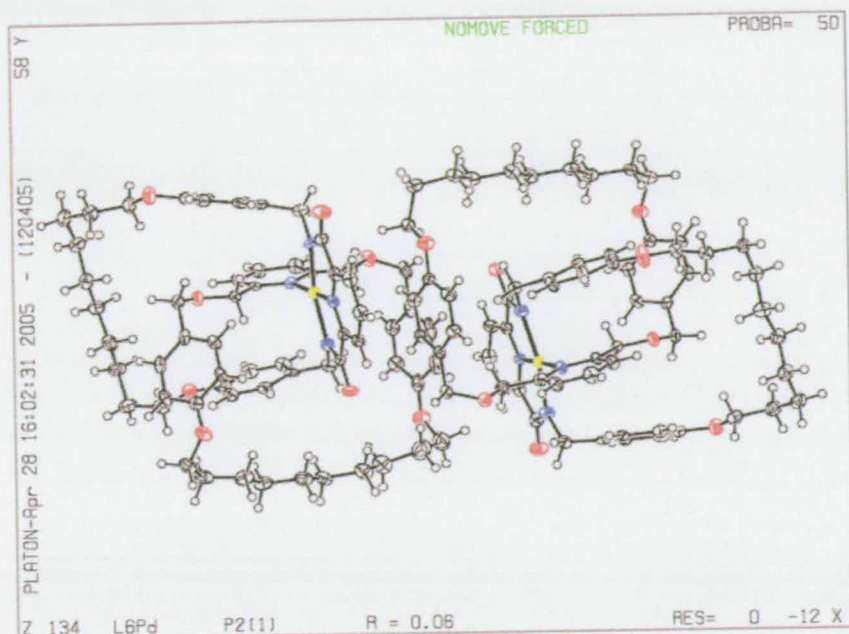
L3Pd



L4PdL5



L6Pd



3.5 References and Notes

- For reviews on interlocked molecules assembled about transition metal templates see: (a) Sauvage, J.-P.; Dietrich-Buchecker, C., Eds. *Molecular Catenanes, Rotaxanes and Knots*; Wiley-VCH: Weinheim, **1999**. (b) Hubin, T. J.; Busch, D. H.; *Coord. Chem. Rev.* **2000**, *200-202*, 5-52. (c) Collin, J.-P.; Dietrich-Buchecker, C.; Gaviña, P.; Jimenez-Molero, M. C.; Sauvage, J.-P. *Acc. Chem. Res.* **2001**, *34*, 477-487. (d) Menon, S. K.; Guha, T. B.; Agrawal, Y. K. *Rev. Inorg. Chem.* **2004**, *24*, 97-133. (e) Cantrill, S. J.; Chichak, K. S.; Peters, A. J.; Stoddart, J. F. *Acc. Chem. Res.* **2005**, *38*, 1-9.
- (a) Fujita, M.; Ibukuro, F.; Hagihara, H.; Ogura, K. *Nature* **1994**, *367*, 720-723. (b) Fujita, M.; Ibukuro, F.; Yamaguchi, K.; Ogura, K. *J. Am. Chem. Soc.* **1995**, *117*, 4175-4176. (c) Piguet, C.; Bernardinelli, G.; Williams, A. F.; Bocquet, B. *Angew. Chem., Int. Ed. Engl.* **1995**, *34*, 582-584. (d) Mingos, D. M. P.; Yau, J.; Menzer, S.; Williams, D. J. *Angew. Chem., Int. Ed. Engl.* **1995**, *34*, 1894-1895. (e) Fujita, M.; Ogura, K. *Bull. Chem. Soc. Jpn.* **1996**, *69*, 1471-1482. (f) Fujita, M.; Ogura, K. *Coord. Chem. Rev.* **1996**, *148*, 249-264. (g) Fujita, M.; Ibukuro, F.; Seki, H.; Kamo, O.; Imanari, M.; Ogura, K. *J. Am. Chem. Soc.* **1996**, *118*, 899-900. (h) Cárdenas, D. J.; Sauvage, J.-P. *Inorg. Chem.* **1997**, *36*, 2777-2783. (i) Cárdenas, D. J.; Gaviña, P.; Sauvage, J.-P. *J. Am. Chem. Soc.* **1997**, *119*, 2656-2664. (j) Fujita, M.; Aoyagi, M.; Ibukuro, F.; Ogura, K.; Yamaguchi, K. *J. Am. Chem. Soc.* **1998**, *120*, 611-612. (k)

Whang, D.; Park, K.-M.; Heo, J.; Kim, K. *J. Am. Chem. Soc.* **1998**, *120*, 4899-4900. (l) Try, A. C.; Harding, M. M.; Hamilton, D. G.; Sanders, J. K. M. *J. Chem. Soc., Chem. Commun.* **1998**, 723-724. (m) Fujita, M.; Fujita, N.; Ogura, K.; Yamaguchi, K. *Nature* **1999**, *400*, 52-55. (n) Fujita, M. *Acc. Chem. Res.* **1999**, *32*, 53-61. (o) Dietrich-Buchecker, C.; Geum, N.; Hori, A.; Fujita, M.; Sakamoto, S.; Yamaguchi, K.; Sauvage, J.-P. *Chem. Commun.* **2001**, 1182-1183. (p) Padilla-Tosta, M. E.; Fox, O. D.; Drew, M. G. B.; Beer, P. D. *Angew. Chem. Int. Ed.* **2001**, *40*, 4235-4239. (q) Park, K.-M.; Kim, S.-Y.; Heo, J.; Whang, D.; Sakamoto, S.; Yamaguchi, K.; Kim, K. *J. Am. Chem. Soc.* **2002**, *124*, 2140-2147. (r) Kim, K. *Chem. Soc. Rev.* **2002**, *31*, 96-107. (s) McArdle, C. P.; Irwin, M. J.; Jennings, M. C.; Vittal, J. J.; Puddephatt, R. J., *Chem. Eur. J.* **2002**, *8*, 723-734. (t) McArdle, C. P.; Van, S.; Jennings, M. C.; Puddephatt, R. J. *J. Am. Chem. Soc.* **2002**, *124*, 3959-3965 (u) Dietrich-Buchecker, C.; Colasson, B.; Fujita, M.; Hori, A.; Geum, N.; Sakamoto, S.; Yamaguchi, K.; Sauvage, J.-P. *J. Am. Chem. Soc.* **2003**, *125*, 5717-5725. (v) Hori, A.; Kataoka, H.; Akasaka, A.; Okano, T.; Fujita, M. *J. Polym. Sci. Part A: Polym. Chem.* **2003**, *41*, 3478-3485. (w) Mohr, F.; Eisler, D. J.; McArdle, C. P.; Atieh, K.; Jennings, M. C.; Puddephatt, R. J. *J. Organomet. Chem.* **2003**, *670*, 27-36. (x) Mohr, F.; Jennings, M. C.; Puddephatt, R. J. *Eur. J. Inorg. Chem.* **2003**, 217-223. (y) Colasson, B. X.; Sauvage, J.-P. *Inorg. Chem.* **2004**, *43*, 1895-1901. (z) Hori, A.; Yamashita, K.; Kusukawa, T.; Akasaka, A.; Biradha, K.; Fujita, M. *Chem. Commun.* **2004**, 1798-1799. (aa) Burchell, T. J.; Eisler, D. J.; Puddephatt, R. J. *Dalton Trans.* **2005**, 268-272. (bb) Wong, W. W. H.; Cookson, J.; Evans, E. A. L.; McInnes, E. J. L.; Wolowska, J.; Maher, J. P.; Bishop, P.; Beer, P. D. *Chem. Commun.* **2005**, 2214-2216.

3. For *catenates* assembled around a tetrahedral four-coordinate Cu(I) template see: (a) Dietrich-Buchecker, C. O.; Sauvage, J.-P.; Kintzinger, J.-P. *Tetrahedron Lett.* **1983**, *24*, 5095-5098. (b) Dietrich-Buchecker, C. O.; Sauvage, J.-P.; Kern, J.-M. *J. Am. Chem. Soc.* **1984**, *106*, 3043-3045. (c) Cesario, M.; Dietrich-Buchecker, C. O.; Guilhem, J.; Pascard, C.; Sauvage, J.-P. *J. Chem. Soc., Chem. Commun.* **1985**, 244-247. (d) Dietrich-Buchecker, C. O.; Guilhem, J.; Khemiss, A. K.; Kintzinger, J.-P.; Pascard, C.; Sauvage, J.-P. *Angew. Chem., Int. Ed. Engl.* **1987**, *26*, 661-663. (e) Dietrich-Buchecker, C. O.; Edel, A.; Kintzinger, J.-P.; Sauvage, J.-P. *Tetrahedron* **1987**, *43*, 333-344. (f) Jørgensen, T.; Becher, J.; Chambron, J.-C.; Sauvage, J.-P. *Tetrahedron Lett.* **1994**, *35*, 4339-4342. (g) Kern, J.-M.; Sauvage, J.-P.; Weidmann,

- J.-L. *Tetrahedron* **1996**, *52*, 10921-10934. (h) Kern, J.-M.; Sauvage, J.-P.; Weidmann, J.-L.; Armaroli, N.; Flamigni, L.; Ceroni, P.; Balzani, V. *Inorg. Chem.* **1997**, *36*, 5329-5338. (i) Mohr, B.; Weck, M.; Sauvage, J.-P.; Grubbs, R. H. *Angew. Chem., Int. Ed.* **1997**, *36*, 1308-1310. (j) Amabilino, D. B.; Sauvage, J.-P. *New J. Chem.* **1998**, *22*, 395-409. (k) Weidmann, J.-L.; Kern, J.-M.; Sauvage, J.-P.; Muscat, D.; Mullins, S.; Köhler, W.; Rosenauer, C.; Räder, H. J.; Martin, K.; Geerts, Y. *Chem. Eur. J.* **1999**, *5*, 1841-1851. (l) Raehm, L.; Hamann, C.; Kern, J.-M.; Sauvage, J.-P. *Org. Lett.* **2000**, *2*, 1991-1994.
4. For *chiral [2]catenates* assembled around tetrahedral four-coordinate Cu(I) templates see: (a) Chambron, J.-C.; Mitchell, D. K.; Sauvage, J.-P. *J. Am. Chem. Soc.* **1992**, *114*, 4625-4631. (b) Kaida, Y.; Okamoto, Y.; Chambron, J.-C.; Mitchell, D. K.; Sauvage, J.-P. *Tetrahedron Lett.* **1993**, *34*, 1019-1022.
5. For *doubly interlocked [2]catenates* assembled around tetrahedral four-coordinate Cu(I) templates see: Nierengarten, J.-F.; Dietrich-Buchecker, C. O.; Sauvage, J.-P. *J. Am. Chem. Soc.* **1994**, *116*, 375-376.
6. For *rotaxanes* assembled around a tetrahedral four-coordinate Cu(I) template see: (a) Wu, C.; Lecavalier, P. R.; Shen, Y. X.; Gibson, H. W. *Chem. Mater.* **1991**, *3*, 569-572. (b) Chambron, J.-C.; Heitz, V.; Sauvage, J.-P. *J. Chem. Soc., Chem. Commun.* **1992**, 1131-1133. (c) Chambron, J.-C.; Heitz, V.; Sauvage, J.-P. *J. Am. Chem. Soc.* **1993**, *115*, 12378-12384. (d) Diederich, F.; Dietrich-Buchecker, C.; Nierengarten, J.-F.; Sauvage, J.-P. *J. Chem. Soc., Chem. Commun.* **1995**, 781-782. (e) Cárdenas, D. J.; Gaviña, P.; Sauvage, J.-P. *Chem. Commun.* **1996**, 1915-1916. (f) Solladié, N.; Chambron, J.-C.; Dietrich-Buchecker, C. O.; Sauvage, J.-P. *Angew. Chem., Int. Ed. Engl.* **1996**, *35*, 906-909. (g) Armaroli, N.; Diederich, F.; Dietrich-Buchecker, C. O.; Flamigni, L.; Marconi, G.; Nierengarten, J.-F.; Sauvage, J.-P. *Chem. Eur. J.* **1998**, *4*, 406-416. (h) Armaroli, N.; Balzani, V.; Collin, J.-P.; Gaviña, P.; Sauvage, J.-P.; Ventura, B. *J. Am. Chem. Soc.* **1999**, *121*, 4397-4408. (i) Solladié, N.; Chambron, J.-C.; Sauvage, J.-P. *J. Am. Chem. Soc.* **1999**, *121*, 3684-3692. (j) Weber, N.; Hamann, C.; Kern, J.-M.; Sauvage, J.-P. *Inorg. Chem.* **2003**, *42*, 6780-6792. (k) Poleschak, I.; Kern, J.-M.; Sauvage, J.-P. *Chem. Commun.* **2004**, 474-476. (l) Kwan, H. P.; Swager, T. M. *J. Am. Chem. Soc.* **2005**, *127*, 5902-5909.
7. For a *rotaxane dimer* assembled around tetrahedral four-coordinate Cu(I) templates see: Jiménez, M. C.; Dietrich-Buchecker, C.; Sauvage, J.-P. *Angew. Chem. Int. Ed.* **2000**, *39*, 3284-3287.

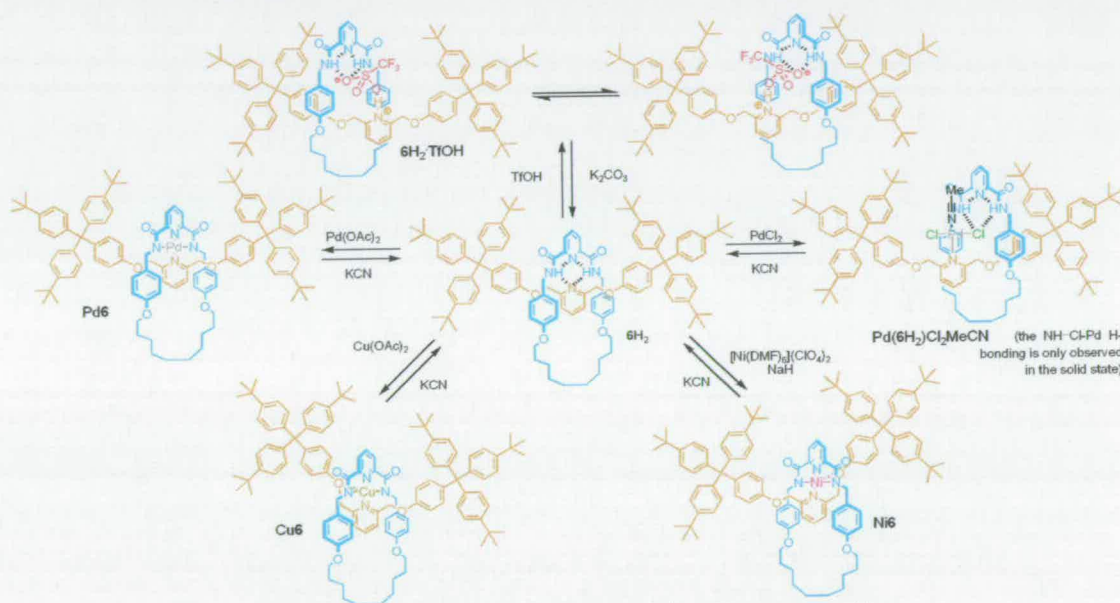
8. For *knots* assembled around tetrahedral four-coordinate Cu(I) templates see: (a) Dietrich-Buchecker, C. O.; Sauvage, J.-P. *Angew. Chem. Int. Ed. Engl.* **1989**, *28*, 189-192. (b) Dietrich-Buchecker, C. O.; Nierengarten, J.-F.; Sauvage, J.-P. *Tetrahedron Lett.* **1992**, *33*, 3625-3628. (c) Dietrich-Buchecker, C. O.; Sauvage, J.-P.; Kintzinger, J.-P.; Maltese, P.; Pascard, C.; Guilhem, J. *New. J. Chem.* **1992**, *16*, 931-942. (d) Dietrich-Buchecker, C. O.; Sauvage, J.-P.; De Cian, A.; Fischer, J. *J. Chem. Soc., Chem. Commun.* **1994**, 2231-2232. (e) Perret-Aebi, L.-E.; von Zelewsky, A.; Dietrich-Buchecker, C.; Sauvage, J.-P. *Angew. Chem. Int. Ed.* **2004**, *43*, 4482-4485.
9. (a) Sokolov V.I.; *Usp. Khim.* **1973**, *42*, 1037-1059; *Russ. Chem. Rev.(Engl. Transl.)* **1973**, *42*, 452-463. For later discussions on possible strategies to catenates based on octahedral metal templates see (b) Busch, D.H. *J. Inclusion Phenom. Mol. Recogn.* **1992**, *12*, 389-395. (c) Gerbeleu, N.V.; Arion, V.B.; Burgess, J. *Template Synthesis of Macrocyclic Compounds*, Wiley-VCH, Weinheim, **1999** and Ref 1b.
10. Belfrekh, N.; Dietrich-Buchecker, C.; Sauvage, J.-P. *Inorg. Chem.* **2000**, *39*, 5169-5172.
11. (a) Leigh, D. A.; Lusby, P. J.; Teat, S. J.; Wilson, A. J.; Wong, J. K. Y.; *Angew. Chem. Int. Ed.* **2001**, *40*, 1538-1543. (b) Hogg, L.; Leigh, D. A.; Lusby, P. J.; Morelli, A.; Parsons, S.; Wong, J. K. Y. *Angew. Chem. Int. Ed.* **2004**, *43*, 1218-1221. (c) Mobian, P.; Kern, J.-M.; Sauvage, J.-P. *J. Am. Chem. Soc.* **2003**, *125*, 2016-2017. (d) Arico, F.; Mobian, P.; Kern, J.-M.; Sauvage, J.-P. *Org. Lett.* **2003**, *5*, 1887-1890. (e) Mobian, P.; Kern, J.-M.; Sauvage, J.-P. *Angew. Chem. Int. Ed.* **2004**, *43*, 2392-2395. (f) Chambron, J.-C.; Collin, J.-P.; Heitz, V.; Jouvenot, D.; Kern, J.-M.; Mobian, P.; Pomeranc, D.; Sauvage, J.-P. *Eur. J. Org. Chem.* **2004**, 1627-1638.
12. Hamann, C.; Kern, J.-M.; Sauvage, J.-P. *Inorg. Chem.* **2003**, *42*, 1877-1883.
13. Gruter, G.-J. M.; de Kanter, F. J. J.; Markies, P. R.; Nomoto, T.; Akkerman, O. S.; Bickelhaupt, F. *J. Am. Chem. Soc.* **1993**, *115*, 12179-12180.
14. Flapan, E. *A Knot Theoretic Approach to Molecular Chirality* in Sauvage, J.-P.; Dietrich-Buchecker, C., Eds. *Molecular Catenanes, Rotaxanes and Knots*; Wiley-VCH: Weinheim, **1999**, 7-35.
15. (a) Kickham, J. E.; Loeb, S. J. *Inorg. Chem.* **1994**, *33*, 4351-4359. (b) Kickham, J. E.; Loeb, S. J.; Murphy, S. L. *Chem. Eur. J.* **1997**, *3*, 1203-1213.
16. Hamann, C.; Kern, J.-M.; Sauvage, J.-P. *Dalton. Trans.* **2003**, 3770-3775.

17. (a) Fuller, A.-M.; Leigh, D. A.; Lusby, P. J.; Oswald, I. D. H.; Parsons, S.; Walker, D. B.; *Angew. Chem. Int. Ed.* **2004**, *43*, 3914-3918. (b) Furusho, Y.; Matsuyama, T.; Takata, T.; Moriuchi, T.; Hirao, T. *Tetrahedron Lett.* **2004**, *45*, 9593-9597. (c) Leigh, D. A.; Lusby, P. J.; Slawin, A. M. Z.; Walker, D. B. *Angew. Chem. Int. Ed. in press*.
18. (a) Schwab, P.; France, M. B.; Ziller, J. W.; Grubbs, R. H. *Angew. Chem., Int. Ed. Engl.* **1995**, *34*, 2039-2041. (b) Grubbs, R. H.; Miller, S. J.; Fu, G. C. *Acc. Chem. Res.* **1995**, *28*, 446-452.
19. Vance, A. L.; Alcock, N. W.; Busch, D. H.; Heppert, J. A. *Inorg. Chem.* **1997**, *36*, 5132-5134.
20. At least as long as the RCM reaction is not under thermodynamic control. However, metathesis of internal olefins is generally much slower than terminal olefins. See, for example, Kidd, T. J.; Leigh, D. A.; Wilson, A. J. *J. Am. Chem. Soc.* **1999**, *121*, 1599-1600.
21. The term 'atropisomerism' technically refers to conformers which can be isolated as separate chemical species as a result of restricted rotation about a single bond [IUPAC Compendium of Chemical Terminology 2nd Edition, 1997]. We stretch this definition slightly in applying it to Pd(7)(endo-8) and Pd(7)(exo-8), which are isolable as a result of restricted rotation about various single bonds in particular ligand orientations.
22. The term "co-conformation" is generally used to refer to the relative positions of mechanically interlocked components with respect to each other[Fyfe, M. C. T.; Glink, P. T.; Menzer, S.; Stoddart, J. F.; White, A. J. P.; Williams, D. J. *Angew. Chem., Int. Ed. Engl.* **1997**, *36*, 2068-2070]. However, since the two components in Pd(7)(endo-8) and Pd(7)(exo-8) are connected by a continuous sequence of covalent and coordination bonds, in this case "conformation" is a sufficient descriptor.
23. The hydrogenation conditions employed in Routes I and III led to a complex mixture when applied to the products of metathesis in Route II. Not only was significant decomplexation of the somewhat strained non-interlocked double macrocycle complex observed, but the resulting free monodentate ligand, **10**, was degraded, presumably by hydrogenolysis of the benzyl ether moieties. Although the use of Na₂CO₃ did not prevent the ligand decomplexation during the hydrogenation step, it reduced the degradation of the free monodentate macrocycle [Cook, G. R.; Behloz, L. G.; Stille, J. R. *J. Org. Chem.* **1994**, *59*, 3575-3582].

- 24 Hogg, L.; Leigh, D. A.; Lusby, P. J.; Morelli, A.; Parsons, S.; Wong, J. K. Y. *Angew. Chem. Int. Ed.* **2004**, *43*, 1218-1221.
25. Fuller, A.-M.; Leigh, D. A.; Lusby, P. J.; Oswald, I. D. H.; Parsons, S.; Walker, D. B.; *Angew. Chem. Int. Ed.* **2004**, *43*, 3914-3918.
26. Donahoe, H. B.; Benjamin, L. E.; Fennoy, L. V.; Greiff, D. *J. Org. Chem.* **1961**, *26*, 474-476.
27. Schalley, C. A.; Silva, G.; Nising, C. F.; Linnartz, P. *Helv. Chim. Acta.* **2002**, *85*, 1578-1596.
28. Bremeyer, N.; Ley, S. V.; Ramarao, C.; Shirley, I. M.; Smith, S. C. *Synlett* **2002**, 1843-1844.

Chapter Four Synopsis

In chapters two and three the synthesis of a [2]rotaxane and a [2]catenane are described. Following the development of these new routes for the assembly of mechanically interlocked architectures, we examined the properties of the demetallated species $6H_2$ and $11H_2$ more closely. The initial proposition that the two kinetically held fragments (e.g. the macrocycle and the thread in $6H_2$) were H-bonding through a bifurcated pyridine-amide-pyridine motif was based on 1H NMR observations. This was confirmed in the solid state by X-ray crystallography. A search of the literature suggested such a motif was in fact quite unusual and was thus investigated more closely.



Scheme 1. Binding modes observed for [2]rotaxane $6H_2$.

The raised energy of the interlocked components – brought about by the enforced high local concentration of convergent functional groups, the limitation in the number of conformations and co-conformations each component can adopt, and the poor solvation of their inner surfaces – facilitates (kinetically and thermodynamically) the formation of internal and external binding motifs that are either not observed or are much weaker when the same groups are not confined in this way. The effect is illustrated through a remarkable series of binding modes – including orthogonal bifurcated bis-pyridine hydrogen bonding, cooperative binding to a sulfonic acid ‘guest’ through de-protonation by one component and anion-amide hydrogen bonding by the other, enforced square pyramidal coordination of Cu(II)

and Ni(II), and second sphere coordination in a square planar Pd(II)Cl complex - exhibited in solution and the solid state by a [2]rotaxane and an analogous [2]catenane, but not seen with either threadable (but non-mechanically interlocked) versions of the components or flexible covalently bonded systems.

Chapter 4: Rare and diverse binding modes introduced through mechanical bonding

Published as “Rare and diverse binding modes introduced through mechanical bonding” D. A. Leigh, P. J. Lusby, A. M. Z. Slawin, D. B. Walker *Angew. Chem. Int. Ed.* **2005**, *44*, 4557-4564.

Acknowledgements

The following people are gratefully acknowledged for their contribution to this chapter: Dr. P. Lusby for many useful discussions; Prof. A. M. Z. Slawin solved the X-ray crystal structures of **6H₂**, **11H₂**, **6H₂.HOTf**, **Cu₆**, **Ni₆** and **Pd(6H₂)Cl₂(CH₃CN)**.

4.1 Introduction

Interest in catenanes and rotaxanes has largely focused on the stimuli-induced change in position of their components for possible exploitation in molecular-level devices,^[1] but other properties and features of these architectures are becoming apparent.^[2] Here we report on a previously unrecognized consequence of kinetically stabilizing an otherwise unfavorable association of molecular fragments through mechanically bonding (Figure 4.1). The raised energy of the interlocked components – brought about by the enforced high local concentration of convergent functional groups, the limitation in the number of conformations and co-conformations each component can adopt, and the poor solvation of their inner surfaces – facilitates (kinetically and thermodynamically) the formation of internal and external binding motifs that are either not observed or are much weaker when the same groups are not confined in this way. The effect is illustrated through a remarkable series of binding modes – including orthogonal bifurcated bis-pyridine hydrogen bonding, cooperative binding to a sulfonic acid ‘guest’ through de-protonation by one component and anion-amide hydrogen bonding by the other, enforced square pyramidal coordination of Cu(II) and Ni(II), and second sphere coordination in a square planar Pd(II)Cl complex – exhibited in solution and the solid state by a [2]rotaxane and an analogous [2]catenane, but not seen with either threadable (but non-mechanically interlocked) versions of the components or flexible covalently bonded systems (Figure 4.2).

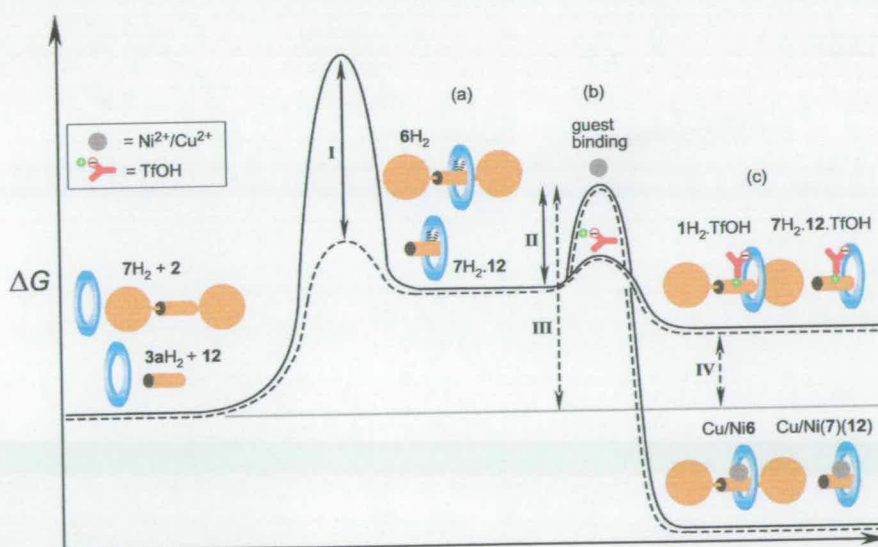


Figure 4.1. Effects of kinetically stabilizing an otherwise unfavorable association of molecular fragments through mechanical bonding. (a) The kinetic stabilization (I) of a mechanically interlocked architecture that features only weakly attractive interactions between the macrocycle and thread

permits non-covalent interactions to be observed (as in $6H_2$) that are too weak to stabilize the corresponding host-guest complex ($7H_2.12$). (b) For a rotaxane that is not thermodynamically stable with respect to its free components, the activation energy for tertiary component complex formation is, in principle, lower than for the analogous non-interlocked system, i.e. barrier **II** is less than **III**. This arises because the entropic cost of bringing the two components of the rotaxane together has already been paid, some degrees of freedom of the components are already restricted in the mechanically interlocked architecture, and the desolvation of the internal rotaxane surfaces is less energetically demanding than those of the free components. (c) The higher energy of such a rotaxane means that a host-guest complex involving the rotaxane can be favorable, e.g. $6H_2.TfOH$, even when the equivalent trimolecular complex ($7H_2.12.TfOH$) is not (**IV**). It also ensures that metal complexes derived from such rotaxanes, such as Cu_6 and Ni_6 , are inherently thermodynamically more stable than the analogous complexes derived from non-interlocked fragments and, in principle, kinetically easier to form.

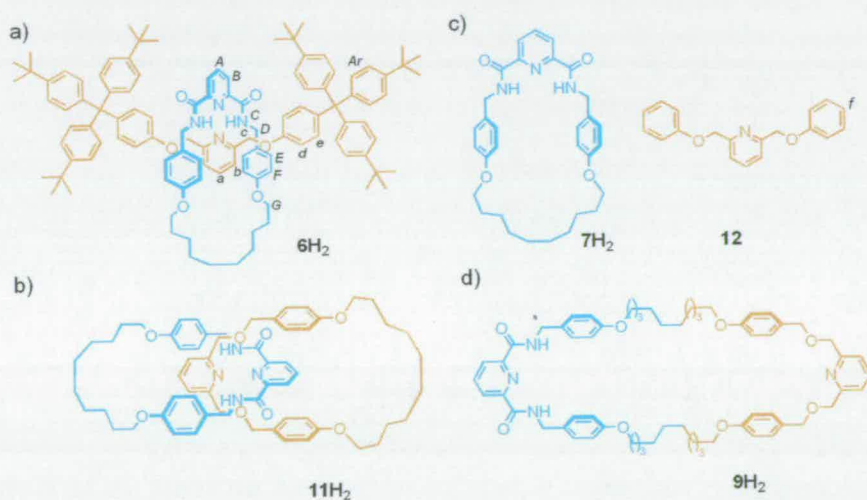


Figure 4.2. Different ways of linking a 2,6-dialkyl pyridine unit with a 2,6-dicarboxamide pyridine unit which lead to significantly different non-covalent binding properties: (a) on different components within a [2]rotaxane architecture, $6H_2$; (b) on different components within a [2]catenane architecture, $11H_2$; (c) on separate threadable, but not mechanically interlocked, molecular components $7H_2$ and **12**; (d) on a flexible but wholly covalently bonded system, $4H_2$. Lettering shows assignments for the 1H NMR spectra shown in Figure 4.4.

4.2 Results and Discussion

Most catenanes and rotaxanes are synthesized by utilizing templates to thermodynamically favor interlocking,^[1a] but subsequent removal of the template can leave a molecule that is thermodynamically unstable with respect to the uninterlocked components and is only held together by the mechanical bond. We recently described^[3] the assembly of a mechanically interlocked architecture about a Pd(II) template to give a square planar [2]rotaxane-metal coordination complex, Pd6.^[4] We were intrigued to find that upon protic de-metallation of the complex to give **6H₂**, the ¹H NMR spectrum in CDCl₃ indicated significant (the macrocycle amide protons appear at 1.7 ppm lower field than the equivalent protons in the free macrocycle) intercomponent hydrogen bonding between the amide groups of the macrocycle and the pyridine nitrogen of the rotaxane thread. Such a binding motif – requiring essentially orthogonal pyridine rings with the nitrogen atoms bridged by bifurcated hydrogen bonds – is rare (a search of the Cambridge Crystallographic Database reveals only one other example^[5]) but it is somewhat reminiscent of the H-bonding 90° to the plane of the lone pairs of amide groups in threads seen in many other hydrogen bonded rotaxanes.^[6] Slow cooling of a hot, saturated solution of **6H₂** in acetonitrile:chloroform (10:1) yielded single crystals which allowed the interaction also to be confirmed in the solid state by X-ray crystallography (Figure 4.3 a and 4.3 b) but the crystals were of insufficient quality to confidently characterize it in detail.^[7] However, when we prepared a [2]catenane incorporating the same functional groups, **11H₂**, a similar non-covalent interaction was found to be present in CDCl₃ solution and, in this case, single crystals of excellent quality for diffraction studies were obtained by slow cooling of a hot, saturated solution of **11H₂** in acetonitrile. The solid state structure of **11H₂** (Figure 4.3 c) closely mirrors the hydrogen bonding motif seen in the crystal structure of **6H₂**, with unsymmetrical intercomponent H-bond distances (2.28 and 3.10 Å in **11H₂**; 2.3 and 2.8 Å in **6H₂**) and the angle between the planes of the pyridine rings nearly orthogonal (90.7° in **11H₂**; 82° in **6H₂**) but tilted (30.0° in **11H₂** (Fig. 4.3 c inset); 34° in **6H₂**) away from linearity to avoid too close an interaction between the two pyridine nitrogen lone pairs.

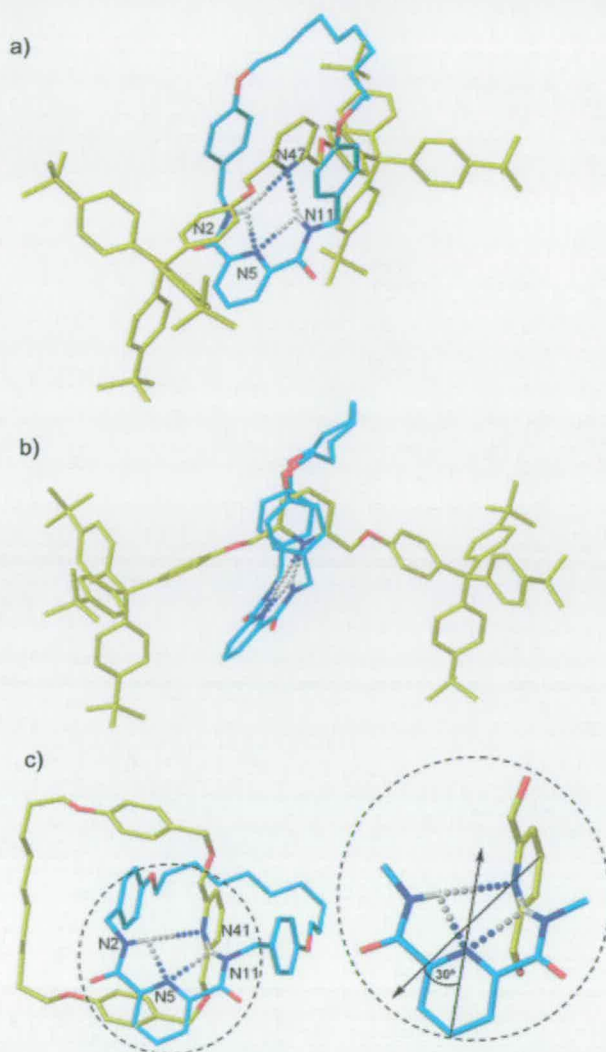


Figure 4.3. X-ray crystal structures^[7] of [2]rotaxane **6H₂** and [2]catenane **11H₂**: (a) **6H₂** (twisted view); (b) **6H₂** (side view, showing the macrocycle circumscribing the pyridine residue of the thread. Disorder in the alkyl chain region and solvate molecules, not the central H-bonding region, results in a high overall *R* factor of 33%); (c) **11H₂** (*R* factor <5%, intercomponent H-bond motif mirrors that shown in (a) and (b)). The lone pairs of the pyridine atoms do not point directly at each other, but are tilted 30.0° apart (inset). Carbon atoms of the macrocycle are shown in light blue and those of the thread in yellow; oxygen atoms are red, nitrogen dark blue, hydrogen white. For clarity only nitrogen-bound hydrogen atoms are shown. Selected bond lengths for **6H₂** [Å]: N2H-N5 2.4; N11H-N5 2.6; N2H-N47 2.8; N11H-N47 2.3. Selected bond angles for **6H₂** [°]: N2H-N5 151; N11H-N5 153; N2H-N47 96; N11H-N47 108. Selected bond lengths for **11H₂** [Å]: N2H-N5 2.18; N11H-N5 2.33; N2H-N41 2.28; N11H-N41 3.10. Selected bond angles for **11H₂** [°]: N2H-N5 107.1; N11H-N5 102.2; N2H-N41 146.5; N11H-N41 129.0.

In order to investigate this atypical binding motif further, we titrated an unstoppered analogue of the thread, **12**, with the free macrocycle, **7H₂**, to determine the energetics

of the interaction in the absence of the kinetic barrier to dissociation provided by the mechanical bond. However, there was virtually no shift in the amide protons of **7H₂** in the presence of up to 20 equiv of **12** (4-80 mM) by ¹H NMR spectroscopy in CDCl₃, indicating that the bimolecular association constant must be less than 5 M⁻¹, the approximate limit of this detection method with the large shifts typically observed through amide H-bonding. Of further interest is that the ¹H NMR of the wholly covalently linked analogue **9H₂** also gives no indication of H-bonding interactions between the pyridine-2,6-carboxamide protons and the second pyridine residue in CDCl₃, even though this very large macrocycle is certainly flexible enough to adopt such a geometry without steric hindrance.

Rare (e.g. amide *NH* to ester acyl oxygen atom)^[8,9] and thus far unique (e.g. amide *NH* to ester alkyl oxygen atom)^[9] hydrogen bond motifs have previously been observed within rotaxane architectures. The propensity for such unusual interactions in mechanically bonded structures probably arises for a number of reasons: (i) the enforced high local concentration of functional groups for which there is a low steric cost to relative movement within the vector of the thread, (ii) the relatively limited number of conformations and co-conformations each component can adopt which does not put functional groups into convergent orientations, (iii) the imposed orthogonalization of components which can preclude normally preferred non-covalent bonding geometries, (iv) freezing out of a single co-conformation for an inter-component binding event only costs a reduction of two degrees of freedom (translation and rotation of the macrocycle about the thread), compared, for example, with the multiple degrees of rotational freedom of the alkyl chains that would be lost by internal hydrogen bonding in **9H₂**, (v) the inefficient solvation of internal or congested surfaces of an interpenetrated architecture means that de-solvation of binding sites is likely to occur at a lower energetic cost than for conventional structures. All of these factors effectively do the same thing: raise the energy of the rotaxane with respect to the free components. However, the kinetic stabilization of the architecture provided by the stoppers prevents dethreading (i.e. the rotaxane is not in equilibrium with the free components). This raising of the internal energy is actually a form of 'host preorganisation', serving to enhance binding properties as outlined by Cram over 30 years ago.^[10] The result is that interactions that are not

strong enough to stabilize a host-guest complex can become thermodynamically favorable if the components are held together by a mechanical bond (Figure 4.1).

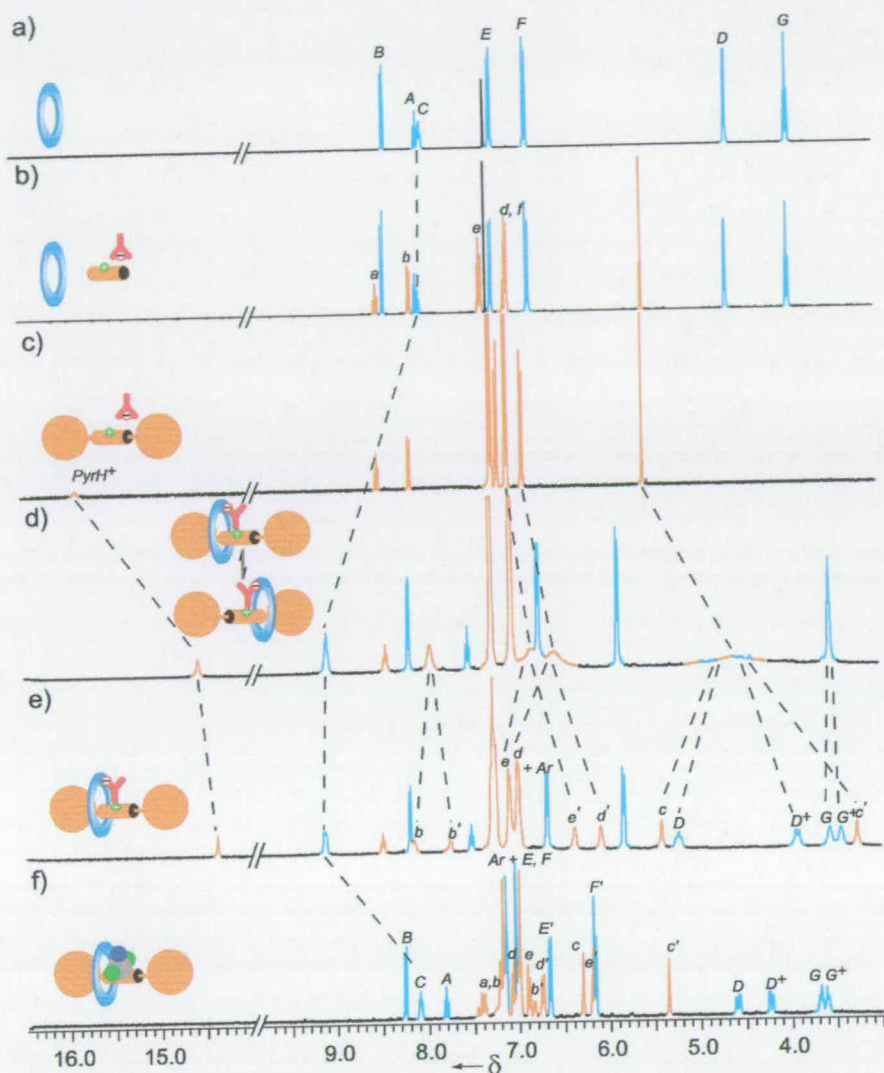
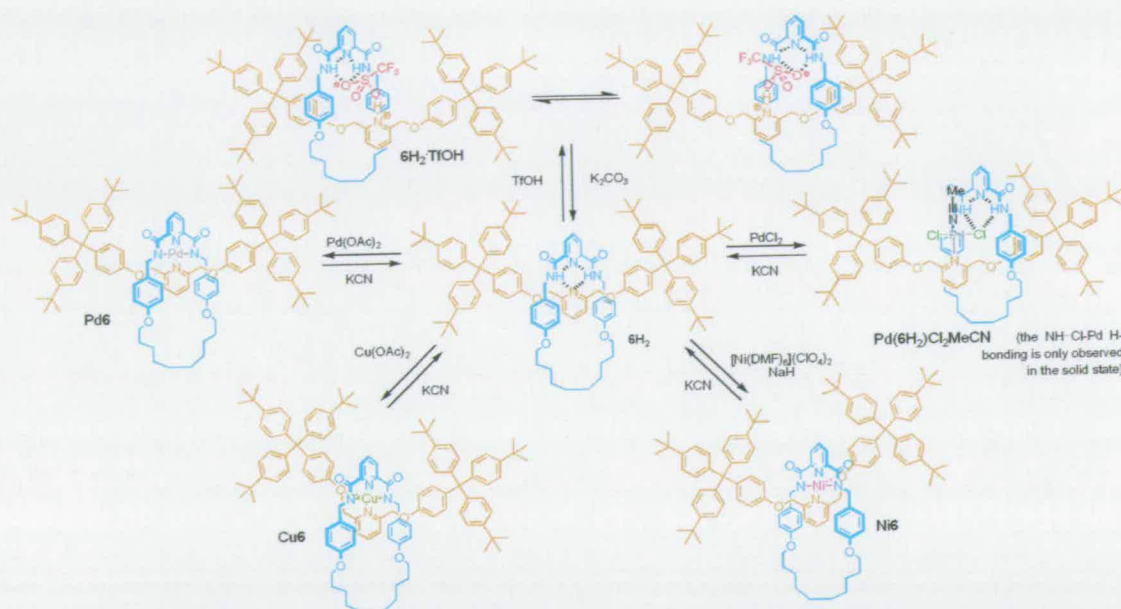


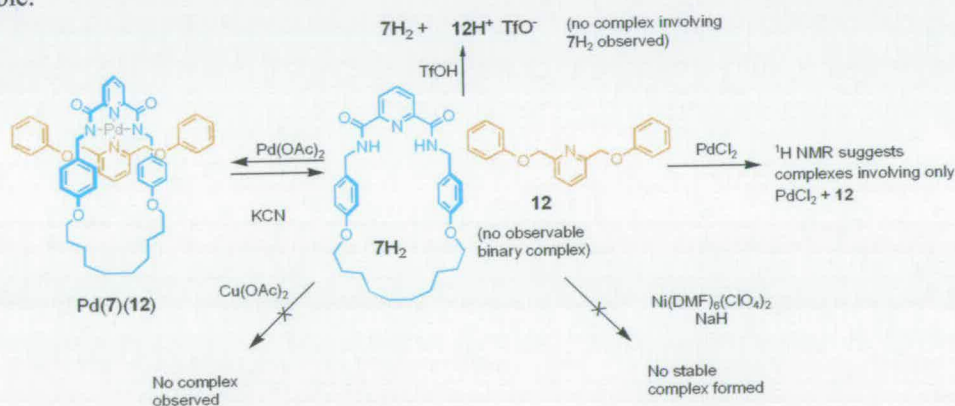
Figure 4.4. ^1H NMR (CDCl_3 , 400 MHz, 298 K except (e)) of: (a) macrocycle 7H_2 , (b) 7H_2 + unstoppered thread 12 + HOTf; (c) thread + HOTf, (d) [2]rotaxane complex 6H_2 .HOTf showing fast exchange (shuttling) of the macrocycle between equivalent sites on both halves of the thread, (e) [2]rotaxane complex 6H_2 .HOTf at 238 K showing slow exchange (reversible non-covalent bonding of the triflate anion provides a transient steric barrier to shuttling), (f) $\text{Pd}(6\text{H}_2)\text{Cl}_2\text{MeCN}$ showing slow exchange (coordination of PdCl_2MeCN provides a fixed steric barrier to shuttling up to at least 325 K).

We reasoned that it should be possible to disrupt the intercomponent H-bonding interaction in 6H_2 by protonating the more basic 2,6-dioxymethylenepyridine nitrogen atom (Scheme 4.1). However, although treatment of 6H_2 with one equivalent of $\text{CF}_3\text{SO}_3\text{H}$ (TfOH) resulted in protonation of the desired site (Figure 4.4 d), the downfield shift of the H_C amide protons indicated that strong hydrogen

bonding was still present! The shielding and broadening of particular thread signals at 298 K (Figure 4.4 d) suggested that instead of residing over the pyridine residue as in **6H₂**, the macrocycle is displaced to the side and shuttles between the two halves of the thread relatively slowly on the NMR timescale. This was confirmed by the 238 K ¹H NMR spectrum (Figure 4.4 e) in which many of the thread resonances are split into two inequivalent sets ($H_b/H_{b'}$, $H_c/H_{c'}$, $H_d/H_{d'}$, $H_e/H_{e'}$) corresponding to exposed-to-solvent and encapsulated (and thus magnetically shielded by the macrocycle) protons, respectively. The rationale for this behaviour was provided by the X-ray structure of single crystals grown from acetonitrile (Figure 4.5a). The [2]rotaxane acts as a host for an entire trifluorosulfonic acid molecule; one component (the thread) de-protonating the acid and both components hydrogen bonding to the resulting anion to generate a neutral complex, **6H₂.HOTf**. The X-ray structure is consistent with the specific shielding effects seen in the ¹H NMR spectra – including the upfield shift of the pyridinium proton cf. Fig. 4.4c as a consequence of other H-bond donors binding to the triflate anion – and with the non-covalent binding of the sulfonic acid acting as a transient steric barrier to shuttling of the macrocycle between the two halves of the thread.^[12] In contrast (Scheme 4.2), a 1:1 mixture of **7H₂** and **12·H⁺ TfO⁻** in CDCl₃ shows no upfield shift of resonances H_c , H_d and H_e (Figure 4.4 b) cf. the protonated thread (Figure 4.4c), nor downfield shifts of the **7H₂** amide protons. Similarly, the absence of shifts in the amide resonances of the protonated covalently linked structure **9H₂.H⁺ TfO⁻** suggests that it does not internally associate through H-bonding.



Scheme 4.1. Binding modes observed for [2]rotaxane $6H_2$. The X-ray crystal structures are shown in Figures 3 and 5. A similar range of complexes is exhibited by [2]catenane $11H_2$ (for X-ray crystal structures of Pd11 and Pd($11H_2$)Cl₂MeCN see ref. [12]). All of the complexation reactions are fully reversible.



Scheme 4.2. Attempted complexation experiments involving $7H_2/12$. Similar results were obtained with macrocycle $9H_2$ (for an X-ray crystal structure of Pd9 see ref. [12]).

The mechanically interlocked assemblies also differ from their non-interlocked counterparts in their ability to adopt a range of overall neutral binding modes with metals. Treatment of $6H_2$ or $11H_2$ with $Cu(OAc)_2$ in refluxing $MeOH/CH_2Cl_2$ resulted in double de-protonation of the ligand and the generation of the corresponding 1:1 neutral metal-interlocked ligand complex. Recrystallization of the copper [2]rotaxane complex, Cu6, from acetonitrile gave single crystals suitability for investigation by X-ray crystallography (Figure 4.6 a). The solid state structure shows a square based pyramidal coordination motif, involving one of the thread oxygen

atoms in addition to the four nitrogens of the rotaxane which form the near-planar (N47 is $\sim 10^\circ$ above the plane defined by N2-N11-N5-Cu) base of the pyramid. Treatment of $7H_2/12$ or $9H_2$ with $Cu(OAc)_2$ under the same conditions gave no indication of any complex formation and there was no de-protonation of the macrocycle amide groups.

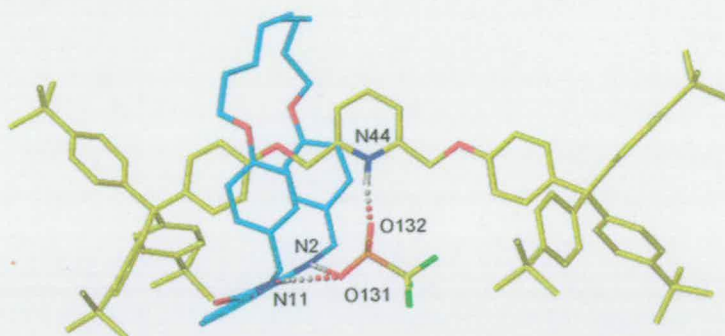


Figure 4.5. X-ray crystal structures^[7] of neutral [2]rotaxane-trifluoromethanesulfonic acid complex, $6H_2.HOTf$. Note the macrocycle is displaced to one side of the central region of the thread compared to free $6H_2$ (Figure 3b). Carbon atoms of the macrocycle are shown in light blue and those of the thread in yellow; oxygen atoms are red, chlorine green, nitrogen dark blue, sulfur orange, fluorine green, hydrogen white. For clarity only amide hydrogen atoms are shown. Selected H-bond lengths for $6H_2.HOTf$ [Å]: N2H-O131 2.14; N11H-O131 2.17; N44H-O132 1.72. Selected bond angles for $6H_2.HOTf$ [°]: N2H-O131 159.0; N11H-O131 148.1; N44H-O132 159.7.

The formation of complexes of the mechanical interlocked ligands with nickel required more vigorous conditions ($[Ni(DMF)_6](ClO_4)_2$, NaH, DMF, $60^\circ C$, 1 h) but nonetheless resulted in Ni6 and Ni11, both orange crystalline compounds. In this case, a similarly colored complex could also be generated with $7H_2/12$, but unlike Ni6 or Ni11 it rapidly decomposes and we were unable to isolate or characterize it. The X-ray structure of single crystals of Ni6 grown from slow cooling of a saturated acetonitrile solution is shown in Figure 4.6b and is closely related to the structure obtained for Cu6. Treatment of any of the rotaxane or catenane metal complexes with KCN in $CH_2Cl_2/MeOH$ regenerates the original interlocked molecule, $6H_2$ or $11H_2$. The difference in both the ease of formation and the stability of the metal complexes with the catenane and rotaxane compared to the non-interlocked ligands is again consistent with the intrinsic effects of kinetically stabilizing a mechanically interlocked architecture (Figure 4.1 c).

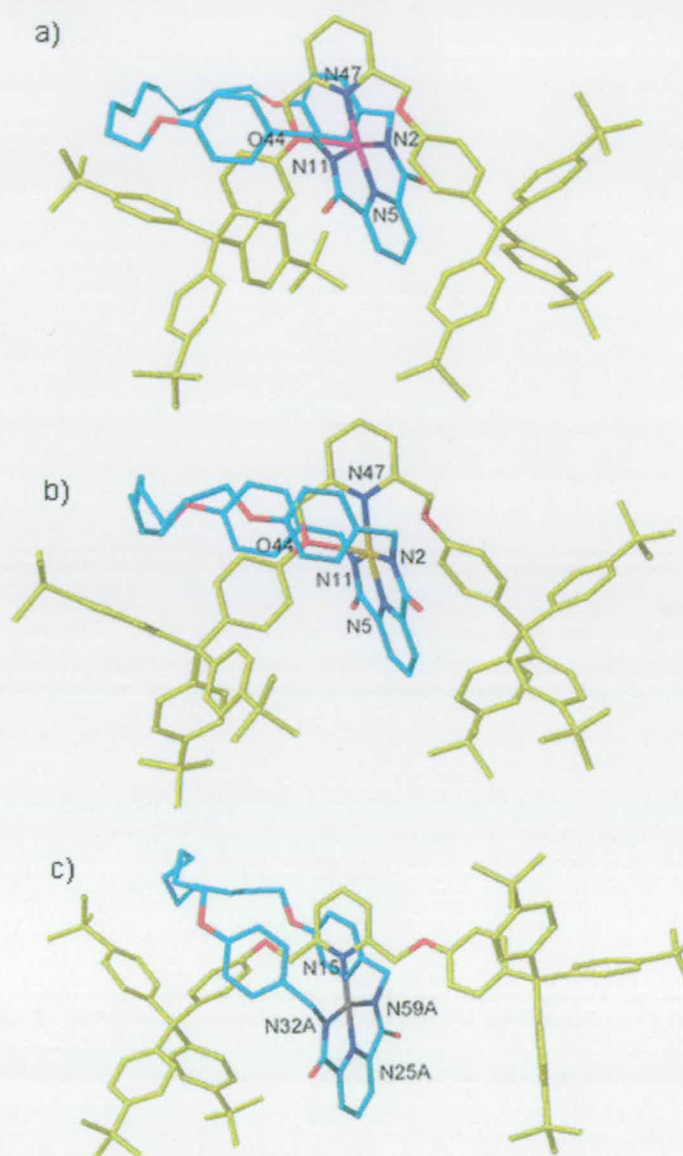


Figure 4.6. X-ray crystal structures^[7] of various complexes of **6**: (a) square pyramidal coordination complex Cu6. (b) square pyramidal coordination complex Ni6. (c) square planar coordination complex Pd6. Carbon atoms of the macrocycle are shown in light blue and those of the thread in yellow; oxygen atoms are red, nitrogen dark blue, hydrogen white, copper brown, nickel pink, palladium grey. Selected bond lengths for Cu6 [Å]: N2-Cu 2.00; N11-Cu 1.98; N5-Cu 1.92; N47-Cu 2.02; O44-Cu 2.41. Selected bond angles for Cu6[°]: N2-Cu-N5 80.3; N5-Cu-N11 80.7; N11-Cu-N47 101.3; N5-Cu-O44 116.6; N5-Cu-N47 169.7. Selected bond lengths for Ni6 [Å]: N2-Ni 1.94; N11-Ni 1.93; N5-Ni 1.81; N47-Ni 1.93; O44-Cu 2.52. Selected bond angles for Ni6: N2-Ni-N5 82.6; N5-Ni-N11 82.4; N11-Ni-N47 98.5; N5-Ni-O44 113.8; N5-Ni-N47 172.1. Selected bond lengths for Pd6: [Å]: Pd-N15 1.95, Pd-N25 1.86, Pd-N32 2.04, Pd-N59 2.02; other selected distance [Å]: N15-N25 3.81; Selected bond angles for Pd6[°] N59-Pd-N32 160.0.

Each of the four ligand sets reacts with Pd(OAc)₂ (**6H**₂, **11H**₂ and **9H**₂ directly in MeCN/CH₂Cl₂; **7H**₂/**12** requires preliminary reaction of Pd(OAc)₂ with **7H**₂ in MeCN

followed by reaction of the resulting complex with **12** in CH_2Cl_2) to give the corresponding square planar coordination complexes (Schemes 1 and 2, Figure 4.6 c). However, the rotaxane and catenane also formed a different type of neutral square planar coordination complex when treated with PdCl_2 , an initial palladium salt bearing significantly more strongly coordinating ligands. Slow cooling of saturated solutions of either complex in acetonitrile rendered crystals suitable for X-ray crystallography and the structure of the rotaxane complex, $\text{Pd}(\mathbf{6H}_2)\text{Cl}_2\text{MeCN}$, is shown in Figure 4.7 (the solid state structure of the [2]catenane complex is similar but features intermolecular rather than intramolecular $\text{NH}\cdots\text{Cl}\cdots\text{Pd}$ H-bonding). From the crystal structures it can be seen that although the Pd coordinates to the thread as in $\text{Pd}\mathbf{6}$, the original metal chloride ligands remain intact and the macrocycle amides are not de-protonated. In solution the coordination of the PdCl_2MeCN unit to the pyridine ring of the thread acts as a steric barrier to shuttling (Figure 4.4 f) similar to that seen with $\mathbf{6H}_2\cdot\text{TfOH}$ but, unlike the complex held together by H-bonds, the coordination to the metal is not kinetically labile and persists as a barrier to shuttling up to at least 325 K (close to the boiling point of the CDCl_3 solvent).^[11]

The solid state structure of $\text{Pd}(\mathbf{6H}_2)\text{Cl}_2\text{MeCN}$ features hydrogen bonding between the amide groups of the macrocycle and the chloride ligands of the metal (Figure 4.7). However, the ^1H NMR spectrum (Figure 4.4f) shows this interaction is not present to any significant extent in CDCl_3 (the chemical shift of H_C is virtually unchanged compared to $\mathbf{7H}_2$). Wisner's group recently^[13] used a similar interaction to direct an elegant synthesis of a pseudorotaxane. In the course of that work a macrocycle binding constant largely resulting from two sets of isophthalamide groups H-bonding to the chloride ligands of a Pd(II) complex was determined to be $5 \times 10^3 \text{ M}^{-1}$ in CDCl_3 .^[13] In contrast, Crabtree found^[14] the association constant of a single isophthalamide group with Cl^- to be $6 \times 10^4 \text{ M}^{-1}$ in CD_2Cl_2 . Accordingly, a $\text{CONH}\cdots\text{Cl}\cdots\text{Pd}$ interaction must be somewhat less than half the strength of a $\text{CONH}\cdots\text{Cl}^-$ H-bond. This is consistent with the observation that it is too weak to significantly bind the macrocycle of $\text{Pd}(\mathbf{6H}_2)\text{Cl}_2\text{MeCN}$ in CDCl_3 , despite the high effective molarity introduced by the mechanical bond, and in marked contrast to the bifurcated bis-pyridine H-bonding that does do so so effectively in $\mathbf{6H}_2$. This shows that the intercomponent binding mode in $\mathbf{6H}_2$ is not particularly weak and its scarcity

as an observed interaction may be because the geometry of the interlocked architecture precludes other normally preferred non-covalent bonding geometries.

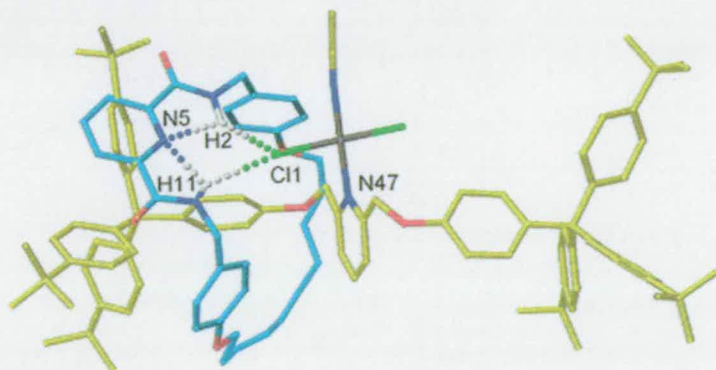


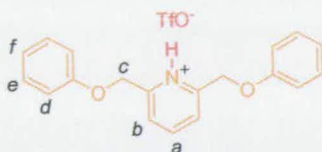
Figure 4.7. X-ray crystal structure^[7] of square planar coordination complex $\text{Pd}(\text{6H}_2)\text{Cl}_2\text{MeCN}$. Carbon atoms of the macrocycle are shown in light blue and those of the thread in yellow; oxygen atoms are red, chlorine green, nitrogen dark blue, hydrogen white, palladium grey. For clarity only amide hydrogen atoms are shown. Selected bond lengths for $\text{Pd}(\text{6H}_2)\text{Cl}_2\text{MeCN}$ [Å]: Pd-N47 1.98, Pd-Cl1 2.27, Cl1-H2 2.67, Cl1-H11 2.64, N5-H2 2.36, N5-H11 2.15; Selected bond angles for $\text{Pd}(\text{6H}_2)\text{Cl}_2\text{MeCN}$ [°]: N2-H2-Cl1 139.8, N11-H11-N5 114.1, N11-H11-Cl1 125.0.

In conclusion, the kinetically enforced association of molecular fragments within an interlocked architecture can lead to a diverse series of sometimes rare and unusual binding motifs both in solution and the solid state. These interactions can produce interesting effects in their own right; the co-operative hydrogen bonding of an organic guest by both components of a [2]rotaxane can present an effective barrier to shuttling at low temperatures, whereas a stronger metal-ligand coordination mode can be used to restrict the same motion even at higher temperatures. The fact that many of the observed modes of binding are weaker or not seen at all when the components are not mechanically interlocked makes this previously unappreciated consequence of the mechanical bond particularly noteworthy.^[15]

4.3 Experimental Section

4.3.1 Solution Host-Guest Binding Experiments

12 (2,6-bisphenoxyethylpyridine) was prepared according to a literature procedure and displayed identical spectroscopic data to those reported.^[16]



12H⁺OTf⁻: To a solution of **12** (0.200 g, 6.9×10^{-1} mmol) in dichloromethane (5 mL) was added TfOH (6.9 mL of a 0.01 M solution) and the solution stirred for 20 min. The resulting precipitate was filtered off and washed with further portions of dichloromethane (2 x 2 mL) to furnish the title compound as a colourless solid (0.294 g, yield = 97%). m.p. 104-105 °C; ¹H NMR (400 MHz, CDCl₃, 298 K): δ = 5.53 (s, 4H, H_c), 7.02 (m, 6H, H_e + H_f), 7.32 (t, J = 9.1 Hz, 4H, H_d), 8.02 (d, J = 8.1 Hz, 2H, H_b), 8.38 (t, J = 8.1 Hz, 1H H_a); ¹³C NMR (100 MHz, CDCl₃, 298 K): δ = 65.5, 114.7, 122.5, 123.3, 130.0 (x2), 154.0, 156.9, 184.1; ESI-MS m/z = 292 [MH]⁺.

¹H NMR titration experiments were performed in CDCl₃ with an initial 7H₂ concentration of 4.0×10^{-3} M and appropriate aliquots of a 4.0×10^{-2} M **12** or **12H⁺** TfO⁻ solution added (up to 20 equivalents) using a Gilson microlitre pipette. In addition a 1:1:1 solution (4.0×10^{-2} M) of 7H₂, **12** and TfOH was prepared, but no evidence of ternary complex formation was observed (the chemical shifts of all the macrocycle protons remained virtually unchanged). The binding constants were calculated using pro-Fit 5.5.3.^[17]

Guest Vol. (mL)	Guest Equiv.	Guest Conc. (M)	Chemical Shift	
			$\delta (\pm 0.05)$	$\Delta\delta (\pm 0.05)$
0	0	0	7.822	0
0.005	0.05	0.0002	7.825	0.003
0.01	0.1	0.0004	7.829	0.007
0.02	0.2	0.0008	7.835	0.013
0.04	0.4	0.0016	7.831	0.009
0.06	0.6	0.0024	7.841	0.019
0.08	0.8	0.0032	7.829	0.007
0.1	1	0.004	7.834	0.012
0.15	1.5	0.006	7.843	0.021
0.2	2	0.008	7.904	0.082
1	10	0.04	7.901	0.079
2	20	0.08	7.907	0.085

Table 4.1 ^1H NMR titration experimental data. 7H_2 host, 12 guest.

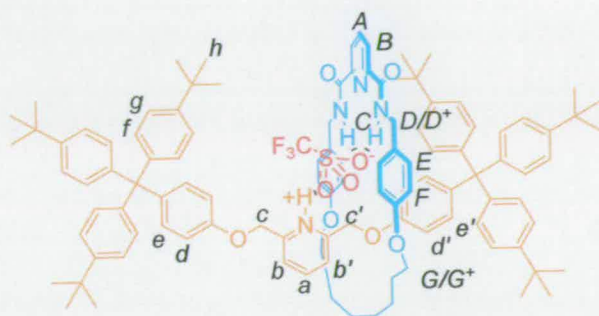
$$K = 7.8 \pm 10 \text{ M}^{-1}$$

Guest Vol. (mL)	Guest Equiv	Guest Conc. (M)	Chemical Shift	
			δ	$\Delta\delta$
0	0	0	7.791	0
0.005	0.05	0.0002	7.789	-0.002
0.01	0.1	0.0004	7.79	-0.001
0.02	0.2	0.0008	7.793	0.002
0.04	0.4	0.0016	7.795	0.004
0.06	0.6	0.0024	7.796	0.005
0.08	0.8	0.0032	7.794	0.003
0.1	1	0.004	7.798	0.007
0.15	1.5	0.006	7.858	0.067
0.2	2	0.008	7.894	0.103
1	10	0.04	7.915	0.124
2	20	0.08	7.934	0.143

Table 4.2 ^1H NMR titration experimental data. 7H_2 host, 12.TfOH guest.

$$K = 200 \pm 200 \text{ M}^{-1}$$

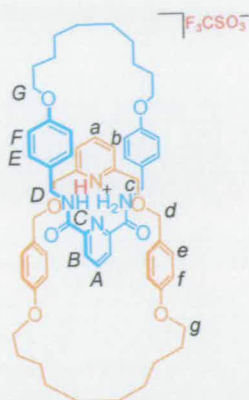
4.3.2. Preparation of Sulfonic Acid Complexes



6H₂.HOTf: To a solution of **6H₂** (0.020 g, 1.2×10^{-2} mmol) in CDCl₃ (0.7 mL) was added TfOH (0.12 mL of a 0.12 M solution CDCl₃). Slow evaporation of the solvent afforded the complex **6H₂.HOTf** as large colourless crystals (0.015 g, 70%), m.p. 176 °C (dec); ¹H NMR (400 MHz, CDCl₃, 238 K): 1.03-1.39 (m, 12H, H_{alkyl}), 1.24 (s, 54H, H_h), 1.54 (m, 4H, H_{alkyl}), 3.27 (m, 2H, H_{c'}), 3.42 (m, 2H, H_{G+}), 3.55 (m, 2H, H_G), 3.92 (m, 2H, H_{D+}), 5.25 (m, 2H, H_D), 5.41 (s, 2H, H_C), 5.86 (d, 4H, $J = 8.5$ Hz, H_F), 6.10 (m, 2H, H_{d'}), 6.42 (m, 2H, H_{e'}), 6.71 (d, 4H, $J = 8.5$ Hz, H_E), 6.89-7.35 (m, 28H, H_e + H_d + H_f + H_g), 7.51 (t, 1H, $J = 7.8$ Hz, H_A), 7.73 (m, 1H, H_b), 8.11-8.28 (m, 3H, H_B + H_b), 8.54 (t, 1H, $J = 7.6$ Hz, H_a), 9.12 (br, 2H, H_C), 14.90 (s, 1H, pyrH⁺).



9H₂.HOTf: To a solution of **9H₂** (0.010 g, 1.0×10^{-2} mmol) in CH₂Cl₂ (5 mL) was added TfOH (1 mL of a 0.01 M CH₂Cl₂ solution). The resulting precipitate was filtered and dried to furnish the title compound as white/pink solid (0.011 g, yield = 95%). m.p. = 225 °C (dec); ¹H NMR (400 MHz, CDCl₃, 298 K): 1.06-1.40 (m, 24H, H_{alkyl}), 1.62-1.72 (m, 8H, H_{alkyl}), 3.84 (m, 8H, H_G + H_G), 4.52 (d, 4H, $J = 5.6$ Hz, H_D), 4.58 (s, 4H, H_d), 4.81 (s, 4H, H_c), 6.75 (d, 4H, $J = 8.3$ Hz, H_E), 7.19 (m, 12H, H_F + H_e + H_f), 7.67 (d, 2H, H_b), 7.88 (m, 2H, H_C), 7.98 (t, 1H, $J = 7.4$ Hz, H_A), 8.14 (m, 1H, H_a), 7.32 (d, 2H, $J = 7.4$ Hz, H_B); ESI-MS $m/z = 1006$ [MH]⁺.



11H₂.HOTf: To a solution of **11H₂** (0.010 g, 1×10^{-2} mmol) in CDCl₃ (1 mL) was added TfOH (1 mL of a 0.01 M CDCl₃ solution). Following analysis, the solvent was removed under reduced pressure to furnish the title compound as a colourless solid (0.011 g, yield = 95%). m.p. = 197 °C (dec); ¹H NMR (400 MHz, CDCl₃, 298 K): 0.51-0.73 (m, 8H, H_{alkyl}), 1.07 (m, 8H, H_{alkyl}), 1.14-1.70 (m, 16H, H_{alkyl}), 3.37 (m, 4H, H_G), 3.71-4.00 (m, 8H, H_D + H_G), 4.15 (s, 4H, H_c), 4.41 (s, 4H, H_d), 5.59 (m, 4H, H_E), 6.45 (m, 4H, H_F), 6.76 (m, 4H, H_e), 6.93 (m, 4H, H_f), 7.47 (m, 2H, H_b), 8.05 (m, 2H, H_B), 8.50 (m, 1H, H_A), 8.78 (m, 1H, H_a), 9.02 (m, 2H, H_C), 12.31 (bs, 1H, Pyr-H⁺); ESI-MS $m/z = 1006 [MH]^+$.

4.3.3 Preparation of TM Complexes

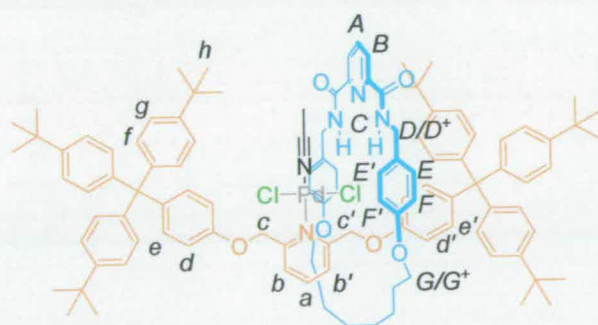
Cu6: Cu(OAc)₂.H₂O (0.013 g, 3×10^{-2} mmol) was added to a 1:1 methanol/dichloromethane solution (10 mL) of **6H₂** (0.025 g, 1.5×10^{-2} mmol) and heated at reflux for 12 h. Following solvent removal under reduced pressure, the crude blue/purple residue was recrystallised from acetonitrile to yield purple needles of **Cu6** (0.021 g, 83%). m.p. 228 °C (dec); LRFAB-MS (3-NOBA matrix) $m/z = 1690 [M]^+$; HRFAB-MS (3-NOBA matrix): $m/z = 1689.92392$, (calcd. for ¹²C₁₁₁¹³CH₁₂₉N₄O₆⁶³Cu, 1689.92437).

Cu11: Cu(OAc)₂ (0.022 g, 5×10^{-2} mmol) was added to a 1:1 methanol/dichloromethane solution (10 mL) of **11H₂** (0.025 g, 2.5×10^{-2} mmol) and heated at reflux for 12 h. Following solvent removal under reduced pressure, the crude blue residue was redissolved in dichloromethane (10 mL) and filtered to remove excess Cu(OAc)₂. The solvent was then removed under reduced pressure to furnish the title compound as a dark blue powder (0.019 g, yield = 71%). m.p. 197

°C (dec); LRFAB-MS (3-NOBA matrix): $m/z = 1066 [M]^+$; HRFAB-MS (3-NOBA matrix): $m/z = 1066.48523$, (calcd. for $C_{62}H_{75}N_4O_8^{63}Cu$, 1066.48829).

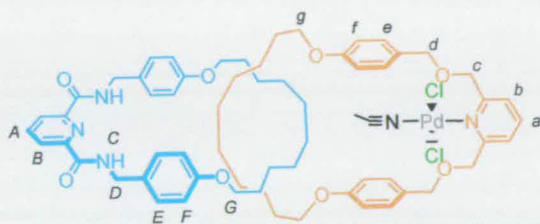
Ni6: To a solution of **6H₂** (0.025 g, 1.5×10^{-2} mmol) in dry DMF (3 mL) was added $Ni(DMF)_6 \cdot (ClO_4)_2$ (0.011 g, 1.5×10^{-2} mmol) and sodium hydride (0.003 g, 3×10^{-2} mmol) and the mixture was heated at 60 °C for 1 h under an atmosphere of nitrogen. The solvent was then removed under reduced pressure and the crude residue was recrystallised from acetonitrile to furnish orange needles of **Ni6** (0.015 g, 59%). m.p. 185 °C (dec); LRFAB-MS (3-NOBA matrix): $m/z = 1685 [M]^+$; HRFAB-MS (3-NOBA matrix): $m/z = 1684.93295$, (calcd. for $^{12}C_{111}^{13}CH_{129}N_4O_6^{58}Ni$, 1684.92987).

Ni11 To a solution of **11H₂** (0.025 g, 0.025 mmol) in anhydrous DMF (3 mL) was added $Ni(DMF)_6 \cdot (ClO_4)_2$ (0.018 g 0.025 mmol) and sodium hydride (0.003 g 0.06 mmol) and the mixture was heated at reflux for 1 h under an atmosphere of nitrogen. The solvent was then removed under reduced pressure and the crude residue was dispersed in diethyl ether and filtered to yield to furnish the title compound as an orange/red powder (0.019 g, yield = 73%). m.p. 201 °C (dec); LRFAB-MS (3-NOBA matrix): $m/z = 1061 [M]^+$; HRFAB-MS (3-NOBA matrix): $m/z = 1061.49385$, (calcd. for $C_{62}H_{75}N_4O_8^{58}Ni$, 1061.49379).

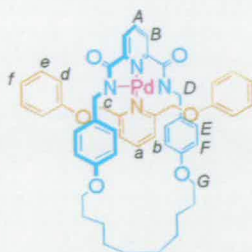


Pd(6H₂)Cl₂MeCN: To a solution of **6H₂** (0.02 g, 1.2×10^{-2} mmol) in 1:1 acetonitrile/dichloromethane (5 mL) was added $PdCl_2$ (0.004 g, 2.3×10^{-2} mmol) and the mixture was heated at 40 °C for 1 h to allow complete dissolution of the metal salt. The solvent was removed under reduced pressure and the crude residue recrystallised from acetonitrile to yield orange plates of $Pd(6H_2)Cl_2MeCN$ (0.019 g, 90%). m.p. 204 °C (dec); 1H NMR (400 MHz, $CDCl_3$, 298 K): $\delta = 1.05-1.40$ (m,

12H, H_{alkyl}), 1.23 (s, 54H, H_h), 1.56 (m, 4H, H_{alkyl}), 1.93 (s, 3H, Pd-NCCH₃), 3.65 (m, 4H, $H_{G^+} + H_G$), 4.23 (dd, 2H, $J = 14.7$ Hz, $J = 5.7$ Hz, H_{D^+}), 4.61 (dd, 2H, $J = 14.7$ Hz, $J = 5.7$ Hz, H_D), 5.36 (s, 2H, H_C), 6.19 (m, $J = 4$ Hz, $H_{E'} + H_{F'}$), 6.31 (s, 2H, $H_{C'}$), 6.68 (d, 2H, $J = 8.5$ Hz, $H_{E'}$), 6.76 (d, 2H, $J = 8.7$ Hz, $H_{D'}$), 6.85 (d, 1H, $J = 7.2$ Hz, $H_{b'}$), 6.91 (d, 2H, $J = 8.9$ Hz, H_e), 7.03 (m, 14H, $H_{Ar} + H_E$), 7.08 (d, 4H, $J = 8.9$ Hz, $H_{F'}$), 7.17 (m, 12H, H_{Ar}), 7.44 (m, 2H, $H_a + H_{b'}$), 7.83 (t, 1H, $J = 7.8$ Hz, H_A), 8.11 (t, 2H, $J = 5.7$ Hz, H_C), 8.27 (d, 2H, $J = 7.8$ Hz, H_B).



Pd(11H₂)Cl₂MeCN: To a solution of PdCl₂·(CH₃CN)₂ (0.015 g, 5.7×10⁻² mmol) in MeCN (5 mL) was added a solution of 11H₂ (0.038 g, 3.8×10⁻² mmol) dissolved in dichloromethane (5 mL) and the mixture stirred for 1 h. The crude residue was then concentrated *in vacuo* and recrystallized from acetonitrile to give the title product as orange plates (0.039 g, yield = 85%). m.p. 162-163 °C; ¹H NMR (400 MHz, 9:1 CD₂Cl₂:CD₃CN, 298 K): δ = 0.72-0.88 (m, 16H, H_{alkyl}), 1.01-1.24 (m, 12H, H_{alkyl}), 1.37-1.49 (m, 4H, H_{alkyl}), 1.94 (s, 3H, Pd-NCCH₃), 3.15 (t, 4H, $J = 6.8$ Hz, H_g), 3.57 (t, 4H, $J = 6.0$ Hz, H_G), 4.08 (d, 4H, $J = 6.3$ Hz, H_D), 4.60 (s, 4H, H_d), 5.62 (s, 4H, H_c), 6.25 (d, 4H, $J = 8.6$ Hz, H_F), 6.41 (d, 4H, $J = 8.6$ Hz, H_E), 6.53 (d, 4H, $J = 8.6$ Hz, H_f), 7.13 (d, 4H, $J = 8.6$ Hz, H_e), 7.21 (d, 2H, $J = 7.8$ Hz, H_b), 7.48 (t, 1H, $J = 7.8$ Hz, H_a), 8.01 (t, 1H, $J = 7.8$ Hz, H_A), 8.25 (t, 2H, $J = 6.3$ Hz, H_C), 8.32 (d, 2H, $J = 7.8$ Hz, H_B); ¹³C NMR (100 MHz, 9:1 CD₂Cl₂:CD₃CN, 298 K) δ = 0.5, 24.3, 24.5, 27.1, 27.2, 27.3, 27.5, 27.8, 28.2, 41.2, 65.7, 65.8, 70.3, 72.1, 113.3, 115.6, 120.6, 123.9, 128.2, 128.4, 128.7, 129.3 (x2), 137.7, 137.9, 148.2, 156.7, 157.3, 159.8, 162.0.



Pd(1)(12): To a solution of Pd(1)(CH₃CN) (0.100 g, 0.152 mmol) in dichloromethane (20 mL) was added 12 (0.044 g, 0.152 mmol) and the mixture stirred for 20 min at r.t. The solvent was then removed under reduced pressure and the resultant residue recrystallised from acetone to furnish the title compound as a pale green solid (0.122 g, yield = 87%). m.p. 161 °C (dec); ¹H NMR (400 MHz, CDCl₃, 298 K): δ= 1.21-1.45 (m, 12H, H_{alkyl}), 1.52-1.65 (m, 4H, H_{alkyl}), 3.74 (t, 4H, J = 5.8 Hz, H_G), 4.18 (s, 4H, H_D), 5.21 (s, 4H, H_c), 6.30 (d, 4H, J = 7.8 Hz, H_F), 6.38 (d, 4H, J = 7.8 Hz, H_E), 6.94 (d, 4H, J = 7.8 Hz, H_d), 7.04 (t, 2H, J = 7.6 Hz, H_f), 7.33 (m, 4H, H_e), 7.44 (d, 2H, J = 7.8 Hz, H_b), 7.69 (m, 3H, H_B + H_a), 8.12 (t, 1H, J = 7.8 Hz, H_A); ¹³C NMR (100 MHz, CDCl₃, 298 K): δ= 25.5, 28.5 (x2), 29.4, 49.9, 67.1, 69.8, 114.6, 115.6, 121.8, 122.3, 125.1, 128.1, 129.7, 132.4, 139.2, 140.9, 152.7, 157.3, 157.6, 158.9, 171.5; ESI-MS: m/z = 911 [MH]⁺.

4.4 References and Notes

[1] For reviews see: a) J.-P. Sauvage, C. Dietrich-Buchecker (eds.), *Molecular Catenanes Rotaxanes and Knots: A Journey Through the World of Molecular Topology*, Wiley-VCH, Weinheim, **1999**.; b) V. Balzani, A Credi, F. M. Raymo, J. F. Stoddart, *Angew. Chem.* **2000**, *112*, 3484-3530; *Angew. Chem. Int. Ed.* **2000**, *39*, 3348-3391; c) V. Balzani, M. Venturi, A. Credi, *Molecular Devices and Machines - A Journey into the Nanoworld*, Wiley-VCH: Weinheim, **2003**, d) A. H. Flood, R. J. A. Ramirez, W.-Q. Deng, R. P. Muller, W. A. Goddard, J. F. Stoddart, *Aust. J. Chem.* **2004**, *57*, 301-322. (e) E. R. Kay, D. A. Leigh 'Synthetic Molecular Machines' in *Functional Artificial Receptors*, T. Schrader, A. D. Hamilton (eds.), Wiley-VCH, Weinheim, **2005**.

[2] For examples in which encapsulation and/or preorganization of the coordinating ligand geometry in a mechanically interlocked architecture can bring about significant property effects see: [stabilization of oxidation state/complex geometry]

- (a) C. O. Dietrich-Buchecker, J.-P. Sauvage *J. Am. Chem. Soc.* **1984**, *106*, 3043-3045; (b) N. Armaroli, L. De Cola, V. Balzani, J.-P. Sauvage, C. O. Dietrich-Buchecker, J.-M. Kern, A. Bailal, *J. Chem. Soc. Dalton Trans.* **1993**, 3241-3247; [protection of functional groups] (c) D. Leigh, A. Murphy, J. P. Smart, A. M. Z. Slawin, *Angew. Chem.* **1997**, *109*, 752-756; *Angew. Chem., Int. Ed. Engl.* **1997**, *36*, 728-731; (d) M. R. Craig, M. G. Hutchings, T. D. W. Claridge, H. L. Anderson, *Angew. Chem.* **2001**, *113*, 1105-1108; *Angew. Chem. Int. Ed.* **2001**, *40*, 1071-1074; (e) J. E. H. Buston, F. Marken, H. L. Anderson, *Chem. Commun.* **2001**, 1046-1047; (f) T. Oku, Y. Furusho, T. Takata, *Org. Lett.* **2003**, *6*, 4923-4925; (g) D. A. Leigh, E. M. Pérez, *Chem. Commun.* **2004**, 2262-2263; [solubility] (h) H. W. Gibson, S. Liu, P. Lecavalier, C. Wu, Y. X. Shen, *J. Am. Chem. Soc.* **1995**, *117*, 852-874; (i) A. G. Johnston, D. A. Leigh, A. Murphy, J. P. Smart, M. D. Deegan, *J. Am. Chem. Soc.* **1996**, *118*, 10662-10663; (j) S. Anderson, H. L. Anderson, *Angew. Chem.* **1996**, *108*, 2075-2078; *Angew. Chem., Int. Ed. Engl.*, **1996**, *35*, 1956-1959; [conformation of a component] (k) W. Clegg, C. Gimenez-Saiz, D. A. Leigh, A. Murphy, A. M. Z. Slawin, S. J. Teat, *J. Am. Chem. Soc.* **1999**, *121*, 4124-4129; [electroluminescence] (l) F. Cacialli, J. S. Wilson, J. J. Michels, C. Daniel, C. Silva, R. H. Friend, N. Severin, P. Samori, J. P. Rabe, M. J. O'Connell, P. N. Taylor, H. L. Anderson, *Nature Mater.* **2002**, *1*, 160-164; [membrane transport] (m) V. Dvornikovs, B. E. House, M. Kaetzl, J. R. Dedman, D. B. Smithrud, *J. Am. Chem. Soc.* **2003**, *125*, 8290-8301.
- [3] A.-M. Fuller, D. A. Leigh, P. J. Lusby, I. D. H. Oswald, S. Parsons, D. B. Walker, *Angew. Chem.* **2004**, *116*, 4004-4008; *Angew. Chem. Int. Ed.* **2004**, *43*, 3914-3918.
- [4] For a recent example of a [2]rotaxane utilizing square planar Pd(II) coordination see I. Yoon, M. Narita, T. Shimizu, M. Asakawa, *J. Am. Chem. Soc.* **2004**, *126*, 16740-16741.
- [5] S. L. Jain, P. Bhattacharyya, H. L. Milton, A. M. Z. Slawin, J. A. Crayston, J. D. Woollins, *Dalton Trans.* **2004**, 862-871.
- [6] F. Biscarini, M. Cavallini, D. A. Leigh, S. León, S. J. Teat, J. K. Y. Wong, F. Zerbetto, *J. Am. Chem. Soc.* **2002**, *124*, 225-233.
- [7] Data for 6H_2 , Cu_6 and Ni_6 were collected at 93 K using a Rigaku Saturn (MM007 high flux RA/Mo $\text{K}\alpha$ radiation, confocal optic), for 11H_2 and $\text{Pd}(6\text{H}_2)\text{Cl}_2\text{MeCN}$ at 93 K using a Rigaku Mercury (MM007 high flux RA/Mo $\text{K}\alpha$

radiation, confocal optic), and for $6\text{H}_2\text{TfOH}$ at 125 K using a Bruker SMART diffractometer (sealed tube $\text{MoK}\alpha$ radiation, graphite monochromator, $\lambda = 0.71073 \text{ \AA}$). All data collections employed narrow frames ($0.3\text{--}1.0^\circ$) to obtain at least a full hemisphere of data. Intensities were corrected for Lorentz polarisation and absorption effects (multiple equivalent reflections). Structures were solved by direct methods, non-H atoms were refined anisotropically with C-H protons being refined in riding geometries (SHELXTL) against F^2 . In most cases amide protons were refined isotropically subject to a distant constraint. Any other restraints or additional features of the refinement are detailed for each structure below. The structure determination for 6H_2 proved particularly problematical; we collected full datasets using a variety of collection routines on more than 15 different crystals from several different crystallisation experiments. The data were always poor, principally because of disorder arising from the alkyl chain and solvate molecules. The structure was refined isotropically with no protons included in the refinement. 6H_2 : $\text{C}_{112}\text{H}_{130}\text{N}_4\text{O}_6$, $M = 1628$, crystal size $0.2 \times 0.1 \times 0.03 \text{ mm}$, orthorhombic, $Pbca$, $a = 18.338(4)$, $b = 23.545(5)$, $c = 44.922(9) \text{ \AA}$, $V = 19396(7) \text{ \AA}^3$, $Z = 8$, $\rho_{\text{calcd}} = 1.115 \text{ Mg m}^{-3}$; $\mu = 0.068 \text{ mm}^{-1}$, 18573 data (17303 unique) $R = 0.3339$ for F values of reflections with $F_o > 4\sigma(F_o)$, $S = 4.90$ for 463 parameters. Residual electron density extremes were 1.665 and -4.557 e\AA^{-3} . 11H_2 : $\text{C}_{62}\text{H}_{76}\text{N}_4\text{O}_8$, $M = 1005.27$, colourless prism, crystal size $0.2 \times 0.2 \times 0.2 \text{ mm}$, triclinic, $P-1$, $a = 11.3539(11)$, $b = 12.0635(11)$, $c = 20.445(2) \text{ \AA}$, $\alpha = 82.323(6)$, $\beta = 88.351(7)$, $\gamma = 80.397(7)^\circ$, $V = 2736.2(5) \text{ \AA}^3$, $Z = 2$, $\rho_{\text{calcd}} = 1.220 \text{ Mg m}^{-3}$; $\mu = 0.080 \text{ mm}^{-1}$, 15494 data (8824 unique, $R_{\text{int}} = 0.0176$) $R = 0.0499$, $S = 0.987$ for 677 parameters. Residual electron density extremes were 0.759 and -0.336 e\AA^{-3} . $6\text{H}_2\text{TfOH}$: $\text{C}_{113}\text{H}_{131}\text{F}_3\text{N}_4\text{O}_9\text{S}$, $M = 1778.28$, colourless prism, crystal size $0.15 \times 0.1 \times 0.1 \text{ mm}$, monoclinic, $P2_1/c$, $a = 20.555(2)$, $b = 18.7503(19)$, $c = 27.853(3) \text{ \AA}$, $\beta = 109.574(2)^\circ$, $V = 10114.6(17) \text{ \AA}^3$, $Z = 4$, $\rho_{\text{calcd}} = 1.168 \text{ Mg m}^{-3}$; $\mu = 0.096 \text{ mm}^{-1}$, 59606 data (18472 unique, $R_{\text{int}} = 0.0449$), $R = 0.1058$, $S = 1.028$ for 1149 parameters. Residual electron density extremes were 1.366 and -0.649 e\AA^{-3} . Cu6 : $\text{C}_{117}\text{H}_{135.5}\text{CuN}_{6.5}\text{O}_6$, $M = 1792.36$, violet platelet, crystal size $0.2 \times 0.1 \times 0.01 \text{ mm}$, triclinic, $P-1$, $a = 16.404(3)$, $b = 17.516(3)$, $c = 20.046(4) \text{ \AA}$, $\alpha = 100.573(3)$, $\beta = 106.016(3)$, $\gamma = 96.178(3)^\circ$, $V = 5365.3(17) \text{ \AA}^3$, $Z = 2$, $\rho_{\text{calcd}} = 1.109 \text{ Mg m}^{-3}$; $\mu = 0.258 \text{ mm}^{-1}$, 41166 data (17787 unique, $R_{\text{int}} = 0.0318$) $R = 0.1507$, $S = 1.812$ for 1163 parameters. Residual electron density extremes were 2.325 and -1.107 e\AA^{-3} . The half

weight acetonitrile solvate molecules were refined isotropically. Ni6: $C_{117}H_{137.5}N_{6.5}NiO_7$, $M = 1805.54$, orange needle, crystal size $0.15 \times 0.015 \times 0.015$ mm, triclinic, $P-1$ $a = 16.423(3)$, $b = 17.582(3)$ $c = 20.056(3)$ Å, $\alpha = 100.0161(19)$, $\beta = 106.234(3)$, $\gamma = 96.2695(18)^\circ$, $V = 5398.6(15)$ Å³, $Z = 2$, $\rho_{\text{calcd}} = 1.111$ Mg m⁻³; $\mu = 0.235$ mm⁻¹, 40853 data (17841 unique, $R_{\text{int}} = 0.0506$) $R = 0.1302$, $S = 1.465$ for 1184 parameters. Residual electron density extremes were 1.874 and -0.891. The half weight acetonitrile and quarter weight water solvate molecules were refined isotropically. The protons on all solvate molecules were not allowed for in the refinement. Pd(6H₂)Cl₂CH₃CN: $C_{122}H_{145}N_9O_6Cl_2Pd$, $M = 2010.77$, yellow platelet $0.2 \times 0.1 \times 0.01$ mm, monoclinic, $C2/c$, $a = 29.6525(12)$, $b = 23.2314(10)$, $c = 32.6559(14)$ Å, $\beta = 99.071(3)^\circ$, $V = 22214.3(16)$ Å³, $Z = 8$, $\rho_{\text{calcd}} = 1.202$ Mg m⁻³, $\mu = 0.273$ mm⁻¹, 58779 data (19158 unique, $R_{\text{int}} = 0.1733$) $R = 0.1416$, $S = 1.090$ for 1253 parameters. Residual electron density extremes were 0.946 and -0.925 eÅ⁻³. The half weight acetonitrile solvate molecules were refined isotropically. The protons on solvate molecules were not allowed for in the refinement. Crystallographic data have been deposited with the Cambridge Crystallographic Data Centre as supplementary publication no's. CCDC-259162 to CCDC-259166. These data can be obtained free of charge via <http://www.ccdc.cam.ac.uk/conts/retrieving.html> or from the Cambridge Crystallographic Data Centre, 12 Union Road, Cambridge CB2 1EZ, UK; fax: +44 1223 336033; or deposit@ccdc.cam.ac.uk.

[8] F. G. Gatti, D. A. Leigh, S. A. Nepogodiev, A. M. Z. Slawin, S. J. Teat, J. K. Y. Wong, *J. Am. Chem. Soc.* **2001**, *123*, 5983-5989.

[9] J. S. Hannam, S. M. Lacy, D. A. Leigh, C. G. Saiz, A. M. Z. Slawin, S. G. Stichelell, *Angew. Chem.* **2004**, *116*, 3322-3326; *Angew. Chem. Int. Ed.* **2004**, *43*, 3260-3264.

[10] D. J. Cram, *Angew. Chem.* **1988**, *100*, 1041-1052; *Angew. Chem., Int. Ed. Engl.* **1988**, *27*, 1009-1020.

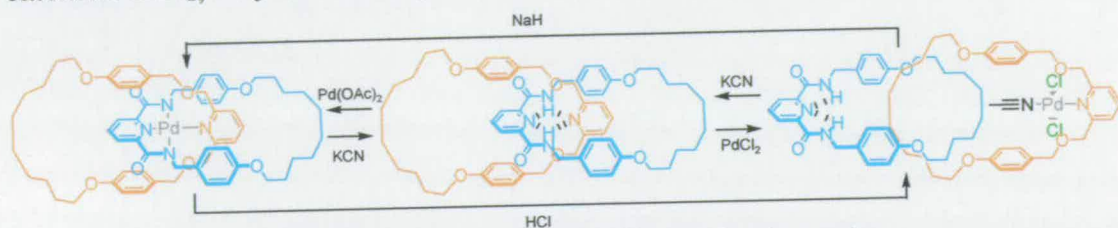
[11] For temporary steric barriers to shuttling see: a) A. S. Lane, D. A. Leigh, A. Murphy, *J. Am. Chem. Soc.* **1997**, *119*, 11092-11093. b) L. Jiang, J. Okano, A. Orita, J. Otera, *Angew. Chem.* **2004**, *116*, 2173-2176; *Angew. Chem. Int. Ed.* **2004**, *43*, 2121-2124.

[12] A.-M. L. Fuller, D. A. Leigh, P. J. Lusby, A. M. Z. Slawin and D. B. Walker, *J. Am. Chem. Soc.* **2005**, *127*, 12612-12619.

- [13] B. A. Blight, K. A. Van Noortwyck, J. A. Wisner, M. C. Jennings, *Angew. Chem.* **2005**, *117*, 1523-1528; *Angew. Chem. Int. Ed.* **2005**, *44*, 1499-1504.
- [14] K. Kavallieratos, S. R. de Gala, D. J. Austin, R. H. Crabtree, *J. Am. Chem. Soc.* **1997**, *119*, 2325-2326.
- [15] A paper has recently appeared [Y. Furusho, T. Matsuyama, T. Takata, T. Moriuchi, T. Hirao, *Tetrahedron Lett.* **2004**, *45*, 9593–9597] based on our earliest work on this system[ref 3]. Although the authors do not comment on it, the ^1H chemical shifts show that the bifurcated bis-pyridine hydrogen bonding motif discussed in the present manuscript is also present in the de-metallated Takata/Hirao rotaxane.
- [16] M. Lämsä, S. Kiviniemi, E. R. Kettukangas, M. Nissinen, J. Pursiainen, K. Rissanen, *J. Phys. Org. Chem.* **2001**, *14*, 551-558.
- [17] The changes in the chemical shifts are so small in this experiment that the limit of the curve fitting software was reached hence the large error margin. For a more detailed description of the technique see [A. P. Bisson, C. A. Hunter, J. C. Morales and K. Young, *Chem. Eur. J.*, **1998**, *4*, 845-851].

Chapter Five Synopsis

In chapter four the diverse range of binding modes accessible through mechanical bonding were discussed. One particular interaction, the 1st and 2nd sphere coordination of PdCl_2 , resulted in a large amplitude topographical rearrangement in catenane 11H_2 , the full details of which are described in chapter five.



Scheme 1. Interconversion of 11H_2 coordination modes.

Reaction of the [2]catenane 11H_2 with $\text{Pd}(\text{OAc})_2$ binds both macrocycles to the metal, locking them in position; treatment with PdCl_2 , however, results in coordination of only one ring, producing a half-turn in the relative orientation of the [2]catenane components in both solution and the solid state (Scheme 1).

Chapter 5: Half-Rotation in a [2]catenane *via* Interconvertible Pd(II) Coordination modes

Published as “*Half-rotation in a [2]catenane via interconvertible Pd(II) coordination modes*” D. A. Leigh, P. J. Lusby, A. M. Z. Slawin, D. B. Walker *Chem. Commun.*

(Published online 13/9/05)

Acknowledgement

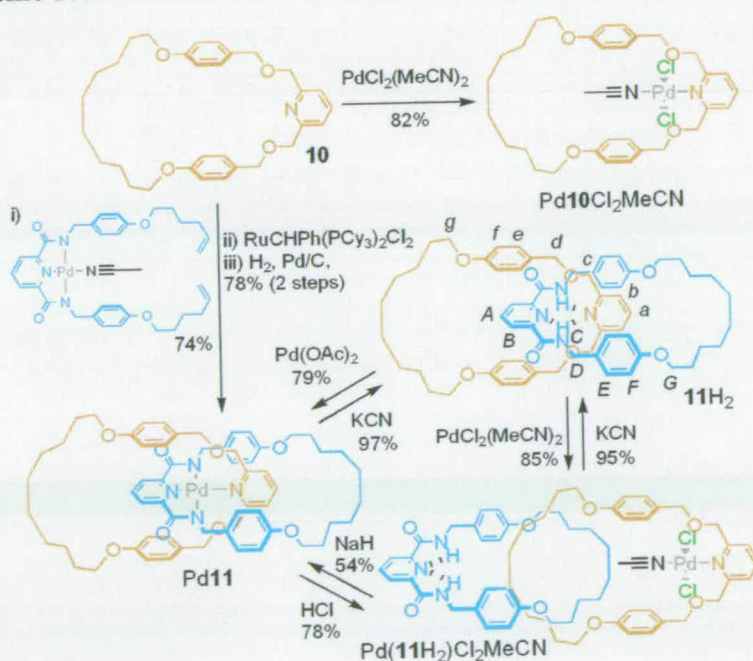
Prof. A. M. Z. Slawin is gratefully acknowledged for solving the crystal structure of Pd(11H₂)Cl₂MeCN.

5.1 Introduction

The development of novel ways to bring about changes in the relative positions of mechanically interlocked sub-molecular components is an important area of investigation in the emerging field of synthetic molecular machines.¹ In terms of rotational processes, a formal half-turn of a ring in a [2]catenane² not only corresponds to a simple mechanical switch,³ but is also a step towards the more demanding requirements of a synthetic rotary molecular motor.⁴ Here we report on a simple [2]catenane system in which the different binding modes of the interlocked rings to Pd(II) cause a major change in position and orientation of the macrocycles in the resulting complexes.

5.2 Results and Discussion

The square planar coordination preference of Pd(II) can be used to direct the macrocyclization of suitable tridentate ligands around 2,6-dimethyleneoxy-pyridine-based threads to form rotaxanes.^{5,6} We reasoned that a similar strategy could be used to make a palladium [2]catenane by incorporating the monodentate unit into a macrocycle. Pleasingly, Pd11 was isolated in 58% yield from **10** via the three step (ligand coordination, ring-closing olefin metathesis, hydrogenation) reaction sequence shown in Scheme 5.1.⁷



Scheme 5.1 Synthesis and interconversion of Pd11, 11H_2 and $\text{Pd}(\text{11H}_2)\text{Cl}_2\text{MeCN}$.

De-metallation of Pd11 (KCN, MeOH/CH₂Cl₂, 20→40 °C, 1.5 h, 97%) afforded the catenand 11H₂ in which pyridine-amide-pyridine H-bonding⁶ holds the macrocycles in a similar position to that seen for Pd11 in both solution and the solid state. The well defined orientation of the two fragments is clearly apparent from comparison of the ¹H NMR spectra of the two catenanes (Figs. 5.1 b and c) with those of the non-interlocked component macrocycles (Fig 5.1 a and e). In the room temperature spectra of both 11H₂ (Fig 5.1b) and Pd11 (Fig 5.1 c) the upfield shift of the H_D, H_E and H_F resonances indicate a π -stacking arrangement between the benzylic amide rings of the 'blue' macrocycle and the pyridine group of the 'orange' macrocycle. In contrast, the alkyl chain protons are not shielded by interactions with aromatic rings in either catenane. The solution geometries suggested by ¹H NMR correspond well to the solid state structures of 11H₂ (Fig 5.2 a) and Pd11 (Fig 5.2 b) determined by X-ray crystallography. Reaction of 11H₂ with Pd(OAc)₂ (MeCN, 60 °C, 4 h, 79%) re-forms the co-conformationally locked catenate, Pd11.

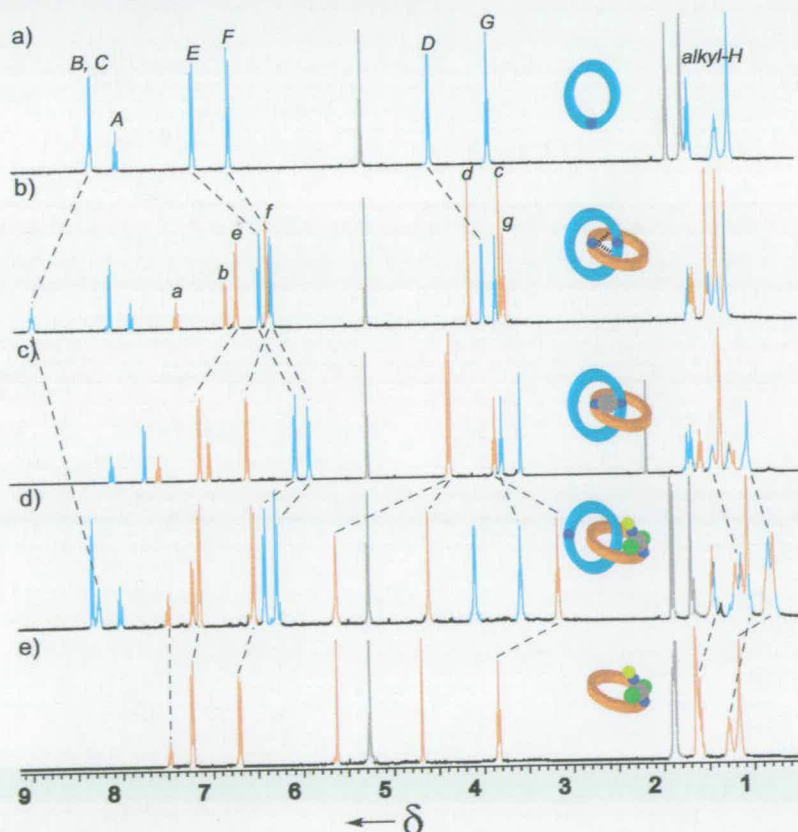


Figure 5.1 ¹H NMR spectra (400 MHz, 9:1 CD₂Cl₂:CD₃CN, 298 K, 2.5 mM) (a) non-interlocked bis-amide macrocycle (b) 11H₂ (c) Pd11 (d) Pd(11H₂)Cl₂MeCN (e) Pd10Cl₂MeCN (non-interlocked tetra-ether macrocycle bound to PdCl₂MeCN). The grey signals correspond to residual solvents. The dark blue circles in the cartoon rings indicate the position of the pyridine nitrogen atoms.

Reaction of $11H_2$ with $PdCl_2(MeCN)_2$ in MeCN (20 °C, 1 h, 85%) afforded a second catenane Pd(II) complex in which the amide protons (H_C) of the 'blue' macrocycle were clearly still present (Fig 5.1 d). X-ray crystallography (Fig 5.2 c and d) of a single crystal obtained from slow cooling of a saturated acetonitrile solution confirmed this complex to be $Pd(11H_2)Cl_2MeCN$, in which only one of the macrocyclic rings is coordinated to the palladium metal ion, presumably as a consequence of both the greater strength of the Pd-Cl bond compared to Pd-OAc and the poor basicity of the Cl^- ion.

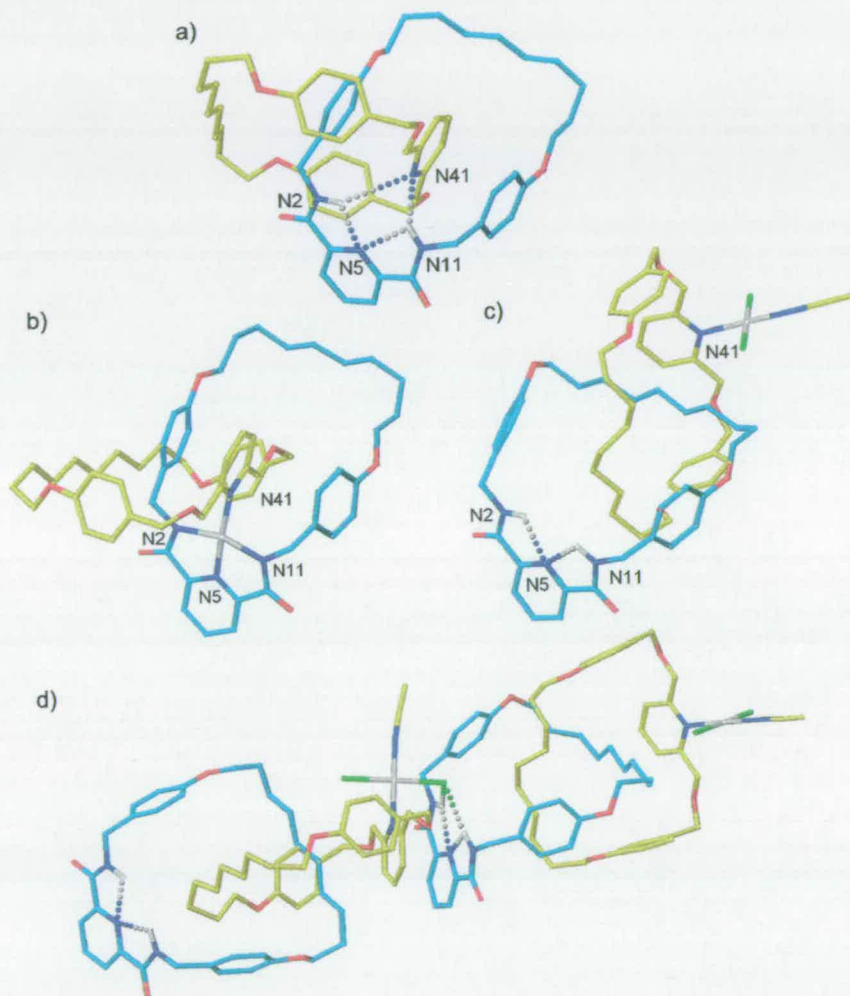


Figure 5.2 X-ray crystal structures of: (a) [2]catenane $11H_2$,⁶ (b) $Pd11$,⁷ (c) $Pd(11H_2)Cl_2MeCN$ ⁸ (single molecule view; note the change of position and orientation of the yellow macrocycle compared to $Pd11$ and $11H_2$) and (d) adjacent molecules of $Pd(11H_2)Cl_2MeCN$ showing intermolecular Pd-Cl \cdots HN hydrogen bonding. Carbon atoms of the bis-amide macrocycle are shown in light blue and those of the tetra-ether macrocycle and coordinated acetonitrile molecule in yellow; oxygen atoms are red, nitrogen dark blue, hydrogen white, palladium grey, chlorine green. For clarity only amide hydrogen atoms are shown. Selected bond lengths for $11H_2$ [Å]: N2H-N5 2.18; N11H-N5 2.33; N2H-N41 2.28; N11H-N41 3.10; N5-N41 3.67. Selected bond angles for $11H_2$ [°]: N2H-N5 107.1; N11H-

N5 102.2; N2H-N41 146.5; N11H-N41 129.0. Selected bond lengths for Pd**11** [Å]: Pd-N2 1.934, Pd-N5 2.041, Pd-N11 2.036, Pd-N41 2.079; Pd**11** bite angle [°]: N2-Pd-N11 160.2. Selected bond lengths for Pd(**11H**₂)Cl₂MeCN [Å]: N2H-N5 2.21; N11H-N5 2.30; N5-N41 12.93. Selected bond angles for Pd(**11H**₂)Cl₂MeCN [°]: N2H-N5 109.0; N11H-N5 104.7.

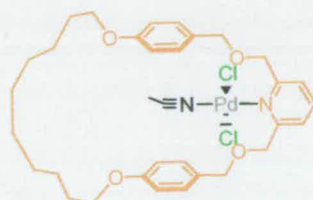
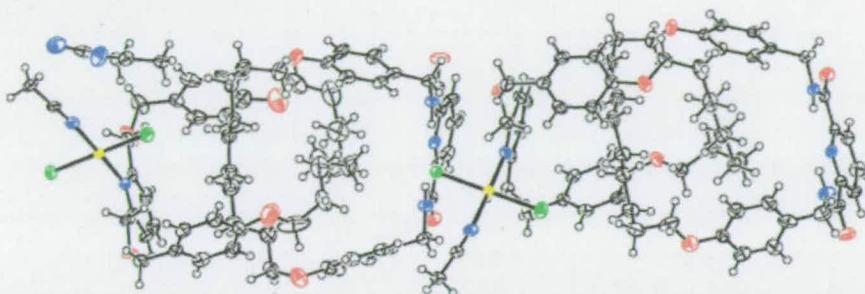
The effect of the different coordination mode on the relative positions and orientation of the two macrocycles in the catenane is dramatic. In the ¹H NMR spectrum of Pd(**11H**₂)Cl₂MeCN (Fig. 5.1 d) the resonances corresponding to H_G, H_g and H_{alkyl} are shifted significantly upfield, indicating that each macrocycle is located preferentially over the aliphatic region of the other.⁹ The X-ray crystal structure (Fig 5.2 c and d) shows a similar geometry exists in the solid state. An additional feature of the X-ray crystal structure of Pd(**11H**₂)Cl₂MeCN is the presence of intermolecular Pd-Cl...HNCO hydrogen bonds between adjacent molecules (Fig 5.2 d). The negligible change in the chemical shift of the amide protons (H_C) between **11H**₂ (Fig 5.1a) and Pd(**11H**₂)Cl₂MeCN (Fig 5.1 d) suggests this interaction is weak in solution,⁶ nevertheless it has been successfully utilised¹⁰ to direct the formation of pseudorotaxanes.

The three catenanes **11H**₂, Pd**11** and Pd(**11H**₂)Cl₂MeCN are all directly interconvertible (Scheme 5.1): The palladium complexes are de-metallated with KCN; Pd(**11H**₂)Cl₂MeCN is converted into Pd**11** by treatment with NaH, and the reverse reaction is promoted by HCl in MeCN. It is interesting to note the macrocycles adopt similar positions and orientations in Pd**11** and **11H**₂ but in the former they are locked in place by a coordination bond whereas in the latter they are held in the thermodynamic minimum only by weak and dynamic H-bonds. The preferred co-conformation of Pd(**11H**₂)Cl₂MeCN is very different to the other two, presumably on steric grounds, and as such its formation from either of the others corresponds to a large amplitude rotational switch. It is rare to find such a rich variation in structure and dynamics possible through a simple manipulation of coordination modes.

5.3 Experimental Section

5.3.1 Compound Analysis

Ellipsoid plot of Pd(**11H**)₂Cl₂MeCN:



Pd10Cl₂MeCN: To a solution of PdCl₂·(CH₃CN)₂ (0.039 g 1.5×10⁻¹ mmol) in MeCN (5 mL) was added a solution of **10** (0.050 g, 1.0×10⁻¹ mmol) dissolved in dichloromethane (5 mL) and the mixture stirred for 1 h. The crude residue was then concentrated *in vacuo* and recrystallized from acetonitrile to give the title product as a pale orange solid (0.058 g, yield = 82%). m.p. 158°C (decomp); ¹H NMR (400 MHz, 9:1 CD₂Cl₂:CD₃CN, 298 K): δ = 1.10-1.31 (m, 8H, H_{alkyl}), 1.55-1.67 (m, 8H, H_{alkyl}), 1.92 (s, 3H, Pd-NCCH₃), 3.83 (t, 4H, J = 6.6 Hz, H_g), 4.68 (s, 4H, H_d), 5.62 (s, 4H, H_c), 6.69 (d, 4H, J = 8.6 Hz, H_f), 7.21 (m, 6H, H_b + H_e), 7.46 (t, 1H, J = 7.8 Hz, H_a); ¹³C NMR (100 MHz, 9:1 CD₂Cl₂:CD₃CN, 298 K) δ = 0.62, 24.5, 27.5 (x2), 28.1, 66.5, 70.5, 72.1, 113.5, 115.9, 120.8, 128.2, 129.4, 137.7, 157.9, 159.2.

5.3.2 Interconversion of [2]Catenane Species

11H₂-Pd11: To a stirred solution of 11H₂ (0.050 g, 5.0x10⁻² mmol) in anhydrous acetonitrile (10 mL) and dichloromethane (10 mL), palladium(II) acetate (0.011 g, 5.0x10⁻² mmol) was added and the solution refluxed for 18 h under an atmosphere of nitrogen. The resulting precipitate was filtered, washed with acetonitrile (25 mL) and dried under suction to yield Pd11 (0.044 g, 79%).

Pd11-Pd(11H₂)Cl₂MeCN: A solution of HCl in CDCl₃ was added dropwise to a solution of Pd11 (0.015 g, 1.4x10⁻² mmol) in CDCl₃/CD₃CN until complete interconversion to Pd(11H₂)Cl₂MeCN was indicated by ¹H NMR spectroscopy. The resultant orange solution was filtered through a plug of NaHCO₃ and concentrated *in vacuo* to yield Pd(11H₂)Cl₂MeCN (0.012 g, 78%).

Pd(11H₂)Cl₂MeCN-Pd11: Sodium hydride (0.0018 g, 4.5x10⁻² mmol) (60% dispersion in oil). was added to a solution of Pd(11H₂)Cl₂MeCN (0.018 g, 1.5 x10⁻² mmol) in dry CH₃CN/CH₂Cl₂ (2 mL/1 mL) and the reaction mixture stirred for 20 minutes under an atmosphere of nitrogen. The crude solution was filtered, concentrated *in vacuo* and purified using column chromatography (99:1 CH₂Cl₂:MeOH) to yield Pd11 (0.009 g, 54%).

5.4 References and Notes

1. V. Balzani, A. Credi, F. M. Raymo and J. F. Stoddart, *Angew. Chem. Int. Ed.*, 2000, **39**, 3349; J.-P. Sauvage, *Chem. Commun.*, 2005, 1507; K. Kinbara and T. Aida, *Chem. Rev.*, 2005, **105**, 1377
2. For examples of catenanes which undergo stimuli-induced half-rotations see: M. Cesario, C. O. Dietrich-Buchecker, J. Guilhem, C. Pascard and J.-P. Sauvage, *J. Chem. Soc., Chem. Commun.*, 1985, 244; A. Livoreil, C. O. Dietrich-Buchecker and J.-P. Sauvage, *J. Am. Chem. Soc.*, 1994, **116**, 9399; D. B. Amabilino, C. O. Dietrich-Buchecker, A. Livoreil, L. Perez-Garcia, J.-P. Sauvage and J. F. Stoddart, *J. Am. Chem. Soc.*, 1996, **118**, 3905; D. A. Leigh, K. Moody, J. P. Smart, K. J. Watson and A. M. Z. Slawin, *Angew. Chem., Int. Ed. Engl.*, 1996, **35**, 306;

- A. Livoreil, J. P. Sauvage, N. Armaroli, V. Balzani, L. Flamigni and B. Ventura, *J. Am. Chem. Soc.*, 1997, **119**, 12114; C. P. Collier, G. Mattersteig, E. W. Wong, Y. Luo, K. Beverly, J. Sampaio, F. M. Raymo, J. F. Stoddart and J. R. Heath, *Science*, 2000, **289**, 1172; V. Balzani, A. Credi, S. J. Langford, F. M. Raymo, J. F. Stoddart and M. Venturi, *J. Am. Chem. Soc.*, 2000, **122**, 3542; D. W. Steuerman, H. R. Tseng, A. J. Peters, A. H. Flood, J. O. Jeppesen, K. A. Nielsen, J. F. Stoddart and J. R. Heath, *Angew. Chem. Int. Ed.*, 2004, **43**, 6486; B. Korybut-Daszkiewicz, A. Wieckowska, R. Bilewicz, S. Domagala, K. Wozniak, *Angew. Chem. Int. Ed.*, 2004, **43**, 1668.
3. A 'switch' influences a system as a function of state; a 'motor' influences a system as a function of trajectory. For a discussion see: E. R. Kay and D. A. Leigh *Top. Curr. Chem.* (in press).
 4. D. A. Leigh, J. K. Y. Wong, F. Dehez and F. Zerbetto, *Nature*, 2003, **424**, 174; J. V. Hernandez, E. R. Kay and D. A. Leigh, *Science*, 2004, **306**, 1532.
 5. A.-M. Fuller, D. A. Leigh, P. J. Lusby, I. D. H. Oswald, S. Parsons and D. B. Walker, *Angew. Chem. Int. Ed.*, 2004, **43**, 3914; Y. Furusho, T. Matsuyama, T. Takata, T. Moriuchi, T. Hirao, *Tetrahedron Lett.* 2004, **45**, 9593.
 6. D. A. Leigh, P. J. Lusby, A. M. Z. Slawin and D. B. Walker, *Angew. Chem. Int. Ed.*, 2005, **44**, 4557.
 7. For various synthetic routes to Pd11 see A.-M. L. Fuller, D. A. Leigh, P. J. Lusby, A. M. Z. Slawin and D. B. Walker, *J. Am. Chem. Soc.*, in press.
 8. Single crystals of sufficient quality for X-ray analysis were grown by slow cooling a saturated MeCN solution of Pd(1H₂)Cl₂MeCN. C₆₆H₈₂Cl₂N₆O₈Pd, *M* = 1264.68, orange plate, crystal size 0.2×0.1×0.03 mm, triclinic, *P*-1, *a* = 9.8106(8), *b* = 25.305(2), *c* = 26.820(2) Å, α = 73.971(4)°, β = 82.771(6)°, γ = 88.050(6)°, *V* = 6348.3(9) Å³, *Z* = 4, ρ_{calcd} = 1.323 Mg m⁻³; MoK α radiation (confocal optic, λ = 0.71073 Å), μ = 0.435 mm⁻¹, *T* = 93(2) K. 40751 data (21993 unique, *R*_{int} = 0.0258, 1.58 < θ < 25.35°), were collected on a Rigaku MM007/Saturn70 CCD diffractometer and were corrected for absorption. The structure was solved by direct methods and refined by full-matrix least-squares on *F*² values of all data (G. M. Sheldrick, SHELXTL, Bruker AXS Madison WI, USA, 2001, version 6.1) to give *wR* = { $\Sigma[w(F_o^2 - F_c^2)^2] / \Sigma[w(F_o^2)^2]$ }^{1/2} = 0.1351, conventional *R* = 0.0525 for *F* values of reflections with *F*_o² > 2 σ (*F*_o²) [40751 observed reflections], *S* = 1.036 for 1516

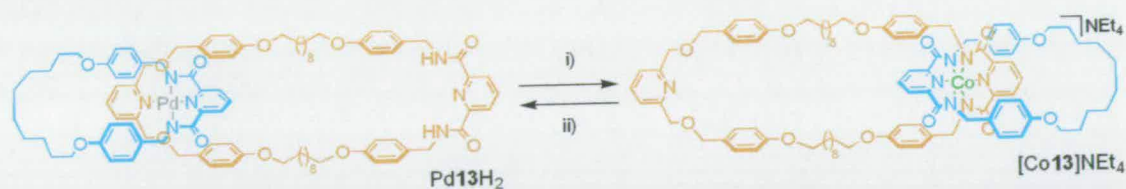
parameters. Residual electron density extremes were 2.301 and -0.992 eÅ⁻³.CCDC no. 279771.

9. The downfield shift of H_c and H_d in Pd(**11**H₂)Cl₂MeCN compared to **11**H₂ is probably caused by coordination of the Pd(II) rather than the absence of macrocyclic shielding. Similar chemical shifts are observed in Pd**10**Cl₂MeCN (Fig. 5.1e).

10. B. A. Blight, K. A. Van Noortwyk, J. A. Wisner and M. C. Jennings, *Angew. Chem. Int. Ed.*, 2005, **44**, 1499.

Chapter Six Synopsis

In chapter five a novel way to bring about a large amplitude rearrangement using interconvertible coordination modes was described. In chapter six a second method for inducing a reversible 180 turn in a [2]catenane is reported where both states are kinetically 'locked' through TM ion coordination.



Scheme 1. Interconversion of co-conformers. Reagents and conditions: i) 1. KCN, $\text{CH}_2\text{Cl}_2/\text{MeOH}$, 98%; 2. $\text{Co}(\text{OAc})_2$, NaH Et_4NOAc , air MeOH, 81%. (ii) 1. Zn, AcOH/MeOH 90%; 2. $\text{Pd}(\text{OAc})_2$, $\text{CH}_2\text{Cl}_2/\text{MeOH}$, 83%.

[2]catenane Pd13H_2 was synthesised in three steps from $\mathbf{9H}_2$ using the same protocol applied to the synthesis of Pd11 . Pd13H_2 is a kinetically stable complex with the smaller 'blue' ring trapped in a specific co-conformation via binding to the Pd(II) ion. Facile de-metallation using KCN 'frees' the ring, although it still shows an affinity for the 2,6-bis(oxymethylene)pyridine moiety via H-bonding. Removal of the four amide protons using sodium hydride followed by introduction of a Co(III) ion induces a 180 degree rotation in the molecule forming $[\text{Co13}]\text{NEt}_4$. The blue ring is now locked on the other side of the molecule due through mutual binding to the Co(III) ion by both submolecular fragments. The 180 degree rotation can be reversed by first removing the Co(III) ion with Zn/acetic acid and then addition of $\text{Pd}(\text{OAc})_2$.

Chapter 6: Kinetically fixed half-rotation in a [2]catenane via transition metal chelation

Submitted for publication as "*Kinetically fixed half-rotation in a [2]catenane via transition metal chelation*" D. A. Leigh, P. J. Lusby, A. M. Z. Slawin, D. B. Walker.

Acknowledgements

Prof. A. M. Z. Slawin is gratefully acknowledged for solving the crystal structures of Pd13H₂ and 13H₄.

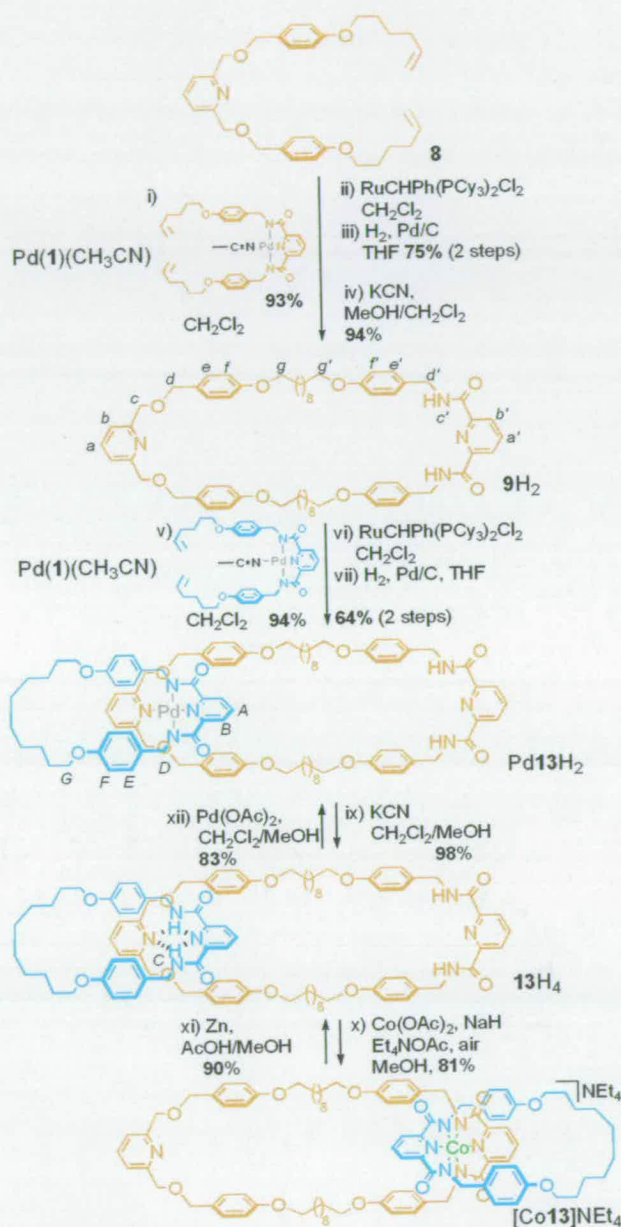
6.1 Introduction

Insight into the physical basis of artificially exploiting molecular level motion has been expedited by concurrent advances in both the theoretical understanding of the mechanism of dynamic natural processes^[1] and the study of controlled molecular motion in prototypical synthetic assemblies.^[2, 3] With respect to the latter, mechanically interlocked molecules have proved particularly valuable due to the restricted number of co-conformations enforced by their topological profile that limits any large amplitude molecular motions to within predefined constraints. When considering the criteria for controlled nanoscale rotational processes, an induced half turn in a [2]catenane is an essential feature. Several examples of switchable [2]catenanes have previously been reported^[4] and, in almost all cases, thermodynamic control of the intercomponent non-covalent interactions is executed via an external stimulus prompting the observed shuttling motion. However there are only a few examples – utilizing either transition metal (TM) coordination or bulky protecting groups – that are kinetically ‘fixed’ in a given co-conformation. Here we would like to report on a simple [2]catenane that can be kinetically locked at two different stations through binding to different TM ions, specifically Pd(II) and Co(III). The mechanism of formal rotation consists of a two stage process, the ‘unlocking’ of the system by removing the TM ion and addition of the alternative ion to induce the rotational motion and fix the molecule in its new topographical arrangement.

6.2 Results and Discussion

The last five years has seen the development of several new strategies employing TM ions as templates in the synthesis of mechanically interlocked molecules^[5] that compliment the original bisphenanthroline/Cu(I) motif so successfully developed by Sauvage. Our recent application of Pd(II) as a template in the synthesis of mechanically interlocked molecules^[6] has yielded several unexpected findings,^[7] one of which was the fortuitous synthesis of a large macrocycle, **9H₂**, from readily prepared ligands, **1H₂** and **8** (Scheme 1, i-iv). **9H₂** contains both a 2,6-bis(oxymethylene)pyridine moiety that is a structural requirement for the assembly of interlocked molecules around Pd(II) and a 2,6-pyridinedicarboxamide binding site

that in its deprotonated (carboxamido) form – apart from forming a stable tridentate complex with Pd(II) – has been previously shown to bind a selection of ‘hard’ TM ions, including Co(III).^[8] It was thus reasoned that ‘clipping’ a second ring around $9H_2$ – by applying the same pyridinecarboxamido/Pd(II) protocol – would fashion a [2]catenane containing two different TM binding sites.



Scheme 6.1. Synthesis of [2]catenane $Pd10H_2$ and conditions required for conversion to $10H_4$ and then $[Co10]NET_4$.

The [2]catenane $Pd13H_2$ was conveniently prepared in three steps (overall 60% yield) with the key transformation being the RCM of the macrocyclic precursor

(shown in blue) around $9H_2$ (shown in orange) using the Grubbs' first generation catalyst (Scheme 6.1, v-vii). The shielding of specific signals in the 1H NMR spectrum of the catenate $Pd10H_2$ (H_E , H_e , H_F and H_f) suggests that the molecule is kinetically locked by the metal ion in the anticipated co-conformation. More surprising is the large downfield shift of the signal corresponding to the amide protons of the $9H_2$ fragment ($H_{c'}$) most likely caused by enhanced H-bonding to the carboxamido oxygens of the small ring fragment. The co-conformation of $Pd13H_2$ was confirmed by X-ray crystallography after slow cooling of a hot saturated solution of the complex in acetonitrile rendered single crystals suitable for solid state analysis (Figure 6.2 a).

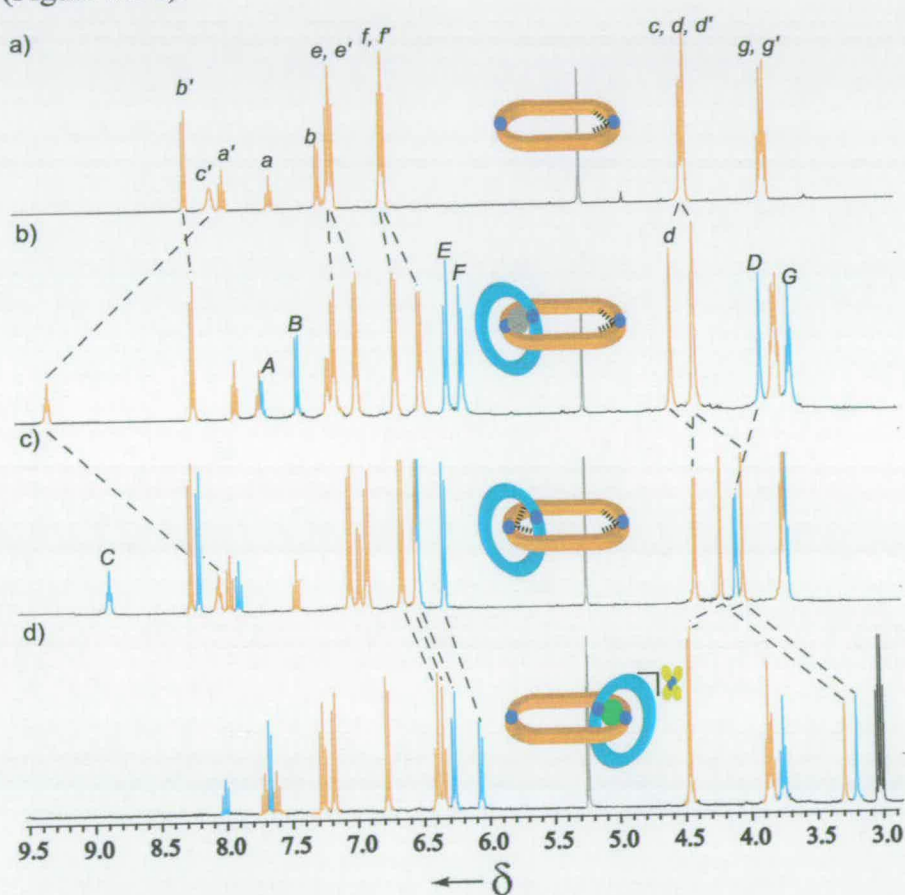


Figure 6.1. 1H NMR spectra (400 MHz, CD_2Cl_2 298 K) of: (a) $9H_2$ (b) $Pd13H_2$ (c) $13H_4$ (d) $[Co13]NEt_4$. The lettering refers to the assignment given in scheme 6.1.

Conversion of the Pd(II) bound catenate into its analogous octahedral Co(III) complex was carried out sequentially. Initial abstraction of the Pd(II) ion with KCN furnished the free ligand $13H_4$, which was then treated first with $Co(OAc)_2$ and Et_4NOAc followed by sodium methoxide to rapidly generate $[Co13]NEt_4$ (Scheme

6.1 viii-ix). Interestingly, the co-conformation of Pd $13H_2$ is retained in the free ligand $13H_4$ through a distinctive intercomponent pyridine-NH-pyridine bifurcated H-bond motif as evidenced by the downfield shift of the amide signal H_C and the pronounced shielding of signals H_c and H_d in its 1H NMR spectrum (Figure 6.1 c). X-ray analysis of single crystals of $13H_4$ confirms that this favourable arrangement is maintained in the solid state (Figure 6.2 b).



Figure 6.2. X-ray crystal structures of [2]catenane Pd $13H_2$ and [2]catenane $13H_4$.^[9] (a) Pd $13H_2$; (b) $13H_4$. Carbon atoms of the small macrocycle are shown in light blue and those of the large macrocycle in yellow; oxygen atoms are red, nitrogen dark blue, hydrogen white. For clarity only nitrogen-bound hydrogen atoms are shown. Selected bond lengths for Pd $13H_2$ [Å]: Pd-N2 2.04; Pd-N5 1.94; Pd-N11 2.04; Pd-N41 2.07; N77-H74 2.38; N77-H83 2.19; other selected distance [Å]: N5-N41 4.00. Selected bond angles for Pd $13H_2$ [°]: N2-Pd-N22 160.5; N74H-N77-N83H 73.5. Selected bond lengths for $13H_4$ [Å]: N2H-N5 2.43; N11H-N5 2.20; N2H-N41 2.25; N11H-N41 2.39. Selected bond angles for $13H_4$ [°]: N2H-N5 92.9; N11H-N5 110.0; N2H-N41 167.3; N11H-N41 139.8.

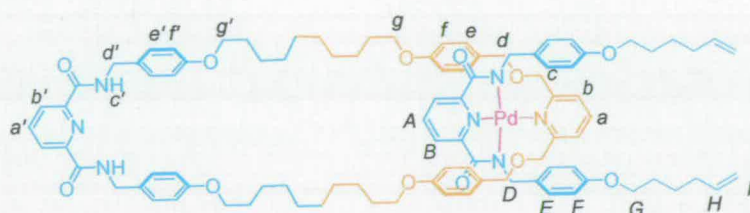
Critically, introduction of a Co(III) ion into the interlocked ligand system introduces several pronounced changes to the 1H NMR spectrum of [Co 13]NEt $_4$ (Figure 6.1 d) verifying that the two macrocyclic fragments have undergone a large amplitude shuttling motion (following deprotonation of the amide groups) in order to accommodate the trivalent TM ion. Firstly, the two NH signals H_C and H_C' are now

absent, suggesting that both 2,6-pyridinedicarboxamide units are now stabilised in their deprotonated form. Secondly, resonances corresponding to benzylic groups H_D and $H_{d'}$ are now shielded, whilst the chemical shifts of signals H_c and H_d are now identical to those observed for the free macrocycle $9H_2$ signifying that they are no longer in close proximity to the aromatic groups of the small amide macrocycle. $Pd13H_2$ was easily regenerated by treating $[Co13]NEt_4$ with Zn /acetic acid and then stirring the free ligand $13H_4$ with $Pd(OAc)_2$.

In summary, a switchable [2]catenane has been prepared wherein the conformation is controlled by the coordination preference of the TM ion it binds to. The [2]catenane is kinetically stable when bound to either metal and switching between the two sides is permitted by first abstracting the TM ion (either Pd(II) or Co(III)), allowing the sub-molecular fragments to rotate more freely, and then locking the structure again through TM ion coordination.

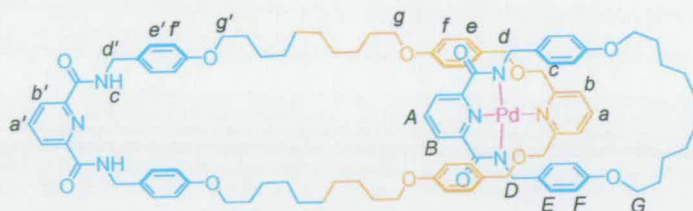
6.3 Experimental

6.3.1 Compound analysis



$Pd(1)(9H_2)$: A solution of $9H_2$ (0.288 g, 2.87×10^{-1} mmol) and $Pd(1)(CH_3CN)$ (0.197 g, 2.87×10^{-1} mmol) in anhydrous dichloromethane (50 mL) was stirred for 1 h at room temperature. The solution was concentrated *in vacuo* and the crude residue purified by column chromatography, (98:2 CH_2Cl_2 :MeOH) to yield $Pd(1)(9H_2)$ as a yellow solid (0.450 g, yield = 95%). m.p. 98-99 °C; 1H NMR (400 MHz, $CDCl_3$, 298 K): δ = 1.15-1.91 (m, 48H, H_{alkyl}), 3.72 (t, 4H, J = 6.6 Hz, H_g), 3.80 (m, 8H, $H_{g'}$ + H_D), 3.86 (t, 4H, J = 6.3 Hz, H_G), 4.26 (s, 4H, H_d), 4.45 (s, 4H, H_c), 4.48 (d, 4H, J = 6.1 Hz, $H_{d'}$), 4.91 (m, 4H, H_H), 5.72 (m, 2H, H_I), 6.35 (d, 4H, J = 8.6 Hz, H_F), 6.46 (d, 4H, J = 8.6 Hz, H_E), 6.69 (d, 4H, J = 8.6 Hz, H_f), 6.74 (d, 4H, J = 8.6 Hz, H_f), 7.12 (m, 8H, H_e + $H_{e'}$), 7.40 (d, 2H, J = 7.8 Hz, H_b), 7.67 (d, 2H, J = 7.8 Hz, $H_{b'}$),

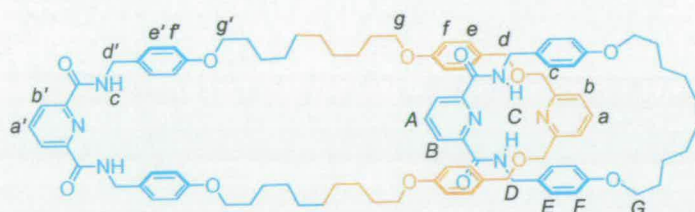
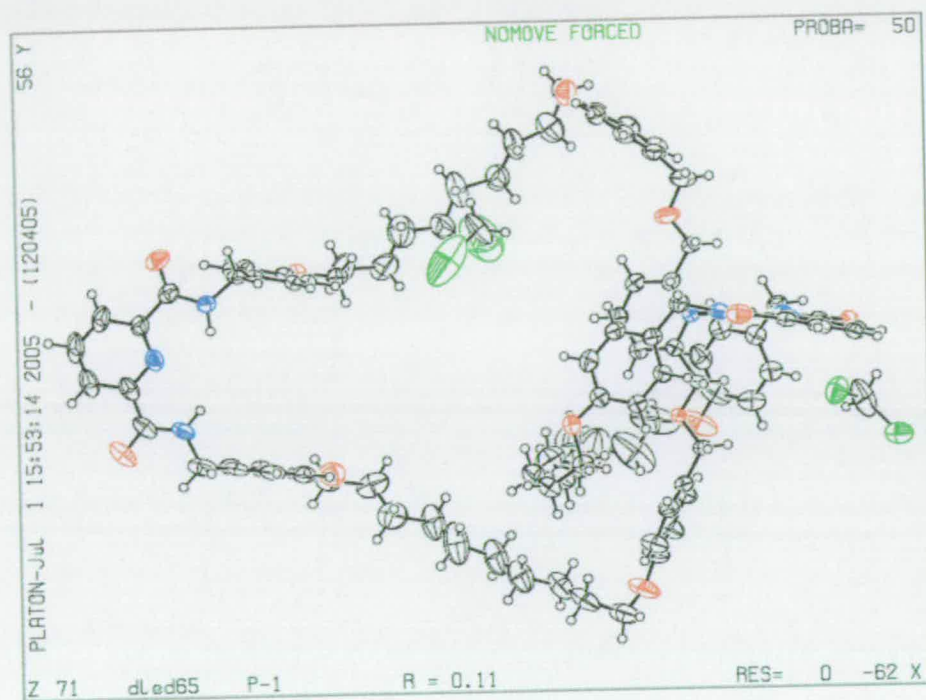
7.80 (t, 1H, $J = 7.8$ Hz, H_a), 7.91 (t, 1H, $J = 7.8$ Hz, H_a), 7.96 (t, 1H, $J = 7.8$ Hz, H_a), 8.31 (d, $J = 7.8$ Hz, 2H, H_b), 8.43 (t, $J = 6.3$ Hz, 2H, H_c); (^{13}C NMR (100 MHz, CDCl_3 , 298 K) $\delta = 25.3, 25.6, 25.7, 25.9, 26.1, 26.3, 26.9, 27.0, 28.8$ (x2), 29.0, 29.1, 29.2, 42.9, 48.7, 67.8, 67.9, 71.4, 73.3, 114.1, 114.6, 122.1, 124.6, 125.2, 128.9, 129.0, 129.1, 129.3, 130.2, 132.9, 138.5, 138.9, 139.1, 140.4, 149.0, 152.5, 157.9, 158.5 (x2), 158.9, 160.4, 163.6, 171.1; LRFAB-MS (3-NOBA matrix): $m/z = 1650$ $[M]^+$.



Pd13H₂: (a) A solution of Pd(1)(9H₂) (0.44 g, 2.6×10^{-1} mmol) in anhydrous dichloromethane (100 mL) was added via a double ended needle to a solution of first generation Grubbs' catalyst (0.064 g, 7.7×10^{-2} mmol) in anhydrous dichloromethane (500 mL) under an atmosphere of nitrogen. The solution was stirred at room temperature for 18 h, concentrated *in vacuo* and the crude residue purified by column chromatography (98:2 CH_2Cl_2 :MeOH) to yield a yellow solid (0.28 g).

(b) To a stirred solution of the yellow solid obtained in part (a) (0.28 g) in THF (50 mL), was added 10% w/w Pd-C (0.04 g) and the resultant suspension stirred under an atmosphere of hydrogen for 18 h. The suspension was filtered through a plug of Celite, and the solution concentrated *in vacuo*. The crude product was purified using column chromatography (2:98, MeOH: CH_2Cl_2) to yield the title compound as a yellow solid (0.272 g, yield = 64% over two steps). m.p. 158-159 °C; ^1H NMR (400 MHz, CD_2Cl_2 , 298 K): $\delta = 1.10$ -1.38 (m, 36H, H_{alkyl}), 1.55-1.66 (m, 12H, H_{alkyl}), 3.65 (t, 4H, $J = 6.5$ Hz, H_g), 3.76 (m, 8H, $H_g + H_g$), 3.87 (s, 4H, H_D), 4.37 (m, 8H, $H_d + H_d'$), 4.55, (s, 4H, H_d), 6.15 (d, 4H, $J = 8.6$ Hz, H_F), 6.26 (d, 4H, $J = 8.6$ Hz, H_E), 6.46 (d, 4H, $J = 8.4$ Hz, H_f), 6.65 (d, 4H, $J = 8.6$ Hz, H_f), 6.95 (d, 4H, $J = 8.4$ Hz, H_e), 7.12 (d, 4H, $J = 8.6$ Hz, H_e), 7.17 (d, 2H, $J = 7.8$ Hz, H_b), 7.40 (d, 2H, $J = 7.8$ Hz, H_b), 7.68 (m, 2H, $H_a + H_a'$), 7.87 (t, 1H, $J = 7.8$ Hz, H_A), 8.19 (d, 2H, $J = 7.8$ Hz, H_B), 9.3 (t, 2H, $J = 6.3$ Hz, H_c); ^{13}C NMR (100 MHz, CD_2Cl_2 , 298 K): $\delta = 26.5, 26.6, 27.0, 27.2, 27.3, 27.5, 28.0, 28.4, 28.8, 28.9, 29.1, 29.2, 43.0, 49.9, 67.3, 68.2$ (x2), 73.5, 76.7, 114.4, 114.7, 115.1, 122.2, 123.9, 125.1, 128.5, 129.2, 130.7, 139.1,

139.3, 140.6, 149.5, 152.3, 157.9 (x2), 158.2 (x2), 159.4, 160.3, 164.1, 171.6, 175.9;
 LRFAB-MS (3-NOBA matrix): $m/z = 1624 [M]^+$; HRFAB-MS (3-NOBA matrix):
 $m/z = 1624.73425$ (calcd. for $^{12}\text{C}_{92}^{13}\text{C}_1\text{H}_{111}\text{N}_7\text{O}_{12}\text{Pd}$, 1624.73563).



13H₄: To a solution of Pd13H₂ (0.215 g, 1.32×10^{-1} mmol) in dichloromethane (20 mL) and methanol (20 mL) was added potassium cyanide (0.086 g, 1.32 mmol) in methanol (5 mL). The solution was stirred at room temperature for 1 h, until it was colourless, and then heated gently to reduce the overall volume to less than 5 mL. The resultant mixture was dispersed in water (25 mL) and washed with dichloromethane (3 x 25 mL). The combined organic extracts were washed with further water (25 mL) and dried over anhydrous magnesium sulfate. After filtration, the solution was concentrated *in vacuo* and the crude residue recrystallised from acetonitrile to give the title compound as a colorless solid (0.198 g, yield = 98%). m.p. 139-141 °C; ¹H NMR (400 MHz, CD₂Cl₂, 298 K): $\delta = 1.13$ -1.39 (m, 36H, H_{alkyl}), 1.54-1.68 (m, 12H, H_{alkyl}), 3.73 (m, 12H, H_G + H_g + H_{g'}), 4.05 (s, 4H, H_c), 4.09 (d, 4H, $J = 6.2$ Hz, H_D), 4.21 (s, 4H, H_d), 4.40 (d, 4H, $J = 6.1$ Hz, H_{d'}), 6.32 (d,

resultant sodium ethoxide solution added drop-wise to the reaction mixture. The solution was left to stir for 3 h at room temperature whilst being exposed to a gentle flow of air. The resultant green suspension was filtered, the solvent removed *in vacuo* and the crude solid redissolved in acetone. Small portions of diethyl ether (3 x 10 mL) were then added to the solution precipitating the title compound as a dark green solid (0.084 g, yield = 81%). m.p. 91-92 °C; ¹H NMR (400 MHz, CD₂Cl₂, 298 K): δ = 1.11 (t, 12H, *J* = 7.3 Hz, N(CH₂CH₃)₄), 1.16-1.42 (m, 36H, H_{alkyl}), 1.56-1.75 (m, 12H, H_{alkyl}), 3.02 (q, 8H, *J* = 7.3 Hz, N(CH₂CH₃)₄), 3.20 (s, 4H, H_D), 3.29 (s, 4H, H_{d'}), 3.76 (t, 4H, *J* = 6.6 Hz, H_G), 3.86 (m, 8H, H_g + H_{g'}), 4.46 (s, 4H, H_c), 4.47 (s, 4H, H_d), 6.07 (d, 4H, *J* = 8.6 Hz, H_F), 6.27 (d, 4H, *J* = 8.6 Hz, H_E), 6.35 (d, 4H, *J* = 8.8 Hz, H_f), 6.40 (d, 4H, *J* = 8.8 Hz, H_{e'}), 6.78 (d, 4H, *J* = 8.6 Hz, H_j), 7.19 (d, 4H, *J* = 8.6 Hz, H_e), 7.27 (m, 4H, H_b + H_{b'}), 7.62 (t, 1H, *J* = 7.6 Hz, H_a), 7.67 (d, 2H, *J* = 7.8 Hz, H_β), 7.72 (t, 1H, *J* = 7.6 Hz, H_{a'}), 8.02 (t, 1H, *J* = 7.8 Hz, H_A); ¹³C NMR (100 MHz, CD₂Cl₂, 298 K): δ = 7.8, 25.9, 26.3, 26.4 (x2), 28.6, 28.7 (x2), 29.5 (x2), 29.6 (x2), 29.8, 46.2, 46.5, 52.9, 67.9, 68.3, 68.4, 72.7, 73.0, 113.7, 114.6, 114.7, 120.6, 122.1, 122.9, 127.9, 129.1, 129.9 (x2), 130.4, 133.3, 134.3, 137.4, 138.7, 157.0, 157.5, 157.9, 158.4, 158.5, 159.3, 168.8, 169.0; LRFAB-MS (3-NOBA matrix): *m/z* = 1577 [MH]⁺; HRFAB-MS (3-NOBA matrix): *m/z* = 1576.75653 (calcd. for C₉₂¹³CH₁₁₀N₇O₁₂Co, 1576.75780).

6.3.2 Interconversion of [2]Catenane Species

[Co10]NEt₄→10H₄: To a solution of [Co10]NEt₄ (0.050 g, 3.17x10⁻² mmol) in acetic acid (2 mL) was added powdered zinc (0.02 g) and the suspension stirred for 1 h. The mixture was then filtered through a plug of Celite and the solvent removed *in vacuo*. The crude product was then recrystallised from acetonitrile to give the title compound as a colorless solid (0.044 g, yield = 90%).

10H₄→Pd10H₂: To a solution of 10H₄ (0.020 g, 1.31x10⁻² mmol) in CH₂Cl₂/CH₃CN was added Pd(OAc)₂ (0.003 g, 1.31x10⁻² mmol) and the solution stirred for 10 h. The solvent was then removed *in vacuo* and the crude product was purified using column chromatography (2:98, MeOH:CH₂Cl₂) to yield the title compound as a yellow solid (0.018 g, yield = 83%).

6.4 References and Notes

- [1] R. D. Astumian, *Science* **1997**, *276*, 917-922; R. D. Astumian, I. Derényi, *Eur. Biophys. J. Biophys. Lett.* **1998**, *27*, 474-489; R. D. Astumian, I. Derényi, *Biophys. J.* **1999**, *77*, 993-1002; R. D. Astumian, P. Hänggi, *Phys. Today*, **2002**, *55(11)*, 33-39; *Molecular Motors*, (Ed. M. Schliwa) Wiley-VCH, Weinheim, **2003**; H. Hess, G. D. Bachand, V. Vogel, *Chem. Eur. J.* **2004**, *10*, 2110-2116.
- [2] For examples of molecular machine prototypes based on non-interlocked molecules see: T. R. Kelly, M. C. Bowyer, K. V. Bhaskar, D. Bebbington, A. Garcia, F. R. Lang, M. H. Kim, M. P. Jette, *J. Am. Chem. Soc.* **1994**, *116*, 3657-3658; T. R. Kelly, I. Tellitu, J. P. Sestelo, *Angew. Chem. Int. Ed. Engl.* **1997**, *36*, 1866-1868; T. R. Kelly, H. De Silva, R. A. Silva, *Nature* **1999**, *401*, 150-152; N. Koumura, R. W. J. Zijlstra, R. A. van Delden, N. Harada, B. L. Feringa, *Nature* **1999**, *401*, 152-155; T. R. Kelly, R. A. Silva, H. De Silva, S. Jasmin, Y. J. Zhao, *J. Am. Chem. Soc.* **2000**, *122*, 6935-6949; N. Koumura, E. M. Geertsema, A. Meetsma, B. L. Feringa, *J. Am. Chem. Soc.* **2000**, *122*, 12005-12006; *Molecular Switches* (Ed: B. L. Feringa), Wiley-VCH, Weinheim, **2001**; B. L. Feringa, *Acc. Chem. Res.* **2001**, *34*, 504-513; T. R. Kelly, *Acc. Chem. Res.* **2001**, *34*, 514-522; B. L. Feringa, N. Koumura, R. A. van Delden, M. K. J. ter Wiel, *Appl. Phys. A.*, **2002**, *75*, 301-308; E. M. Geertsema, N. Koumura, M. K. J. ter Wiel, A. Meetsma, B. L. Feringa, *Chem. Commun.* **2002**, 2962-2963; N. Koumura, E. M. Geertsema, M. B. van Gelder, A. Meetsma, B. L. Feringa, *J. Am. Chem. Soc.* **2002**, *124*, 5037-5051; R. A. van Delden, N. Koumura, N. Harada, B. L. Feringa, *Proc. Natl. Acad. Sci. U. S. A.* **2002**, *99*, 4945-4949; B. L. Feringa, R. A. van Delden, M. K. J. ter Wiel, *Pure Appl. Chem.* **2003**, *75*, 563-575; S. M. Hou, T. Sagara, D. C. Xu, T. R. Kelly, E. Ganz, *Nanotechnology*, **2003**, *14*, 566-570; M. K. J. ter Wiel, R. A. van Delden, A. Meetsma, B. L. Feringa, *J. Am. Chem. Soc.* **2003**, *125*, 15076-15086.
- [3] For examples of molecular machine prototypes based on mechanically interlocked molecules see V. Balzani, M. Gómez-López, J. F. Stoddart, *Acc. Chem. Res.* **1998**, *31*, 405-414; J.-C. Chambron, J.-P. Sauvage, *Chem. Eur. J.* **1998**, *4*, 1362-1366; J.-P. Collin, P. Gaviña, V. Heitz, J.-P. Sauvage, *Eur. J. Inorg. Chem.* **1998**, 1-14; M.-J. Blanco, M. C. Jiménez, J.-C. Chambron, V. Heitz, M. Linke, J.-P. Sauvage, *Chem. Soc. Rev.* **1999**, *28*, 293-305; *Molecular Catenanes, Rotaxanes and Knots*,

- (Eds.: J.-P. Sauvage, C. Dietrich-Buchecker), Wiley-VCH, Weinheim, 1999; V. Balzani, A. Credi, F. M. Raymo, J. F. Stoddart, *Angew. Chem. Int. Ed.* **2000**, *39*, 3349-3391; R. Ballardini, V. Balzani, A. Credi, M. T. Gandolfi, M. Venturi, *Acc. Chem. Res.* **2001**, *34*, 445-455; J.-P. Collin, C. Dietrich-Buchecker, P. Gaviña, M. C. Jiménez-Molero, J.-P. Sauvage, *Acc. Chem. Res.* **2001**, *34*, 477-487; A. R. Pease, J. O. Jeppesen, J. F. Stoddart, Y. Luo, C. P. Collier, J. R. Heath, *Acc. Chem. Res.* **2001**, *34*, 433-444; J.-P. Sauvage, in *Structure and Bonding, Vol. 99*, Springer, Berlin, **2001**; B. X. Colasson, C. Dietrich-Buchecker, M. C. Jiménez-Molero, J.-P. Sauvage, *J. Phys. Org. Chem.* **2002**, *15*, 476-483; C. Dietrich-Buchecker, M. C. Jiménez-Molero, V. Sartor, J.-P. Sauvage, *Pure Appl. Chem.* **2003**, *75*, 1383-1393; E. R. Kay, D. A. Leigh, in *Functional Artificial Receptors* (Eds.: T. Schrader, A. D. Hamilton), Wiley-VCH, Weinheim, **2005**, pp. 333-406; K. Kinbara, T. Aida, *Chem. Rev.* **2005**, *105*, 1377-1400; J.-P. Sauvage, *Chem. Commun.* **2005**, 1507-1510.
- [4] M. Cesario, C. O. Dietrich-Buchecker, J. Guilhem, C. Pascard, J.-P. Sauvage, *J. Chem. Soc. Chem. Commun.* **1985**, 244-247; A. Livoreil, C. O. Dietrich-Buchecker, J.-P. Sauvage, *J. Am. Chem. Soc.* **1994**, *116*, 9399-9400; D. B. Amabilino, C. O. Dietrich-Buchecker, A. Livoreil, L. Pérez-García, J.-P. Sauvage, J. F. Stoddart, *J. Am. Chem. Soc.* **1996**, *118*, 3905-3913; D. A. Leigh, K. Moody, J. P. Smart, K. J. Watson, A. M. Z. Slawin, *Angew. Chem. Int. Ed. Engl.* **1996**, *35*, 306-310; A. Livoreil, J.-P. Sauvage, N. Armaroli, V. Balzani, L. Flamigni, B. Ventura, *J. Am. Chem. Soc.* **1997**, *119*, 12114-12124; V. Balzani, A. Credi, S. J. Langford, F. M. Raymo, J. F. Stoddart, M. Venturi, *J. Am. Chem. Soc.* **2000**, *122*, 3542-3543; C. P. Collier, G. Mattersteig, E. W. Wong, Y. Luo, K. Beverly, J. Sampaio, F. M. Raymo, J. F. Stoddart, J. R. Heath, *Science* **2000**, *289*, 1172-1175; D. A. Leigh, J. K. Y. Wong, F. Dehez, F. Zerbetto, *Nature* **2003**, *424*, 174-179; J. V. Hernández, E. R. Kay, D. A. Leigh, *Science* **2004**, *306*, 1532-1537; B. Korybut-Daszkiewicz, A. Wieckowska, R. Bilewicz, S. Domagala, K. Wozniak, *Angew. Chem. Int. Ed.* **2004**, *43*, 1668-1672; D. W. Steuerman, H.-R. Tseng, A. J. Peters, A. H. Flood, J. O. Jeppesen, K. A. Nielsen, J. F. Stoddart, J. R. Heath, *Angew. Chem. Int. Ed.* **2004**, *43*, 6486-6491; P. Mobian, J.-M. Kern, J.-P. Sauvage, *Angew. Chem. Int. Ed.* **2004**, *43*, 2392-2395.
- [5] D. A. Leigh, P. J. Lusby, S. J. Teat, A. J. Wilson, J. K. Y. Wong, *Angew. Chem. Int. Ed.* **2001**, *40*, 1538-1543; F. Arico, P. Mobian, J.-M. Kern, J.-P. Sauvage, *Org. Lett.* **2003**, *5*, 1887-1890; P. Mobian, J.-M. Kern, J.-P. Sauvage, *J. Am. Chem.*

Soc. **2003**, *125*, 2016-2017; P. Mobian, J.-M. Kern, J.-P. Sauvage, *Inorg. Chem.* **2003**, *42*, 8633-8637; P. Mobian, J.-M. Kern, J.-P. Sauvage, *Helv. Chim. Acta* **2003**, *86*, 4195-4213; D. Pomeranc, D. Jouvenot, J.-C. Chambron, J. P. Collin, V. Heitz, J.-P. Sauvage, *Chem. Eur. J.* **2003**, *9*, 4247-4254; J.-C. Chambron, J.-P. Collin, V. Heitz, D. Jouvenot, J.-M. Kern, P. Mobian, D. Pomeranc, J.-P. Sauvage, *Eur. J. Org. Chem.* **2004**, 1627-1638; L. Hogg, D. A. Leigh, P. J. Lusby, A. Morelli, S. Parsons, J. K. Y. Wong, *Angew. Chem. Int. Ed.* **2004**, *43*, 1218-1221.

[6] A.-M. Fuller, D. A. Leigh, P. J. Lusby, I. D. H. Oswald, S. Parsons, D. B. Walker, *Angew. Chem. Int. Ed.* **2004**, *43*, 3914-3918; A.-M. L. Fuller, D. A. Leigh, P. J. Lusby, A. M. Z. Slawin, D. B. Walker, *J. Am. Chem. Soc.* **2005**, *127*, 12612-12619.

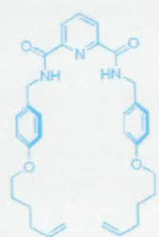
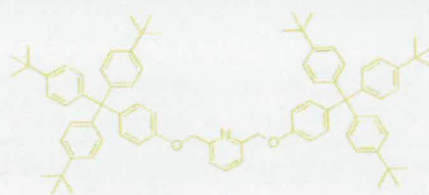
[7] D. A. Leigh, P. J. Lusby, A. M. Z. Slawin, D. B. Walker, *Angew. Chem. Int. Ed.* **2005**, *44*, 4557-4564.

[8] F. A. Chavez, J. M. Rowland, M. M. Olmstead, P. K. Mascharak, *J. Am. Chem. Soc.* **1998**, *120*, 9015-9027; J. C. Noveron, M. M. Olmstead, P. K. Mascharak, *Inorg. Chem.* **1998**, *37*, 1138-1139; D. S. Marlin, M. M. Olmstead, P. K. Mascharak, *Inorg. Chem.* **1999**, *38*, 3258-3260; J. C. Noveron, M. M. Olmstead, P. K. Mascharak, *J. Am. Chem. Soc.* **1999**, *121*, 3553-3554; F. A. Chavez, P. K. Mascharak, *Acc. Chem. Res.* **2000**, *33*, 539-545; D. S. Marlin, P. K. Mascharak, *Chem. Soc. Rev.* **2000**, *29*, 69-74; L. A. Tyler, J. C. Noveron, M. M. Olmstead, P. K. Mascharak, *Inorg. Chem.* **2000**, *39*, 357-362; J. C. Noveron, M. M. Olmstead, P. K. Mascharak, *J. Am. Chem. Soc.* **2001**, *123*, 3247-3259.

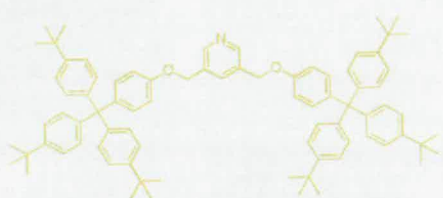
[9] Data for Pd₁₃H₂ were collected at 93 K using a Rigaku Saturn (MM007 high flux RA/MoK_α radiation, confocal optic) and data for 13H₄ were collected at 173 K using a Rigaku Saturn (MM007 high flux RA/CuK_α radiation, confocal optic). At least a full hemisphere of data was collected. Intensities were corrected for Lorentz polarisation and absorption effects (multiple equivalent reflections). Structures were solved by direct methods, non-H atoms were refined anisotropically with C-H protons being refined in riding geometries (SHELXTL) against F^2 . In most cases amide protons were refined isotropically subject to a distant constraint. Pd₁₃H₂: C₉₃H₁₁₁N₇O₁₂Pd·CH₂Cl₂, $M = 1710.21$, yellow prism, crystal size 0.1×0.1×0.1 mm, triclinic, $P-1$, $a = 13.6450(9)$, $b = 17.6906(12)$, $c = 19.4878(14)$ Å, $\alpha = 77.415(4)$, $\beta = 74.874(4)$, $\gamma = 81.360(4)^\circ$ $V = 4410.2(5)$ Å³, $Z = 2$, $\rho_{\text{calcd}} = 1.288$ Mg m⁻³; $\mu = 0.335$

mm^{-1} , 31243 data (14083 unique, $R_{\text{int}} = 0.0585$) $R = 0.1132$, $S = 1.124$ for 1081 parameters. Residual electron density extremes were 1.990 and $-0.742 \text{ e}\text{\AA}^{-3}$. 13H_4 : $\text{C}_{93}\text{H}_{113}\text{N}_7\text{O}_{12}(\text{H}_2\text{O})_{0.25}$, $M = 1525.41$, colourless prism, crystal size $0.1 \times 0.1 \times 0.1 \text{ mm}$, monoclinic, $P2_1/c$, $a = 28.678(3)$, $b = 11.6588(10)$, $c = 27.999(3) \text{ \AA}$, $\beta = 116.174(3)^\circ$, $V = 8401.6(13) \text{ \AA}^3$, $Z = 4$, $\rho_{\text{calcd}} = 1.206 \text{ Mg m}^{-3}$; $\mu = 0.637 \text{ mm}^{-1}$, 103523 data (14154 unique, $R_{\text{int}} = 0.1938$) $R = 0.1349$, $S = 1.061$ for 1035 parameters. Residual electron density extremes were 0.530 and $-0.370 \text{ e}\text{\AA}^{-3}$.

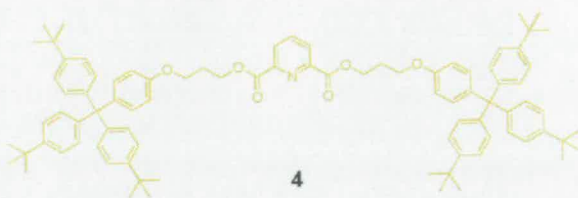
Appendix 1: Glossary of Compounds

1H₂

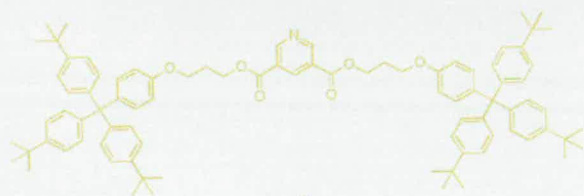
2



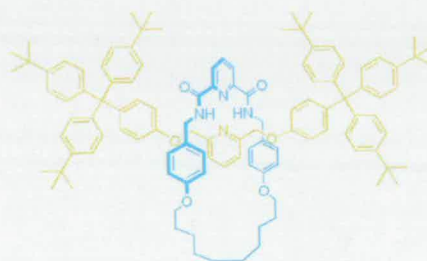
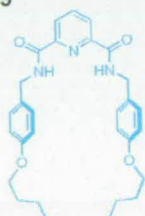
3



4



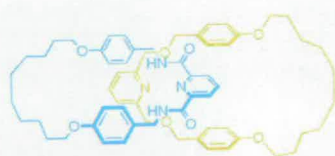
5

6H₂7H₂

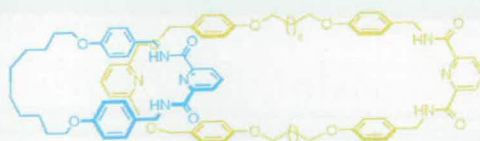
8

9H₂

10

11H₂

12

13H₄

Appendix 2: Published Papers

Rotaxane Synthesis


A 3D Interlocked Structure from a 2D Template: Structural Requirements for the Assembly of a Square-Planar Metal-Coordinated [2]Rotaxane**

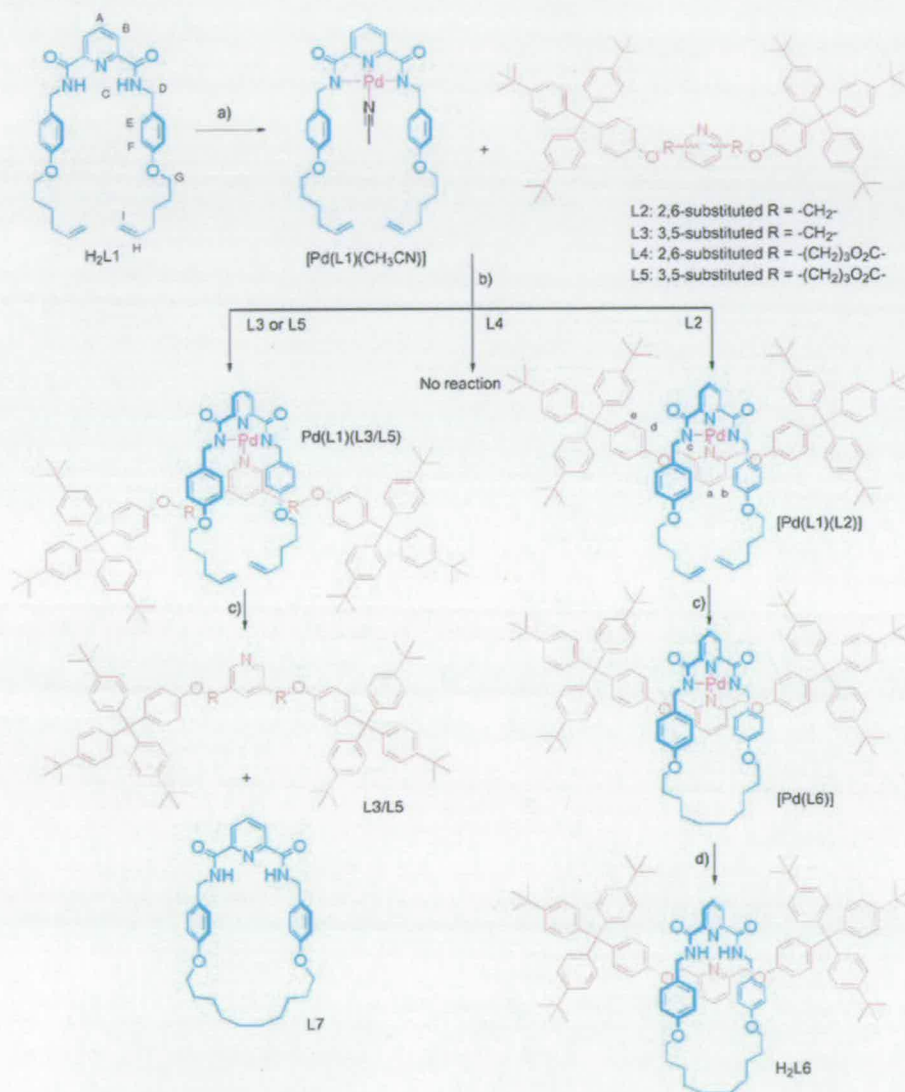
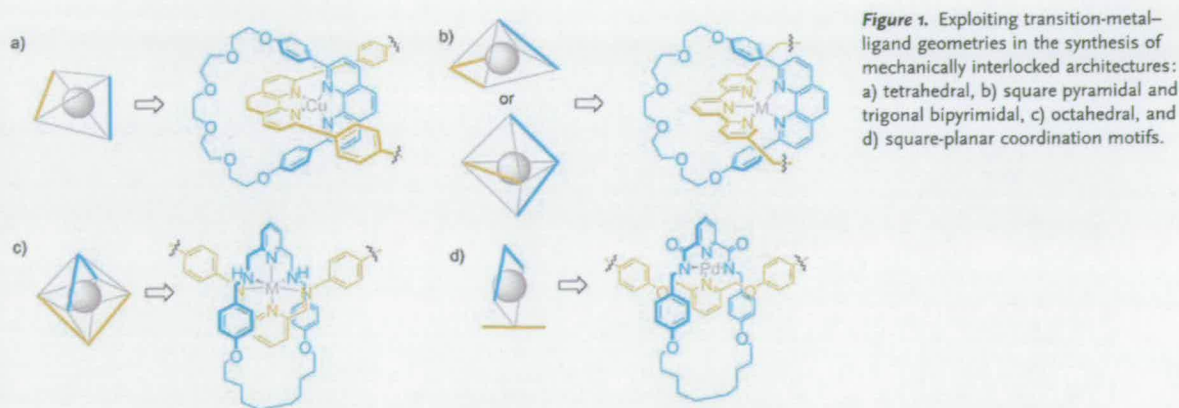
Anne-Marie Fuller, David A. Leigh,* Paul J. Lusby, Iain D. H. Oswald, Simon Parsons, and D. Barney Walker

The starting point for the revolution in catenane and rotaxane synthesis that occurred during the last part of the 20th century was the realization by Sauvage and co-workers that metal–ligand coordination geometries could fix molecular fragments in three-dimensional space such that they were predisposed to form mechanically interlocked architectures through macrocyclization or “stoppering” reactions.^[1] Efficient synthetic methods to rotaxanes were subsequently developed based on four- (tetrahedral)^[2], five- (trigonal bipyramidal and square pyramidal)^[3] and, most recently, six-coordinate (octahedral)^[4] metal templates (Figure 1).^[5] One of the benefits of using specific coordination motifs for such assemblies is that the resulting interlocked ligands often do not permit other metal geometries in their binding site, which can consequently be exploited either to lock a metal in an unusual geometry for its oxidation state^[6] or to bring about large-amplitude “shuttling” of the ligand components.^[3,7] Here we show that three-dimensional interlocked architectures can also be assembled from two-dimensional coordination templates by using steric and electronic restrictions to direct the synthesis in the third

[*] A.-M. Fuller, Prof. D. A. Leigh, Dr. P. J. Lusby, I. D. H. Oswald, Dr. S. Parsons, D. B. Walker
School of Chemistry, University of Edinburgh
The King's Buildings, West Mains Road, Edinburgh EH9 3JJ (UK)
Fax: (+44) 131-667-9085
E-mail: David.Laugh@ed.ac.uk

[**] We thank E. R. Kay for assistance with the graphics and crystallography data. This work was supported by the European Union Future and Emerging Technology Program MechMol and the EPSRC.

 Supporting information for this article is available on the WWW under <http://www.angewandte.org> or from the author.



Scheme 1. Reagents and conditions: a) Pd(OAc)₂, CH₃CN, 76%; b) CHCl₃, 50 °C; L2: 63%, L3: 96%, L4: 0%, L5: 97%; c) 1. Grubbs catalyst (0.1 equiv), CH₂Cl₂; 2. H₂, Pd/C, THF, H₂L6: 98%, L3 + L7: 63%, L5 + L7: 69% (over 2 steps); d) KCN, MeOH, CH₂Cl₂, 20 °C, 1 h and then 40 °C, 0.5 h, 97%.

dimension. The resulting [2]rotaxane is the first example of a mechanically interlocked ligand that forms a four-coordinate square-planar metal complex.^[8]

The square-planar [2]rotaxane ligand design consists of a tridentate benzylic amide macrocycle and a monodentate thread (Figure 1d). The macrocycle incorporates a 2,6-dicarboxyamidopyridine unit to exploit the palladium chemistry recently developed^[9] by Hirao and co-workers. The thread contains a pyridine donor group substituted with appropriately bulky stoppers in either the 2,6- or 3,5-positions. It was envisioned that in the key intermediate, [Pd(L1)(L2–L5)] (see Scheme 1), the geometry of the precursor to the macrocycle (previously used to direct hydrogen bond assembly processes^[10]) would promote intercomponent π - π stacking, thus encouraging the pyridine donor of the thread to bind the metal ion orthogonally to the N₃ ligand (complementing the normally preferred orientation^[11]) and directing the assembly in the third dimension. A series of readily available threads L2–L5 was investigated during the study.

The rotaxane synthesis was carried out according to Scheme 1. Treatment of H₂L1 with Pd(OAc)₂ in acetonitrile smoothly generated a complex [Pd(L1)(CH₃CN)] in which the fourth coordination site of the metal is occupied by a normally labile acetonitrile molecule. Nevertheless, displacement of the acetonitrile by bis-ester pyridine ligand L4 was unsuccessful (see below). However, simple combination of L5 or either of the bis-ether pyridine threads (L2 and L3) with [Pd(L1)(CH₃CN)] in either dichloromethane or chloroform gave the desired complexes [Pd(L1)(L5/L2/L3)] in 97, 63 and 96% yields, respectively. The ¹H NMR spectrum of [Pd(L1)(L2)] is shown in Figure 2c. Comparison with the spectra of [Pd(L1)(CH₃CN)] and H₂L1 (Figure 2b and 2a, respectively) shows features clearly indicative of metal coordination (the absence of H_C and shifts in H_A and H_B) and the anticipated aromatic stacking between the tridentate and monodentate ligands (particularly H_E and H_F). Similar chemical shift differences were observed for [Pd(L1)(L3)] and [Pd(L1)(L5)], however, ring closing olefin metathesis (RCM) followed by hydrogenation (Scheme 1, step c) of the three complexes produced very different results. Whilst cyclization of [Pd(L1)(L2)] gave the corresponding [2]rotaxane [Pd(L6)] in 77% yield following hydrogenation of the olefin, no [2]rotaxane was produced from RCM of either [Pd(L1)(L3)] or [Pd(L1)(L5)], the only products in each case being the free macrocycle and thread. Why does only one of the four threads direct rotaxane synthesis in the desired manner?

The ¹H NMR spectra of the [2]rotaxane ([Pd(L6)], Figure 2d), mass spectrometric analysis, and the preserved association of the organic fragments upon demetalation, unambiguously confirmed the interlocked structure. In addition to the loss of the terminal alkene protons, some subtle differences in the ¹H NMR spectrum of [Pd(L6)] compared to [Pd(L1)(L2)] (Figure 2c) indicates that some rearrangement of the ligands does occur on formation of the rotaxane. Single crystals of [Pd(L6)] suitable for X-ray crystallography^[12] were grown by slow cooling of a warm, saturated solution of the [2]rotaxane in acetonitrile. The solid-state structure (Figure 3) shows the interlocked architecture and the

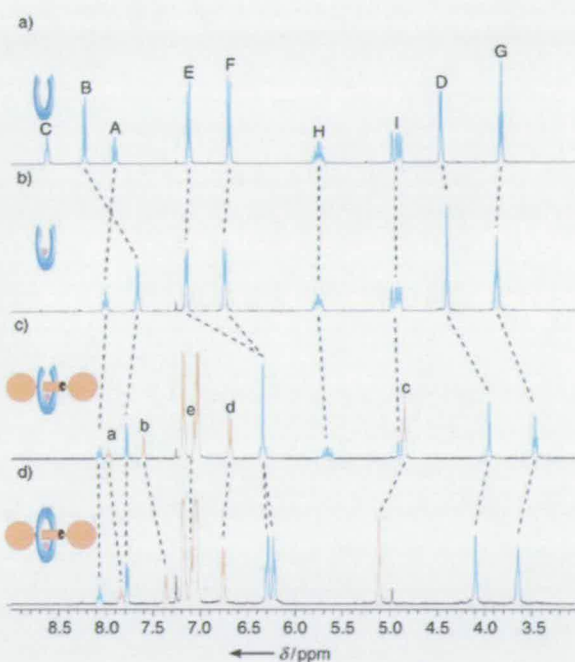


Figure 2. ¹H NMR spectra (400 MHz, 9:1 CDCl₃:CD₃CN, 298 K) of a) H₂L1; b) [Pd(L1)(CH₃CN)]; c) [Pd(L1)(L2)]; d) [2]rotaxane [Pd(L6)]. The lettering refers to the assignments in Scheme 1.

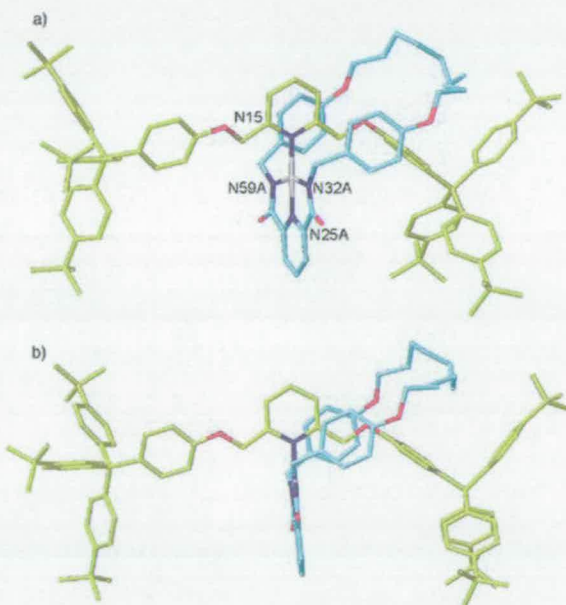


Figure 3. X-ray crystal structure of rotaxane [Pd(L6)] showing a) staggered and b) side-on views.^[12] Carbon atoms of the macrocycle are shown in light blue and those of the thread in yellow; oxygen atoms are red, nitrogen dark blue, palladium gray. Selected bond lengths [Å]: Pd-N15 1.95, Pd-N25 1.86, Pd-N32 2.04, Pd-N59 2.02; other selected distance [Å]: N15-N25 3.81; macrocycle bite angle [°]: N59-Pd-N32 160.0. The macrocycle is disordered over two similar sites (50:50), but one is omitted for clarity together with the hydrogen atoms.

pseudo-square-planar geometry (the N_3 bite angle is 160.0°) around the palladium center. The π stacking between the macrocycle and the pyridine ring of the thread so apparent in solution from the 1H NMR shifts is significantly offset in the solid state (see the side-on view, Figure 3b). The co-conformation adopted by the macrocycle and thread in the crystal structure of the rotaxane clearly illustrates why RCM of the complexes formed with the 3,5-disubstituted threads ($[Pd(L1)(L3)]$ and $[Pd(L1)(L5)]$) can lead to uninterlocked products; even with both fragments attached to the metal, cyclization of L1 can readily occur without encircling a 3,5-substituted pyridine thread. Similarly, the conformation of the thread suggests a possible reason for the lack of reactivity of the 2,6-bis-ester thread L4 towards $[Pd(L1)(CH_3CN)]$. In the crystal structure the electron density of the ether oxygen atoms of the thread is directed away from the occupied d_{z^2} orbital lobes which lie above and below the plane of the square-planar geometry at the d^8 palladium center. Chelation of L4 to $[Pd(L1)]$ has to occur orthogonally for steric reasons. Such an arrangement would force electron density from the ester carbonyl groups into this high-energy space.

Demetalation of $[Pd(L6)]$ with potassium cyanide (Scheme 1, step d) generates the free [2]rotaxane $H_2(L6)$ in 97% yield, thus confirming that the coordination bonds are not required to stabilize the interlocked architecture once it is formed. The 1H NMR spectrum of $H_2(L6)$ and its uninterlocked components in $CDCl_3$ are shown in Figure 4. The shielding of the benzyl groups in the rotaxane relative to the free macrocycle, together with the large ($\delta = 1.7$ ppm) downfield shift of the amide protons (H_C), indicate that specific

hydrogen-bonding interactions between the thread and the macrocycle are "switched on" by the demetalation/protonation procedure. It appears that the amide groups of H_2L6 simultaneously hydrogen bond to the pyridine groups in both the macrocycle and thread.

In conclusion, we have described methodology for assembling a three-dimensional interlocked molecular architecture from a two-dimensional metal template. A combination of steric and electronic factors direct the synthesis in the third dimension, either promoting or preventing interlocking. The resulting [2]rotaxane is the first example derived from a square-planar-coordinated metal center and completes the series of mechanically interlocked ligands for common transition-metal geometries initiated by Sauvage and co-workers in 1983.

Received: December 29, 2003 [Z53622]

Keywords: coordination modes · palladium · rotaxanes · template synthesis

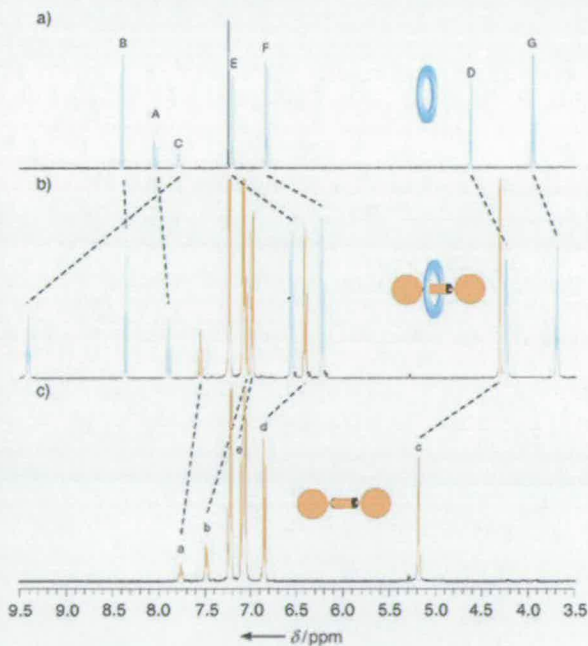


Figure 4. 1H NMR spectra (400 MHz, $CDCl_3$, 298 K) of a) macrocycle; b) demetalated [2]rotaxane H_2L6 ; c) thread L2. The lettering refers to the assignments in Scheme 1.

- [1] C. O. Dietrich-Buchecker, J.-P. Sauvage, J.-P. Kintzinger, *Tetrahedron Lett.* **1983**, 24, 5095–5098.
- [2] a) J.-P. Sauvage, C. Dietrich-Buchecker, G. Rapenne in *Molecular Catenanes, Rotaxanes and Knots* (Eds.: J.-P. Sauvage, C. Dietrich-Buchecker), Wiley-VCH, Weinheim, **1999**; b) J.-P. Collin, C. Dietrich-Buchecker, P. Gaviña, M. C. Jimenez-Molero, J.-P. Sauvage, *Acc. Chem. Res.* **2001**, 34, 477–487.
- [3] a) N. Armaroli, V. Balzani, J.-P. Collin, P. Gaviña, J.-P. Sauvage, B. Ventura, *J. Am. Chem. Soc.* **1999**, 121, 4397–4408; b) L. Raehm, J.-M. Kern, J.-P. Sauvage, *Chem. Eur. J.* **1999**, 5, 3310–3317.
- [4] a) D. Pomeranc, D. Jouvenot, J.-C. Chambron, J.-P. Collin, V. Heitz, J.-P. Sauvage, *Chem. Eur. J.*, **2003**, 9, 4247–4254; b) L. Hogg, D. A. Leigh, P. J. Lusby, A. Morelli, S. Parsons, J. K. Y. Wong, *Angew. Chem.* **2004**, 116, 1238–1241; *Angew. Chem. Int. Ed.* **2004**, 43, 1218–1221.
- [5] For complexes in which metal coordination forms part of the macrocycle in a rotaxane, see a) K.-S. Jeong, J. S. Choi, S.-Y. Chang, H.-Y. Chang, *Angew. Chem.* **2000**, 112, 1758–1761; *Angew. Chem. Int. Ed.* **2000**, 39, 1692–1695; b) S.-Y. Chang, J. S. Choi, K.-S. Jeong, *Chem. Eur. J.* **2001**, 7, 2687–2697; c) S.-Y. Chang, K.-S. Jeong, *J. Org. Chem.* **2003**, 68, 4014–4019; d) S.-Y. Chang, H.-Y. Jang, K.-S. Jeong, *Chem. Eur. J.* **2003**, 9, 1535–1541; for complexes in which metal coordination forms part of the thread in a rotaxane, see e) K.-M. Park, D. Whang, E. Lee, J. Heo, K. Kim, *Chem. Eur. J.* **2002**, 8, 498–508; for complexes in which metal coordination forms the stoppers in a rotaxane, see f) R. B. Hannak, G. Färber, R. Konrat, B. Kräutler, *J. Am. Chem. Soc.* **1997**, 119, 2313–2314; g) J.-C. Chambron, J.-P. Collin, J.-O. Dalbavie, C. O. Dietrich-Buchecker, V. Heitz, F. Odobel, N. Solladié, J.-P. Sauvage, *Coord. Chem. Rev.* **1998**, 178–180, 1299–1312; h) A. J. Baer, D. H. Macartney, *Inorg. Chem.* **2000**, 39, 1410–1417; i) G. J. E. Davidson, S. J. Loeb, N. A. Parekh, J. A. Wisner, *J. Chem. Soc. Dalton Trans.* **2001**, 3135–3136; for polyrotaxanes based on metal-coordination polymers, see j) S. R. Batten, R. Robson, *Angew. Chem.* **1998**, 110, 1558–1595; *Angew. Chem. Int. Ed.* **1998**, 37, 1460–1494; k) A. J. Blake, N. R. Champness, P. Hubberstey, W.-S. Li, M. A. Withersby, M. Schröder, *Coord. Chem. Rev.* **1999**, 183, 117–138; l) K. Kim, *Chem. Soc. Rev.* **2002**, 31, 96–107.

- [6] N. Armaroli, L. De Cola, V. Balzani, J.-P. Sauvage, C. O. Dietrich-Buchecker, J.-M. Kern, A. Bailal, *J. Chem. Soc. Dalton Trans.* **1993**, 3241–3247.
- [7] M. Consuelo Jiménez, C. Dietrich-Buchecker, J.-P. Sauvage, *Angew. Chem.* **2000**, *112*, 3422–3425; *Angew. Chem. Int. Ed.* **2000**, *39*, 3284–3287.
- [8] For a rotaxane which utilizes square-planar metal complexes as the stoppers, see S. J. Loeb, J. A. Wisner, *Chem. Commun.* **1998**, 2757–2758; for a pseudo-rotaxane based on a square-planar metal geometry, see C. Hamann, J.-M. Kern, J.-P. Sauvage, *Dalton Trans.* **2003**, 3770–3775.
- [9] T. Moriuchi, S. Bandoh, M. Miyaishi, T. Hirao, *Eur. J. Inorg. Chem.* **2001**, 651–657.
- [10] a) T. J. Kidd, D. A. Leigh, A. J. Wilson, *J. Am. Chem. Soc.* **1999**, *121*, 1599–1600; b) J. S. Hannam, T. J. Kidd, D. A. Leigh, A. J. Wilson, *Org. Lett.* **2003**, *5*, 1907–1910.
- [11] a) J. E. Kickham, S. J. Loeb, *Inorg. Chem.* **1994**, *33*, 4351–4359; b) G. R. Newkome, T. Kawato, D. K. Kohli, W. E. Puckett, B. D. Olivier, G. Chiari, F. R. Fronczek, W. A. Deutsch, *J. Am. Chem. Soc.* **1981**, *103*, 3423–3429; c) this particular combination of metal coordination and π stacking to control the interaction of tridentate and monodentate ligands is very reminiscent of a series of metalloreceptors for DNA bases [J. E. Kickham, S. J. Loeb, S. L. Murphy, *Chem. Eur. J.* **1997**, *3*, 1203–1213].
- [12] [Pd(L6)]: $C_{12}H_{141.5}N_{8.5}O_6Pd$, $M_r = 1917.33$, yellow block, crystal size $0.47 \times 0.31 \times 0.27$ mm³, triclinic, space group $P\bar{1}$, $a = 15.7840(10)$, $b = 15.9967(10)$, $c = 22.8029(14)$ Å, $\alpha = 84.9850(10)$, $\beta = 71.8430(10)$, $\gamma = 80.5460(10)^\circ$, $V = 5392.5(6)$ Å³, $Z = 2$, $\rho_{\text{calc}} = 1.193$ Mg m⁻³; $MoK\alpha$ radiation (graphite monochromator, $\lambda = 0.71073$ Å), $\mu = 0.231$ mm⁻¹, $T = 150(2)$ K. 34 043 data (15 412 unique, $R_{\text{int}} = 0.0331$, $2.06 < \theta < 23.26^\circ$), were collected on a Bruker SMART CCD diffractometer using narrow frames (0.5° in ω), and were corrected semiempirically for absorption and incident beam decay. Data beyond 0.9 Å were weak and were not used for refinement. The structure was solved by direct methods (SIR92)^[13] and refined by full-matrix least-squares against F^2 .^[14] Phenyl groups were constrained to be rigid hexagons and hydrogen atoms were placed in calculated positions. The whole macrocyclic component, inclusive of the Pd atom, is disordered (50:50) over two positions. The alkyl chain is further disordered and the refinement of this portion of the structure was controlled by application of restraints to both 1,2 and 1,3 distances and use of a common isotropic displacement parameter for all C atoms forming the chain. The only disorder present in the thread is in two of the *tert*-butyl groups. That based on C244 is rotationally disordered (70:30) with the central carbon atom (C244) fully occupied and the two alternative sets of methyl positions related by a 60° rotation about the C244–C243 bond. All atoms in the groups were refined with anisotropic displacement parameters (adps), those of “opposite” C atoms being constrained to be equal. The *tert*-butyl group attached to C263 is disordered (70:30) over two positions and was refined isotropically. Similarity restraints were applied to chemically equivalent 1,2 and 1,3 distances in both disordered *tert*-butyl groups. In the latter stages of refinement there was still significant unassigned electron density associated with diffuse solvent. This density was modeled by using the procedure of van der Sluis and Spek,^[15] comprising 199 electrons per unit cell, and corresponds to approximately 4.5 MeCN solvent molecules per asymmetric unit; values of M_r , $F(000)$, μ etc. have been calculated on this assumption. $wR = \{\sum[w(F_o^2 - F_c^2)]^2 / \sum[w(F_o^2)]^2\}^{1/2} = 0.2527$, conventional $R = 0.0806$ for F values of 15 412 reflections with $F_o^2 > 2\sigma F_o^2$, $S = 1.115$ for 885 parameters. Residual electron density extremes were 1.03 and -0.94 e Å⁻³. CCDC-229418 contains the supplementary crystallographic data for this paper. These data can be obtained free of charge via www.ccdc.cam.ac.uk/conts/retrieving.html (or from the Cambridge Crystallographic Data Centre, 12 Union Road, Cambridge CB21EZ, UK; fax: (+44) 1223-336-033; or deposit@ccdc.cam.ac.uk).
- [13] A. Altomare, G. Casciaro, C. Giacovazzo, A. Guagliardi, *J. Appl. Crystallogr.* **1993**, *26*, 343–350.
- [14] G. M. Sheldrick, University of Göttingen, Germany, **1997**.
- [15] P. van der Sluis, A. L. Spek, *Acta. Crystallogr. Sect. A* **1990**, *46*, 194–201.

Selecting Topology and Connectivity through Metal-Directed Macrocyclization Reactions: A Square Planar Palladium [2]Catenate and Two Noninterlocked Isomers

Anne-Marie L. Fuller,[†] David A. Leigh,^{*,†} Paul J. Lusby,[†]
Alexandra M. Z. Slawin,[‡] and D. Barney Walker[†]

Contribution from the School of Chemistry, University of Edinburgh, The King's Buildings, West Mains Road, Edinburgh EH9 3JJ, United Kingdom, and the School of Chemistry, University of St. Andrews, Purdie Building, St. Andrews, Fife, KY16 9ST, United Kingdom

Received May 8, 2005; E-mail: David.L Leigh@ed.ac.uk

Abstract: We report the synthesis of a [2]catenane using a square planar palladium(II) template, together with two isomers of the interlocked structure: a single tetradentate macrocycle that adopts a "figure of eight" conformation to encapsulate the metal and a complex in which the two macrocycles of the catenane are not interlocked. The three isomers can each be selectively formed depending on how the building blocks are assembled and cyclized. Olefin metathesis of both building blocks while they are attached to the metal gives the single large macrocycle in 77% yield. Cyclizing the monodentate unit prior to attaching both ligands to the metal gives the [2]catenane in 78% yield. Performing the tridentate macrocycle produces a complex in two atropisomeric forms—threaded and nonthreaded—in a 2:3 ratio, which do not interconvert in dichloromethane at room temperature over 7 days. RCM of the nonthreaded atropisomer affords the complex with two noninterlocked macrocyclic ligands; RCM of the threaded atropisomer generates the topologically isomeric [2]catenane. Heating the acyclic atropisomers in acetonitrile provides a mechanism for their interconversion via ligand exchange, allowing the threaded:nonthreaded ratio to be varied from 2:3 to 8:1. All three fully ring-closed complexes were characterized unambiguously by ¹H NMR spectroscopy and X-ray crystallography. As far as we are aware, this is the first time such a set of three formal topological and constitutional isomers has been described.

Introduction

The use of transition metal ions to direct the synthesis of interlocked architectures remains among the most efficient strategies available.^{1–8} In addition to exploiting reversible coordination chemistry to deliver high yields of thermodynamically privileged catenanes incorporating metals in their ring frameworks,² catenanes—metal complexes of interlocked organic macrocyclic ligands—can be formed through metal template macrocyclization reactions. However, while the use of tetrahedral copper(I) geometry to hold bidentate ligands in an orientation suitable for subsequent interlocking macrocyclization reactions has been extensively developed over a 20 year period,^{3–8} the transposition of this basic concept to other coordination modes has been slow to develop. Although Sokolov alluded to the possibility of using octahedral ions to template catenane synthesis as early as 1973,⁹ attempts to prepare interlocked architectures in this way initially met with limited

success,^{2c,10} and it is only recently¹¹ that efficient synthetic routes based on octahedral coordination have been developed. There is also a single example¹² of five-coordinate zinc(II) being used to direct the formation of a [2]catenane and a remarkable crown ether-threaded organometallic catenane templated about a magnesium atom that also forms part of one ring.¹³

At first sight, the use of a template strategy to produce interlocked macrocyclic ligands for metals with a square planar coordination geometry might appear somewhat counter-intuitive. Square planar coordination obviously involves a 2D donor set, while interlocking of the two rings requires two crossing points (one positive, one negative¹⁴) necessitating control over the nature of covalent bond formation in the third dimension. However, by using a tridentate—monodentate ligand combination, the relative orientation of the ligands coordinated to the metal can be varied (formally by rotation about the monodentate ligand—metal bond), and therefore, in principle, systems can be designed to extend above and below the plane of the square planar coordination mode and direct a subsequent ring closure reaction. Indeed, there are several examples^{15,16} of the orthogonal alignment of organic fragments using such a "3 + 1" donor set of ligands, and we recently found that it was possible to exploit this effect to form a mechanically interlocked structure (Scheme 1).¹⁷ Through a combination of electronic and steric factors, the square planar palladium holds the monodentate 2,6-

[†] University of Edinburgh.

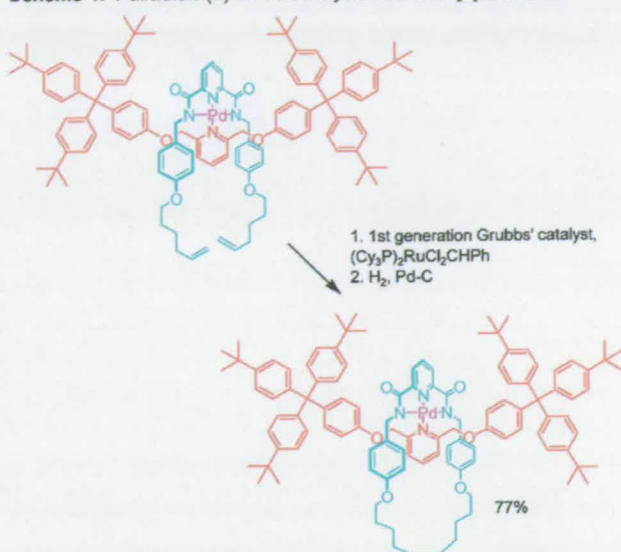
[‡] University of St. Andrews.

(1) For reviews on interlocked molecules assembled about transition metal templates, see: (a) Sauvage, J.-P.; Dietrich-Buchecker, C. *Molecular Catenanes, Rotaxanes and Knots*; Wiley-VCH: Weinheim, Germany, 1999. (b) Hubin, T. J.; Busch, D. H. *Coord. Chem. Rev.* **2000**, *200–202*, 5–52. (c) Collin, J.-P.; Dietrich-Buchecker, C.; Gaviña, P.; Jimenez-Molero, M. C.; Sauvage, J.-P. *Acc. Chem. Res.* **2001**, *34*, 477–487. (d) Menon, S. K.; Guha, T. B.; Agrawal, Y. K. *Rev. Inorg. Chem.* **2004**, *24*, 97–133. (e) Cantrill, S. J.; Chichak, K. S.; Peters, A. J.; Stoddart, J. F. *Acc. Chem. Res.* **2005**, *38*, 1–9.

dimethyleneoxyppyridine thread orthogonal to a bis-olefin-terminated tridentate benzylic amide macrocycle precursor such that cyclization by ring closing olefin metathesis (RCM) results in a [2]rotaxane in 77% yield.

However, extending this strategy to catenane synthesis is not straightforward. Even though oligomer and polymer formation could be minimized by metal chelation of the acyclic building blocks, a double macrocyclization strategy could produce three different isomeric products (1–3, Scheme 2), and even performing one of the rings prior to attaching the building blocks to the metal could still afford either the interlocked (1) or noninterlocked (3) complex. Therefore we explored several potential routes to a square planar coordination [2]catenane, varying the sequence that the rings were cyclized and whether or not the building blocks were attached to the metal prior to

Scheme 1. Palladium(II)-Directed Synthesis of a [2]Rotaxane¹⁷



macrocyclization. Remarkably, it proved possible to find synthetic routes to each of the isomers 1–3 shown in Scheme 2.

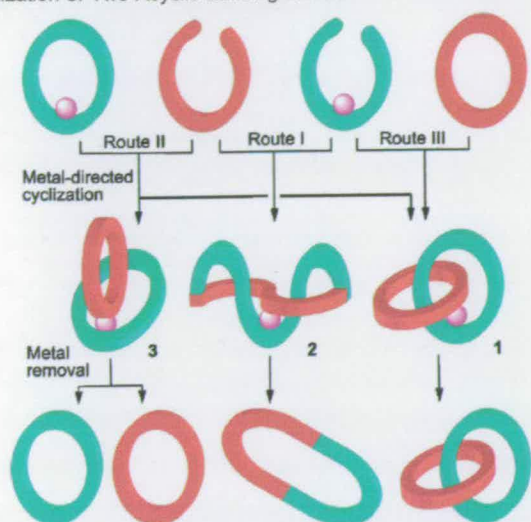
Results and Discussion

Route I: Simultaneous Metal-Directed Olefin Metathesis of L1 and L2. The first route investigated was the possible

- (2) (a) Fujita, M.; Ibukuro, F.; Hagihara, H.; Ogura, K. *Nature* **1994**, *367*, 720–723. (b) Fujita, M.; Ibukuro, F.; Yamaguchi, K.; Ogura, K. *J. Am. Chem. Soc.* **1995**, *117*, 4175–4176. (c) Piguet, C.; Bernardinelli, G.; Williams, A. F.; Bocquet, B. *Angew. Chem., Int. Ed. Engl.* **1995**, *34*, 582–584. (d) Mingos, D. M. P.; Yau, J.; Menzer, S.; Williams, D. *J. Angew. Chem., Int. Ed. Engl.* **1995**, *34*, 1894–1895. (e) Fujita, M.; Ogura, K. *Bull. Chem. Soc. Jpn.* **1996**, *69*, 1471–1482. (f) Fujita, M.; Ogura, K. *Coord. Chem. Rev.* **1996**, *148*, 249–264. (g) Fujita, M.; Ibukuro, F.; Seki, H.; Kamo, O.; Imanari, M.; Ogura, K. *J. Am. Chem. Soc.* **1996**, *118*, 899–900. (h) Cárdenas, D. J.; Sauvage, J.-P. *Inorg. Chem.* **1997**, *36*, 2777–2783. (i) Cárdenas, D. J.; Gaviña, P.; Sauvage, J.-P. *J. Am. Chem. Soc.* **1997**, *119*, 2656–2664. (j) Fujita, M.; Aoyagi, M.; Ibukuro, F.; Ogura, K.; Yamaguchi, K. *J. Am. Chem. Soc.* **1998**, *120*, 611–612. (k) Whang, D.; Park, K.-M.; Heo, J.; Kim, K. *J. Am. Chem. Soc.* **1998**, *120*, 4899–4900. (l) Try, A. C.; Harding, M. M.; Hamilton, D. G.; Sanders, J. K. M. *J. Chem. Soc., Chem. Commun.* **1998**, 723–724. (m) Fujita, M.; Fujita, N.; Ogura, K.; Yamaguchi, K. *Nature* **1999**, *400*, 52–55. (n) Fujita, M. *Acc. Chem. Res.* **1999**, *32*, 53–61. (o) Dietrich-Buchecker, C.; Geum, N.; Hori, A.; Fujita, M.; Sakamoto, S.; Yamaguchi, K.; Sauvage, J.-P. *Chem. Commun.* **2001**, 1182–1183. (p) Padilla-Tosta, M. E.; Fox, O. D.; Drew, M. G. B.; Beer, P. D. *Angew. Chem., Int. Ed.* **2001**, *40*, 4235–4239. (q) Park, K.-M.; Kim, S.-Y.; Heo, J.; Whang, D.; Sakamoto, S.; Yamaguchi, K.; Kim, K. *J. Am. Chem. Soc.* **2002**, *124*, 2140–2147. (r) Kim, K. *Chem. Soc. Rev.* **2002**, *31*, 96–107. (s) McArdle, C. P.; Irwin, M. J.; Jennings, M. C.; Vittal, J. J.; Puddephatt, R. J. *Chem.-Eur. J.* **2002**, *8*, 723–734. (t) McArdle, C. P.; Van, S.; Jennings, M. C.; Puddephatt, R. J. *J. Am. Chem. Soc.* **2002**, *124*, 3959–3965. (u) Dietrich-Buchecker, C.; Colasson, B.; Fujita, M.; Hori, A.; Geum, N.; Sakamoto, S.; Yamaguchi, K.; Sauvage, J.-P. *J. Am. Chem. Soc.* **2003**, *125*, 5717–5725. (v) Hori, A.; Kataoka, H.; Akasaka, A.; Okano, T.; Fujita, M. *J. Polym. Sci. Part A: Polym. Chem.* **2003**, *41*, 3478–3485. (w) Mohr, F.; Eisler, D. J.; McArdle, C. P.; Atieh, K.; Jennings, M. C.; Puddephatt, R. J. *J. Organomet. Chem.* **2003**, *670*, 27–36. (x) Mohr, F.; Jennings, M. C.; Puddephatt, R. J. *Eur. J. Inorg. Chem.* **2003**, 217–223. (y) Colasson, B. X.; Sauvage, J.-P. *Inorg. Chem.* **2004**, *43*, 1895–1901. (z) Hori, A.; Yamashita, K.; Kusukawa, T.; Akasaka, A.; Biradha, K.; Fujita, M. *Chem. Commun.* **2004**, 1798–1799. (aa) Burchell, T. J.; Eisler, D. J.; Puddephatt, R. J. *Dalton Trans.* **2005**, 268–272. (bb) Wong, W. H. H.; Cookson, J.; Evans, E. A. L.; McInnes, E. J. L.; Wolowska, J.; Maher, J. P.; Bishop, P.; Beer, P. D. *Chem. Commun.* **2005**, 2214–2216.
- (3) For catenanes assembled around a tetrahedral four-coordinate Cu(I) template, see: (a) Dietrich-Buchecker, C. O.; Sauvage, J.-P.; Kintzinger, J.-P. *Tetrahedron Lett.* **1983**, *24*, 5095–5098. (b) Dietrich-Buchecker, C. O.; Sauvage, J.-P.; Kern, J.-M. *J. Am. Chem. Soc.* **1984**, *106*, 3043–3045. (c) Cesario, M.; Dietrich-Buchecker, C. O.; Guilhem, J.; Pascard, C.; Sauvage, J.-P. *J. Chem. Soc., Chem. Commun.* **1985**, 244–247. (d) Dietrich-Buchecker, C. O.; Guilhem, J.; Khemiss, A. K.; Kintzinger, J.-P.; Pascard, C.; Sauvage, J.-P. *Angew. Chem., Int. Ed. Engl.* **1987**, *26*, 661–663. (e) Dietrich-Buchecker, C. O.; Edel, A.; Kintzinger, J.-P.; Sauvage, J.-P. *Tetrahedron* **1987**, *43*, 333–344. (f) Jørgensen, T.; Becher, J.; Chambon, J.-C.; Sauvage, J.-P. *Tetrahedron Lett.* **1994**, *35*, 4339–4342. (g) Kern, J.-M.; Sauvage, J.-P.; Weidmann, J.-L. *Tetrahedron* **1996**, *52*, 10921–10934. (h) Kern, J.-M.; Sauvage, J.-P.; Weidmann, J.-L.; Armaroli, N.; Flamigni, L.; Ceroni, P.; Balzani, V. *Inorg. Chem.* **1997**, *36*, 5329–5338. (i) Mohr, B.; Weck, M.; Sauvage, J.-P.; Grubbs, R. H. *Angew. Chem., Int. Ed. Engl.* **1997**, *36*, 1308–1310. (j) Amabilino, D. B.; Sauvage, J.-P. *New J. Chem.* **1998**, *22*, 395–409. (k) Weidmann, J.-L.; Kern, J.-M.; Sauvage, J.-P.; Muscat, D.; Mullins, S.; Köhler, W.; Rosenauer, C.; Räder, H. J.; Martin, K.; Geerts, Y. *Chem.-Eur. J.* **1999**, *5*, 1841–1851. (l) Raehm, L.; Hamann, C.; Kern, J.-M.; Sauvage, J.-P. *Org. Lett.* **2000**, *2*, 1991–1994.
- (4) For chiral [2]catenanes assembled around tetrahedral four-coordinate Cu(I) templates, see: (a) Chambon, J.-C.; Mitchell, D. K.; Sauvage, J.-P. *J. Am. Chem. Soc.* **1992**, *114*, 4625–4631. (b) Kaida, Y.; Okamoto, Y.; Chambon, J.-C.; Mitchell, D. K.; Sauvage, J.-P. *Tetrahedron Lett.* **1993**, *34*, 1019–1022.
- (5) For doubly interlocked [2]catenanes assembled around tetrahedral four-coordinate Cu(I) templates, see: Nierengarten, J.-F.; Dietrich-Buchecker, C. O.; Sauvage, J.-P. *J. Am. Chem. Soc.* **1994**, *116*, 375–376.

- (6) For rotaxanes assembled around a tetrahedral four-coordinate Cu(I) template, see: (a) Wu, C.; Lecavalier, P. R.; Shen, Y. X.; Gibson, H. W. *Chem. Mater.* **1991**, *3*, 569–572. (b) Chambon, J.-C.; Heitz, V.; Sauvage, J.-P. *J. Chem. Soc., Chem. Commun.* **1992**, 1131–1133. (c) Chambon, J.-C.; Heitz, V.; Sauvage, J.-P. *J. Am. Chem. Soc.* **1993**, *115*, 12378–12384. (d) Diederich, F.; Dietrich-Buchecker, C.; Nierengarten, J.-F.; Sauvage, J.-P. *J. Chem. Soc., Chem. Commun.* **1995**, 781–782. (e) Cárdenas, D. J.; Gaviña, P.; Sauvage, J.-P. *Chem. Commun.* **1996**, 1915–1916. (f) Solladié, N.; Chambon, J.-C.; Dietrich-Buchecker, C. O.; Sauvage, J.-P. *Angew. Chem., Int. Ed. Engl.* **1996**, *35*, 906–909. (g) Armaroli, N.; Diederich, F.; Dietrich-Buchecker, C. O.; Flamigni, L.; Marconi, G.; Nierengarten, J.-F.; Sauvage, J.-P. *Chem.-Eur. J.* **1998**, *4*, 406–416. (h) Armaroli, N.; Balzani, V.; Collin, J.-P.; Gaviña, P.; Sauvage, J.-P.; Ventura, B. *J. Am. Chem. Soc.* **1999**, *121*, 4397–4408. (i) Solladié, N.; Chambon, J.-C.; Sauvage, J.-P. *J. Am. Chem. Soc.* **1999**, *121*, 3684–3692. (j) Weber, N.; Hamann, C.; Kern, J.-M.; Sauvage, J.-P. *Inorg. Chem.* **2003**, *42*, 6780–6792. (k) Poleschak, I.; Kern, J.-M.; Sauvage, J.-P. *Chem. Commun.* **2004**, 474–476. (l) Kwan, H. P.; Swager, T. M. *J. Am. Chem. Soc.* **2005**, *127*, 5902–5909.
- (7) For a rotaxane dimer assembled around tetrahedral four-coordinate Cu(I) templates, see: Jiménez, M. C.; Dietrich-Buchecker, C.; Sauvage, J.-P. *Angew. Chem., Int. Ed.* **2000**, *39*, 3284–3287.
- (8) For knots assembled around tetrahedral four-coordinate Cu(I) templates, see: (a) Dietrich-Buchecker, C. O.; Sauvage, J.-P. *Angew. Chem., Int. Ed. Engl.* **1989**, *28*, 189–192. (b) Dietrich-Buchecker, C. O.; Nierengarten, J.-F.; Sauvage, J.-P. *Tetrahedron Lett.* **1992**, *33*, 3625–3628. (c) Dietrich-Buchecker, C. O.; Sauvage, J.-P.; Kintzinger, J.-P.; Maltese, P.; Pascard, C.; Guilhem, J. *New J. Chem.* **1992**, *16*, 931–942. (d) Dietrich-Buchecker, C. O.; Sauvage, J.-P.; De Cian, A.; Fischer, J. *J. Chem. Soc., Chem. Commun.* **1994**, 2231–2232. (e) Perret-Aebi, L.-E.; von Zelewsky, A.; Dietrich-Buchecker, C.; Sauvage, J.-P. *Angew. Chem., Int. Ed.* **2004**, *43*, 4482–4485.
- (9) (a) Sokolov, V. I. *Usp. Khim.* **1973**, *42*, 1037–1059; *Russ. Chem. Rev. (Engl. Transl.)* **1973**, *42*, 452–463. For later discussions on possible strategies to catenanes based on octahedral metal templates, see: (b) Busch, D. H. *J. Inclusion Phenom. Mol. Recognit.* **1992**, *12*, 389–395. (c) Gerbeleu, N. V.; Arion, V. B.; Burgess, J. *Template Synthesis of Macrocyclic Compounds*; Wiley-VCH: Weinheim, Germany 1999; and ref 1b.
- (10) Belfrekh, N.; Dietrich-Buchecker, C.; Sauvage, J.-P. *Inorg. Chem.* **2000**, *39*, 5169–5172.
- (11) (a) Leigh, D. A.; Lusby, P. J.; Teat, S. J.; Wilson, A. J.; Wong, J. K. Y.; *Angew. Chem., Int. Ed.* **2001**, *40*, 1538–1543. (b) Mobian, P.; Kern, J.-M.; Sauvage, J.-P. *J. Am. Chem. Soc.* **2003**, *125*, 2016–2017. (c) Arico, F.; Mobian, P.; Kern, J.-M.; Sauvage, J.-P. *Org. Lett.* **2003**, *5*, 1887–1890. (d) Hogg, L.; Leigh, D. A.; Lusby, P. J.; Morelli, A.; Parsons, S.; Wong, J. K. Y. *Angew. Chem., Int. Ed.* **2004**, *43*, 1218–1221. (e) Mobian, P.; Kern, J.-M.; Sauvage, J.-P. *Angew. Chem., Int. Ed.* **2004**, *43*, 2392–2395. (f) Chambon, J.-C.; Collin, J.-P.; Heitz, V.; Jouvenot, D.; Kern, J.-M.; Mobian, P.; Pomeranc, D.; Sauvage, J.-P. *Eur. J. Org. Chem.* **2004**, 1627–1638.

Scheme 2. Schematic Representation of the Three Isomers that Result from Synchronous or Simultaneous Metal-Directed Cyclization of Two Acyclic Building Blocks^a



^a Homodimerization is avoided by using one tridentate ligand (blue) and one monodentate ligand (orange) and a metal with a preferred square planar coordination geometry. Other possible reaction products could potentially include knots (although knotted isomers of 1–3 are easily precluded by limiting the size of the building blocks) and higher cyclic, catenated and knotted oligomers and polymers resulting from the condensation of more than just one of each building block (minimized by carrying out the cyclization reactions at high dilution).

double macrocyclization of the tridentate (H_2L1) and monodentate ($L2$) building blocks, with both ligands already coordinated to a square planar metal, $L1PdL2$ (Scheme 3, Route I). The monodentate ligand $L2$ was prepared in two steps from 4-hydroxybenzyl alcohol (see Supporting Information) and when combined with the known $L1Pd(CH_3CN)$ complex in dichloromethane, this provided the tetra-terminal olefin complex, $L1PdL2$, in 93% yield (Scheme 3, ii). 1H NMR confirms the exchange of the acetonitrile ligand for $L2$ (Figure 1a,b; note the upfield shift of the aromatic resonances of $L1$ (H_E and H_F) by 0.8 and 0.2 ppm, respectively, due to stacking with the pyridine group of $L2$).

Subjecting $L1PdL2$ to RCM using the first-generation Grubbs' olefin metathesis catalyst,¹⁸ followed by hydrogenation of the resulting internal double bond (Scheme 3, iii), gave a single species in 75% isolated yield for the two steps. FAB mass spectrometry confirmed that the complex had the molecular weight ($m/z = 1110, MH^+$) necessary to be one of the isomers 1–3, and the 1H NMR spectrum (Figure 1c) showed significant

differences to $L1PdL2$, most notably in the region of 2.5–5.5 ppm, indicating that some change in orientation of the building blocks had occurred upon RCM. Treatment of the complex with potassium cyanide (Scheme 3, iv) gave a single organic compound (confirmed by mass spectrometry and 1H NMR), ruling out the possibility that the product of the RCM was the two noninterlocked ring isomer, 3; that is, the product of Route I could not be $L4PdL5$.

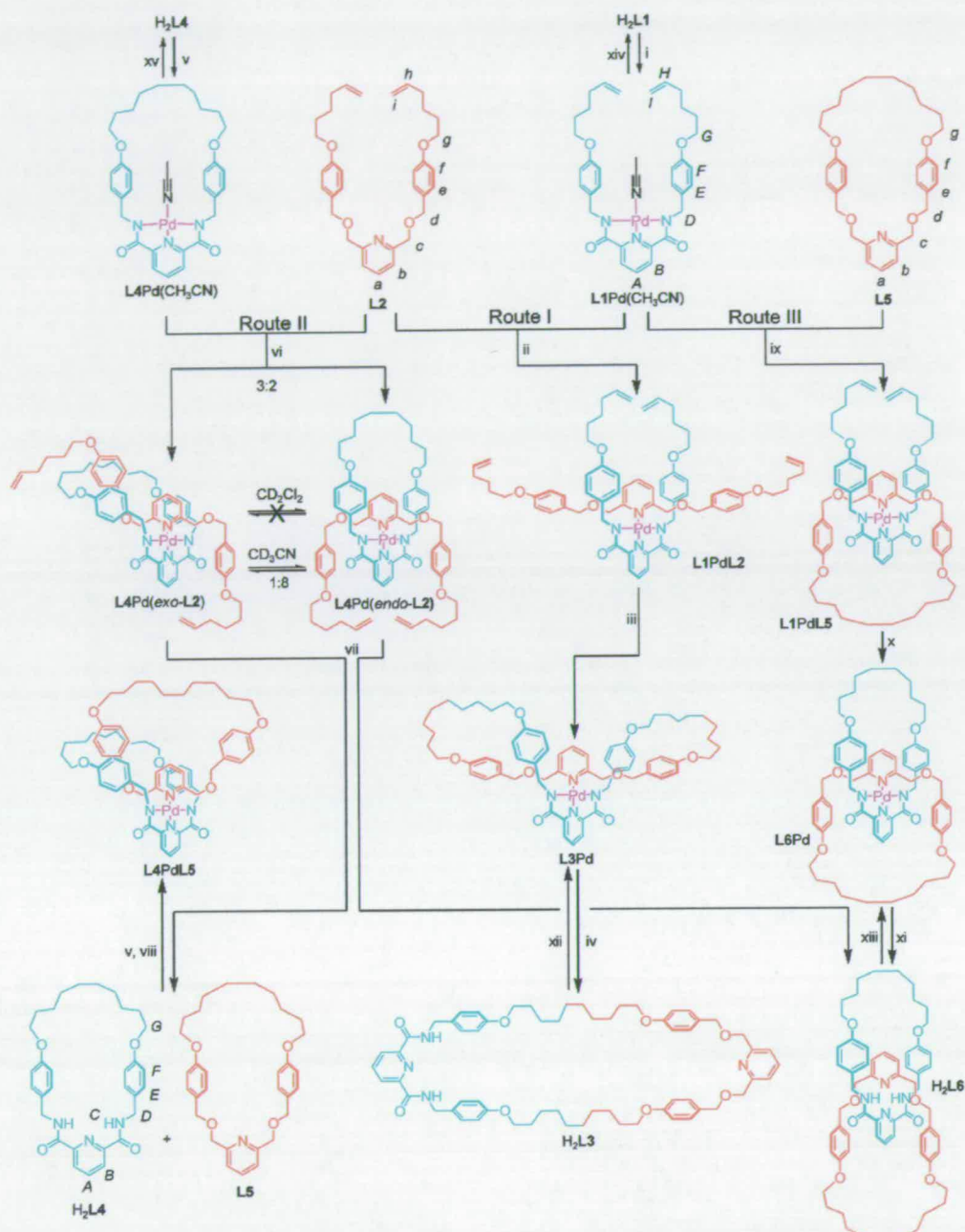
The 1H NMR spectrum (Figure 2c) of the demetalated structure did not show the shielding effects characteristic of benzylic amide macrocycle interlocked systems, the chemical shifts being virtually identical to the independently prepared free ligands, H_2L4 and $L5$ (Figure 2a and d, respectively). This suggested that the ligand isomer formed from Route I was probably H_2L3 , the single large macrocycle (2) resulting from intercomponent metathesis between the $L1$ and $L2$ olefin groups. This assignment was confirmed when single crystals suitable for X-ray crystallography were grown from slow cooling of a hot, saturated acetonitrile solution of the complex formed by Route I. The solid state structure (Figure 3) shows the tetradentate 58-membered single macrocycle satisfying the square planar coordination geometry of the palladium, with the tridentate 2,6-dicarboxamidopyridine moiety held orthogonally to the monodentate 2,6-bis(oxyethylene)pyridine group. This results in twisting of the macrocycle, providing a single crossover point in a distinctive figure-of-eight conformation (Figure 3b). Although rare, this shape is not unique among coordination complexes of large flexible macrocycles, with other examples—based on octahedral metals—reported by the groups of Sauvage (a 58-membered hexadentate bis-terpy macrocycle bound to iron(II))¹⁰ and Busch (a 40-membered ring coordinating to nickel(II) via 2,6-diiminopyridine groups).¹⁹ In all cases, the metal ion provides the crossover point, imposing helical chirality on what would otherwise be intrinsically achiral macrocycles (for $L3Pd$, both enantiomers are observed in the unit cell). Re-examination of the 1H NMR spectrum (Figure 1c) reveals that the ring conformation of $L3Pd$ is conserved from the solid state to solution. The low (C_2) symmetry results in the individual protons of the H_D , H_C , and H_A methylene groups (H_D , $H_{D'}$, H_C , $H_{C'}$, H_A , and $H_{A'}$) being held in diastereotopic environments; the magnitude of the splittings following their proximity to the crossover point (H_D and $H_{D'}$ are split by nearly 2.5 ppm, H_C and $H_{C'}$ by 1.0 ppm, and H_A and $H_{A'}$ by just 0.4 ppm). Interestingly, the aromatic region of $L3Pd$ is virtually identical to that of $L1PdL2$ (Figure 1b), suggesting that while the alkyl residues may be mobile, the rest of the acyclic precursor complex is well-organized for intercomponent olefin metathesis.

Since the attempted simultaneous double macrocyclization strategy had given rise to intercomponent bond formation, we sought to exclude this possibility²⁰ by performing one or the other of the rings prior to the second, metal-directed, cyclization reaction (Scheme 3, Routes II and III).

Route II: Metal-Directed RCM of $L2$. Tridentate macrocycle H_2L4 was prepared in 57% yield by treatment of 2,6-

- (12) Hamann, C.; Kern, J.-M.; Sauvage, J.-P. *Inorg. Chem.* **2003**, *42*, 1877–1883.
 (13) Gruter, G.-J. M.; de Kanter, F. J. J.; Markies, P. R.; Nomoto, T.; Akkerman, O. S.; Bickelhaupt, F. *J. Am. Chem. Soc.* **1993**, *115*, 12179–12180.
 (14) Flapan, E. A Knot Theoretic Approach to Molecular Chirality. In *Molecular Catenanes, Rotaxanes and Knots*; Sauvage, J.-P., Dietrich-Buchecker, C., Eds.; Wiley-VCH: Weinheim, Germany, 1999; pp 7–35.
 (15) (a) Kickham, J. E.; Loeb, S. J. *Inorg. Chem.* **1994**, *33*, 4351–4359. (b) Kickham, J. E.; Loeb, S. J.; Murphy, S. L. *Chem.-Eur. J.* **1997**, *3*, 1203–1213.
 (16) Hamann, C.; Kern, J.-M.; Sauvage, J.-P. *Dalton. Trans.* **2003**, 3770–3775.
 (17) (a) Fuller, A.-M.; Leigh, D. A.; Lusby, P. J.; Oswald, I. D. H.; Parsons, S.; Walker, D. B. *Angew. Chem., Int. Ed.* **2004**, *43*, 3914–3918. (b) Furusho, Y.; Matsuyama, T.; Takata, T.; Moriuchi, T.; Hirao, T. *Tetrahedron Lett.* **2004**, *45*, 9593–9597. (c) Leigh, D. A.; Lusby, P. J.; Slawin, A. M. Z.; Walker, D. B. *Angew. Chem., Int. Ed.* **2005**, *44*, 4557–4564.
 (18) (a) Schwab, P.; France, M. B.; Ziller, J. W.; Grubbs, R. H. *Angew. Chem., Int. Ed. Engl.* **1995**, *34*, 2039–2041. (b) Grubbs, R. H.; Miller, S. J.; Fu, G. C. *Acc. Chem. Res.* **1995**, *28*, 446–452.

- (19) Vance, A. L.; Alcock, N. W.; Busch, D. H.; Heppert, J. A. *Inorg. Chem.* **1997**, *36*, 5132–5134.
 (20) At least as long as the RCM reaction is not under thermodynamic control. However, metathesis of internal olefins is generally much slower than that of terminal olefins. See, for example: Kidd, T. J.; Leigh, D. A.; Wilson, A. J. *J. Am. Chem. Soc.* **1999**, *121*, 1599–1600.

Scheme 3^a

^a Reagents and conditions: (i) Pd(OAc)₂, CH₃CN, 1 h, 76%; (ii) CH₂Cl₂, 1 h, 93%; (iii) a. first-generation Grubbs' catalyst (Cy₃P)₂Cl₂RuCHPh, 0.2 equiv, CH₂Cl₂, 20 h; b. H₂, Pd-C, THF, 4 h, 75% (over two steps); (iv) KCN, MeOH, CH₂Cl₂, 20 °C, 1 h and then 40 °C, 0.5 h, 94%; (v) Pd(OAc)₂, CH₃CN, 1 h, 93%; (vi) CH₂Cl₂, 1 h, a 3:2 ratio of L4Pd(exo-L2):L4Pd(endo-L2), isolated in 89% yield; (vii) a. first-generation Grubbs' catalyst (0.1 equiv), CH₂Cl₂, 22 h; b. H₂ (50 bar), Pd EnCat, THF, 18 h; c. KCN, MeOH, CH₂Cl₂, 20 °C, 1 h and then 40 °C, 0.5 h, H₂L4, L5, and H₂L6 (25% over three steps); (viii) part (v) and then CH₂Cl₂, 1 h, 78%; (ix) CH₂Cl₂, 1 h, 69%; (x) a. first-generation Grubbs' catalyst (0.1 equiv), CH₂Cl₂, 22 h; b. H₂, Pd-C, THF, 4 h, 78% (over two steps); (xi) KCN, MeOH, CH₂Cl₂, 20 °C, 1 h and then 40 °C, 0.5 h, 97%; (xii) Pd(OAc)₂, CH₃CN, 60 °C, 4 h, 85%; (xiii) Pd(OAc)₂, CH₃CN, 60 °C, 4 h, 79%; (xiv) KCN, MeOH, CH₂Cl₂, 20 °C, 1 h and then 40 °C, 0.5 h, 98%; (xv) KCN, MeOH, CH₂Cl₂, 20 °C, 1 h and then 40 °C, 0.5 h, 95%.

pyridinedicarbonyl dichloride with the appropriate diamine under high dilution conditions (see Supporting Information). Subsequent complexation with palladium(II) acetate afforded L4Pd(CH₃CN) (93%, Scheme 3, v). Threading of L2 through the cavity of L4Pd(CH₃CN) via the substitution of the coordinated acetonitrile was attempted by simple mixing of the two in dichloromethane at room temperature (Scheme 3, vi). While

mass spectrometry confirmed the ligand exchange, the ¹H NMR spectrum of the crude product was unexpectedly complex. Closer inspection of the thin layer chromatograph of the reaction mixture revealed two products with very similar R_f values in a ratio of approximately 2:3. Despite their proximity, these proved amenable to separation by preparative thin-layer chromatography on silica gel-coated plates (CH₂Cl₂:MeOH, 98.5:1.5 as eluent).

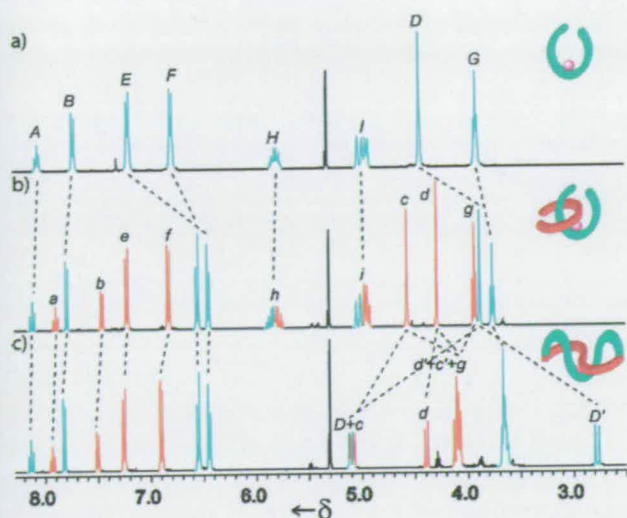


Figure 1. ^1H NMR spectra (400 MHz, 19:1 CD_2Cl_2 : CD_3CN , 298 K) of (a) $\text{L1Pd}(\text{CH}_3\text{CN})$, (b) L1PdL2 , and (c) L3Pd . The lettering refers to the assignments shown in Scheme 3.

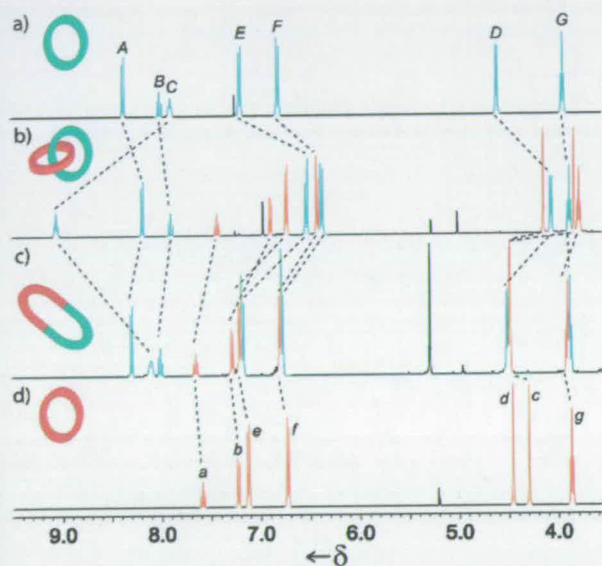


Figure 2. ^1H NMR spectra (400 MHz, CDCl_3 , 298 K) of (a) $\text{H}_2\text{L4}$, (b) $\text{H}_2\text{L6}$, (c) $\text{H}_2\text{L3}$, and (d) L5 . The lettering refers to the assignments shown in Scheme 3.

The isolated complexes gave indistinguishable fragmentation patterns by electrospray ionization mass spectrometry, the molecular mass ion suggesting they were both isomers of L4PdL2 . However, the ^1H NMR spectra exhibited important differences between the two products. When compared to the spectra of the starting materials, the minor isomer (lower R_f , Figure 4d) showed significant shielding of the L4 benzyl rings (H_E and H_F), indicative of aromatic stacking with the pyridine group of L2 . In contrast, the major isomer (higher R_f , Figure 4b) showed no evidence of stacking interactions but a greater degree of complexity in both the L2 signals (two sets of nonequivalent H_b , H_c , H_d , H_e , and H_f resonances) and the H_D methylene groups (an AB system with a 2.5 ppm separation between the two proton environments) of L4 . From this, we tentatively assigned the two products as “threaded” (minor

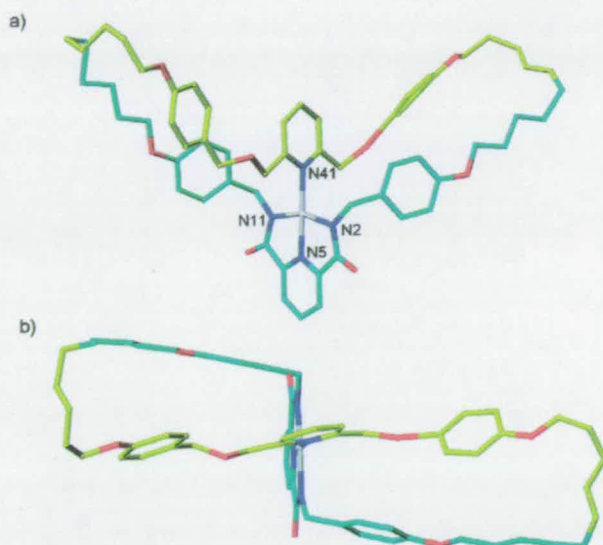


Figure 3. X-ray crystal structure of “figure-of-eight” complex L3Pd grown by slow cooling of a warm, saturated solution of the complex in acetonitrile. (a) Side-on and (b) top views. Carbon atoms originating from L1 are shown in light blue, those from L2 in yellow. Oxygen atoms are red, nitrogen dark blue, palladium gray. Selected bond lengths [\AA]: Pd–N2 2.015, Pd–N5 1.941, Pd–N11 2.027, Pd–N41 2.052; tridentate fragment bite angle [$^\circ$]: N2–Pd–N11 161.0.

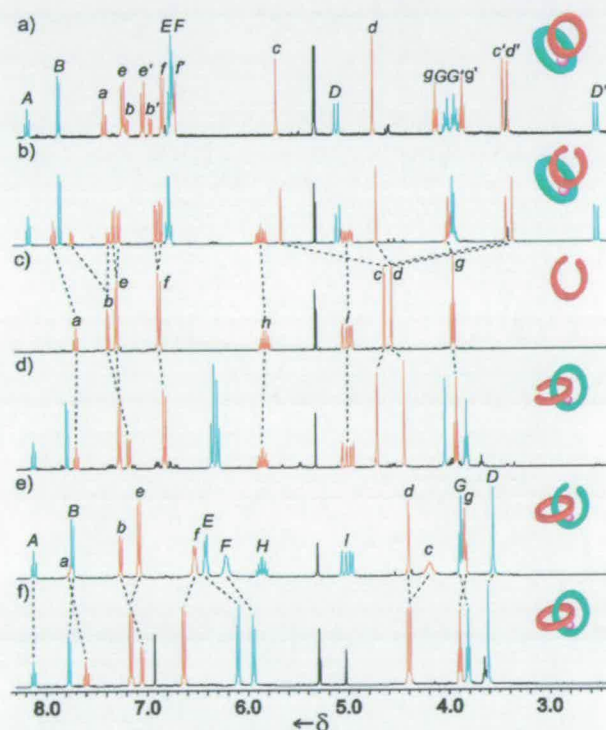


Figure 4. ^1H NMR spectra (400 MHz, CD_2Cl_2 , 298 K) of (a) L4PdL5 , (b) $\text{L4Pd}(\text{exo-L2})$, (c) L2 , (d) $\text{L4Pd}(\text{endo-L2})$, (e) L1PdL5 , and (f) L6Pd . The lettering refers to the assignments shown in Scheme 3.

isomer) and “threaded” (minor isomer) atropisomers,²¹ $\text{L4Pd}(\text{exo-L2})$ and $\text{L4Pd}(\text{endo-L2})$, respectively (Scheme 3).

Intriguingly, CPK models suggested that cyclization of L2 could occur with *each* atropisomer of L4PdL2 , suggesting that two compounds of identical connectivity but different conformations²² are predisposed to form topological isomeric products

upon RCM—the [2]catenate, **1**, and the analogous noninterlocked double macrocycle structure, **3**. Sure enough, treatment of the 2:3 mixture of atropisomers with Grubbs' catalyst in CH_2Cl_2 , followed by hydrogenation and demetalation (Scheme 3, vii (three steps—the mixtures of topological and olefin isomers preventing the isolation of pure products until the end of the reaction sequence)), afforded three products: macrocycles $\text{H}_2\text{L4}$ and L5 arising from complex **3**, and a further compound, which mass spectrometry confirmed to be a different isomer of $\text{H}_2\text{L3}$, in 25% overall yield for the three steps.²³

^1H NMR spectroscopy of the new compound in CDCl_3 (Figure 2b) revealed shielding of most resonances compared to the free macrocycles $\text{H}_2\text{L4}$ (Figure 2a) and L5 (Figure 2d) characteristic of interdigitation, suggesting that it was indeed the [2]catenand $\text{H}_2\text{L6}$. The exception to the upfield trend in shifts was the amide protons (H_c), which were shifted significantly downfield (ca. 1.3 ppm) in the catenand compared to those of $\text{H}_2\text{L4}$, indicative of a significant hydrogen-bonding interaction between the amide protons of one ring and the pyridine nitrogen of the other. In contrast, the analogous amide protons in the 58-membered free macrocycle $\text{H}_2\text{L3}$ occur at 8.11 ppm in CDCl_3 (Figure 2c), only slightly downfield of their position in $\text{H}_2\text{L4}$ (7.88 ppm, Figure 2a), meaning that little intramolecular hydrogen bonding is occurring in the large flexible macrocycle. Why is this internal hydrogen bonding absent when it is so clearly present in the mechanically bonded isomer $\text{H}_2\text{L6}$? First, the size and nature of the solvent-exposed surfaces of the compact [2]catenand structure and the large, relatively open, macrocycle must be very different, making desolvation of the amide and pyridine residues in the catenane a significantly less energetically costly process. Second, with the 2,6-bis(oxymethylene)pyridine and 2,6-pyridinecarboxamide groups on different components, the macrocycles in $\text{H}_2\text{L6}$ can orientate themselves for inter-residue hydrogen bonding with little more than the loss of a single rotational degree of freedom. In contrast, alignment of the groups to enable a similar interaction within $\text{H}_2\text{L3}$ would significantly restrict the number of conformations accessible by the alkyl chains in the large flexible ring, the resulting losses in degrees of freedom raising the energy of the hydrogen-bonded structure. This unusual orthogonal double bifurcated bis-pyridine hydrogen-bonding interaction is also observed in the related [2]rotaxane system.¹⁷

Reintroduction of Pd(II) into the free ligand systems ($\text{H}_2\text{L3} \rightarrow \text{L3Pd}$, Scheme 3, xii; $\text{H}_2\text{L6} \rightarrow \text{L6Pd}$, Scheme 3, xiii; $\text{H}_2\text{L4} \rightarrow \text{L4Pd}(\text{CH}_3\text{CN}) + \text{L5} \rightarrow \text{L4PdL5}$, Scheme 3, v, viii) proceeded smoothly in each case, the last two providing pure samples of complexes formed previously as intermediates during each pathway of the Route II syntheses. ESI mass spectrometry initially identified the formation of L4PdL5 , confirming that both macrocycles could simultaneously bind to palladium without being interlocked. ^1H NMR spectroscopy (Figure 4a)

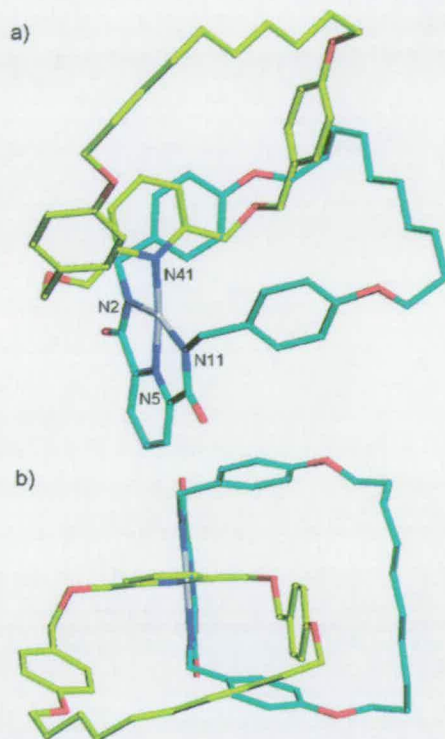


Figure 5. X-ray crystal structure of noninterlocked double macrocycle complex L4PdL5 grown from a saturated solution of the complex in acetone. (a) Side-on and (b) top views. Carbon atoms of the L4 macrocycle are shown in light blue, and those of the L5 macrocycle in yellow; oxygen atoms are red, nitrogen dark blue, and palladium gray. Selected bond lengths [\AA]: N2-Pd 2.032, N5-Pd 1.943, N11-Pd 2.032, N41-Pd 2.077; tridentate fragment bite angle [$^\circ$]: N2-Pd-N11 160.8.

corroborated this result and showed significant similarity (a diastereotopic environment for H_d , and two sets of signals for each H_b , H_c , H_d , H_e , H_f , and H_g) to the presumed nonthreaded isomer of L4PdL2 (Figure 4b). These spectral features are consistent with orthogonal binding of the rings to the square planar geometry metal, with neither macrocycle being able to pass through the cavity of the other nor rotate (at least not rapidly on the NMR time scale in the case of the monodentate ligand) about the plane of the square planar coordination geometry. This means both macrocycles are performed desymmetrized in the plane that they coordinate to the metal, that is, top from bottom in L4 and left from right in L5 (as L4PdL5 is depicted in Figure 5a).

Pleasingly, the pure samples of L4PdL5 and L6Pd both provided single crystals suitable for structure elucidation by X-ray crystallography (Figure 5 and Figure 6, respectively). Between them, the X-ray crystal structures of L3Pd , L4PdL5 , and L6Pd confirm not only the identity of the metal complexes—a unique set of topological (L4PdL2 and L6Pd) and constitutional (L3Pd and L4PdL5/L6Pd) isomers—but also the structural assignments of the free ligands inferred by the earlier ^1H NMR and mass spectrometry analysis.

Atropisomer-Specific Synthesis of Different Topological Isomers. Although RCM (and subsequent hydrogenation and demetalation) of the mixture of the two L4PdL2 atropisomers gives a ratio of isolated interlocked to noninterlocked products similar to the starting atropisomer ratio, it does not necessarily follow that one atropisomer leads solely to one product. The

(21) The term "atropisomerism" technically refers to conformers which can be isolated as separate chemical species as a result of restricted rotation about a single bond [IUPAC Compendium of Chemical Terminology 2nd ed.; 1997]. We stretch this definition slightly in applying it to $\text{L4Pd}(\text{endo-L2})$ and $\text{L4Pd}(\text{exo-L2})$, which are isolable as a result of restricted rotation about various single bonds in particular ligand orientations.

(22) The term "co-conformation" is generally used to refer to the relative positions of mechanically interlocked components with respect to each other [Fyfe, M. C. T.; Glink, P. T.; Menzer, S.; Stoddart, J. F.; White, A. J. P.; Williams, D. J. *Angew. Chem., Int. Ed. Engl.* 1997, 36, 2068–2070]. However, since the two components in $\text{L4Pd}(\text{endo-L2})$ and $\text{L4Pd}(\text{exo-L2})$ are connected by a continuous sequence of covalent and coordination bonds, in this case "conformation" is a sufficient descriptor.

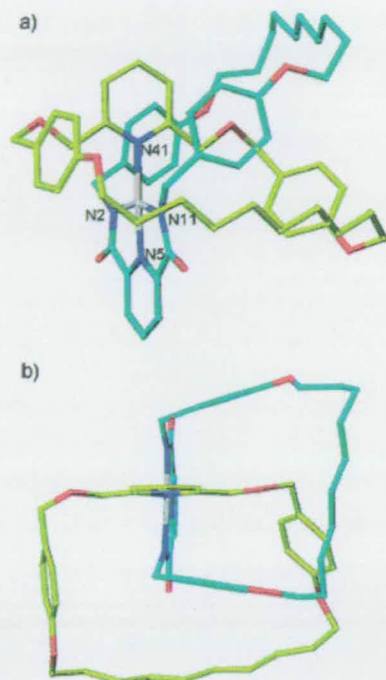


Figure 6. X-ray crystal structure of palladium[2]catenate **L6Pd** grown by slow cooling of a warm, saturated solution of the complex in acetonitrile. (a) Side-on and (b) top views. Carbon atoms of the **L4** macrocycle are shown in light blue, and those of the **L5** macrocycle in yellow; oxygen atoms are red, nitrogen dark blue, and palladium gray. Selected bond lengths [Å]: Pd–N2 1.934, Pd–N5 2.041, Pd–N11 2.036, Pd–N41 2.079; tridentate fragment bite angle [°]: N2–Pd–N11 160.2.

interconversion of the two **L4PdL2** atropisomers in solution was investigated by ^1H NMR spectroscopy. The initial threaded:nonthreaded ratio of ca. 2:3 remained unchanged over 7 days in CD_2Cl_2 at room temperature. Similarly, spectra of pure samples of each of the compounds were invariant under these conditions, demonstrating that the atropisomers are kinetically stable at room temperature in a noncoordinating solvent. However, addition of $\sim 10\%$ CD_3CN to either of the pure atropisomer solutions or the 2:3 mixture led to a gradual change in the threaded:nonthreaded ratio, increasing to ca. 7:3 after 4 days. This suggests that the threaded isomer is thermodynamically favored, and that atropisomer interconversion can take place via the dissociation of **L2** from either form of **L4PdL2**, the vacant coordination site being temporarily filled by a molecule of CD_3CN . Accordingly, the reaction between **L2** and **L4Pd**(CH_3CN) was repeated in refluxing acetonitrile. After several hours, ^1H NMR spectroscopy showed a 7:3 ratio of the threaded:nonthreaded forms of **L4PdL2**. Heating over 2 days increased the ratio to 8:1, after which no further change occurred.

RCM of single atropisomer samples of **L4PdL2** in CH_2Cl_2 did, indeed, generate a single new species in each case. The product of RCM of the presumed **L4Pd**(*endo*-**L2**) complex was hydrogenated to give solely the [2]catenate, **L6Pd**; the product of RCM of presumed **L4Pd**(*exo*-**L2**) proved unstable to hydrogenation,²³ so the metal was removed instead (KCN, MeOH, CH_2Cl_2 , 20 °C, 1 h and then 40 °C, 0.5 h), liberating two different macrocycles, $\text{H}_2\text{L4}$ (96%) and the unsaturated olefin analogue of **L5** (93%).

Route III: Metal-Directed RCM of L1. Finally, we investigated the product distribution arising from performing the monodentate macrocycle and applying metal-directed cyclization of the tridentate ligand (Scheme 3, Route III).²⁴ **L1Pd**(CH_3CN) and **L5** were stirred together in dichloromethane at room temperature (Scheme 3, ix) and, in contrast to the analogous step in Route II, reacted to give a single product rather than a mixture of atropisomers. The ^1H NMR spectrum of **L1PdL5** (Figure 4e) suggests the two ligands are threaded; the upfield shift of H_E and H_F compared to similar protons in the nonthreaded **L4PdL5** and **L4Pd**(*exo*-**L2**) complexes (Figure 4a and b, respectively), indicating π -stacking of the benzyl groups of **L1** with the pyridine unit of **L5**. It is difficult to distinguish between whether **L1PdL5** can exist as threaded/nonthreaded atropisomers but is formed solely as the (*exo*-**L1**)**PdL5** isomer, or rather threaded and nonthreaded forms of **L1PdL5** are in equilibrium with the threaded conformation being thermodynamically preferred by several kcal mol⁻¹. In any event, RCM of **L1PdL5** and subsequent hydrogenation (Scheme 3, x) afforded exclusively the [2]catenate, **L6Pd**, in 78% yield, making this route both synthetically efficient and completely selective for the mechanically interlocked topological isomer.

Conclusions

A [2]catenate and the isomeric single macrocycle and double macrocycle metal complexes can each be efficiently assembled about a palladium(II) template via RCM. The order in which the tridentate and monodentate ligand cyclization reactions and coordination steps are performed determines the outcome of the synthetic pathway, providing selective routes to each of the three topological and constitutional isomers. In one case, performing the tridentate macrocycle followed by its coordination along with the acyclic monodentate ligand to the Pd produces threaded and nonthreaded atropisomers. These can be isolated and, while the individual forms are stable in dichloromethane, they can be interconverted in a coordinating solvent through ligand exchange. Each atropisomer was shown to be a true intermediate to a different topological product, meaning that, in this reaction, the choice of solvent can determine whether the [2]catenate is formed or its noninterlocked isomer. It is remarkable to see how topology and connectivity can be selected so exquisitely—in three different forms—using just one set of organic building blocks and a metal atom with a two-dimensional coordination geometry.

Experimental Section

Selected Spectroscopic Data for the Set of Three Constitutional and Topological Isomers. **L3Pd**: ^1H NMR (400 MHz, CD_2Cl_2 , 298 K): δ = 1.09–1.84 (m, 32H, alkyl-H), 2.70 (d, 2H, J = 14.4 Hz, H_D), 3.64 (m, 4H, H_C), 4.00–4.13 (m, 8H, H_E + H_F + H_G), 4.39 (d, 2H, J = 10.6 Hz, H_D), 5.04–5.14 (m, 4H, H_C + H_D), 6.38 (d, 4H, J = 8.6 Hz, H_E), 6.49 (d, 4H, J = 8.6 Hz, H_F), 6.84 (d, 4H, J = 8.6 Hz,

- (23) The hydrogenation conditions employed in Routes I and III led to a complex mixture when applied to the products of metathesis in Route II. Not only was significant decomplexation of the somewhat strained noninterlocked double macrocycle complex observed but also the resulting free monodentate ligand, **L5**, was degraded, presumably by hydrogenolysis of the benzyl ether moieties. Although the use of Pd EnCat did not prevent the ligand decomplexation during the hydrogenation step, it significantly reduced the degradation of the free monodentate macrocycle [Bremeyer, N.; Ley, S. V.; Ramarao, C.; Shirley, I. M.; Smith, S. C. *Synlett* **2002**, 1843–1844].
- (24) Leigh, D. A.; Lusby, P. J.; Slawin, A. M. Z.; Walker, D. B. Submitted for publication.

H_f), 7.20 (d, 4H, $J = 8.6$ Hz, H_e), 7.45 (d, 2H, $J = 7.8$ Hz, H_b), 7.76 (d, 2H, $J = 7.8$ Hz, H_b), 7.88 (t, 1H, $J = 7.8$ Hz, H_a), 8.08 (t, 1H, $J = 7.8$ Hz, H_a). ¹³C NMR (100 MHz, CD₂Cl₂, 293 K): $\delta = 23.7, 25.2, 25.5, 27.5, 27.5, 27.5, 28.6, 29.5, 48.5, 67.1, 68.1, 71.8, 73.2, 114.0, 114.8, 121.2, 124.8, 128.5, 128.7, 129.5, 132.8, 139.1, 140.7, 152.8, 158.1, 158.6, 160.6, 171.1$. HRMS (FAB, NOBA): Calcd for C₆₂H₇₅N₄O₈-Pd [M + H]⁺ 1109.46169. Found 1109.46275. L4PdL5: ¹H NMR (400 MHz, CD₂Cl₂, 298 K): $\delta = 0.81-1.74$ (m, 32H, alkyl-H), 2.50 (d, 2H, $J = 14.8$ Hz, H_D), 3.34-3.44 (m, 4H, H_d + H_e), 3.78-4.02 (m, 6H, H_e + H_f + H_g), 4.09 (t, 2H, $J = 6.3$ Hz, H_e), 4.72 (s, 2H, H_d), 5.08 (d, 2H, $J = 14.8$ Hz, H_D), 5.67 (s, 2H, H_e), 6.64-6.84 (m, 12H, H_f + H_f + H_e + H_g), 6.92 (d, 1H, $J = 7.8$ Hz, H_e), 6.99 (d, 2H, $J = 8.6$ Hz, H_e), 7.12-7.22 (m, 3H, H_b + H_e), 7.38 (t, 1H, $J = 7.8$ Hz, H_a), 7.83 (d, 2H, $J = 7.8$ Hz, H_b), 8.13 (t, 1H, $J = 7.8$ Hz, H_a). ¹³C NMR (100 MHz, CD₂Cl₂, 298 K): $\delta = 25.6, 25.9, 25.9, 28.5, 29.0, 29.1, 29.3, 29.4, 29.4, 29.6, 29.8, 29.9, 49.2, 67.8, 67.9, 68.3, 72.1, 72.8, 73.4, 76.3, 114.8, 114.9, 115.4, 122.0, 122.7, 125.1, 128.3, 129.9, 130.3, 130.5, 131.4, 133.0, 138.4, 141.3, 153.0, 158.2, 158.7, 159.6, 160.6, 161.9, 171.6$. LRMS (ESI) $m/z = 1132$ [M + Na]⁺. L6Pd: ¹H NMR (400 MHz, CD₂Cl₂, 293 K): $\delta = 1.04-1.50$ (m, 24H, alkyl-H), 1.60 (m, 4H, alkyl-H), 1.70 (m, 4H, alkyl-H), 3.60 (s, 4H, H_D), 3.81

(t, 4H, $J = 6.3$ Hz, H_g), 3.89 (t, 4H, $J = 6.3$ Hz, H_g), 4.36-4.42 (m, 8H, H_d + H_e), 5.94 (d, 4H, $J = 8.6$ Hz, H_f), 6.10 (d, 4H, $J = 8.6$ Hz, H_e), 6.63 (d, 4H, $J = 8.6$ Hz, H_g), 7.05 (d, 2H, $J = 7.8$ Hz, H_b), 7.15 (d, 4H, $J = 8.6$ Hz, H_e), 7.60 (t, 1H, $J = 7.8$ Hz, H_a), 7.76 (d, 2H, $J = 7.6$ Hz, H_b), 8.13 (t, 1H, $J = 7.6$ Hz, H_a). ¹³C NMR (100 MHz, CD₂Cl₂, 293 K): $\delta = 25.8, 26.0, 28.5, 28.7, 28.9, 29.2, 30.0, 30.1, 49.4, 67.1, 67.7, 69.6, 72.9, 114.5, 114.8, 121.2, 124.5, 128.2, 128.6, 131.7, 132.9, 138.8, 140.6, 153.1, 157.4, 159.5, 160.0, 171.1$. HRMS (FAB, NOBA): Calcd for C₆₂H₇₅N₄O₈ Pd [M + H]⁺ 1109.46169. Found 1109.46152.

Acknowledgment. This work was supported by the European Union Future and Emerging Technology program, *MechMol*, and the EPSRC.

Supporting Information Available: Experimental procedures and spectroscopic data for all new compounds, and thermal ellipsoids for the crystal structures of L3Pd, L4PdL5, and L6Pd. This material is available free of charge via the Internet at <http://pubs.acs.org>.

JA053005A

Supramolecular Chemistry

Rare and Diverse Binding Modes Introduced through Mechanical Bonding**

David A. Leigh,* Paul J. Lusby,
Alexandra M. Z. Slawin, and D. Barney Walker

Interest in catenanes and rotaxanes has largely focused on the stimuli-induced change in the position of their components for possible exploitation in molecular devices,^[1] but other properties and features of these architectures are becoming apparent.^[2] Here, we report a previously unrecognized consequence of kinetic stabilization of an otherwise unfavorable association of molecular fragments through mechanical bonding (Figure 1). The raised energy of the interlocked components—brought about by the enforced high local concentration of convergent functional groups, the limitation in the number of conformations and co-conformations that each component can adopt, and the poor solvation of their inner surfaces—facilitates (kinetically and thermodynamically) the formation of internal and external binding motifs that are either not observed or much weaker when the same groups are not confined in this way. The effect is illustrated through a remarkable series of binding modes (including orthogonal bifurcated pyridine–pyridine hydrogen bonding,

[*] Prof. D. A. Leigh, Dr. P. J. Lusby, D. B. Walker
School of Chemistry
University of Edinburgh
The King's Buildings
West Mains Road, Edinburgh EH9 3JJ (UK)
Fax: (+44) 131-667-9085
E-mail: david.leigh@ed.ac.uk

Prof. A. M. Z. Slawin
School of Chemistry
University of St. Andrews
Purdie Building, St. Andrews, Fife KY16 9ST (UK)

[**] We thank Anne-Marie Fuller for the synthesis of H₂4. This work was supported by the European Union Future and Emerging Technology Program MechMol and by the EPSRC.



Supporting information for this article is available on the WWW under <http://www.angewandte.org> or from the author.

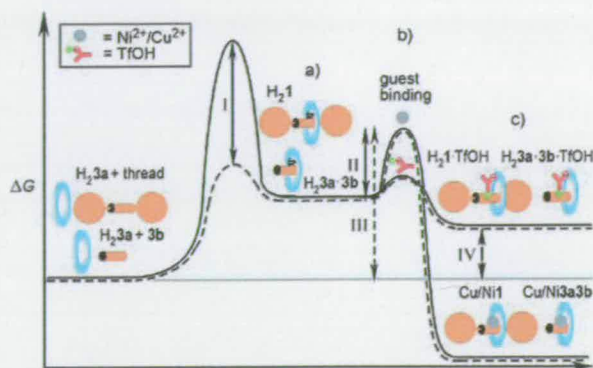


Figure 1. Effects of kinetic stabilization of an otherwise unfavorable association of molecular fragments through mechanical bonding. a) The kinetic stabilization (I) of a mechanically interlocked architecture that features only weakly attractive interactions between the macrocycle and thread permits noncovalent interactions to be observed (as in H_2 1) which are too weak to stabilize the corresponding host-guest complex (H_2 3a-3b). b) For a rotaxane that is not thermodynamically stable with respect to its free components, the activation energy for tertiary component complex formation is lower than for the analogous noninterlocked system (barrier II is less than III). This arises because the entropic cost of bringing the two components of the rotaxane together has already been paid, some degrees of freedom of the components are already restricted in the mechanically interlocked architecture, and the desolvation of the internal rotaxane surfaces is less energetically demanding than those of the free components. c) The higher energy of such a rotaxane means that a host-guest complex which involves the rotaxane can be favorable (e.g. H_2 1·TfOH) even when the equivalent trimolecular complex (H_2 3a-3b·TfOH) is not (IV). It also ensures that metal complexes derived from such rotaxanes, such as Cu1 and Ni1, are inherently thermodynamically more stable than the analogous complexes derived from noninterlocked fragments and, in principle, kinetically easier to form. The association/dissociation pathways are shown by black solid (interlocked components) and dashed (noninterlocked components) lines; the horizontal gray line corresponds to the free energy of the nonassociated individual components.

cooperative binding to a sulfonic acid guest through deprotonation by one component and anion-amide hydrogen bonding by the other, enforced square-pyramidal coordination of Cu^{II} and Ni^{II} , and second-sphere coordination in a square-planar $Pd^{II}Cl$ complex) exhibited in solution and the solid state by a [2]rotaxane and an analogous [2]catenane, but not seen with either threadable (but nonmechanically interlocked) versions of the components or flexible covalently bonded systems (Figure 2).

Most catenanes and rotaxanes are synthesized by utilizing templates to thermodynamically favor interlocking,^[1a] but subsequent removal of the template can leave a molecule that is energetically unstable with respect to the noninter-

locked components and is only held intact by virtue of the mechanical bond. We recently described^[3] the assembly of a mechanically interlocked architecture about a Pd^{II} template to give a square-planar [2]rotaxane-metal coordination complex, Pd1.^[4] We were intrigued to find that upon protic demetalation of the complex to give H_2 1, the 1H NMR spectrum in $CDCl_3$ indicated significant intercomponent hydrogen bonding between the amide groups of the macrocycle and the pyridine nitrogen atom of the rotaxane thread (the protons of the amide groups in the macrocycle appear 1.7 ppm downfield relative to the corresponding protons in the free macrocycle). Such a binding motif, which requires essentially orthogonal pyridine rings with the nitrogen atoms bridged by bifurcated hydrogen bonds, is extremely rare (a search of the Cambridge Crystallographic Database reveals only one other example^[5]) but is somewhat reminiscent of the hydrogen bonding that occurs at 90° to the plane of the lone pairs of amide groups in threads seen extensively in other hydrogen-bonded rotaxanes.^[6] Slow cooling of a hot, saturated solution of H_2 1 in acetonitrile/chloroform (10:1) yielded single crystals that were of sufficient quality to confirm the interaction in the solid state by X-ray crystallography (Figure 3a,b) but were inadequate to confidently characterize the interaction in detail.^[7] However, when we prepared a [2]catenane that incorporated the same functional groups, H_2 2, a similar noncovalent interaction was observed in solution in $CDCl_3$ and, in this case, single crystals of excellent quality were obtained by slow cooling of a hot, saturated solution of H_2 2 in acetonitrile. The solid-state structure of H_2 2 (Figure 3c) closely mirrors the hydrogen-bonding motif seen in the crystal structure of H_2 1, with unsymmetrical intercomponent hydrogen-bond distances (2.28 and 3.10 Å in H_2 2; 2.3 and 2.8 Å in H_2 1) and the angle between the planes of the

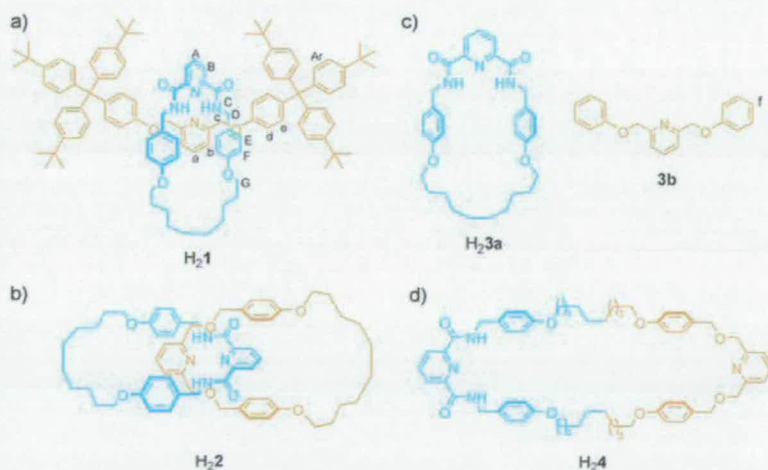


Figure 2. Different ways of linking a 2,6-dialkylpyridine unit with a 2,6-dicarboxamidepyridine unit which lead to significantly different noncovalent binding properties: a) on different components within a [2]rotaxane architecture, H_2 1; b) on different components within a [2]catenane architecture, H_2 2; c) on separate threadable, but not mechanically interlocked, molecular components H_2 3a and 3b; and d) on a flexible but wholly covalently bonded system, H_2 4. For 1H NMR spectroscopic assignments (see Figure 4), hydrogen atoms have been labeled A-G and a-f/Ar for the macrocycle and thread, respectively.

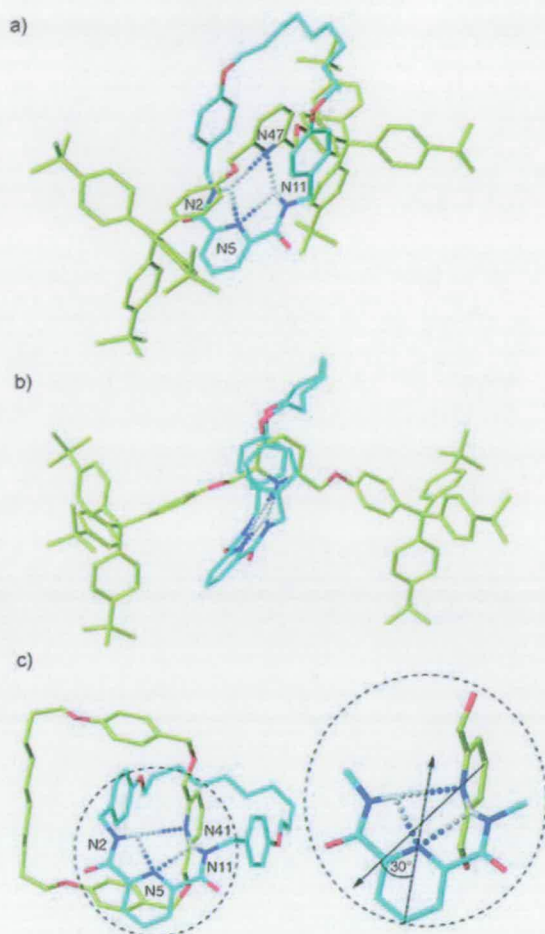


Figure 3. X-ray crystal structures^[7] of [2]rotaxane **H₂1** and [2]catenane **H₂2**: a) **H₂1** (twisted view); b) **H₂1** (side view which shows the macrocycle circumscribing the pyridine residue of the thread; disorder in the alkyl chain region and solvent molecules, not the central hydrogen-bonding region, results in a high overall *R* factor of 33 %); c) **H₂2** (*R* factor < 5%; the intercomponent hydrogen-bond motif mirrors that shown in (a) and (b)). Inset: the lone pairs of the pyridine nitrogen atoms do not point directly at each other, but are tilted 30.0° apart. C (macrocycle) turquoise; C (thread) yellow; O red; N dark blue; H white. For clarity only nitrogen-bound hydrogen atoms are shown. Selected bond lengths [Å] for **H₂1**: N2H–N5 2.4; N11H–N5 2.6; N2H–N47 2.8; N11H–N47 2.3. Selected bond angles [°] for **H₂1**: N2H–N5 151; N11H–N5 153; N2H–N47 96; N11H–N47 108. Selected bond lengths [Å] for **H₂2**: N2H–N5 2.18; N11H–N5 2.33; N2H–N41 2.28; N11H–N41 3.10. Selected bond angles [°] for **H₂2**: N2H–N5 107.1; N11H–N5 102.2; N2H–N41 146.5; N11H–N41 129.0.

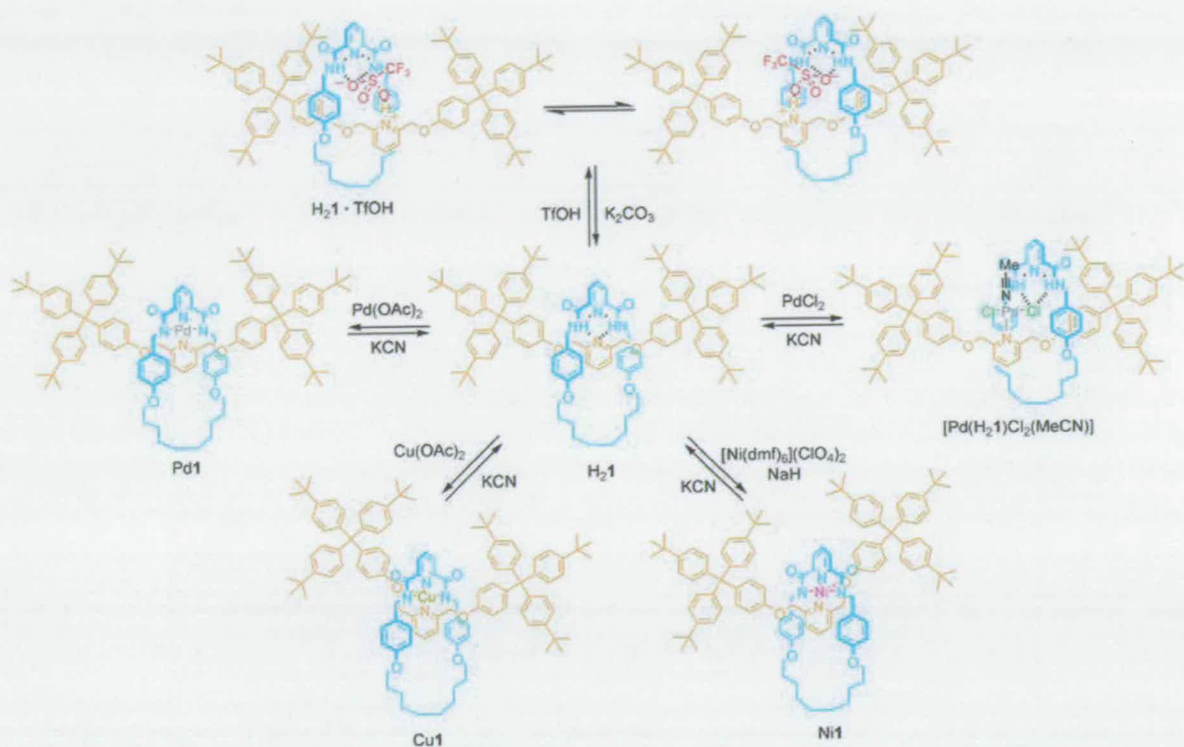
pyridine rings nearly orthogonal (90.7° in **H₂2**; 82° in **H₂1**) but tilted (30.0° in **H₂2** (Figure 3c, inset); 34° in **H₂1**) away from linearity to avoid too close an interaction between the lone pairs on the pyridine nitrogen atoms.

To investigate this atypical binding motif further, we titrated an unstoppered analogue of the thread, **3b**, with the free macrocycle, **H₂3a**, and monitored the titration by ¹H NMR spectroscopy (CDCl₃) to determine the energetics

of the interaction in the absence of the kinetic barrier to dissociation provided by the mechanical bond. However, there was virtually no shift in the amide protons of **H₂3a** in the presence of up to 20 equivalents of **3b** (4–80 mM) which indicates that the bimolecular association constant must be less than 5 M⁻¹—the approximate limit of this detection method with the large shifts typically observed through hydrogen-bonding amide groups. Interestingly, the ¹H NMR spectrum of the wholly covalently linked analogue **H₂4** in CDCl₃ also gave no indication of hydrogen-bonding interactions between the pyridine-2,6-carboxamide protons and the second pyridine residue, even though this very large macrocycle is certainly flexible enough to adopt such a geometry without steric hindrance.

Rare hydrogen-bond motifs have previously been observed within rotaxane architectures (e.g. amide NH to ester acyl oxygen atoms,^[8,9] and amide NH to ester alkyl oxygen atoms^[9]). The propensity for such unusual interactions in mechanically bonded structures presumably arises for a number of reasons: 1) the enforced high local concentration of functional groups for which there is a low steric cost to relative movement within the vector of the thread; 2) the limited number of conformations and co-conformations that each component can adopt that do not put functional groups into convergent orientations; 3) the imposed orthogonalization of components which can preclude normally preferred noncovalent bonding geometries; 4) freezing out of a single co-conformation for an intercomponent binding event only costs a reduction of two degrees of freedom (translation and rotation of the macrocycle about the thread) in contrast to the multiple degrees of rotational freedom of the alkyl chains that would be lost by internal hydrogen bonding in **H₂4**; 5) the inefficient solvation of internal or congested surfaces of an interpenetrated architecture means that desolvation of binding sites is likely to occur at a lower energetic cost than for conventional structures. All of these factors effectively do the same thing, that is, raise the energy of the rotaxane with respect to the free components. However, the kinetic stabilization of the architecture provided by the stoppers prevents dethreading (the rotaxane is not in equilibrium with the free components). This increase in free energy is actually a form of host preorganization, which serves to enhance binding properties as outlined by Cram over 30 years ago.^[10] The result is that interactions which are not strong enough to stabilize a host–guest complex can become thermodynamically favorable if the components are held together by a mechanical bond (Figure 1).

We reasoned that it should be possible to disrupt the intercomponent hydrogen-bonding interaction in **H₂1** by protonation of the more basic 2,6-dioxymethylenepyridine nitrogen atom (Scheme 1). Although treatment of **H₂1** with one equivalent of trifluoromethanesulfonic acid (TfOH) resulted in protonation of the desired site (Figure 4d), the downfield shift of the H_C amide protons indicated that strong hydrogen bonding was still present. The shielding and broadening of particular thread signals at 298 K (Figure 4d) suggests that instead of residing over the pyridine residue as in **H₂1**, the macrocycle is displaced to the side and shuttles between the two halves of the thread relatively slowly on the



Scheme 1. Binding modes observed for [2]rotaxane $\text{H}_2\cdot\text{1}$. All of the complexation reactions are fully reversible. A similar range of complexes are exhibited by [2]catenane $\text{H}_2\cdot\text{2}$ (for an X-ray crystal structure of Pd2, see ref. [12]). The hydrogen bonding in $[\text{Pd}(\text{H}_2\cdot\text{1})\text{Cl}_2(\text{MeCN})]$ is observed only in the solid state. Tf = trifluoromethanesulfonyl, DMF = *N,N*-dimethylformamide.

NMR timescale. This was confirmed by the ^1H NMR spectrum recorded at 238 K (Figure 4e) in which many of the thread resonances were split into two inequivalent sets (H_b/H_c , H_d/H_e , H_f/H_g , H_h/H_i) that correspond to solvent-exposed and encapsulated (and thus magnetically shielded by the macrocycle) protons, respectively. The rationale for this behavior was provided by the crystal structure of single crystals grown from acetonitrile (Figure 5a). The [2]rotaxane acts as a host for an entire molecule of TfOH; one component (the thread) deprotonates the acid, and both components hydrogen bond to the resulting anion to generate a neutral complex, $\text{H}_2\cdot\text{1}\cdot\text{HOTf}$. The X-ray crystal structure is consistent with the specific shielding effects seen in the ^1H NMR spectra, including the upfield shift of the signal for the pyridinium proton (see Figure 4c) as a consequence of other hydrogen-bond donors binding to the triflate anion, and with the noncovalent binding of the sulfonic acid acting as a transient steric barrier to shuttling of the macrocycle between the two halves of the thread.^[12] In contrast (Scheme 2), a 1:1 mixture of $\text{H}_2\cdot\text{3a}$ and $\text{3bH}^+\text{TfO}^-$ in CDCl_3 shows neither upfield shift of resonances H_c , H_d , and H_e (compare Figure 4b with the spectrum of the protonated thread in Figure 4c) nor downfield shifts of the protons from the amide groups in $\text{H}_2\cdot\text{3a}$. Similarly, the absence of shifts in the amide resonances of the protonated covalently linked structure $\text{H}_2\cdot\text{4}\cdot\text{H}^+\text{TfO}^-$ suggests that it does not internally associate through hydrogen bonding.

The mechanically interlocked assemblies also differ from their noninterlocked counterparts in their ability to adopt a range of overall neutral binding modes with metals. Treatment of $\text{H}_2\cdot\text{1}$ or $\text{H}_2\cdot\text{2}$ with $\text{Cu}(\text{OAc})_2$ in $\text{MeOH}/\text{CH}_2\text{Cl}_2$ with heating at reflux resulted in double deprotonation of the ligand and the generation of the corresponding 1:1 neutral metal-interlocked ligand complex. Recrystallization of the copper [2]rotaxane complex, Cu1, from acetonitrile gave single crystals that were suitable for X-ray crystallographic studies (Figure 5b). The solid-state structure shows a square-based pyramidal coordination motif that involves one of the thread oxygen atoms as well as the four nitrogen atoms of the rotaxane which form the near-planar base of the pyramid (N47 lies approximately 10° above the plane defined by N2-N11-N5-Cu). Treatment of $\text{H}_2\cdot\text{3a}/\text{3b}$ or $\text{H}_2\cdot\text{4}$ with $\text{Cu}(\text{OAc})_2$ under the same conditions gave no indication of formation of a complex nor deprotonation of the amide groups of the macrocycle.

The synthesis of complexes of the mechanically interlocked ligands with nickel required more vigorous conditions ($[\text{Ni}(\text{dmf})_6](\text{ClO}_4)_2$, NaH, DMF, 60°C , 1 h) but nonetheless resulted in Ni1 and Ni2, both isolated as orange crystalline compounds. In this case, a similarly colored complex could also be generated with $\text{H}_2\cdot\text{3a}/\text{3b}$, but unlike Ni1 or Ni2 the isolated compound rapidly decomposed and we were unable to isolate or characterize it. The X-ray crystal structure of single crystals of Ni1 grown from slow cooling of a saturated

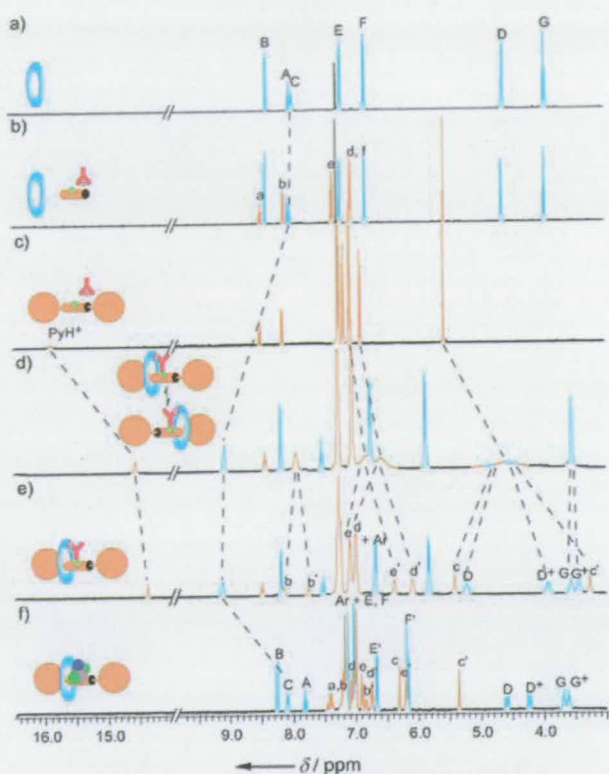


Figure 4. ^1H NMR spectra (CDCl_3 , 400 MHz, 298 K unless otherwise stated): a) macrocycle $\text{H}_2\mathbf{3a}$; b) $\text{H}_2\mathbf{3a}$ and unstoppered thread $\mathbf{3b}$ and HOTf; c) thread and HOTf (Py=pyridine); d) [2]rotaxane complex $\text{H}_2\mathbf{1}$ -HOTf showing fast exchange (shuttling) of the macrocycle between equivalent sites on both halves of the thread; e) [2]rotaxane complex $\text{H}_2\mathbf{1}$ -HOTf at 238 K showing slow exchange (reversible noncovalent bonding of the triflate anion provides a transient steric barrier to shuttling); f) $[\text{Pd}(\text{H}_2\mathbf{1})\text{Cl}_2(\text{MeCN})]$ showing slow exchange (coordination of $[\text{PdCl}_2(\text{MeCN})]$ provides a fixed steric barrier to shuttling up to at least 325 K). See Figure 2 for atom labeling scheme.

solution in acetonitrile is shown in Figure 5c and is closely related to the structure obtained for $\text{Cu}\mathbf{1}$. Treatment of any of the rotaxane or catenane metal complexes with KCN in $\text{CH}_2\text{Cl}_2/\text{MeOH}$ regenerated the original interlocked molecule, $\text{H}_2\mathbf{1}$ or $\text{H}_2\mathbf{2}$. The differences in both the ease of formation and the stability of the metal complexes with the catenane and rotaxane relative to the noninterlocked ligands is, again,

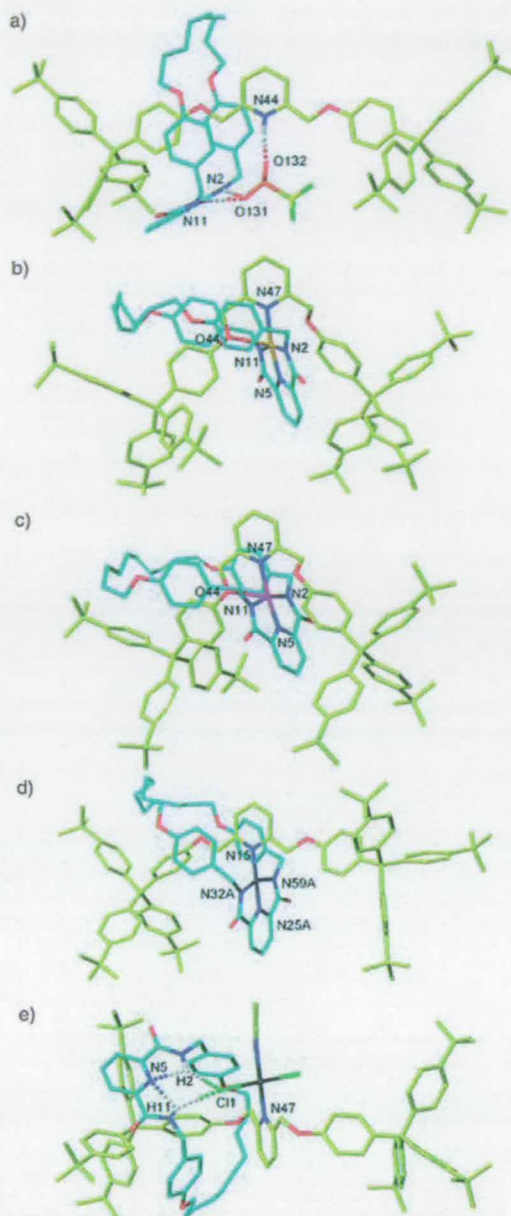
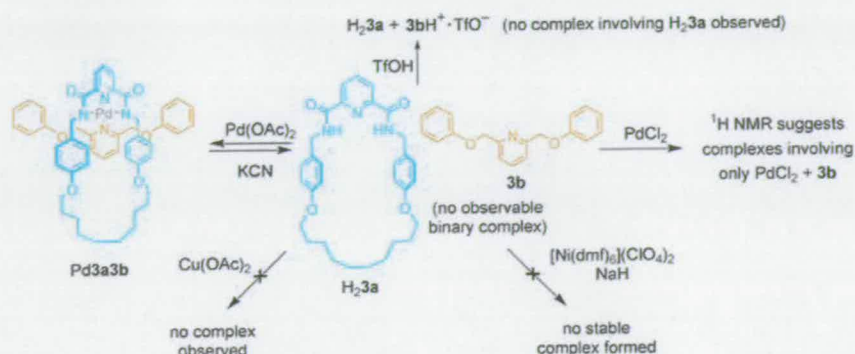


Figure 5. X-ray crystal structures^[7] of various complexes of $\mathbf{1}$: a) neutral [2]rotaxane-triflic acid complex, $\text{H}_2\mathbf{1}$ -HOTf. Note the macrocycle is displaced to one side of the central region of the thread relative to free $\text{H}_2\mathbf{1}$ (Figure 3b); b) square-pyramidal coordination complex $\text{Cu}\mathbf{1}$; c) square-pyramidal coordination complex $\text{Ni}\mathbf{1}$; d) square-planar coordination complex $\text{Pd}\mathbf{1}$; e) square-planar coordination complex $[\text{Pd}(\text{H}_2\mathbf{1})\text{Cl}_2(\text{MeCN})]$. C (macrocycle) turquoise; C (thread) yellow; O red; N dark blue; H white; S orange; F light green; Cl dark green; Cu tan; Ni pink; Pd dark gray. For clarity only amide hydrogen atoms are shown. Selected hydrogen-bond lengths [Å] for $\text{H}_2\mathbf{1}$ -HOTf: N2H–O131 2.14; N11H–O131 2.17; N44H–O132 1.72. Selected bond angles [°] for $\text{H}_2\mathbf{1}$ -HOTf: N2H–O131 159.0; N11H–O131 148.1; N44H–O132 159.7. Selected bond lengths [Å] for $\text{Cu}\mathbf{1}$: N2–Cu 2.00; N11–Cu 1.98; N5–Cu 1.92; N47–Cu 2.02; O44–Cu 2.41. Selected bond angles [°] for $\text{Cu}\mathbf{1}$: N2–Cu–N5 80.3; N5–Cu–N11 80.7; N11–Cu–N47 101.3; N5–Cu–O44 116.6; N5–Cu–N47 169.7. Selected bond lengths [Å] for $\text{Ni}\mathbf{1}$: N2–Ni 1.94; N11–Ni 1.93; N5–Ni 1.81; N47–Ni 1.93; O44–Cu 2.52. Selected bond angles [°] for $\text{Ni}\mathbf{1}$: N2–Ni–N5 82.6; N5–Ni–N11 82.4; N11–Ni–N47 98.5; N5–Ni–O44 113.8; N5–Ni–N47 172.1. Selected bond lengths [Å] for $\text{Pd}\mathbf{1}$: Pd–N15 1.95, Pd–N25 1.86, Pd–N32 2.04, Pd–N59 2.02, N15–N25 3.81. Selected bond angles [°] for $\text{Pd}\mathbf{1}$: N59–Pd–N32 160.0. Selected bond lengths [Å] for $[\text{Pd}(\text{H}_2\mathbf{1})\text{Cl}_2(\text{MeCN})]$: Pd–N47 1.98, Pd–Cl1 2.27, Cl1–H2 2.67, Cl1–H11 2.64, N5–H2 2.36, N5–H11 2.15. Selected bond angles [°] for $[\text{Pd}(\text{H}_2\mathbf{1})\text{Cl}_2(\text{MeCN})]$: N2–H2–Cl1 139.8, N11–H11–N5 114.1, N11–H11–Cl1 125.0.



Scheme 2. Attempted complexation experiments involving $\text{H}_2\mathbf{3a}/\mathbf{3b}$. Similar results were obtained with macrocycle $\text{H}_2\mathbf{4}$ (for an X-ray crystal structure of $\text{Pd}\mathbf{4}$, see ref. [12]).

consistent with the intrinsic effect of kinetic stabilization of a mechanically interlocked architecture (Figure 1c).

Each of the four ligand sets reacts with $\text{Pd}(\text{OAc})_2$ ($\text{H}_2\mathbf{1}$, $\text{H}_2\mathbf{2}$, and $\text{H}_2\mathbf{4}$ directly in $\text{MeCN}/\text{CH}_2\text{Cl}_2$; $\text{H}_2\mathbf{3a}/\mathbf{3b}$ requires preliminary reaction of $\text{Pd}(\text{OAc})_2$ with $\text{H}_2\mathbf{3a}$ in MeCN followed by treatment of the resulting complex with $\mathbf{3b}$ in CH_2Cl_2) to give the corresponding square-planar coordination complexes (Schemes 1 and 2 and Figure 5d). However, the rotaxane and catenane also formed a different type of neutral square-planar coordination complex when treated with PdCl_2 , an initial palladium salt that features significantly stronger coordinating ligands (chloride is also less basic than acetate). Slow cooling of saturated solutions of either complex in acetonitrile afforded crystals that were suitable for X-ray crystallography, and the structure of the rotaxane complex, $[\text{Pd}(\text{H}_2\mathbf{1})\text{Cl}_2(\text{MeCN})]$, is shown in Figure 5e (the solid-state structure of the [2]catenane complex is similar but features intermolecular rather than intramolecular $\text{NH}\cdots\text{Cl}\cdots\text{Pd}$ hydrogen bonding). From the crystal structures it can be seen that although Pd coordinates to the thread as in $\text{Pd}\mathbf{1}$, the original metal chloride ligands remain intact and the macrocycle amides are not deprotonated. In solution the coordination of the $[\text{PdCl}_2(\text{MeCN})]$ unit to the pyridine ring of the thread acts as a steric barrier to shuttling (Figure 4f). This is similar to the effect seen with $\text{H}_2\mathbf{1}\cdot\text{TiOH}$, but unlike the complex held together by hydrogen bonds the coordination to the metal is not kinetically labile and persists as a barrier to shuttling up to at least 325 K (close to the boiling point of the solvent CDCl_3).^[11]

The solid-state structure of $[\text{Pd}(\text{H}_2\mathbf{1})\text{Cl}_2(\text{MeCN})]$ features hydrogen bonding between the amide groups of the macrocycle and the chloride ligands of the metal (Figure 5e). However, the $^1\text{H NMR}$ spectrum shows that this interaction is not present to any significant extent in CDCl_3 (the chemical shift of H_C is virtually unchanged compared to $\text{H}_2\mathbf{3a}$, Figure 4f). Wisner and co-workers recently used a similar interaction to direct an elegant synthesis of a pseudorotaxane.^[13] During the course of that work, a macrocycle binding constant that largely results from two sets of isophthalamide

groups hydrogen bonding to the chloride ligands of a Pd^{II} complex was determined to be $5 \times 10^3 \text{ M}^{-1}$ in CDCl_3 .^[13] In contrast, Crabtree and co-workers determined the association constant for a single isophthalamide group with Cl^- to be $6 \times 10^4 \text{ M}^{-1}$ in CD_2Cl_2 .^[14] Accordingly, a $\text{C}(\text{O})\text{NH}\cdots\text{Cl}\cdots\text{Pd}$ interaction must be somewhat less than half the strength of a $\text{C}(\text{O})\text{NH}\cdots\text{Cl}^-$ hydrogen bond. This is consistent with the observation that the interaction is too weak to significantly bind the macrocycle in $[\text{Pd}(\text{H}_2\mathbf{1})\text{Cl}_2(\text{MeCN})]$ in CDCl_3 , despite the high effective molarity introduced by the mechanical bond, and is in marked contrast to the effective bifurcated pyridine–pyridine hydrogen bonding in $\text{H}_2\mathbf{1}$. This suggests that the intercomponent binding mode in $\text{H}_2\mathbf{1}$ is not particularly weak and its scarcity as an observed interaction may arise because the geometry of the interlocked architecture precludes otherwise preferred noncovalent bonding geometries.

In conclusion, the kinetically enforced association of molecular fragments within an interlocked architecture facilitates the formation of diverse, and sometimes rare and unusual, binding motifs both in solution and the solid state. These interactions can produce interesting effects in their own right; the cooperative hydrogen bonding of an organic guest by both components of a [2]rotaxane can present an effective barrier to shuttling at low temperatures, whereas a stronger metal–ligand coordination mode can be used to restrict the same motion even at higher temperatures. The fact that many of the observed modes of binding are weaker or not seen at all when the components are not mechanically interlocked makes this consequence of the mechanical bond particularly noteworthy.^[15]

Received: January 1, 2005
 Revised: February 18, 2005
 Published online: June 23, 2005

Keywords: catenanes · coordination modes · hydrogen bonds · noncovalent interactions · rotaxanes

- [1] For reviews, see: a) *Molecular Catenanes, Rotaxanes, and Knots: A Journey Through the World of Molecular Topology* (Eds.: J.-P. Sauvage, C. Dietrich-Buchecker), Wiley-VCH, Weinheim, 1999; b) V. Balzani, A. Credi, F. M. Raymo, J. F. Stoddart, *Angew. Chem.* **2000**, *112*, 3484–3530; *Angew. Chem. Int. Ed.* **2000**, *39*, 3348–3391; c) V. Balzani, M. Venturi, A. Credi, *Molecular Devices and Machines—A Journey into the Nanoworld*, Wiley-VCH, Weinheim, 2003; d) A. H. Flood, R. J. A. Ramirez, W.-Q. Deng, R. P. Muller, W. A. Goddard, J. F. Stoddart, *Aust. J. Chem.* **2004**, *57*, 301–322; e) “Synthetic Molecular Machines”: E. R. Kay, D. A. Leigh in *Functional Artificial Receptors* (Eds.: T. Schrader, A. D. Hamilton), Wiley-VCH, Weinheim, 2005, 333–406.
- [2] For examples in which encapsulation and/or preorganization of the coordinating ligand geometry in a mechanically interlocked architecture can bring about significant property effects, see: (stabilization of oxidation state/complex geometry) a) C. O. Dietrich-Buchecker, J.-P. Sauvage, *J. Am. Chem. Soc.* **1984**, *106*, 3043–3045; b) N. Armadori, L. De Cola, V. Balzani, J.-P. Sauvage, C. O. Dietrich-Buchecker, J.-M. Kern, A. Bailal, *J. Chem. Soc. Dalton Trans.* **1993**, 3241–3247; (protection of functional groups) c) D. Leigh, A. Murphy, J. P. Smart, A. M. Z. Slawin, *Angew. Chem.* **1997**, *109*, 752–756; *Angew. Chem. Int. Ed. Engl.* **1997**, *36*, 728–731; d) M. R. Craig, M. G. Hutchings, T. D. W. Claridge, H. L. Anderson, *Angew. Chem.* **2001**, *113*, 1105–1108; *Angew. Chem. Int. Ed.* **2001**, *40*, 1071–1074; e) J. E. H. Buston, F. Marken, H. L. Anderson, *Chem. Commun.* **2001**, 1046–1047; f) T. Oku, Y. Furusho, T. Takata, *Org. Lett.* **2003**, *5*, 4923–4925; g) D. A. Leigh, E. M. Pérez, *Chem. Commun.* **2004**, 2262–2263; (solubility) h) H. W. Gibson, S. Liu, P. Lecavalier, C. Wu, Y. X. Shen, *J. Am. Chem. Soc.* **1995**, *117*, 852–874; i) A. G. Johnston, D. A. Leigh, A. Murphy, J. P. Smart, M. D. Deegan, *J. Am. Chem. Soc.* **1996**, *118*, 10662–10663; j) S. Anderson, H. L. Anderson, *Angew. Chem.* **1996**, *108*, 2075–2078; *Angew. Chem. Int. Ed. Engl.* **1996**, *35*, 1956–1959; (conformation of a component) k) W. Clegg, C. Gimenez-Saiz, D. A. Leigh, A. Murphy, A. M. Z. Slawin, S. J. Teat, *J. Am. Chem. Soc.* **1999**, *121*, 4124–4129; (electroluminescence) l) F. Cacialli, J. S. Wilson, J. J. Michels, C. Daniel, C. Silva, R. H. Friend, N. Severin, P. Samori, J. P. Rabe, M. J. O’Connell, P. N. Taylor, H. L. Anderson, *Nat. Mater.* **2002**, *1*, 160–164; (membrane transport) m) V. Dvornikovs, B. E. House, M. Kaetzl, J. R. Dedman, D. B. Smithrud, *J. Am. Chem. Soc.* **2003**, *125*, 8290–8301.
- [3] A.-M. Fuller, D. A. Leigh, P. J. Lusby, I. D. H. Oswald, S. Parsons, D. B. Walker, *Angew. Chem.* **2004**, *116*, 4004–4008; *Angew. Chem. Int. Ed.* **2004**, *43*, 3914–3918.
- [4] For a recent example of a [2]rotaxane that utilizes square-planar Pd^{II} coordination, see: I. Yoon, M. Narita, T. Shimizu, M. Asakawa, *J. Am. Chem. Soc.* **2004**, *126*, 16740–16741.
- [5] S. L. Jain, P. Bhattacharyya, H. L. Milton, A. M. Z. Slawin, J. A. Crayston, J. D. Woollins, *Dalton Trans.* **2004**, 862–871.
- [6] F. Biscarini, M. Cavallini, D. A. Leigh, S. León, S. J. Teat, J. K. Y. Wong, F. Zerbetto, *J. Am. Chem. Soc.* **2002**, *124*, 225–233.
- [7] Structural data for H₂I, CuI, and NiI were collected at 93 K using a Rigaku Saturn diffractometer (MM007 high-flux RA/MoK α radiation, confocal optic); for H₂2 and [Pd(H₂I)Cl₂(MeCN)] at 93 K using a Rigaku Mercury diffractometer (MM007 high-flux RA/MoK α radiation, confocal optic); and for H₂1-TfOH at 125 K using a Bruker SMART diffractometer (sealed tube MoK α radiation, graphite monochromator, λ = 0.71073 Å). All data collections employed narrow frames (0.3–1.0°) to obtain at least a full hemisphere of data. Intensities were corrected for Lorentz polarization and absorption effects (multiple equivalent reflections). Structures were solved by direct methods, non-hydrogen atoms were refined anisotropically with CH protons being refined in riding geometries (SHELXTL) against F². In most cases, amide protons were refined isotropically subject to a distant constraint. Any other restraints or additional features of the refinement are detailed for each structure below. The structure determination for H₂1 proved particularly problematic; we collected full datasets using a variety of collection routines on more than 15 different crystals from several different crystallization experiments. The data were always poor, principally because of disorder arising from the alkyl chain and solvated molecules. The structure was refined isotropically with no protons included in the refinement. H₂1: C₁₁₂H₁₃₀N₄O₆, M_r = 1628, crystal size = 0.2 × 0.1 × 0.03 mm³, orthorhombic, *Pbca*, *a* = 18.338(4), *b* = 23.545(5), *c* = 44.922(9) Å, *V* = 19396(7) Å³, *Z* = 8, ρ_{calcd} = 1.115 Mg m⁻³; μ = 0.068 mm⁻¹, 18573 data (17303 unique), *R* = 0.3339 for *F* values of reflections with *F*_o > 4 σ (*F*_o), *S* = 4.90 for 463 parameters. Residual electron density extremes were 1.665 and -4.557 eÅ⁻³. H₂2: C₆₂H₇₆N₄O₆, M_r = 1005.27, colorless prism, crystal size = 0.2 × 0.2 × 0.2 mm³, triclinic, *P*-1, *a* = 11.3539(11), *b* = 12.0635(11), *c* = 20.445(2) Å, α = 82.323(6), β = 88.351(7), γ = 80.397(7)°, *V* = 2736.2(5) Å³, *Z* = 2, ρ_{calcd} = 1.220 Mg m⁻³; μ = 0.080 mm⁻¹, 15494 data (8824 unique, *R*_{int} = 0.0176), *R* = 0.0499, *S* = 0.987 for 677 parameters. Residual electron density extremes were 0.759 and -0.336 eÅ⁻³. H₂1-TfOH: C₁₁₃H₁₃₁F₃N₄O₉S, M_r = 1778.28, colorless prism, crystal size = 0.15 × 0.1 × 0.1 mm³, monoclinic, *P2₁/c*, *a* = 20.555(2), *b* = 18.7503(19), *c* = 27.853(3) Å, β = 109.574(2)°, *V* = 10114.6(17) Å³, *Z* = 4, ρ_{calcd} = 1.168 Mg m⁻³; μ = 0.096 mm⁻¹, 59606 data (18472 unique, *R*_{int} = 0.0449), *R* = 0.1058, *S* = 1.028 for 1149 parameters. Residual electron density extremes were 1.366 and -0.649 eÅ⁻³. CuI: C₁₁₇H_{135.5}CuN₆O₆, M_r = 1792.36, violet platelet, crystal size = 0.2 × 0.1 × 0.01 mm³, triclinic, *P*-1, *a* = 16.404(3), *b* = 17.516(3), *c* = 20.046(4) Å, α = 100.573(3), β = 106.016(3), γ = 96.178(3)°, *V* = 5365.3(17) Å³, *Z* = 2, ρ_{calcd} = 1.109 Mg m⁻³; μ = 0.258 mm⁻¹, 41166 data (17787 unique, *R*_{int} = 0.0318), *R* = 0.1507, *S* = 1.812 for 1163 parameters. Residual electron density extremes were 2.325 and -1.107 eÅ⁻³. The half-weight acetonitrile solvent molecules were refined isotropically. NiI: C₁₁₇H_{137.5}N_{6.5}NiO₆, M_r = 1805.54, orange needle, crystal size = 0.15 × 0.015 × 0.015 mm³, triclinic, *P*-1 *a* = 16.423(3), *b* = 17.582(3), *c* = 20.056(3) Å, α = 100.016(19), β = 106.234(3), γ = 96.2695(18)°, *V* = 5398.6(15) Å³, *Z* = 2, ρ_{calcd} = 1.111 Mg m⁻³; μ = 0.235 mm⁻¹, 40853 data (17841 unique, *R*_{int} = 0.0506), *R* = 0.1302, *S* = 1.465 for 1184 parameters. Residual electron density extremes were 1.874 and -0.891. The half-weight acetonitrile and quarter-weight water solvent molecules were refined isotropically. The protons on all solvated molecules were discounted in the refinement. [Pd(H₂I)Cl₂(MeCN)]: C₁₂₂H₁₄₅N₉O₆Cl₂Pd, M_r = 2010.77, yellow platelet, crystal size = 0.2 × 0.1 × 0.01 mm³, monoclinic, *C2/c*, *a* = 29.6525(12), *b* = 23.2314(10), *c* = 32.6559(14) Å, β = 99.071(3)°, *V* = 22214.3(16) Å³, *Z* = 8, ρ_{calcd} = 1.202 Mg m⁻³; μ = 0.273 mm⁻¹, 58779 data (19158 unique, *R*_{int} = 0.1733), *R* = 0.1416, *S* = 1.090 for 1253 parameters. Residual electron density extremes were 0.946 and -0.925 eÅ⁻³. The half-weight acetonitrile solvent molecules were refined isotropically. The protons on solvated molecules were discounted in the refinement. CCDC 259162–259166 contain the supplementary crystallographic data for this paper. These data can be obtained free of charge from the Cambridge Crystallographic Data Centre via www.ccdc.cam.ac.uk/data_request/cif.
- [8] F. G. Gatti, D. A. Leigh, S. A. Nepogodiev, A. M. Z. Slawin, S. J. Teat, J. K. Y. Wong, *J. Am. Chem. Soc.* **2001**, *123*, 5983–5989.
- [9] J. S. Hannam, S. M. Lacy, D. A. Leigh, C. G. Saiz, A. M. Z. Slawin, S. G. Stichelell, *Angew. Chem.* **2004**, *116*, 3322–3326; *Angew. Chem. Int. Ed.* **2004**, *43*, 3260–3264.

- [10] D. J. Cram, *Angew. Chem.* **1988**, *100*, 1041–1052; *Angew. Chem. Int. Ed. Engl.* **1988**, *27*, 1009–1020.
- [11] For temporary steric barriers to shuttling, see: a) A. S. Lane, D. A. Leigh, A. Murphy, *J. Am. Chem. Soc.* **1997**, *119*, 11092–11093; b) L. Jiang, J. Okano, A. Orita, J. Otera, *Angew. Chem.* **2004**, *116*, 2173–2176; *Angew. Chem. Int. Ed.* **2004**, *43*, 2121–2124.
- [12] A.-M. L. Fuller, D. A. Leigh, P. J. Lusby, A. M. Z. Slawin, D. B. Walker, unpublished results.
- [13] B. A. Blight, K. A. Van Noortwyck, J. A. Wisner, M. C. Jennings, *Angew. Chem.* **2005**, *117*, 1523–1528; *Angew. Chem. Int. Ed.* **2005**, *44*, 1499–1504.
- [14] K. Kavallieratos, S. R. de Gala, D. J. Austin, R. H. Crabtree, *J. Am. Chem. Soc.* **1997**, *119*, 2325–2326.
- [15] *Note added in proof*: A paper recently appeared (Y. Furusho, T. Matsuyama, T. Takata, T. Moriuchi, T. Hirao, *Tetrahedron Lett.* **2004**, *45*, 9593–9597) that reproduces some of the previous work^[3] on the square-planar template rotaxane system. Although the authors do not comment on it, the ¹H NMR chemical shifts show that the bifurcated pyridine–pyridine hydrogen-bonding motif also exists in their demetalated rotaxane.

Half-rotation in a [2]catenane *via* interconvertible Pd(II) coordination modes†

David A. Leigh,^{*a} Paul J. Lusby,^a Alexandra M. Z. Slawin^b and D. Barney Walker^a

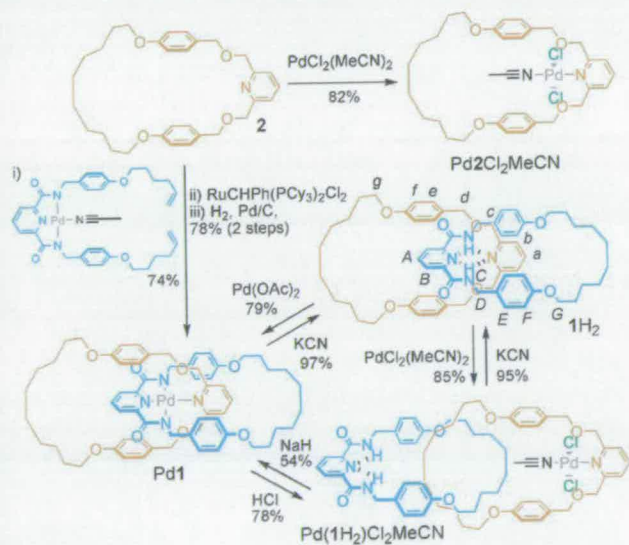
Received (in Cambridge, UK) 27th July 2005, Accepted 15th August 2005

First published as an Advance Article on the web 13th September 2005

DOI: 10.1039/b510663j

Reaction of a [2]catenane with Pd(OAc)₂ binds both macrocycles to the metal, locking them in position; treatment with PdCl₂, however, results in coordination of only one ring, producing a half-turn in the relative orientation of the [2]catenane components in both solution and the solid state.

The development of novel ways to bring about changes in the relative positions of mechanically interlocked sub-molecular components is an important area of investigation in the emerging field of synthetic molecular machines.¹ In terms of rotational processes, a formal half-turn of a ring in a [2]catenane² not only corresponds to a simple mechanical switch,³ but is also a step towards the more demanding requirements of a synthetic rotary molecular motor.⁴ Here we report on a simple [2]catenane system in which the different binding modes of the interlocked rings to Pd(II) cause a major change in the position and orientation of the macrocycles in the resulting complexes.



Scheme 1 Synthesis and interconversion of PdI, 1H₂ and Pd(1H₂)Cl₂MeCN.†

^aSchool of Chemistry, University of Edinburgh, The King's Buildings, West Mains Road, Edinburgh, UK EH9 3JJ.

E-mail: David.L Leigh@ed.ac.uk; Fax: +44-131-667-9085

^bSchool of Chemistry, University of St. Andrews, Purdie Building, St. Andrews, Fife, UK KY16 9ST

† Electronic supplementary information (ESI) available: Experimental procedures and X-ray crystallographic data. See <http://dx.doi.org/10.1039/b510663j>

The square planar coordination preference of Pd(II) can be used to direct the macrocyclization of suitable tridentate ligands around 2,6-dimethyleneoxy-pyridine-based threads to form rotaxanes.^{5,6} We reasoned that a similar strategy could be used to make a palladium [2]catenane by incorporating the monodentate unit into a macrocycle. Pleasingly, PdI was isolated in 58% yield from 2 *via* the three step (ligand coordination, ring-closing olefin metathesis, hydrogenation) reaction sequence shown in Scheme 1.⁷

De-metallation of PdI (KCN, MeOH-CH₂Cl₂, 20 → 40 °C, 1.5 h, 97%) afforded the catenane 1H₂ in which pyridine-amide-pyridine H-bonding⁶ holds the macrocycles in a similar position to that seen for PdI in both solution and the solid state. The well defined orientation of the two fragments is clearly apparent from comparison of the ¹H NMR spectra of the two catenanes (Fig. 1b and c) with those of the non-interlocked component macrocycles (Fig. 1a and 1e). In the room temperature spectra of both 1H₂ (Fig. 1b) and PdI (Fig. 1c) the upfield shift of the H_D, H_E and H_F

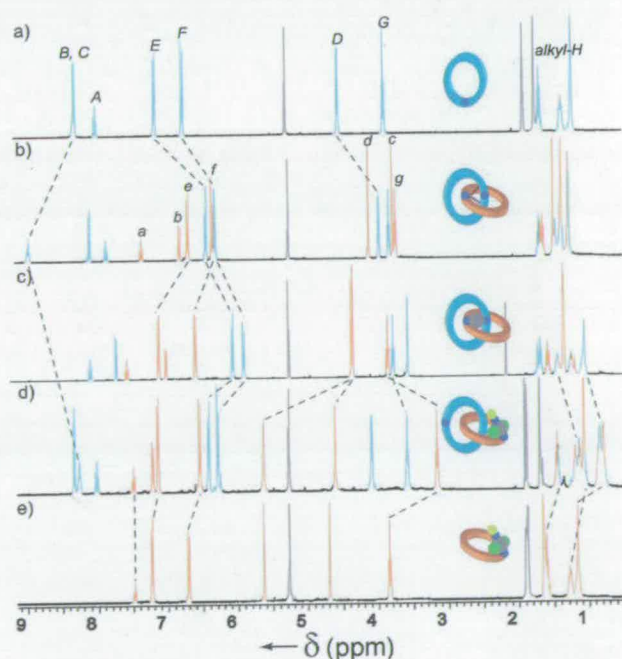


Fig. 1 ¹H NMR spectra (400 MHz, 9 : 1 CD₂Cl₂ : CD₃CN, 298 K, 2.5 mM) (a) non-interlocked bis-amide macrocycle, (b) 1H₂, (c) PdI, (d) Pd(1H₂)Cl₂MeCN and (e) Pd₂Cl₂MeCN (non-interlocked tetra-ether macrocycle bound to PdCl₂MeCN). The grey signals correspond to residual solvents. The dark blue circles in the cartoon rings indicate the position of the pyridine nitrogen atoms.

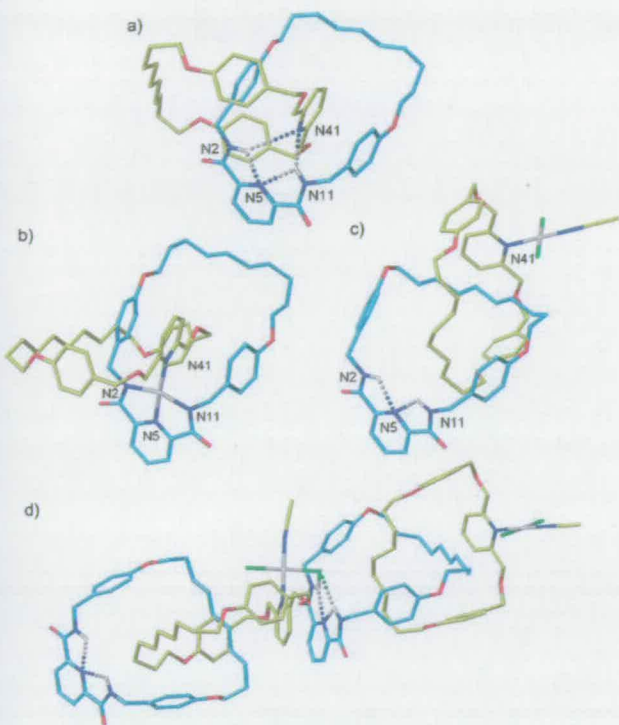


Fig. 2 X-Ray crystal structures of: (a) $1H_2$,⁶ (b) PdI ,⁷ (c) $Pd(1H_2)Cl_2MeCN$ ⁸ (single molecule view; note the change of position and orientation of the yellow macrocycle compared to PdI and $1H_2$) and (d) adjacent molecules of $Pd(1H_2)Cl_2MeCN$ showing intermolecular $Pd-Cl \cdots HN$ hydrogen bonding. Carbon atoms of the bis-amide macrocycle are shown in light blue and those of the tetra-ether macrocycle and coordinated acetonitrile molecule in yellow; oxygen atoms are red, nitrogen dark blue, hydrogen white, palladium grey, chlorine green. For clarity only amide hydrogen atoms are shown. Selected bond lengths for $Pd(1H_2)Cl_2MeCN$ [Å]: $N2H-N5$ 2.21; $N11H-N5$ 2.31; $N5-N41$ 12.93. Selected bond angles for $Pd(1H_2)Cl_2MeCN$ [°]: $N2-H-N5$ 108.8; $N11-H-N5$ 104.1.

resonances indicate a π -stacking arrangement between the benzylic amide rings of the 'blue' macrocycle and the pyridine group of the 'orange' macrocycle. In contrast, the alkyl chain protons are not shielded by interactions with aromatic rings in either catenane. The solution geometries suggested by 1H NMR studies correspond well to the solid state structures of $1H_2$ (Fig. 2a) and PdI (Fig. 2b) determined by X-ray crystallography. Reaction of $1H_2$ with $Pd(OAc)_2$ (MeCN, 60 °C, 4 h, 79%) re-forms the co-conformationally locked catenane, PdI .

Reaction of $1H_2$ with $PdCl_2(MeCN)_2$ in MeCN (20 °C, 1 h, 85%) afforded a second catenane $Pd(II)$ complex in which the amide protons (H_C) of the 'blue' macrocycle were clearly still present (Fig. 1d). X-Ray crystallography (Fig. 2c and d) on a single crystal obtained from slow cooling a saturated acetonitrile solution confirmed this complex to be $Pd(1H_2)Cl_2MeCN$, in which only one of the macrocyclic rings is coordinated to the palladium metal ion, presumably as a consequence of both the greater strength of the $Pd-Cl$ bond compared to $Pd-OAc$ and the poor basicity of the Cl^- ion.

The effect of the different coordination mode on the relative positions and orientations of the two macrocycles in the catenane

is dramatic. In the 1H NMR spectrum of $Pd(1H_2)Cl_2MeCN$ (Fig. 1d) the resonances corresponding to H_G , H_B and H_{alkyl} are shifted significantly upfield, indicating that each macrocycle is located preferentially over the aliphatic region of the other.⁹ The X-ray crystal structure (Fig. 2c and d) shows a similar geometry exists in the solid state. An additional feature of the X-ray crystal structure of $Pd(1H_2)Cl_2MeCN$ is the presence of intermolecular $Pd-Cl \cdots HNCO$ hydrogen bonds between adjacent molecules (Fig. 2d). The negligible change in the chemical shift of the amide protons (H_C) between $1H_2$ (Fig. 1a) and $Pd(1H_2)Cl_2MeCN$ (Fig. 1d) suggests this interaction is weak in solution,⁶ nevertheless it has been successfully utilised¹⁰ to direct the formation of pseudorotaxanes.

The three catenanes $1H_2$, PdI and $Pd(1H_2)Cl_2MeCN$ are all directly interconvertible (Scheme 1): the palladium complexes are de-metallated with KCN; $Pd(1H_2)Cl_2MeCN$ is converted into PdI by treatment with NaH, and the reverse reaction is promoted by HCl in MeCN.¹¹ It is interesting to note the macrocycles adopt similar positions and orientations in PdI and $1H_2$ but in the former they are locked in place by a coordination bond whereas in the latter they are held in the thermodynamic minimum only by weak and dynamic H-bonds. The preferred co-conformation of $Pd(1H_2)Cl_2MeCN$ is very different to the other two, presumably on steric grounds, and as such its formation from either of the others corresponds to a large amplitude rotational switch. It is rare to find such a rich variation in structure and dynamics made possible through simple manipulation of coordination modes.

Notes and references

- V. Balzani, A. Credi, F. M. Raymo and J. F. Stoddart, *Angew. Chem., Int. Ed.*, 2000, **39**, 3348; J.-P. Sauvage, *Chem. Commun.*, 2005, 1507; K. Kinbara and T. Aida, *Chem. Rev.*, 2005, **105**, 1377.
- For examples of catenanes which undergo stimuli-induced half-rotations see: M. Cesario, C. O. Dietrich-Buchecker, J. Guilhem, C. Pascard and J.-P. Sauvage, *J. Chem. Soc., Chem. Commun.*, 1985, 244; A. Livoreil, C. O. Dietrich-Buchecker and J.-P. Sauvage, *J. Am. Chem. Soc.*, 1994, **116**, 9399; D. B. Amabilino, C. O. Dietrich-Buchecker, A. Livoreil, L. Pérez-García, J.-P. Sauvage and J. F. Stoddart, *J. Am. Chem. Soc.*, 1996, **118**, 3905; D. A. Leigh, K. Moody, J. P. Smart, K. J. Watson and A. M. Z. Slawin, *Angew. Chem., Int. Ed. Engl.*, 1996, **35**, 306; A. Livoreil, J. P. Sauvage, N. Armaroli, V. Balzani, L. Flamigni and B. Ventura, *J. Am. Chem. Soc.*, 1997, **119**, 12114; C. P. Collier, G. Matternsteig, E. W. Wong, Y. Luo, K. Beverly, J. Sampaio, F. M. Raymo, J. F. Stoddart and J. R. Heath, *Science*, 2000, **289**, 1172; V. Balzani, A. Credi, S. J. Langford, F. M. Raymo, J. F. Stoddart and M. Venturi, *J. Am. Chem. Soc.*, 2000, **122**, 3542; D. W. Steurman, H. R. Tseng, A. J. Peters, A. H. Flood, J. O. Jeppesen, K. A. Nielsen, J. F. Stoddart and J. R. Heath, *Angew. Chem., Int. Ed.*, 2004, **43**, 6486; B. Korybut-Daszkiewicz, A. Wiecekowska, R. Bilewicz, S. Domagala and K. Wóznik, *Angew. Chem., Int. Ed.*, 2004, **43**, 1668.
- A 'switch' influences a system as a function of state; a 'motor' influences a system as a function of trajectory. For a discussion see: E. R. Kay and D. A. Leigh, *Top. Curr. Chem.* (in press).
- D. A. Leigh, J. K. Y. Wong, F. Dehez and F. Zerbetto, *Nature*, 2003, **424**, 174; J. V. Hernández, E. R. Kay and D. A. Leigh, *Science*, 2004, **306**, 1532.
- A.-M. Fuller, D. A. Leigh, P. J. Lusby, I. D. H. Oswald, S. Parsons and D. B. Walker, *Angew. Chem., Int. Ed.*, 2004, **43**, 3914; Y. Furusho, T. Matsuyama, T. Takata, T. Moriuchi and T. Hirao, *Tetrahedron Lett.*, 2004, **45**, 9593.
- D. A. Leigh, P. J. Lusby, A. M. Z. Slawin and D. B. Walker, *Angew. Chem., Int. Ed.*, 2005, **44**, 4557.
- For various synthetic routes to PdI see: A.-M. L. Fuller, D. A. Leigh, P. J. Lusby, A. M. Z. Slawin and D. B. Walker, *J. Am. Chem. Soc.* web release date 17th August 2005.

- 8 Crystallographic data for Pd(1H₂)Cl₂MeCN: Rigaku MM007/Mercury diffractometer with graphite-monochromated Mo-K α radiation ($\lambda = 0.71073$ Å), 93 K. C₆₄H₇₉Cl₂N₅O₈Pd·CH₃CN, $M = 1264.68$, triclinic, space group $P\bar{1}$, $a = 9.8106(8)$, $b = 25.305(2)$, $c = 26.820(2)$ Å $\alpha = 73.971(4)$, $\beta = 82.771(6)$, $\gamma = 88.050(6)^\circ$, $V = 6348.3(9)$ Å³, $Z = 4$, $D_c = 1.323$ Mg m⁻³, $\mu = 0.435$ mm⁻¹. Of 40751 measured data, 21993 were unique ($R_{\text{int}} = 0.0258$) and 18202 observed ($I > 2\sigma(I)$) to give $R_1 = 0.0524$ and $wR_2 = 0.1226$. CCDC 279771. See <http://dx.doi.org/10.1039/b510663j> for crystallographic data in CIF or other electronic format.
- 9 The downfield shift of H_c and H_d in Pd(1H₂)Cl₂MeCN compared to 1H₂ is probably caused by coordination of the Pd rather than the absence of macrocyclic shielding. Similar chemical shifts are observed in Pd2Cl₂MeCN (Fig. 1e).
- 10 B. A. Blight, K. A. Van Noortwyk, J. A. Wisner and M. C. Jennings, *Angew. Chem., Int. Ed.*, 2005, **44**, 1499.
- 11 For an unusual C-metallated Pd(II) catenate, see: A. J. Blake, C. O. Dietrich-Buchecker, T. I. Hyde, J.-P. Sauvage and M. Schröder, *J. Chem. Soc., Chem. Commun.*, 1989, 1663.